Karl D. von Ellenrieder

Fundamentals of Marine Vehicle Control

Lecture Notes
MTS/IEEE Oceans 2022
Chennai

21 February 2022

Preface

These lecture notes have been prepared for the 2022 MTS/IEEE Oceans Conference and Exposition in Chennai, India. They provide a brief review of the fundamental principles of the nonlinear control of marine vehicles. The intended audience is masters students, PhD students and practitioners who possess, at minimum, some prior experience with the automatic control of linear time invariant systems at the undergraduate student level.

A set of six lectures is provided. Each lecture is intended to take approximately 40-50 minutes, so that the entire tutorial session will take approximately five hours. Lecture 1 provides a physical motivation for focusing on nonlinear control, a brief description of some common approaches to the structure of marine guidance, navigation and control systems, as well as an introduction to their kinematics and dynamics. Lecture 2 introduces important stability concepts needed for the analysis of nonlinear systems. An introduction to the control of underactuated systems is provided in the Lecture 3. Then feedback linearization and backstepping, sliding mode control and adaptive control are introduced in lectures 4-6, respectively.

A list of references and a set of illustrative exercises is provided at the end of each lecture.

The lecture notes draw heavily from the author's textbook *Control of Marine Vehicles* [1]. The author gratefully acknowledges the kind permission of the publisher Springer to reproduce figures, use excerpts from the book in manuscript form, and to reuse selected problems. Please note that unless otherwise indicated each figure was reproduced from this book.

Bolzano, Italy — *Karl von Ellenrieder*
February 2022

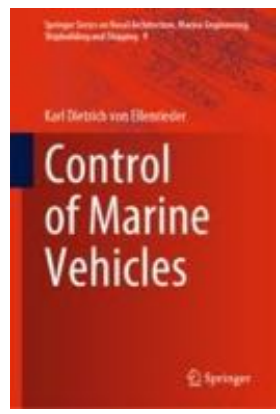

https://link.springer.com/book/10.1007/978-3-030-75021-3

References

1. Karl Dietrich von Ellenrieder. *Control of Marine Vehicles*. Springer Nature, 2021.

Contents

Lecture 1
Introduction

Abstract The architecture of a typical guidance, navigation and control system for marine vehicle systems is discussed. Conventional notations and approaches to the dynamic modeling of marine vehicle systems are presented.

1.1 Overview

Approximately 70% of the Earth's surface is covered by water. The range of environmental conditions that can be encountered within that water is broad. Accordingly, an almost equally broad range of marine vehicles has been developed to operate on and within conditions as disparate as the rough, cold waters of the Roaring Forties and the Furious Fifties in the Southern Hemisphere; the relatively calm, deep waters of the Pacific; and the comparatively warm, shallow, silty waters of the Mississippi and the Amazon rivers.

Here, we will refer to any system, manned or unmanned, which is capable of self-propelled locomotion or positioning at the water's surface, or underwater, as a *marine vehicle*[1]. Thus, this term will be used interchangeably to mean boat, vessel, ship, semi-submersible, submarine, autonomous underwater vehicle (AUV), remotely operated vehicle (ROV), etc.

The main problem in marine vehicle control is to find a way to actuate a vehicle so that it follows a desired behavior as closely as possible. The vehicle should approximate the desired behavior, even when affected by uncertainty in both its ability to accurately sense its environment and to develop control forces with its actuators (e.g. propellers or fins), as well as, when the vehicle is acted upon by external disturbances, such as current, waves and wind.

[1] Some authors similarly use the term *marine craft* in deference to the use of the term *vehicle* to represent a land-borne system.

1.2 Automatic Control

A system is called a *feedback* system when the variables being controlled (e.g. position, speed, etc.) are measured by sensors, and the information is fed back to the controller such that it can process and influence the controlled variables.

Example 1.1. Fig. 1.1 shows a boat trying to maintain a fixed position and heading on the water (station keeping). Imagine that we set up the system to keep the boat as close as possible to the desired position. Without any control, either human control or machine control, the boat is likely to deviate further and further away from the desired position, possibly because of the action of wind, currents or waves. Thus, this system is inherently unstable. The system being controlled, which is the boat in this example, is often called either the *plant* or the *process*. If a human boat captain were present, you could say that the captain is playing the role of the *controller*. One of the purposes of a controller is to keep the controlled system stable, which in this case would mean to keep the boat near the point η_d. The task of keeping the combined system consisting of a plant and controller stable is called *stabilization*.

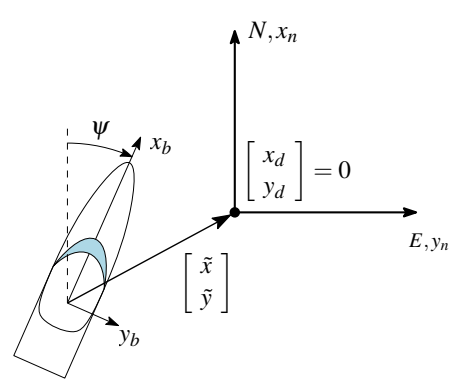

Fig. 1.1 Station–keeping about the desired pose (position and orientation) $\eta_d = [x_d\ y_d\ \psi_d]^T = 0$. Here, $\eta := [x_n\ y_n\ \psi]^T$, where x_n and y_n are the North and East components, respectively, of the vessel's position and ψ is the angle between x_b and N. The error in position and heading is $\tilde{\eta} = \eta_d - \eta$. When $\eta_d = 0$, the pose error is $\tilde{\eta} = -\eta$.

Two possible approaches to stabilizing the system include *open–loop control* and *closed–loop control*:

- Open loop control: This would correspond to: 1) performing a set of detailed experiments to determine the engine throttle and steering wheel positions that keep the boat located at η_d for the expected environmental conditions; 2) setting the boat to η_d, and 3) setting the engine throttle and steering wheel to their experimentally determined positions and hoping that the boat maintains the correct position and heading, even when the environmental conditions vary. As sudden or temporary changes in the environmental conditions (disturbances), such as wind gusts, cannot be predicted, this approach is unlikely to work well. In general, one can never stabilize an unstable plant using open–loop control.

- Closed loop control: This would correspond to using some sort of feedback, such as a human captain monitoring a GPS receiver, to obtain a measure of how well the boat is maintaining the desired position and setting the engine throttle or turning the steering wheel, as needed, to keep the boat in the correct location. As a human captain would use information from the output of the system (the boat's actual position relative to the desired position) to adjust the system input (the positions of the engine throttle and steering wheel), closed–loop control is also called feedback control.

Automatic control is simply the use of machines as controllers. As mentioned above, the plant is the system or process to be controlled. The means by which the plant is influenced is called the *input*, which could be a force or moment acting on the boat, for example. The response of the plant to the input is called the *output*, which would be the deviation of the boat from the desired position and heading. In addition to the input, there are other factors that can influence the output of the plant, but which cannot be predicted, such as the forces and moments generated by wind gusts or waves. These factors are called *disturbances*. In order to predict the behavior of the plant, a model of the plant dynamics is needed. This model may be generated using physical principles, by measuring the output response of the plant to different inputs in a process known as *system identification*, or from a combination of these approaches.

In the human feedback system the captain has to perform several subtasks. He/she has to observe the boat's position and compare it to the measured GPS location, make decisions about what actions to take, and exercise his/her decision to influence the motion of the boat. Normally, these three stages are called *sensing*, *control* and *actuation*, respectively. If we replace the human captain with a machine, we need a sensor, a controller and an actuator. As with the human controlled system, the sensor measures a physical variable that can be used to deduce the behavior of the output, e.g. the deviation of the boat from the desired position and heading. However, with machine control, the output of the sensor must be a signal that the controller can accept, such as an electrical signal. The controller, often a computer or electrical circuit, takes the reading from the sensor, determines the action needed and sends the decision to the actuator. The actuator (e.g. the propeller and rudder) then generates the quantities which influence the plant (such as the forces and moments needed push the boat towards the desired position). A block diagram of a stabilizing closed–loop controller is shown in Fig. 1.2.

□

Example 1.2. Consider another example of maneuvering a boat, as shown in Fig. 1.3. Here, the boat is following a desired, time-dependent, trajectory against a persistent wind so that its speed follows an external command, such as a varying speed limits along a coastal marine channel. There are two subtasks in this example. The first is following the desired trajectory without the wind. This problem is called *tracking*. The second is the reduction (or elimination) of the effects of the wind on the speed and position of the boat. This problem is called *disturbance rejection*. The overall

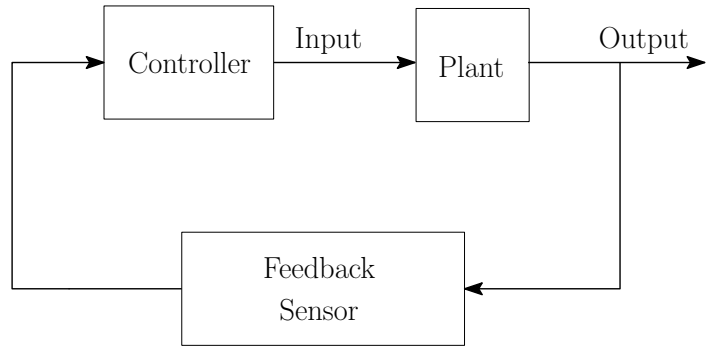

Fig. 1.2 Structure of a feedback system for stabilization purposes.

problem, encompassing both tracking and disturbance rejection, is called *regulation*.

- Open–loop control: This could correspond to adjusting the positions of the steering wheel and throttle according to a precomputed position profile and the wind conditions along different sections of the trajectory, obtained from an accurate weather forecast. One can imagine that the scheme will not work well, since any error in the precomputed position profile or the weather forecast will cause errors in the actual trajectory of the boat.
- Closed–loop control: This could correspond to adjusting the steering and engine throttle according to the measured position and speed of the boat. Since we can steer, accelerate or decelerate the boat in real time, we should be able to control the position, speed and heading of the boat to within a small margin of error. In this case it is not necessary to precisely know the environmental conditions.

□

One can see that the main difference between regulation and stabilization is that there is a command signal, also called a *reference input*, in the regulation problem. The reference input needs to be processed, in addition to other signals, by the stabilizing controller. The structure of a feedback system for regulation is shown in Fig. 1.4. Another difference between regulation and stabilization is that in the regulation problem, the disturbance is often assumed to be persistent and has some known features, such as being piecewise constant. Whereas in the stabilization problem, the disturbance is assumed to be unknown and temporary in nature. The study of stabilization is important because there are many stabilization problems of importance for marine engineering, such as the station keeping problem above, but also because it is a key step in achieving regulation.

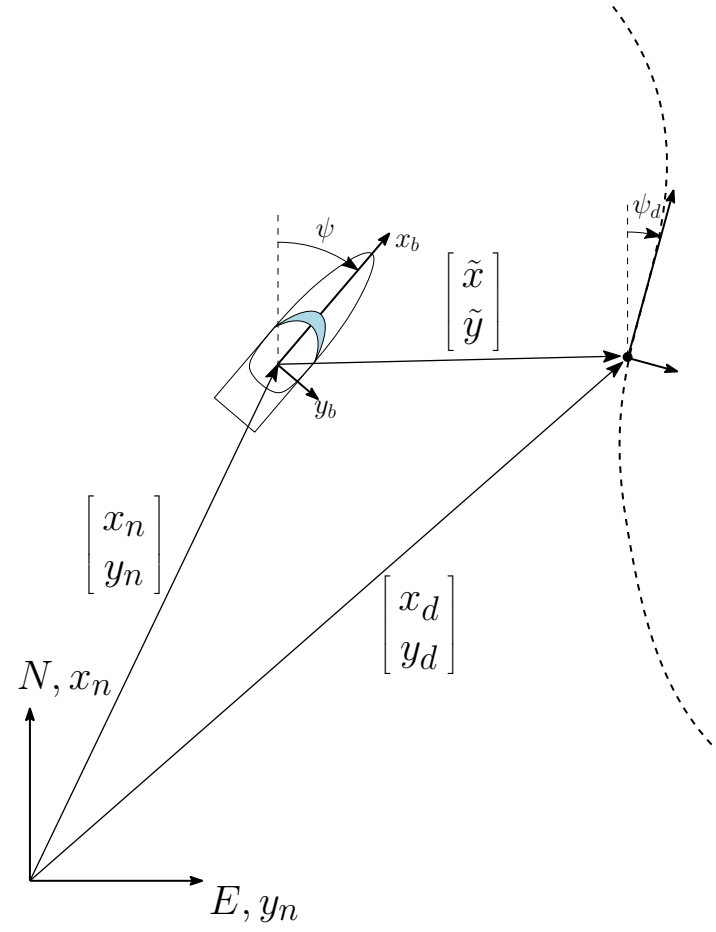

Fig. 1.3 A surface vessel tracking a desired trajectory η_d (dashed curve). Here, $\eta := [x_n\ y_n\ \psi]^T$, where x_n and y_n are the North and East components, respectively, of the vessel's position and the heading angle ψ is the angle between x_b and N. The error in position and heading is $\tilde{\eta} = \eta_d - \eta$. The trajectory may be time-parameterized $\eta_d(t)$ with continuous derivatives, which could also define desired translational and rotational velocities, and desired translational and rotational accelerations, for example.

1.3 Typical Guidance, Navigation and Control Architectures of Marine Vehicles

Systems designed to govern the motion of marine vehicles (as well as air-/spacecraft, cars, etc.) are typically organized along the functional lines of guidance, navigation and control (GNC). A block diagram of a typical GNC system for marine vehicles is shown in Fig. 1.5. The navigation system uses sensors to estimate the vehicle's position, velocity and acceleration, in addition to other knowledge about the state of the vehicle, such as the available propulsive power. Based upon information from the navigation system, and with knowledge of the vehicle's desired operating condition, the guidance system generates a trajectory. When planning a route

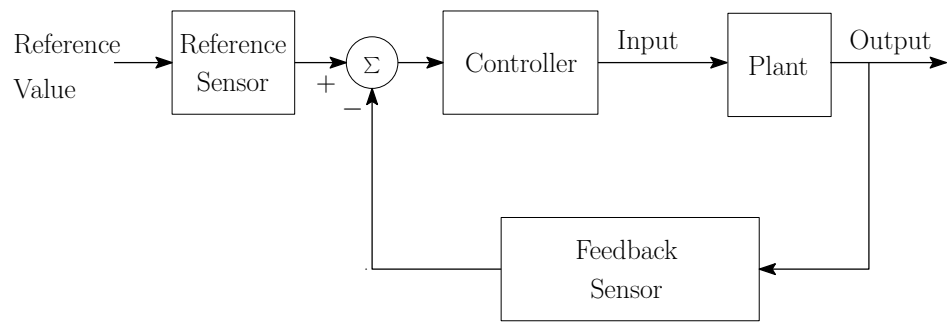

Fig. 1.4 Structure of a feedback controller for regulation.

some guidance systems may use data on weather conditions, sea states, or other information that could affect the vehicle's progress that has been obtained through communication with satellites or remote ground stations. Lastly, the vehicle's control system uses the data input from both the guidance and navigation systems to generate output commands to the vehicle's actuators (propellers, fins, etc.) so that the vehicle follows the desired trajectory as closely as possible.

Based upon its inputs, the guidance system determines a set of waypoints (intermediate target coordinates) that the vehicle should follow. The guidance system also includes a reference computing algorithm, which is sometimes also called a trajectory planner, that generates a smooth feasible trajectory through the desired waypoints based upon the vehicle's dynamic model, its current position and orientation, obstacles or other traffic and the amount of power available.

Sensors commonly found in the navigation systems of marine vehicles include radar, global positioning system (GPS) units, inertial measurement units (IMUs), and electronic compasses. GPS measurements typically include vehicle position, speed and heading. Depending on the number of measurement axes available, IMUs can measure the linear and angular accelerations of the vehicle, and also its rotational rates. The outputs of these sensors can be noisy or have drop-outs where a signal is lost from time to time. For example: 1) underwater vehicles can only acquire GPS positioning information at the surface where they can receive signals from GPS satellites; 2) smaller boats are low to the water and when operating in rough seas radar contacts can fade in and out; and 3) the Earth's magnetic fields around bridges or large metallic underwater structures can be distorted, affecting the outputs of the magnetometers used in electronic compass systems. To mitigate these effects, navigation systems often employ *state estimators*, also called *observers*, that use a combination of redundant sensor inputs and/or computational models of the vehicle's performance to approximate the true state of the vehicle. The vehicle state information that is output from the navigation system is used as a feedback signal to the vehicle control system.

The control system includes a controller and control allocation system. The input to the controller can be combinations of desired position, speed, heading, acceler-

ation, etc. Its output is basically a set of anticipated forces and moments that must be applied to the vehicle, as shown in Fig. 1.5) in order for it to achieve the desired behavior. A *control allocation* system is then used to determine which available actuators (propellers, fins, etc.) should be powered to produce the required forces and moments and to translate the desired forces/moments into actuator commands, such as propeller RPM or fin angle. As it may be possible for more than one combination of actuators to produce the same set of required control forces and moments, the control allocation system often optimizes the choice of actuators to minimize the power or time required to perform a desired maneuver. Note that several different types of controllers may need to be used on the same vehicle, depending upon its operating condition. For example, a vehicle may be required to transit from one port to another, during which time an autopilot (speed and heading controller) is employed. Later it might need to hold position (station–keep) while waiting to be moored, during which time a station–keeping controller may be employed. Systems developed to switch from one type of controller to another, which may have a different dynamic structure, are called *switched-* or *hybrid-control* systems. The system used to select the appropriate controller is known as a *supervisor*.

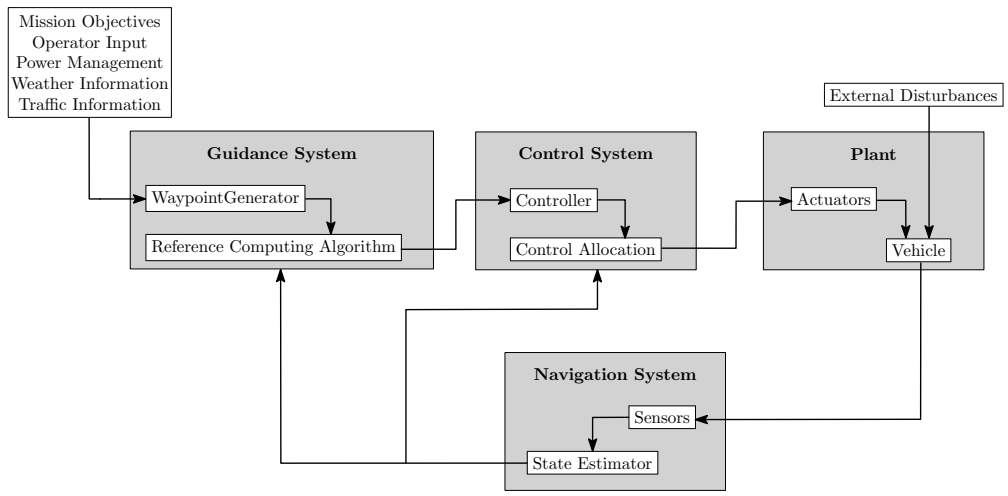

Fig. 1.5 A typical Guidance, Navigation and Control System used for marine vehicles.

1.4 Dynamic Modeling of Marine Vehicles

As discussed in Section 1.2, the goal of feedback control is to either stabilize the output of a controlled dynamic system about a desired equilibrium point, or to cause a controlled system to follow a desired reference input accurately, despite the path that the reference variable may take, external disturbances and changes in the dynamics of the system. Before designing a feedback controller, we must construct a math-

ematical model of the system to be controlled and must understand the dynamic responses expected from the closed–loop system, so that we reasonably predict the resulting performance. Thus, the design of any feedback system fundamentally depends on a sufficiently accurate dynamic model of the system and an appropriate estimate of the closed–loop system's dynamic response.

Thus, the first step in the design of a controller is the development of a suitable dynamic model of the system to be controlled. In addition to physical modeling based on first principles, such as Newton's 2nd Law or the use of Lagrange's Energy Methods for mechanical systems. There are also System Identification techniques that utilize experimental data to determine the parameters in, and sometimes the structure of, the dynamic model of a system.

In this text, we will usually assume that a dynamic model of the system to be controlled has already been developed and focus on how the equations that govern the system's response can be analyzed. However, especially when working with nonlinear and/or underactuated systems, an understanding of the underlying dynamics of a system can assist with controller design. In this vein, some of the basic principles involved in modeling marine vehicle systems are summarized in this section. More detailed information on the dynamic modeling of marine systems can be found in the following references [8, 1, 7, 3, 4].

It is traditional to split the study of the physics of motion of particles and rigid bodies into two parts, kinematics and kinetics. Kinematics generally refers to the study of the geometry of motion and kinetics is the study of the motion of a body resulting from the applied forces and moments that act upon its inertia.

1.4.1 Kinematics of Marine Vehicles

The key kinematic features of interest for the control of marine vessels are the vehicle's position and orientation; linear and angular velocities; and linear and angular accelerations. Controlling the trajectory of a system is an especially important objective in robotics and unmanned vehicle systems research, where the position and orientation of a vehicle are often referred to as its *pose*. When developing a dynamic model of a marine vehicle, it is common to specify its position with respect to a North-East-Down (NED) coordinate system, which is taken to be locally tangent to the surface of the Earth. As shown in Fig. 1.6a, the NED system is fixed at a specific latitude and longitude at the surface of the Earth and rotates with it. Note that the NED frame is not an inertial frame, as it is rotating. Thus, strictly speaking, there are forces arising from the centripetal and Coriolis accelerations caused by the Earth's rotation that act on the vehicle. However, at the speeds that marine vehicles typically travel, these forces are generally much smaller than gravitational, actuator and hydrodynamic forces (such as drag) and so are typically ignored in the equations of motion. However, as we shall see below, there are centripetal and Coriolis effects that arise from the vehicle's rotation about its own axes. Under certain oper-

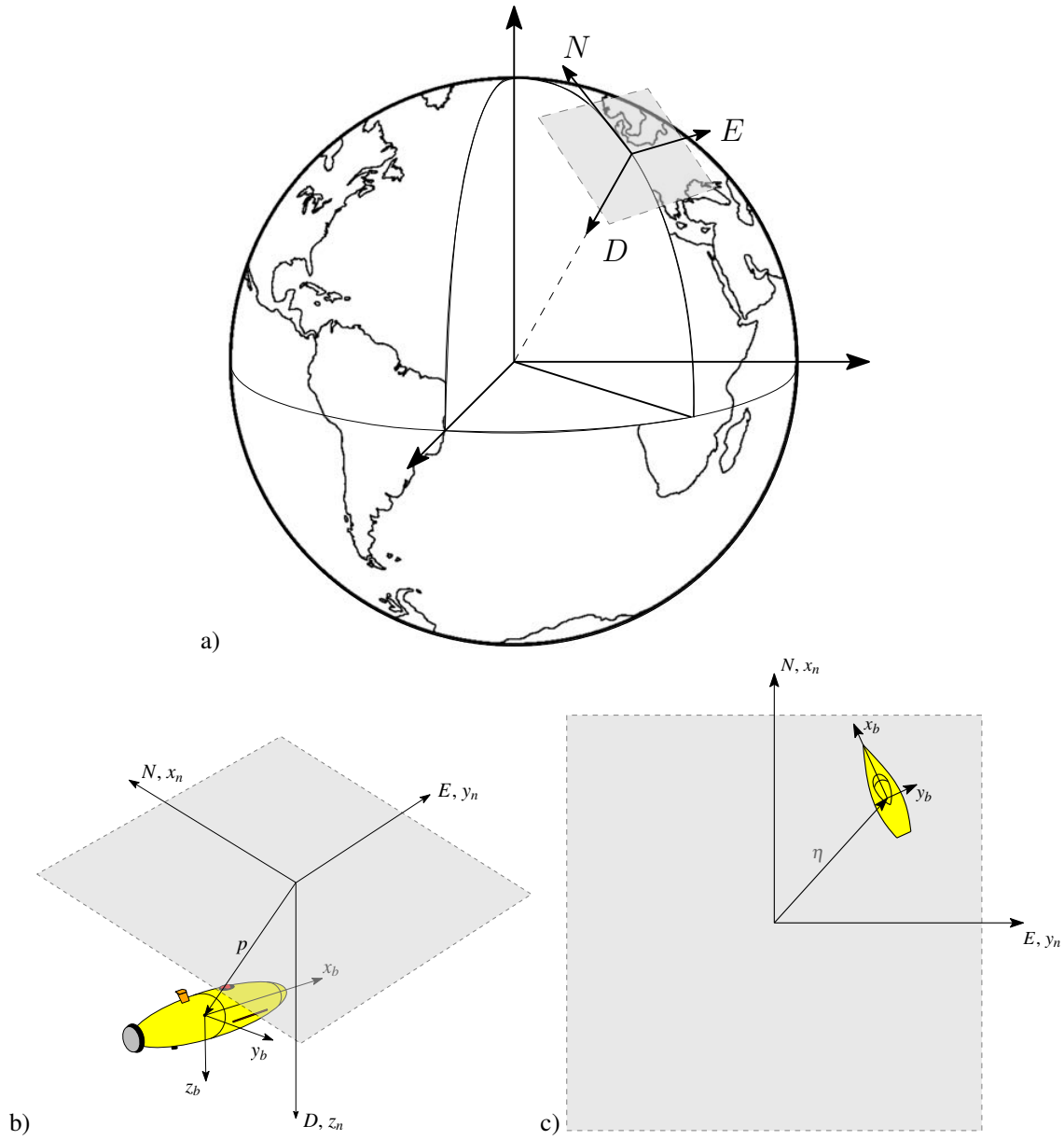

Fig. 1.6 a) The *NED* coordinate system referenced to an Earth–fixed, Earth–centered coordinate system. b) An underwater vehicle referenced with respect to the NED coordinate system. c) A surface vehicle referenced with respect to the NED coordinate system. Note the motion of surface vessels can typically be assumed to lie within the plane of the *N*–*E* axes.

ational conditions, for example when forward and rotational speeds of a vehicle are significant, these effects must be included in a vessel's equations of motion.

The position of the vehicle in NED coordinates is given by

$$\mathbf{p}_{b/n}^{n} = \begin{bmatrix} x_n \\ y_n \\ z_n \end{bmatrix}, \tag{1.1}$$

where we use the superscript n to indicate that the position is in *NED* coordinates and the subscript b/n to indicate that we are measuring the position of the vehicle (body) with respect to the *NED* 'n-frame'. Similarly, the orientation of the vehicle is given by

$$\Theta_{nb} = \begin{bmatrix} \phi \\ \theta \\ \psi \end{bmatrix}, \tag{1.2}$$

where ϕ is defined as the *roll* angle about the x_b axis, θ is the *pitch* angle about the y_b axis, and ψ is the *yaw* angle about the z_b axis. These angles are often referred to as the *Euler angles* and are a measure of the cumulative angular change over time between the *NED* and body-fixed coordinate systems (Fig. 1.7). Note that the origin of the body-fixed coordinate systems shown here has been taken to be the center of gravity G (center of mass) of the vehicle. In some applications it may be more convenient to locate the origin of the coordinate systems elsewhere, such as at the center of buoyancy B of a vehicle or at a position where measurements of a vehicle's motion are collected, such as the location of an IMU. According to D'Alembert's Principle, the forces acting on rigid body can be decomposed into the linear forces applied at the center of gravity of the body and rotational torques applied about the center of gravity [6]. Because of this, when the origin of the coordinate system is not located at the center of gravity additional terms must be included in the equations of motion to determine the local accelerations and velocities in the body-fixed frame, which arise from externally applied forces and moments.

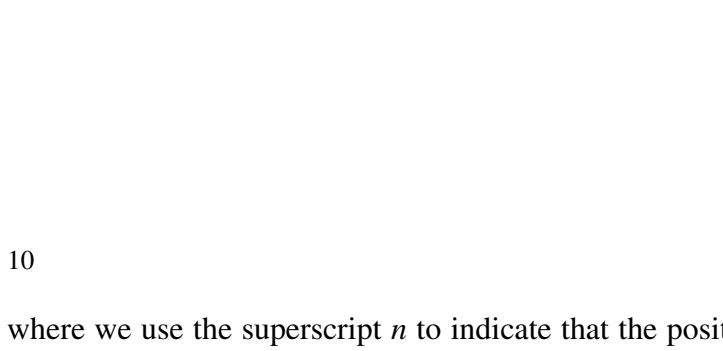

Fig. 1.7 A body-fixed coordinate system with its origin located at the center of gravity G of an Autonomous Underwater Vehicle (AUV).

As shown in Fig. 1.7, the coordinate along the longitudinal (*surge*) axis of the vehicle is x_b, the coordinate along the transverse (*sway*) axis is y_b and the coordinate along the remaining perpendicular (*heave*) axis is z_b. The velocity of the vehicle measured in the body fixed frame is given by

$$\mathbf{v}_{b/n}^{b} = \begin{bmatrix} u \\ v \\ w \end{bmatrix}, \tag{1.3}$$

and the angular velocity of the vehicle in the body–fixed frame is

$$\omega_{b/n}^{b} = \begin{bmatrix} p \\ q \\ r \end{bmatrix} = \begin{bmatrix} \dot{\phi} \\ \dot{\theta} \\ \dot{\psi} \end{bmatrix}. \tag{1.4}$$

Here, p is the *roll rate* about the x_b axis, q is the *pitch rate* about the y_b axis and r is the *yaw rate* about the z_b axis. As also shown in Fig. 1.7, the external linear forces acting on a marine vehicle are written as

$$\mathbf{f}_{b}^{b} = \begin{bmatrix} X \\ Y \\ Z \end{bmatrix}. \tag{1.5}$$

and the corresponding external moments are given by

$$\mathbf{m}_{b}^{b} = \begin{bmatrix} K \\ M \\ N \end{bmatrix}. \tag{1.6}$$

The generalized motion of an unmanned vehicle has six degrees of freedom (DOF), three translational (linear) and three rotational. We can write the full six DOF equations in vector form by introducing the generalized position η, velocity $\mathbf{v}$ and force τ, each of which has six components

$$\eta = \begin{bmatrix} \mathbf{p}_{b/n}^{n} \\ \Theta_{nb} \end{bmatrix} = \begin{bmatrix} x_n \\ y_n \\ z_n \\ \phi \\ \theta \\ \psi \end{bmatrix}, \tag{1.7}$$

$$\mathbf{v} = \begin{bmatrix} \mathbf{v}_{b/n}^{b} \\ \boldsymbol{\omega}_{b/n}^{b} \end{bmatrix} = \begin{bmatrix} u \\ v \\ w \\ p \\ q \\ r \end{bmatrix}, \tag{1.8}$$

and

$$\tau = \begin{bmatrix} \mathbf{f}_{b}^{b} \\ \mathbf{m}_{b}^{b} \end{bmatrix} = \begin{bmatrix} X \\ Y \\ Z \\ K \\ M \\ N \end{bmatrix}. \tag{1.9}$$

Remark 1.1. The use of mathematical symbols for making definitions or assumptions shorter is very common in the robotics and control literature. A short list of some of the symbols commonly encountered is given in Table 1.1.

Table 1.1 Common mathematical symbols used in robotics and control.

Symbol	Meaning
$\in$	an element of
$\subset$	a subset of
$\forall$	for every
$\exists$	there exists
$\mathbb{R}$	the set of real numbers
$\mathbb{R}^{+}$	the set of positive real numbers
$\mathbb{Z}$	the set of integers
$\Rightarrow$	implies

Remark 1.2. In robotics and control research it is often important to keep track of the dimensions and ranges of the components of each vector involved. Typically, the components of vectors, such as speed and position, are defined along

the set of both positive and negative real numbers and so the dimensions of such vectors are specified as $\mathbf{p}^n_{b/n} \in \mathbb{R}^3$, $\mathbf{v}^b_{b/n} \in \mathbb{R}^3$, $\mathbf{f}^b_b \in \mathbb{R}^3$, and $\mathbf{m}^b_b \in \mathbb{R}^3$, for example. However, the principal values of angular measurements have a limited range, e.g. $0 \leq \phi < 2\pi$, and so are often specified as $\Theta_{nb} \in \mathcal{S}^3$, where $\mathcal{S} := [0, 2\pi)$.

Coordinate system conventions for surface vehicles

Unmanned and manned underwater vehicles, such as AUVs and submarines, typically employ the body–fixed coordinate system convention shown in Fig. 1.7. However, the study of the motion of surface vehicles also includes an examination of their response to wave and wind conditions at the water's surface. In the fields of Naval Architecture and Marine Engineering, these surface conditions are often known as a *seaway*. Traditionally, the dynamic modeling of surface vehicles has been split into separate disciplines known as *seakeeping* and *maneuvering* (e.g. [8, 7, 3]). Maneuvering calculations generally examine the dynamic response of a vessel when moving through calm, flat seas and with an eye towards understanding its course-keeping ability and trajectory. Maneuvering calculations do include the wave-making resistance of the vessel (i.e. the drag on the hull generated when the vehicle moves through calm water and creates waves). Seakeeping calculations on the other hand typically examine a vessel's linear and angular displacements from a nominal trajectory when disturbed by the waves already present in a seaway. Seakeeping calculations are typically split into Froude-Kryloff forces caused by the pressure field of waves impacting the hull of a ship, as well as, the 'radiation forces'developed from the ship's own motion [2].

Although, there have been some recent efforts to merge the analyses performed in these two similar disciplines, e.g. [13, 10, 12], the nomenclature and modeling conventions used have traditionally differed slightly, which can lead to confusion. Maneuvering studies have often used a body-fixed coordinate system analogous to that used with underwater vehicles, such as in Fig. 1.8a, with its origin at G, the positive sway axis pointing out of the starboard side of the vessel, and the positive heave axis pointing towards the bottom of the vehicle.

However, in place of the NED plane, seakeeping studies often use a coordinate system with its origin at the centroid of the vessel's waterplane and translating at the vessel's nominal constant forward speed (the dashed x–y–z frame in Fig. 1.8b). A second, body–fixed frame, is used to specify the wave-induced displacement of the vessel η from the x–y–z frame (the x_b–y_b–z_b frame in Fig. 1.8b). In the x_b–y_b–z_b coordinate system the positive heave axis points upward, the positive surge axis points forward and the positive sway axis points towards the port side of the vessel. In this text, we shall always use the traditional maneuvering body–fixed coordinate system convention shown in Figs. 1.7 and 1.8a.

Coordinate System Transformations

When the orientation and position of a marine vehicle changes, the representation of its inertial properties, the inertia tensor, is constant if expressed in a body–fixed

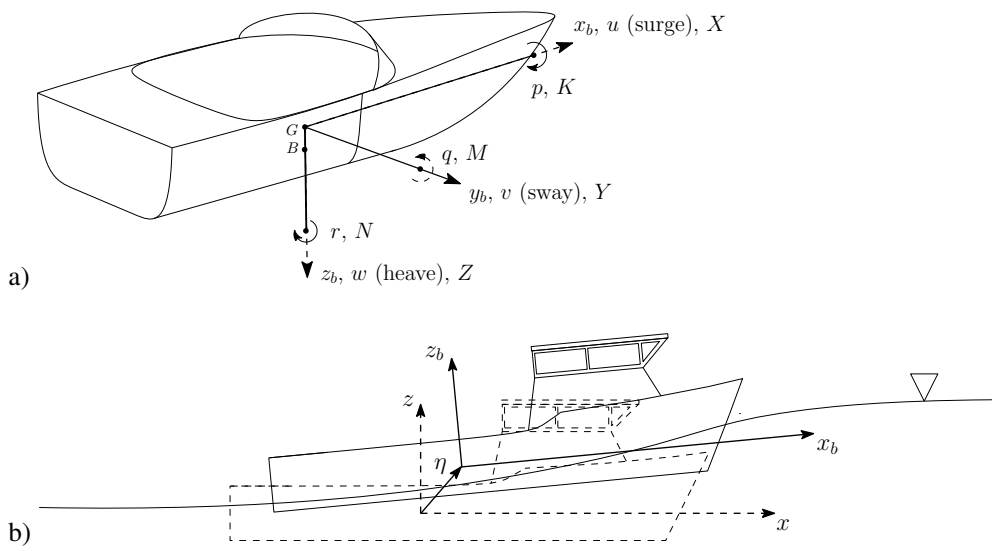

Fig. 1.8 a) A traditional maneuvering body–fixed coordinate system. b) A conventional sea–keeping body–fixed frame.

coordinate system. Thus, the use of body–fixed coordinate systems can substantially simplify the modeling and dynamic simulation of a vehicle. However, one of the main objectives of vehicle simulations is to predict the time–dependent position and orientation of a vehicle in a real operating space, which is usually specified in a *NED* coordinate system. In order to determine position and orientation in the *NED* frame, the velocity of the vehicle in body–fixed coordinates must be converted to *NED* coordinates and integrated in time. Therefore, it is important to understand how one can perform coordinate transformations to express the velocity vector components in multiple reference frames. Coordinate system transformation techniques are equally important in other instances, for example when converting the representation of forces/moments generated by a vectored thruster from a thruster–fixed coordinate system, where the relation between the orientation of the flow entering the thruster and the forces/moments generated is most easily modeled, to a vehicle body–fixed coordinate system, where the thruster forces/moments are best represented during dynamic simulation.

Consider the motion of a boat in the *NED* coordinate system, as shown in Fig. 1.9a. Here we will assume that the motion is confined to the *N–E* plane and restricted to three degrees of freedom, which include rotation about the *D* axis measured with respect to *N* and linear translations in the *N–E* plane. Here the *course* (trajectory) of the boat is represented as a dashed curve. At each time instant the velocity vector $\mathbf{U}$ is tangent to the course. The *course angle* χ, is the angle between $\mathbf{U}$ and *N*. Note that, in general, the bow of the vessel does not need to point in the same direction as the velocity vector. The angle between the x_b axis of the vessel, which usually points through its bow, and *N* is called the *heading angle* ψ. When χ and ψ differ, the angle between them is known as the drift angle β (sometimes also called either the *sideslip angle* or, especially in sailing, the *leeway angle*), and

the component of velocity perpendicular to the longitudinal axis of the boat v (sway speed) is called the *sideslip*.

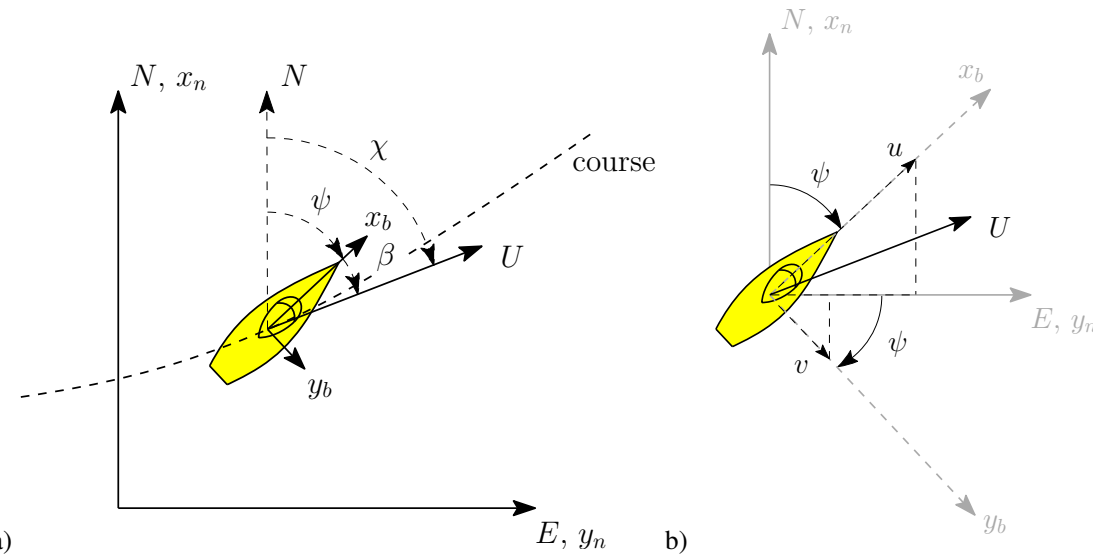

Fig. 1.9 a) 3 DOF maneuvering coordinate system definitions. b) Resolution of the velocity vector components in the *NED* and body–fixed frames.

An examination of the velocity vector **U** in both the body–fixed and the *NED* coordinate systems, as shown in Fig. 1.9b, allows one to see how the velocity vector expressed in components along x_b and y_b can be converted to components in the *NED* frame. Writing the *NED* frame velocity components $\dot{x}_n$ and $\dot{y}_n$ in terms of the u and v components of the body–fixed frame gives

$$\dot{x}_n = u\cos\psi - v\sin\psi, \tag{1.10}$$

$$\dot{y}_n = u\sin\psi + v\cos\psi, \tag{1.11}$$

which can be rewritten in vector form as

$$\begin{pmatrix}\dot{x}_n\\ \dot{y}_n\end{pmatrix} = \begin{bmatrix}\cos\psi & -\sin\psi\\ \sin\psi & \cos\psi\end{bmatrix}\begin{pmatrix}u\\ v\end{pmatrix}. \tag{1.12}$$

Here, in equation 1.12 the matrix in square brackets transforms vectors expressed in *NED* coordinates into a vector expressed in body–fixed frame coordinates. In this relatively simple example, one can see that the coordinate transformation can be thought of as a rotation about the D axis. In three dimensions, the same transformation matrix can be expressed as

$$R_{z_b,\psi} = \begin{bmatrix}\cos\psi & -\sin\psi & 0\\ \sin\psi & \cos\psi & 0\\ 0 & 0 & 1\end{bmatrix}, \tag{1.13}$$

where the subscript z,ψ is used to denote a rotation in heading angle ψ about the z_b axis.

Generally, a three dimensional transformation between any two coordinate systems can be thought of as involving a combination of individual rotations about the three axes of a vehicle in body–fixed coordinates. In this context, the heading angle ψ, pitch angle θ and roll angle ϕ of the vehicle are Euler angles, and the transformations corresponding to rotation about the pitch and roll axes can be respectively represented as

$$R_{y_b,\theta} = \begin{bmatrix} \cos\theta & 0 & \sin\theta \\ 0 & 0 & 1 \\ -\sin\theta & 0 & \cos\theta \end{bmatrix}, \tag{1.14}$$

and

$$R_{x_b,\phi} = \begin{bmatrix} 1 & 0 & 0 \\ 0 & \cos\phi & -\sin\phi \\ 0 & \sin\phi & \cos\phi \end{bmatrix}. \tag{1.15}$$

In order to determine the transformation between any arbitrary total rotation between the body–fixed coordinate system and the *NED* frame, we can use the product of the transformation matrices. For example, the complete transformation for an orientation that can be represented as first a rotation in heading and then a rotation in pitch would be given by the product $R_{y_b,\theta}R_{z_b,\psi}$. As shown in Example 1.3 below, the order in which the rotations are performed is important.

Example 1.3. Consider the successive rotations of a surface vessel, as shown in Fig. 1.10. The final orientation of the vessel after successive $+90^\circ$ rotations in roll first and then pitch, will be different from the final orientation of the vessel after successive $+90^\circ$ rotations in pitch first and then roll. From a mathematical stand-

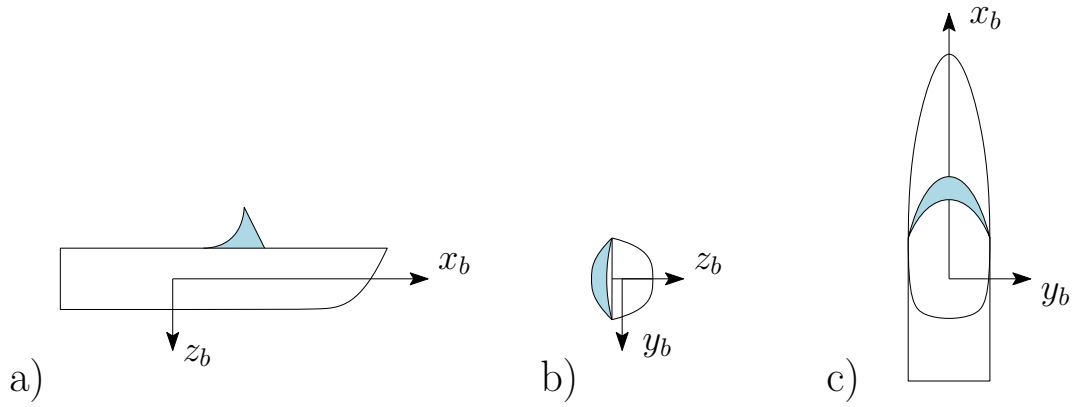

Fig. 1.10 Successive $+90^\circ$ rotations of the boat shown in1.8a: a) Initial orientation. b) Final orientation after roll first and then pitch. c) Final orientation after pitch first and then roll.

point, this is the result of the fact that matrix operations do not commute, such that in general $R_{y_b,\theta}R_{z_b,\psi} \neq R_{z_b,\psi}R_{y_b,\theta}$.

□

Remark 1.3. As the order of the sequence of rotations is important, in both the fields of marine vehicle maneuvering and aeronautical/astronautical engineering it has become accepted practice for the heading angle ψ to be taken first, the pitch angle θ to be taken secondly, and lastly the roll angle ϕ to be taken.

Thus, the transformation matrix corresponding to a general three dimensional rotation between two coordinate systems is defined as

$$\begin{aligned}\mathbf{R}_b^n(\Theta_{nb}) &:= R_{z_b,\psi}R_{y_b,\theta}R_{x_b,\phi} \\ &= \begin{bmatrix} \mathrm{c}\psi\mathrm{c}\theta & -\mathrm{s}\psi\mathrm{c}\phi+\mathrm{c}\psi\mathrm{s}\theta\mathrm{s}\phi & \mathrm{s}\psi\mathrm{s}\phi+\mathrm{c}\psi\mathrm{s}\theta\mathrm{c}\phi \\ \mathrm{s}\psi\mathrm{c}\theta & \mathrm{c}\psi\mathrm{c}\phi+\mathrm{s}\psi\mathrm{s}\theta\mathrm{s}\phi & -\mathrm{c}\psi\mathrm{s}\phi+\mathrm{s}\psi\mathrm{s}\theta\mathrm{c}\phi \\ -\mathrm{s}\theta & \mathrm{c}\theta\mathrm{s}\phi & \mathrm{c}\theta\mathrm{c}\phi \end{bmatrix},\end{aligned} \tag{1.16}$$

where $\mathrm{c}(\cdot)$ and $\mathrm{s}(\cdot)$ are used to represent the $\cos(\cdot)$ and $\sin(\cdot)$ functions, respectively.

Despite the complicated appearance of the rotation matrices, they have some nice mathematical properties that make them easy to implement, and which can be used for validating their correct programming in simulation codes. Rotation matrices belong the *special orthogonal group of order 3*, which can be expressed mathematically as $\mathbf{R}_b^n(\Theta_{nb}) \in \mathrm{SO}(3)$, where

$$\mathrm{SO}(3) := \{\mathbf{R} | \mathbf{R} \in \mathbb{R}^{3\times 3}, \text{ where } \mathbf{R} \text{ is orthogonal and } \det(\mathbf{R}) = \mathbf{1}\}. \tag{1.17}$$

The term $\det(\mathbf{R})$ represents the determinant of $\mathbf{R}$. In words, this means that rotation matrices are orthogonal and their inverse is the same as their transpose $\mathbf{R}^T = \mathbf{R}^{-1}$, so that $\mathbf{R}\mathbf{R}^T = \mathbf{R}\mathbf{R}^{-1} = \mathbf{1}$, where $\mathbf{1}$ is the identity matrix

$$\mathbf{1} := \begin{bmatrix} 1 & 0 & 0 \\ 0 & 1 & 0 \\ 0 & 0 & 1 \end{bmatrix}. \tag{1.18}$$

Use of the transpose can make it very convenient to switch back and forth between vectors in the body–fixed and the *NED* frames, e.g.

$$\dot{\mathbf{p}}_{b/n}^n = \mathbf{R}_b^n(\Theta_{nb})\mathbf{v}_{b/n}^b, \tag{1.19}$$

and

$$\mathbf{v}_{b/n}^b = \mathbf{R}_b^n(\Theta_{nb})^T\dot{\mathbf{p}}_{b/n}^n. \tag{1.20}$$

When the Euler angles are limited to the ranges

$$0 \leq \psi < 2\pi, \quad -\frac{\pi}{2} < \theta < \frac{\pi}{2}, \quad 0 \leq \phi \leq 2\pi, \tag{1.21}$$

any possible orientation of a vehicle can be attained. When $\theta = \pm\pi/2$, ψ and ϕ are undefined, as no unique set of values for them can be found. This condition, wherein the angular velocity component along the x_b axis cannot be represented in terms of the Euler angle rates [6], is known as *gimbal lock*. Marine surface vehicles are unlikely to encounter scenarios in which gimbal lock can occur, however, it is possible for it to occur with ROVs, AUVs or submarines undergoing aggressive maneuvers. In such cases, the kinematic equations could be described by two Euler angle representations with different singularities and the singular points can be avoided by switching between the representations. Alternatively, the use of unit quaternions for performing coordinate transformations, instead of Euler angles, can be used to circumvent the possibility of gimbal lock (see [4]).

Definition 1.1 (Time derivative of $\mathbf{R}_b^n$ and the cross product operator $\mathbf{S}(\lambda)$). When designing controllers for marine vehicles it is often necessary to compute the time derivative of the rotation matrix $\mathbf{R}_b^n$. A convenient way to do this is to use the cross product operator. Let $\lambda := [\lambda_1\ \lambda_2\ \lambda_3]^T$ and $\mathbf{a}$ be a pair of vectors. The cross product between λ and $\mathbf{a}$ can be expressed as

$$\lambda \times \mathbf{a} = \mathbf{S}(\lambda)\mathbf{a}, \tag{1.22}$$

where $\mathbf{S}$ is

$$\mathbf{S}(\lambda) = -\mathbf{S}^T(\lambda) = \begin{bmatrix} 0 & -\lambda_3 & \lambda_2 \\ \lambda_3 & 0 & -\lambda_1 \\ -\lambda_2 & \lambda_1 & 0 \end{bmatrix}. \tag{1.23}$$

Then, the time derivative of the rotation matrix that transforms vectors between the body-fixed and the NED reference frames is

$$\dot{\mathbf{R}}_b^n = \mathbf{R}_b^n \mathbf{S}(\omega_{b/n}^b), \tag{1.24}$$

where

$$\mathbf{S}(\omega_{b/n}^b) = -\mathbf{S}^T(\omega_{b/n}^b) = \begin{bmatrix} 0 & -r & q \\ r & 0 & -p \\ -q & p & 0 \end{bmatrix}. \tag{1.25}$$

□

Since the orientation between the NED frame and the body–fixed coordinate system can change as a vehicle maneuvers, the relation between the rate of change of the Euler angles $\dot{\Theta}_{nb}$ and the angular velocity of the vehicle $\omega_{b/n}^b$ requires the use of a special transformation matrix $\mathbf{T}_\Theta(\Theta_{nb})$. As shown in [6], the angular velocities associated with changes in the Euler angles $\dot{\phi}$, $\dot{\theta}$ and $\dot{\psi}$ are not perpendicular to one another. Another way of thinking about this is that the Euler rotations are not taken about orthogonal body axes, but about axes which change during the rotation process [7]. Projecting $\dot{\Theta}_{nb}$ along the directions of the components of the angular velocity vector $\omega_{b/n}^b$, gives

$$\begin{aligned} p &= \dot{\phi} - \dot{\psi}\sin\theta \\ q &= \dot{\theta}\cos\phi + \dot{\psi}\sin\phi\cos\theta \\ r &= -\dot{\theta}\sin\phi + \dot{\psi}\cos\phi\cos\theta, \end{aligned} \tag{1.26}$$

or in vector form $\omega_{b/n}^{b} = \mathbf{T}_{\Theta}^{-1}(\Theta_{nb})\dot{\Theta}_{nb}$, where

$$\mathbf{T}_{\Theta}^{-1}(\Theta_{nb}) = \begin{bmatrix} 1 & 0 & -\mathrm{s}\theta \\ 0 & \mathrm{c}\phi & \mathrm{c}\theta\mathrm{s}\phi \\ 0 & -\mathrm{s}\phi & \mathrm{c}\theta\mathrm{c}\phi \end{bmatrix}. \tag{1.27}$$

Inverting the relations in equations 1.26, gives

$$\begin{aligned} \dot{\phi} &= p + (q\sin\phi + r\cos\phi)\tan\theta \\ \dot{\theta} &= q\cos\phi - r\sin\phi \\ \dot{\psi} &= (q\sin\phi + r\cos\phi)\sec\theta, \end{aligned} \tag{1.28}$$

or in vector form $\dot{\Theta}_{nb} = \mathbf{T}_{\Theta}(\Theta_{nb})\omega_{b/n}^{b}$ so that

$$\mathbf{T}_{\Theta}(\Theta_{nb}) = \begin{bmatrix} 1 & \mathrm{s}\phi\mathrm{t}\theta & \mathrm{c}\phi\mathrm{t}\theta \\ 0 & \mathrm{c}\phi & -\mathrm{s}\phi \\ 0 & \dfrac{\mathrm{s}\phi}{\mathrm{c}\theta} & \dfrac{\mathrm{c}\phi}{\mathrm{c}\theta} \end{bmatrix}, \tag{1.29}$$

where $\mathrm{t}(\cdot) := \tan(\cdot)$. Note that $\mathbf{T}^{T} \neq \mathbf{T}^{-1}$.

The Kinematic Equations

Putting it all together, the full six DOF kinematic equations relating the motion of a marine vehicle in the NED coordinate system to its representation in the body–fixed coordinate system can be written compactly in vector form as

$$\dot{\eta} = \mathbf{J}_{\Theta}(\eta)\mathbf{v}, \tag{1.30}$$

which, in matrix form, corresponds to

$$\begin{pmatrix} \dot{\mathbf{p}}_{b/n}^{n} \\ \dot{\Theta}_{nb} \end{pmatrix} = \begin{bmatrix} \mathbf{R}_{b}^{n}(\Theta_{nb}) & \mathbf{0}_{3\times3} \\ \mathbf{0}_{3\times3} & \mathbf{T}_{\Theta}(\Theta_{nb}) \end{bmatrix} \begin{pmatrix} \mathbf{v}_{b/n}^{b} \\ \omega_{b/n}^{b} \end{pmatrix}, \tag{1.31}$$

where $\mathbf{0}_{3\times3}$ is a 3×3 matrix of zeros,

$$\mathbf{0}_{3\times3} := \begin{bmatrix} 0 & 0 & 0 \\ 0 & 0 & 0 \\ 0 & 0 & 0 \end{bmatrix}. \tag{1.32}$$

When studying the stability of submarines, it is common to assume that the motion is constrained to a vertical plane, with only surge, heave and pitch motions. Similarly, in many instances the motion of surface vehicles can be assumed to be constrained to the horizontal plane with only three degrees of freedom: surge, sway and yaw. Maneuvering stability for these cases is presented in [7], for example. For surface vehicles, the three DOF kinematic equations reduce to

$$\dot{\eta} = \mathbf{R}(\psi)\mathbf{v}, \tag{1.33}$$

where $\mathbf{R}(\psi) = R_{z_b,\psi}$ (see equation 1.13) and

$$\eta = \begin{pmatrix} x_n \\ y_n \\ \psi \end{pmatrix}, \quad \text{and} \quad \mathbf{v} = \begin{pmatrix} u \\ v \\ r \end{pmatrix}. \tag{1.34}$$

1.4.2 Kinetics of Marine Vehicles

From a control design standpoint, the main goal of developing a dynamic model of a marine vehicle is to adequately describe the vehicle's dynamic response to environmental forces from waves, wind or current and to the control forces applied with actuators, such as fins, rudders, and propellers. The complete equations of motion of a marine vehicle moving in calm, flat water can be conveniently expressed in body-fixed coordinates using the robot-like model of Fossen [4]

$$\dot{\eta} = \mathbf{J}(\eta)\mathbf{v} \tag{1.35}$$

and

$$\mathbf{M}\dot{\mathbf{v}} + \mathbf{C}(\mathbf{v})\mathbf{v} + \mathbf{D}(\mathbf{v})\mathbf{v} + \mathbf{g}(\eta) = \tau + \mathbf{w}_d, \tag{1.36}$$

where the first equation describes the kinematics of the vehicle (as above) and the second equation represents its kinetics. The terms appearing in these equations are defined in Table 1.2. Here n is the number of degrees of freedom. In general, a marine craft with actuation in all DOFs, such as an underwater vehicle, requires a $n = 6$ DOF model for model-based controller and observer design, while ship and semi-submersible control systems can be designed using an $n = 3$, or 4 DOF model.

The terms $\mathbf{M}$, $\mathbf{C}(\mathbf{v})$ and $\mathbf{D}(\mathbf{v})$ have the useful mathematical properties shown in Table 1.3. These symmetry properties can be exploited in controller designs and stability analyses.

Table 1.2 Variables used in (1.35) and (1.36).

Term	Dimension	Description
$\mathbf{M}$	$\mathbb{R}^n \times \mathbb{R}^n$	Inertia tensor (including added mass effects)
$\mathbf{C}(\mathbf{v})$	$\mathbb{R}^n \times \mathbb{R}^n$	Coriolis and centripetal matrix (including added mass effects)
$\mathbf{D}(\mathbf{v})$	$\mathbb{R}^n \times \mathbb{R}^n$	Hydrodynamic damping matrix
$\mathbf{g}(\eta)$	$\mathbb{R}^n$	Gravity and buoyancy (hydrostatic) forces/moments
$\mathbf{J}(\eta)$	$\mathbb{R}^n \times \mathbb{R}^n$	Transformation matrix
$\mathbf{v}$	$\mathbb{R}^n$	Velocity/angular rate vector
η	$\mathbb{R}^n$	Position/attitude vector
τ	$\mathbb{R}^n$	External forces/moments (e.g. wind, actuator forces)
$\mathbf{w}_d$	$\mathbb{R}^n$	Vector of disturbances

Table 1.3 Mathematical properties of $\mathbf{M}$, $\mathbf{C}(\mathbf{v})$ and $\mathbf{D}(\mathbf{v})$.

$\mathbf{M} = \mathbf{M}^T > 0 \Rightarrow \mathbf{x}^T\mathbf{M}\mathbf{x} > 0, \forall \mathbf{x} \neq 0$
$\mathbf{C}(\mathbf{v}) = -\mathbf{C}^T(\mathbf{v}) \Rightarrow \mathbf{x}^T\mathbf{C}(\mathbf{v})\mathbf{x} = 0, \forall \mathbf{x}$
$\mathbf{D}(\mathbf{v}) > 0 \Rightarrow \frac{1}{2}\mathbf{x}^T[\mathbf{D}(\mathbf{v}) + \mathbf{D}^T(\mathbf{v})]\mathbf{x} > 0, \forall \mathbf{x} \neq 0$

Remark 1.4. Notice that the velocity, inertial terms and forces in (1.36) are computed in the body-fixed coordinate system. This substantially simplifies the modeling and dynamic simulation of marine vehicle motion because the representation of the inertia tensor is constant when expressed in a body–fixed coordinate system.

An important advantage of representing the equations of motion in this form is that it is similar to that used for robotic manipulators (see [11], for example), which permits one to draw upon a wealth of control and stability analysis techniques developed for more general robotics applications.

Remark 1.5. The inertia tensor $\mathbf{M}$ includes the effects of *added mass*. These are additional terms added to the true mass, and mass moments of inertia, of a marine vehicle to account for the pressure-related effects acting on the submerged portions of its hull when it accelerates. These pressure-related effects cause forces, which are proportional to the acceleration of the vehicle, and are hence conceptualized to be associated with the effective mass of fluid surrounding the vehicle, which is also accelerated, when the vehicle is accelerated [9].

When a vehicle is operating in a current, or in waves, the equations of motion must be modified slightly. In a current, the hydrodynamic forces (added mass and drag) become dependent on the relative velocity between the vehicle and the surrounding water. When a surface vehicle operates in waves, some of the added mass

and hydrodynamic damping terms are dependent on the encounter frequency of the vessel with the waves and must be altered accordingly. As mentioned above, we will we will normally assume that the dynamic model of the system to be controlled (1.36) has already been developed and focus on how the equations that govern the system's response can be analyzed to design a controller. Detailed descriptions of how maneuvering models can be developed for marine vehicles are presented in the following texts [8, 1, 2, 7, 3, 4].

1.5 Why Study Nonlinear Control?

Marine environments are generally complex, unstructured and uncertain. The disturbances affecting a marine vehicle caused by wind, waves and currents are time varying and generally unpredictable.

Not only are the characteristics of the environment complex, but the dynamics of marine vehicles themselves is usually highly nonlinear. Consider how the wave drag of a surface vessel (also called the *residuary resistance* R_R) varies with its speed U and length L, which is typically characterized using the Froude number $\mathrm{Fr} := U/\sqrt{gL}$, as shown in the figure below. Even within a narrow range of operating conditions (e.g. $0 \leq \mathrm{Fr} \leq 0.6$), the wave drag can vary substantially.

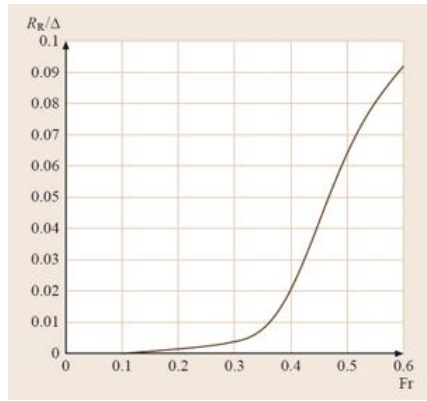

Fig. 1.11 An example of how the residuary resistance (wave-making resistance) of a hull varies with Froude number [14]. Here R_R is normalized by the displacement Δ (weight) of the vessel.

As the speed of a surface vessel increases, the hydrodynamic response of its hull changes substantially because the physical processes involved in generating the lift force that supports the vehicle's weight are Froude number dependent. The dynamics of the lift force transition from a response that can be characterized as:

a) *hydrostatic displacement* — generated mainly by the buoyancy arising from the weight of the water displaced by the underwater portion of the hull, i.e. Archimedes' Principle, ($\mathrm{Fr} \leq 0.4$), to

b) *semi-displacement* — generated from a combination of buoyancy and hydrodynamic lift ($0.4 \leq \text{Fr} \leq 1-1.2$), to
c) *planing* — generated mainly by hydrodynamic lift ($1-1.2 \leq \text{Fr}$).

When a surface vessel operates across a range of Froude numbers the draft of the hull (sinkage) and its trim (pitch angle of the hull) can vary substantially, causing large changes in its drag characteristics.

Normally, the hydrodynamics of the main hull of a marine vessel and its actuators (fins, rudders and propellers) are characterized separately [5]. This can lead to uncertainty in the dynamic response of the vessel, for which correction factors are often used. At the same time nonlinear interactions (vortex shedding from lifting surfaces, such as rudders and fins, and complex changes in the flow around the hull caused by propellers and thrusters) between the actuator and main body of the vessel are almost always present. Such interactions may not always be captured well when fixed parameters are used in the maneuvering equations of motion.

Further, complex, nonlinear hydrodynamic interactions can also arise when a vessel operates at/near the surface, where its damping depends on the encounter frequency (speed/direction-adjusted frequency) of incident waves [2, 3], near the seafloor, where pressure effects can change vessel dynamics, or when multiple vehicles operate near one another. For example, a significant component of the drag of a surface vessel operating in a seaway depends on the heights and frequencies of the waves it traverses. As the encounter frequency of the waves depends on the speed and orientation of the vessel, the drag can vary substantially depending on the relative angles between waves and vehicle (normally, control design is performed using the maneuvering equations, which assume calm flat water with no waves).

Finally, marine vessels are almost never operated in the configuration or at the operating conditions for which they were designed. Thus, the dynamics for which their control systems were originally developed may often no longer apply.

In short, the dynamics of marine vehicles are highly uncertain, both in terms of the model coefficients used (*parametric uncertainties*) and the equations that describe them (e.g. there are often unmodeled dynamics, called *unstructured uncertainties*). The dynamics are also generally nonlinear and time-varying. When coupled with the fact that the external environment imposes time varying and unpredictable disturbances on a vehicle, it becomes clear that the application of special robust nonlinear control techniques, which have been specifically developed to handle time varying nonlinear systems with uncertain models, can help to extend the range of safe operating conditions beyond what is possible using standard linear control techniques.

In the remainder of these lecture notes, we will explore some of the basic tools of nonlinear control and their application to marine systems. The following topics are covered:

- Lyapunov and Lyapunov-like stability analysis techniques for nonlinear systems;
- feedback linearization and integrator backstepping;
- the control of underactuated systems;
- adaptive control; and

- sliding model control, including higher order sliding mode observers and differentiators.

Problems

1.1. Some common feedback control systems are listed below.

(a) Manual steering of a boat in a harbor.
(b) The water level controlled in a tank by a float and valve.
(c) Automatic speed control of an ocean–going ship.

For each system, draw a component block diagram and identify the following:

- the process
- the actuator
- the sensor
- the reference input
- the controlled output
- the actuator output
- the sensor output

1.2. AUVs can only acquire GPS signals when they are at the surface. When underwater, they often use a method known as *dead-reckoning* to estimate their location (when high precision acoustic positioning measurements are not available). The technique involves combining measurements of their orientation with measurements, or estimates, of their speed. When operating near the seafloor, speed can be measured using a sensor known as a Doppler velocimetry logger (DVL). When beneath the surface, but too far above the seafloor for a DVL to function, the speed can be estimated based on knowledge of the correlation between open loop propeller commands and steady state speed. AUVs surface periodically, as their missions permit, to correct the dead-reckoning position estimate using a GPS measurement. Sketch a block diagram depicting this process.

1.3. A vectored thruster AUV uses a gimbal-like system to orient its propeller so that part of the propeller thrust T can be directed along the sway and heave axes (Fig. 1.7) of the vehicle. As shown in Fig. 1.12, let the pitch angle of the the gimbal be $\theta_p \ll 1$ and the yaw angle be $\psi_p \ll 1$. If the thrust of the propeller lies along the symmetry axis of the propeller duct, use the Euler transformation matrices (1.13)–(1.14) to show that the torques produced by the propeller in the vehicle reference frame are

$$\tau = \begin{bmatrix} K \\ M \\ N \end{bmatrix} \approx -lT \begin{bmatrix} 0 \\ \theta_p \\ \psi_p \end{bmatrix},$$

where l is the distance between the center of mass of the AUV and the propeller.

1.4. Find the rotation matrix corresponding to the Euler angles $\phi = \pi/2$, $\theta = 0$ and $\psi = \pi/4$. What is the direction of the x_b axis relative to the NED frame?

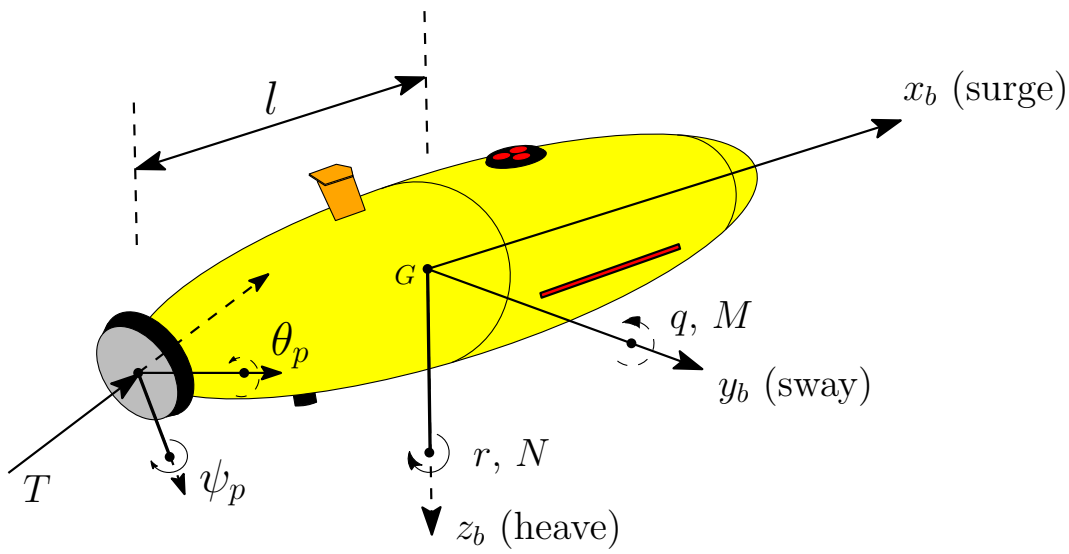

Fig. 1.12 An AUV with a vectored thruster.

References

1. E Eugene Allmendinger, editor. *Submersible vehicle systems design*, volume 96. SNAME, Jersey City, NJ, 1990.
2. Odd Faltinsen. *Sea loads on ships and offshore structures*, volume 1. Cambridge university press, 1993.
3. Odd M Faltinsen. *Hydrodynamics of high-speed marine vehicles*. Cambridge University Press, 2005.
4. Thor I Fossen. *Handbook of marine craft hydrodynamics and motion control*. John Wiley & Sons, 2011.
5. Thomas C Gillmer and Bruce Johnson. *Introduction to Naval Architecture*. Naval Institute Press, 1982.
6. Donald T Greenwood. *Principles of dynamics*. Prentice-Hall Englewood Cliffs, NJ, 1988.
7. Edward M Lewandowski. *The dynamics of marine craft: maneuvering and seakeeping*, volume 22. World scientific, 2004.
8. E V Lewis. *Principles of Naval Architecture*, volume III. SNAME, Jersey City, NJ, 2 edition, 1989.
9. John Nicholas Newman. *Marine hydrodynamics*. MIT Press, 1997.
10. Renato Skejic and Odd M Faltinsen. A unified seakeeping and maneuvering analysis of ships in regular waves. *Journal of marine science and technology*, 13(4):371–394, 2008.
11. Mark W Spong, Seth Hutchinson, and Mathukumalli Vidyasagar. *Robot modeling and control*. Wiley, 2006.
12. Rahul Subramanian and Robert F Beck. A time-domain strip theory approach to maneuvering in a seaway. *Ocean Engineering*, 104:107–118, 2015.
13. Serge Sutulo and C Guedes Soares. A unified nonlinear mathematical model for simulating ship manoeuvring and seakeeping in regular waves. In *Proc. Int. Conf. on Marine Simulation and Ship Manoeuvrability MARSIM*, 2006.
14. Karl Dietrich von Ellenrieder and Manhar R Dhanak. Hydromechanics. In *Springer Handbook of Ocean Engineering*, pages 127–176. Springer, 2016.

Lecture 2
Stability: Basic Concepts

Abstract Here we examine basic stability concepts and methods for analyzing the stability of nonlinear systems. Lyapunov's Direct (Second) Method and LaSalle's Invariant Set Theorem are introduced, together with some common approaches for the determination of candidate Lyapunov functions. The concepts of ultimate boundedness and practical stability are introduced for the analysis of time-varying systems with exogenous disturbances. Lastly, the use of Barbalat's Lemma for analyzing the stability of systems with time-varying parameters is discussed.

2.1 The Stability of Marine Systems

One of the most important questions about the properties of a controlled system is whether or not it is stable: does the output of the system remain near the desired operating condition as the commanded input condition, the characteristics of any feedback sensors and the disturbances acting on the system vary?

For marine systems the question of stability can be especially critical. For example, unmanned underwater vehicles are often used to make measurements of the water column over several hours. When they are underwater, it can be difficult to localize and track them precisely. If their motion is not robustly stable to unknown disturbances, e.g. salinity driven currents under the polar ice caps, strong wind driven currents, etc. the error in their trajectories could grow substantially over time, making their recovery difficult or sometimes impossible. Anyone who has witnessed a team of oceanographers nervously pacing the deck of a research vessel while anxiously watching for a 2 m UUV to return from the immense blackness of the ocean, with significant research funds and countless hours of preparation and time invested its return, can appreciate the importance of knowing that the vehicle's motion is predictable and that one can be reasonably confident in its safe retrieval.

As another example, consider the motion of a large ship. When moving at design speed, some large ships can take more than 10 minutes and require several kilometers to stop or substantially change direction. The ability to precisely control a ship

near populated coastlines, where there could be underwater hazards such as reefs and rocks, is extremely important for ensuring the safety of the lives of the people aboard the ship, as well as for ensuring that the risks of the substantial economic and environmental damage that could occur from a grounding or collision are minimized.

2.2 Basic Concepts in Stability

Many advanced techniques have been developed to determine the stability of both linear and nonlinear systems. However, before embarking on a detailed description of the stability analysis techniques typically applied in control systems engineering practice, we can gain some insight into the stability of controlled systems by first exploring some relatively simple graphical approaches that exploit the simplicity of plotting the trajectories of the state variables in phase space [14, 10, 7].

A state space input–output system has the form

$$\dot{\mathbf{x}} = \mathbf{F}(\mathbf{x}, \mathbf{u}), \quad \mathbf{y} = \mathbf{h}(\mathbf{x}, \mathbf{u}), \tag{2.1}$$

where $\mathbf{x} = \{x_1, \ldots, x_n\} \in \mathbb{R}^n$ is the state, $\mathbf{u} \in \mathbb{R}^p$ is the input and $\mathbf{y} \in R^q$ is the output. The smooth maps $\mathbf{F} : \mathbb{R}^n \times \mathbb{R}^p \to \mathbb{R}^n$ and $\mathbf{h} : \mathbb{R}^n \times \mathbb{R}^p \to \mathbb{R}^q$ represent the dynamics and feedback measurements of the system. Here, we investigate systems where the control signal is a function of the state, $\mathbf{u} = \alpha(\mathbf{x})$. This is one of the simplest types of feedback, in which the system regulates its own behavior. In this way, the equations governing the response of a general n^{th}–order controlled system can be written as a system of n first order differential equations. In vector form, this equation can be written as

$$\dot{\mathbf{x}} = \mathbf{F}(\mathbf{x}, \alpha(\mathbf{x})) := \mathbf{f}(\mathbf{x}), \tag{2.2}$$

and in the corresponding component form, as

$$\begin{aligned} \dot{x}_1 &= f_1(x_1, \ldots, x_n) \\ &\vdots \\ \dot{x}_n &= f_n(x_1, \ldots, x_n). \end{aligned} \tag{2.3}$$

We will start by qualitatively exploring some basic stability concepts using graphical approaches, and then proceed to analytical approaches for analyzing the stability of systems in Sections **??**–2.8. The graphical representations in phase space of systems with $n > 2$ can be computationally and geometrically complex, so we will restrict our attention to first order $n = 1$ and second order $n = 2$ systems. Further, we will assume that $\mathbf{f}$ is a smooth, real–valued, function of $\mathbf{x}(t)$ and that $\mathbf{f}$ is an autonomous function $\mathbf{f} = \mathbf{f}(\mathbf{x})$, i.e. it does not *explicitly* depend on time $\mathbf{f} \neq \mathbf{f}(\mathbf{x}, t)$.

2.3 Flow along a line

To start, consider a one–dimensional system $\dot{x} = f(x)$ and think of x as the position of an imaginary particle moving along the real line, and $\dot{x}$ as the velocity of that particle. Then the differential equation represents a vector field on the line — it dictates the velocity vector at each point x. To sketch the vector field we can plot $\dot{x}$ versus x and then add vectors to the real line so that at each point of the x–axis, the direction of the vector at that point is determined by the sign of $\dot{x}$. The vectors give the trajectory of the imaginary particle on the real axis. Points where $\dot{x} = 0$ correspond to positions where the particle does not move, i.e. *fixed points*, which represent equilibrium solutions of the differential equation. An equilibrium solution corresponds to a *stable* fixed point if the velocity vectors on both sides of it point towards the fixed point. Conversely, an equilibrium solution corresponds to an *unstable* fixed point if the velocity vectors on both sides of it point away from the fixed point. Note that if the velocity vectors on either side of the fixed point differ in sign (point in opposite directions) the assumption that $f(x)$ is a smooth function would be violated. Here, we'll represent stable fixed points with filled circles and unstable fixed points with open circles, as in Example 2.1 below (after [14]).

Example 2.1. Consider the system $\dot{x} = x^2 - 1$. To find the fixed points and examine the stability of the system, we can plot x versus $\dot{x}$, as shown in Fig. 2.1. We can see that the fixed points occur at the locations $x = \pm 1$. Adding velocity vectors to the x–axis we can see that an imaginary particle would travel to the left for $|x| < 1$ and to the right for $|x| > 1$. Thus, the point $x = +1$ is an unstable fixed point and the point $x = -1$ is a stable fixed point. Note that the notion of stable equilibrium is based on small disturbances. A small disturbance to the system at $x = -1$ will return the system to $x = -1$. However, a disturbance that knocks the system from $x = -1$ to the right of $x = 1$ will send the system out to $x \to +\infty$. Thus, $x = -1$ is *locally stable*.

□

Example 2.2. Consider the system $\dot{x} = \sin(x + \pi/4) - x$. An approach to graphically analyzing its stability would be to plot the function $f(x) = \sin(x + \pi/4) - x$ and then sketch the associated vector field. An easier approach is to find the equilibrium point where $\dot{x} = 0$ by separately plotting $y_1 = x$ and $y_2 = \sin(x + \pi/4)$ on the same graph and looking for any intersection points where $\dot{x} = y_2 - y_1 = 0$. When this is done, as in Fig. 2.2, it can be seen that this system has a single equilibrium point. It can also be seen that when the line $y_1 = x$ is above the curve $y_2 = \sin(x + \pi/4)$, $\dot{x} < 0$, and when $y_1 = x$ is below the curve $y_2 = \sin(x + \pi/4)$, $\dot{x} > 0$. Thus, the fixed point is a stable equilibrium point. Here, the fixed point is *globally stable* because it is approached from all initial conditions.

□

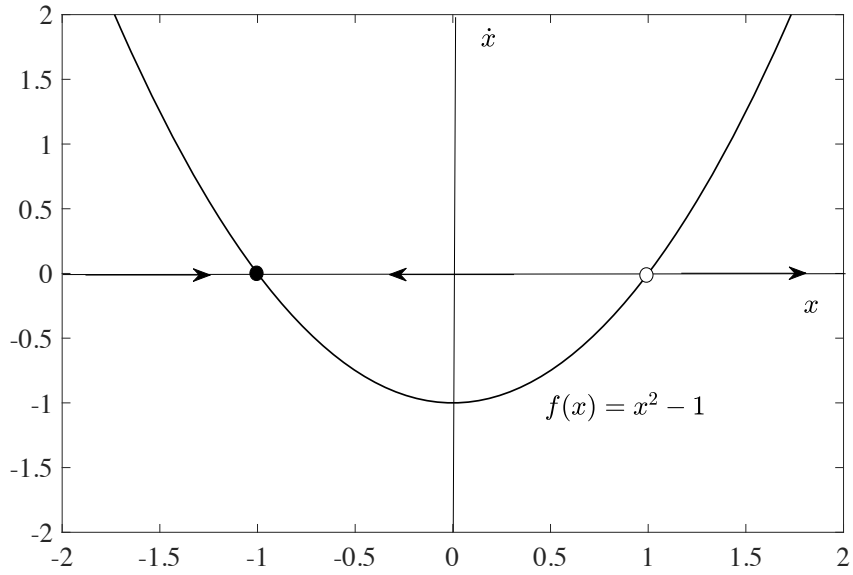

Fig. 2.1 One dimensional phase diagram of the system $\dot{x} = x^2 - 1$.

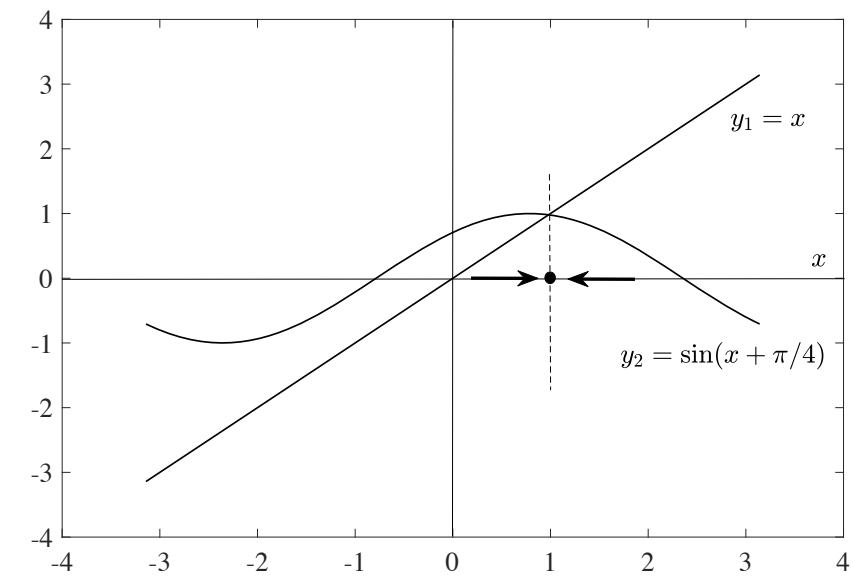

Fig. 2.2 Graphical approach to finding the stability of the system $\dot{x} = \sin(x + \pi/4) - x$.

2.3.1 Linear 1D Stability Analysis

Linearization about a desired operating point x_e of a controlled system can be used to determine a more quantitative measure of stability than provided by graphical approaches. To accomplish this we can perform a Taylor series expansion of the differential equation about x_e. Let η be a small perturbation away from x_e, such

that $\eta(t) = x(t) - x_e$. Thus, near the point x_e, $\dot{\eta} = \dot{x} = f(x) = f(x_e + \eta)$ and using Taylor's expansion gives

$$\begin{aligned} f(x_e+\eta) &= f(x_e) + \eta f'(x_e) + \frac{1}{2}\left.\frac{\mathrm{d}^2 f}{\mathrm{d}x^2}\right|_{x=x_e}\eta^2 + \cdots + \frac{1}{n!}\left.\frac{\mathrm{d}^n f}{\mathrm{d}x^n}\right|_{x=x_e}\eta^n, \\ &= f(x_e) + \eta f'(x_e) + O(\eta^2), \end{aligned} \tag{2.4}$$

where "Big–O" notation $O(\eta^2)$ is used to denote quadratically small terms in η and $f'(x) := \mathrm{d}f/\mathrm{d}x$. We can think of the desired operating point, or set point of our system as a fixed point of the differential equation governing the controlled system, $f(x_e)$. Assuming that the $O(\eta^2)$ terms are neglegible in comparison, we may use the *linear approximation*

$$\dot{\eta} \approx \eta f'(x_e). \tag{2.5}$$

With the initial condition $\eta(t=0) = \eta_0$, the solution to this equation would be

$$\eta = \eta_0 e^{f'(x_e)t}. \tag{2.6}$$

Thus, we can see that if $f'(x_e) > 0$ the perturbation η grows exponentially and decays if $f'(x_e) < 0$. Thus, the sign of the slope $f'(x_e)$ determines whether an operating point is stable or unstable and the magnitude of the slope is a measure of how stable the operating point is (how quickly perturbations grow or decay). When $f'(x_e) = 0$, the $O(\eta^2)$ terms are not negligible and a nonlinear analysis is needed.

Example 2.3 (Speed control of a surface vessel). As discussed in Section 1.2, one of the main purposes of an automatic control system is to make a desired operating point an equilibrium point of the controlled system, such that the system is stable at that point. As much as possible, the controlled system should also be stable about the operating point when external disturbances act on the system. Consider the speed control of the boat shown in Fig. 2.3. The equation of motion is given by

$$m\dot{u} = -cu|u| + T, \tag{2.7}$$

where u is speed, c is a constant related to the drag coefficient of the hull and T is the thrust generated by the propeller. Here, we will use the concepts of flow along a line and linearization to explore the stabilization problem of maintaining a desired constant speed $u = u_0$. We will compare the use of both *open loop control* and *closed loop control*, as described in Example 1.1.

Starting with open loop control, suppose we performed a series of careful measurements and found that when conditions are perfect, we can set the thrust to

$$T = cu_0|u_0|,$$

so that at steady state (when $\dot{u} = 0$), $\lim_{t\to\infty} u = u_{\mathrm{ss}} \to u_0$. By plotting the flow of (2.7), we can see that it is globally stable (Fig. 2.4). However, we have assumed that the conditions under which the boat is operating are perfect, meaning that there

are no external disturbances acting on the system and that we have perfectly characterized the drag-related coefficient c.

Suppose now that there is a very slowly varying external disturbance (for example the boat could be moving into a strong headwind), which we will characterize as a constant d_e. Additionally, assume that there is an uncertainty in the drag-related coefficient, δc. Then, the open loop thrust will be set to

$$T = (c+\delta c)u_0|u_0| = cu_0|u_0| + \delta cu_0|u_0|$$

and (2.7) becomes

$$m\dot{u} = -cu|u| + cu_0|u_0| + \delta cu_0|u_0| + d_e = -cu|u| + cu_0|u_0| + d, \qquad (2.8)$$

where d is a constant that combines the external disturbances and the uncertainty of the drag-related coefficient. Now, we can solve (2.8) to see that when $\dot{u} = 0$ and $u > 0$, the steady state speed is

$$\lim_{t\to\infty} u = u_{\text{ss}} = \sqrt{u_0^2 + d/c}.$$

Owing to d, there will always be a speed error and with open loop control there is no way to mitigate it (see Fig. 2.4).

Now, let's explore the use of closed loop control and see if we can improve the speed error caused by d. As explained in 1.1, closed loop control involves measuring the output of the system and feeding it back to a controller, which produces a signal related to the error between the desired output and the measured output. Here, we want to control the system so that the steady state speed error $(u_{\text{ss}} - u_0)$ is small. Let the thrust commanded by the closed loop controller be

$$T = cu_0|u_0| + \delta cu_0|u_0| - k_p(u-u_0), \qquad (2.9)$$

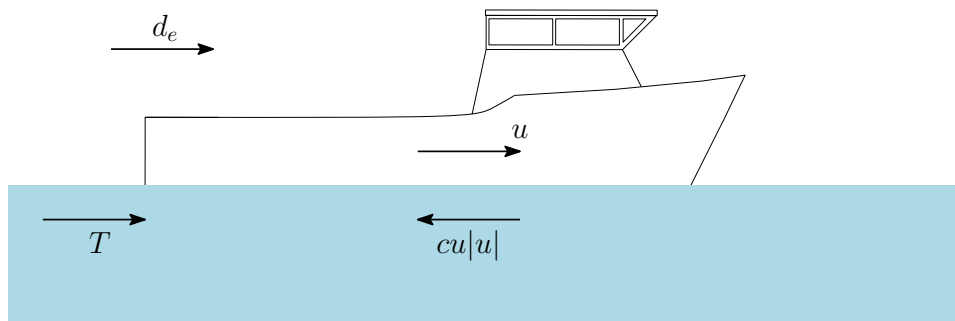

Fig. 2.3 Speed control of a boat: u is speed, T is propeller thrust, $cu|u|$ is hull drag and d_e is a constant external disturbance force, such as wind drag.

where $k_p > 0$ is a controller design parameter called a proportional gain, that can be used to tune the response of the system. Substituting this into (2.7) and accounting for the constant external disturbance d_e, (2.7) becomes

$$\begin{aligned} m\dot{u} &= -cu|u| + cu_0|u_0| + \delta cu_0|u_0| - k_p(u-u_0) + d_e, \\ &= -cu|u| + cu_0|u_0| - k_p(u-u_0) + d. \end{aligned} \tag{2.10}$$

For $u > 0$, the term $u|u|$ can be linearized about the desired operating speed u_0, to get

$$u|u| = u^2 = u_0^2 + 2u_0(u-u_0) + (u-u_0)^2 \approx u_0^2 + 2u_0(u-u_0).$$

Substituting this into (2.10) gives

$$\begin{aligned} m\dot{u} &\approx -c[u_0^2 + 2u_0(u-u_0)] + cu_0^2 - k_p(u-u_0) + d, \\ &\approx -(k_p + 2cu_0)(u-u_0) + d. \end{aligned} \tag{2.11}$$

Now at steady state ($\dot{u} = 0$), we can solve for u to get

$$\lim_{t\to\infty} u = u_{\rm ss} = u_0 + \frac{d}{k_p + 2cu_0} = u_0 + \left[\frac{d_e + \delta cu_0|u_0|}{k_p + 2cu_0}\right]. \tag{2.12}$$

The advantage of closed loop control, is that the effects of the external disturbance d_e and parameter uncertainty δc can be now mitigated by picking a large value of k_p, such that

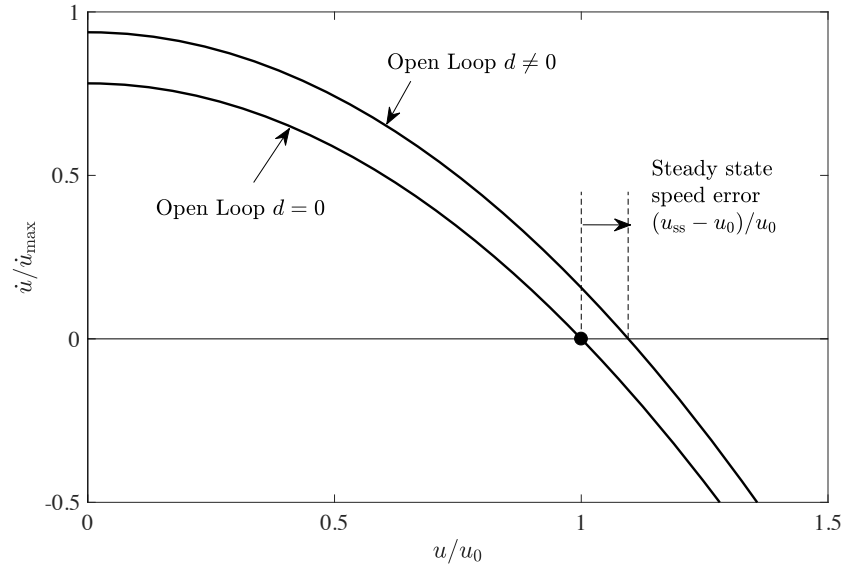

Fig. 2.4 Open loop speed control without ($d = 0$) and with the effects of external disturbances and parameter uncertainty ($d = cu_0|u_0|/5$).

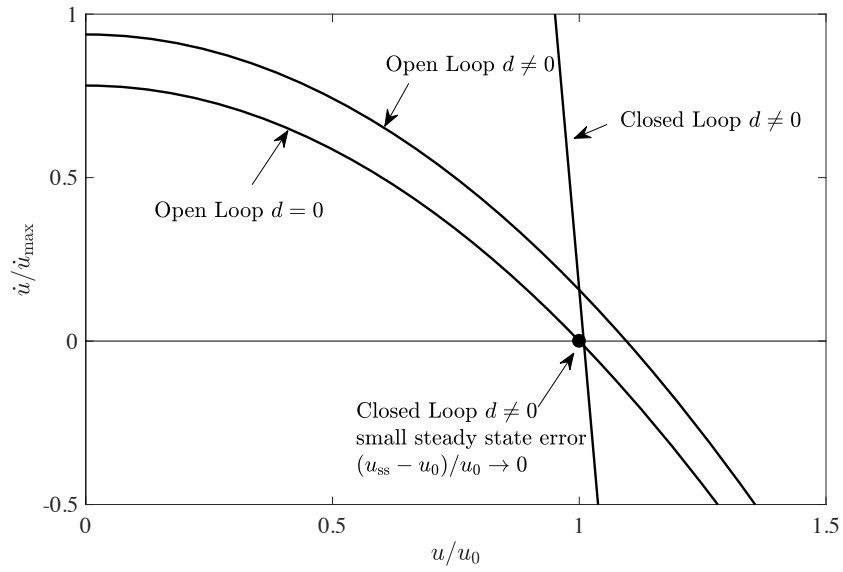

Fig. 2.5 Performance comparison of closed loop speed control and open loop speed control with external disturbances and parameter uncertainty ($d = cu_0|u_0|/5$).

$$\left[\frac{d_e + \delta c u_0 |u_0|}{k_p + 2cu_0}\right] \to 0$$

and $u_{ss} \to u_0$. Closed loop control with $k_p/(2cu_0) = 10$ and $d = cu_0|u_0|/5$ is shown in Fig. 2.5. It can be seen that the system is stable and that the effect of k_p is to make the slope of $\dot{u}$ very large near $u/u_0 = 1$ so that the system is strongly driven towards $u = u_0$. Of course k_p cannot be made infinitely large. From (2.9), it can be seen that the thrust commanded from the controller is proportional to k_p. From a practical standpoint, there are limits to how much thrust a propeller can generate (*actuator saturation*) and how quickly it can respond to changes in the commanded thrust (*actuator rate limits*). As will be discussed later, it can be important to take these actuator limits into account during controller design and stability analysis to ensure that the controller behaves as expected.

□

2.4 Phase plane analysis

The qualitative nature of nonlinear systems is important for understanding some of the key concepts of stability. As mentioned above, the graphical representations in phase space of systems with $n > 2$ can be computationally and geometrically complex. Here we will restrict our attention to second order $n = 2$ systems, where there are two state variables $\mathbf{x} \in \mathbb{R}^2$.

As with our study of one dimensional systems in Section 2.3, we can think of a differential equation

$$\dot{\mathbf{x}} = \mathbf{f}(\mathbf{x}), \tag{2.13}$$

as representing a vector field that describes the velocity of an imaginary particle in the state space of the system. The velocity tells us how $\mathbf{x}$ changes.

For two dimensional dynamical systems, each state corresponds to a point in the plane and $\mathbf{f}(\mathbf{x})$ is a vector representing the velocity of that state. We can plot these vectors on a grid of points in the $\mathbf{x} = \{x_1, x_2\}$ plane, which is often called the *state space* or *phase plane* of the system, to obtain a visual image of the dynamics of the system. The points where the velocities are zero are of particular interest, as they represent the *stationary points* or *fixed points* points: if we start at such a state, we stay at that state. These points are essentially equilibrium points.

A *phase portrait*, or *phase plane diagram* can be constructed by plotting the flow of the vector field corresponding to (2.13). For a given initial condition, this flow is the solution of the differential equation in the phase plane. By plotting the solutions corresponding to different initial conditions, we obtain a phase portrait.

The phase portrait can provide insight into the dynamics of a system. For example, we can see whether all trajectories tend to a single point as time increases, or whether there are more complicated behaviors. However, the phase portrait cannot tell us the rate of change of the states (although, this can be inferred from the length of the vectors in a plot of the vector field).

2.4.1 Linear 2D Stability Analysis

More generally, suppose that we have a nonlinear system (2.13) that has an equilibrium point at $\mathbf{x}_e$. As in Section 2.3.1, let η be a small perturbation away from $\mathbf{x}_e$, such that $\eta(t) = \mathbf{x}(t) - \mathbf{x}_e$. Thus, $\dot{\eta} = \dot{\mathbf{x}} = \mathbf{f}(\mathbf{x}) = \mathbf{f}(\mathbf{x}_e + \eta)$. Computing the Taylor series expansion of the vector field, as in Section 2.3.1, we obtain

$$\dot{\eta} = \mathbf{f}(\mathbf{x}_e) + \left.\frac{\partial \mathbf{f}}{\partial \mathbf{x}}\right|_{\mathbf{x}_e} \eta + O(\eta^T \eta). \tag{2.14}$$

Since $\mathbf{f}(\mathbf{x}_e) = 0$, we write the *linear approximation*, or the *linearization* at $\mathbf{x}_e$, to the original nonlinear system as

$$\frac{\mathrm{d}\eta}{\mathrm{d}t} = \mathbf{A}\eta, \quad \text{where} \quad \mathbf{A} := \left.\frac{\partial \mathbf{f}}{\partial \mathbf{x}}\right|_{\mathbf{x}_e}. \tag{2.15}$$

The fact that a linear model can be used to study the behavior of a nonlinear system near an equilirium point is a powerful one. For example, we could use a local linear approximation of a nonlinear system to design a feedback law that keeps the system near a desired operating point. Also note that, in general, a given dynamical system may have zero, one or more fixed points $\mathbf{x}_e$. When using a phase portrait to analyze

the stability of a system it is important to know where these fixed points are located within the phase plane.

2.4.2 Classification of Linear 2D Systems

Here we will classify the possible phase portraits that can occur for a given $\mathbf{A}$ in (2.15). The simplest trajectories in the phase plane correspond to straight line trajectories. To start we will seek trajectories of the form

$$\mathbf{x}(t) = e^{\lambda t}\mathbf{v}, \tag{2.16}$$

where $\mathbf{v} \neq 0$ is a fixed vector to be determined and λ is a growth rate, also to be determined. If such solutions exist, they correspond to exponential motion along the line spanned by the vector $\mathbf{v}$.

To find the conditions on $\mathbf{v}$ and λ, we substitute $\mathbf{x}(t) = e^{\lambda t}\mathbf{v}$ into $\dot{\mathbf{x}} = \mathbf{A}\mathbf{x}$, and obtain $\lambda e^{\lambda t}\mathbf{v} = e^{\lambda t}\mathbf{A}\mathbf{v}$. Cancelling the nonzero scalar factor $e^{\lambda t}$ yields

$$\mathbf{A}\mathbf{v} = \lambda\mathbf{v}. \tag{2.17}$$

The desired straight line solutions exist if $\mathbf{v}$ is an *eigenvector* of $\mathbf{A}$ with corresponding *eigenvalue* λ.

In general, the eigenvalues of a matrix $\mathbf{A}$ are given by the *characteristic equation* $\det(\mathbf{A} - \lambda\mathbf{1}) = 0$, where $\mathbf{1}$ is the identity matrix. If we define the elements of $\mathbf{A}$, as

$$\mathbf{A} = \begin{bmatrix} a & b \\ c & d \end{bmatrix},$$

the characteristic equation becomes

$$\det(\mathbf{A} - \lambda\mathbf{1}) = \begin{vmatrix} a-\lambda & b \\ c & d-\lambda \end{vmatrix}.$$

Expanding the determinant gives

$$\lambda^2 + \tau\lambda + \Delta = 0, \tag{2.18}$$

where

$$\begin{aligned} \tau &= -\text{trace}(\mathbf{A}) = -(a+d), \\ \Delta &= \det(\mathbf{A}) \qquad ad - bc. \end{aligned} \tag{2.19}$$

Then the solutions of the quadratic characteristic equation (2.18) are

$$\lambda_1 = \frac{-\tau + \sqrt{\tau^2 - 4\Delta}}{2}, \quad \lambda_2 = \frac{-\tau - \sqrt{\tau^2 - 4\Delta}}{2}. \tag{2.20}$$

Thus, the eigenvalues only depend on the trace and the determinant of $\mathbf{A}$.

Most often, the eigenvalues are distinct, i.e. $\lambda_1 \neq \lambda_2$. In this case, the corresponding eigenvectors $\mathbf{v}_1$ and $\mathbf{v}_2$ are linearly independent and span the phase plane (Fig. 2.6). Any initial condition $\mathbf{x}_0$ can be written as a linear combination of eigenvectors, $\mathbf{x}_0 = c_1\mathbf{v}_1 + c_2\mathbf{v}_2$, where $\mathbf{v}_1$ is the solution to (2.17) when $\lambda = \lambda_1$ and $\mathbf{v}_2$ is the solution to (2.17) when $\lambda = \lambda_2$. Thus, the general solution for $\mathbf{x}(t)$ is

$$\mathbf{x} = c_1 e^{\lambda_1 t}\mathbf{v}_1 + c_2 e^{\lambda_2 t}\mathbf{v}_2. \tag{2.21}$$

The reason that this is the general solution is because it is a linear combination of

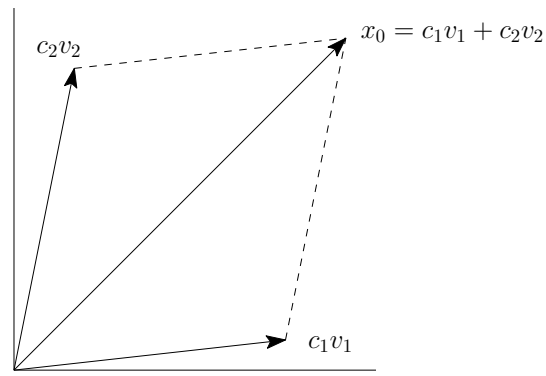

Fig. 2.6 Eigenvectors in the phase plane.

the solutions to, (2.15), which can be written as $\dot{\mathbf{x}} = \mathbf{A}\mathbf{x}$ and because it satisfies the initial condition $\mathbf{x}(0) = \mathbf{x}_0$, and so by the existence and uniqueness of solutions, it is the only solution.

The types of critical points are classified on the chart shown in Fig. 2.7a: nodes, foci, or saddles can be obtained [9]. The type of trajectory depends on the location of a point defined by τ and Δ on the τ—Δ chart. When both of the eigenvalues are real, either nodes or saddles are produced. When the eigenvalues are complex, a focus is obtained. When τ and Δ fall on one of the boundaries indicated by a Roman numeral on the τ—Δ chart, one of the following degenerate critical points exists (Fig. 2.7b):

Case I) For this case $\Delta = 0$. The critical point is known as a node-saddle. The eigenvalues are given by $\lambda_1 = 0$ and $\lambda_2 = \tau$, and the general solution has the form

$$\mathbf{x}(t) = c_1\mathbf{v}_1 + c_2\mathbf{v}_2 e^{\lambda_2 t}$$

so that there will be a line of equilibrium points generated by $\mathbf{v}_1$ and an infinite number of straight line trajectories parallel to $\mathbf{v}_2$.

Case II) This case occurs when the eigenvalues are repeated, $\lambda_1 = \lambda_2$. If the eigenvectors $\mathbf{v}_1$ and $\mathbf{v}_2$ are independent, the critical point is a star node and the trajectories are straight lines. If the eigenvectors are not linearly independent, the critical point is a node-focus with the solution trajectories approaching/leaving the critical point tangent to the single eigenvector.

Case III) The eigenvalues are purely imaginary, so that the trajectories correspond to elliptical orbits about the critical point.

Case IV) Finally, in the last degenerate case both $\tau = 0$ and $\Delta = 0$. This corresponds to a system of either the form

$$\begin{bmatrix} \dot{x}_1 \\ \dot{x}_2 \end{bmatrix} = \begin{bmatrix} 0 & a \\ 0 & 0 \end{bmatrix},$$

or

$$\begin{bmatrix} \dot{x}_1 \\ \dot{x}_2 \end{bmatrix} = \begin{bmatrix} 0 & 0 \\ b & 0 \end{bmatrix},$$

where a and b are constants. In this case, the trajectories are either straight lines parallel to the x_1-axis given by $x_1 = ac_1t + c_2$, $x_2 = c_1$, or straight lines parallel to the x_2-axis given by $x_1 = c_1$, $x_2 = bc_1t + c_2$.

Note that the when the eigenvectors are nonorthogonal, the resulting pattern of trajectories is skewed in the directions of the eigenvectors, when compared to the same case (node or saddle) with orthogonal eigenvectors (Fig. 2.8).

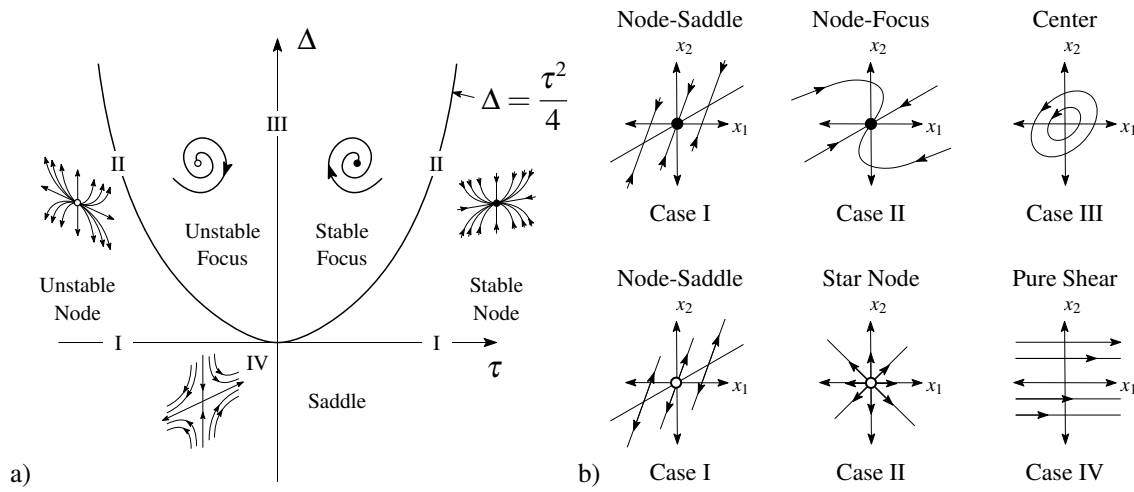

Fig. 2.7 a) Classification of critical points on the τ—Δ chart. b) Degenerate Critical points located on the boundaries I, II, and III and origin IV of the the τ—Δ chart.

Example 2.4. Consider the pitch stability of an autonomous underwater vehicle (AUV) moving at a constant speed U (Fig. 2.9). Here we will explore the use of active control to stabilize the system. When the pitch angle is non-zero, a hydrodynamically-induced pitching moment, called the *Munk moment*, can arise [3]. If we assume the motion is confined to the x_b–z_b plane of the vehicle and neglect drag, the dynamic equation of motion for pitch is

$$(I_y - M_{\dot{q}})\ddot{\theta} = (I_y - M_{\dot{q}})\dot{q} = -U^2 \sin\theta \cos\theta (Z_{\dot{w}} - X_{\dot{u}}). \tag{2.22}$$

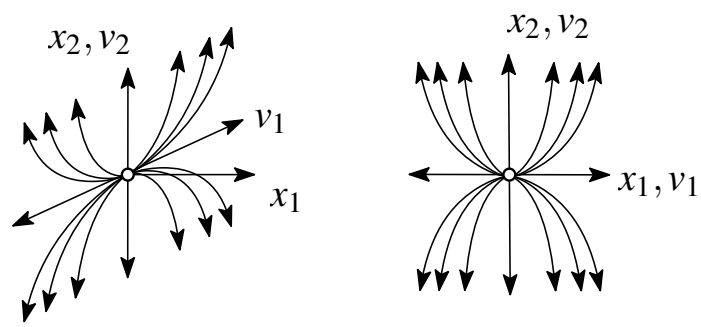

Fig. 2.8 A node with nonorthogonal eigenvectors v_1, v_2 (left) and orthogonal eigenvectors (right).

Here I_y and $M_{\dot{q}}$ are the rigid-body mass and added mass moments of inertia about the sway axis of the AUV. The pitch angle is θ, $q = \dot{\theta}$ is the pitch rate, and $Z_{\dot{w}}$ and $X_{\dot{u}}$ are the added mass in the heave (z_b) and surge (x_b) directions, respectively. Note that the added mass coefficients are defined such that $M_{\dot{q}} < 0$, $Z_{\dot{w}}$, and $X_{\dot{u}}$, in accordance to the 1950 SNAME nomenclature for the dynamic modeling of underwater vehicles [11]. For long slender vehicles that have a large length-to-diameter ratio, like a typical AUV, $|Z_{\dot{w}}| \gg |X_{\dot{u}}|$. An examination of (2.22) shows that when $0 < \theta < \pi/2$ the Munk moment is proportional to the difference between the added mass coefficients $Z_{\dot{w}}$ and $X_{\dot{u}}$ and that it is a destabilizing moment. Positive pitch angles cause a positive pitching moment, which increases the pitch angle, which causes a larger pitching moment. Similarly, a negative pitch angle, produces a negative pitching moment, which makes the pitch angle more negative, and so on. From a qualitative perspective, we might expect the condition $\theta = 0$ to be unstable and the condition $\theta = \pi/2$ to be stable. First consider the uncontrolled system. We can rewrite (2.22)

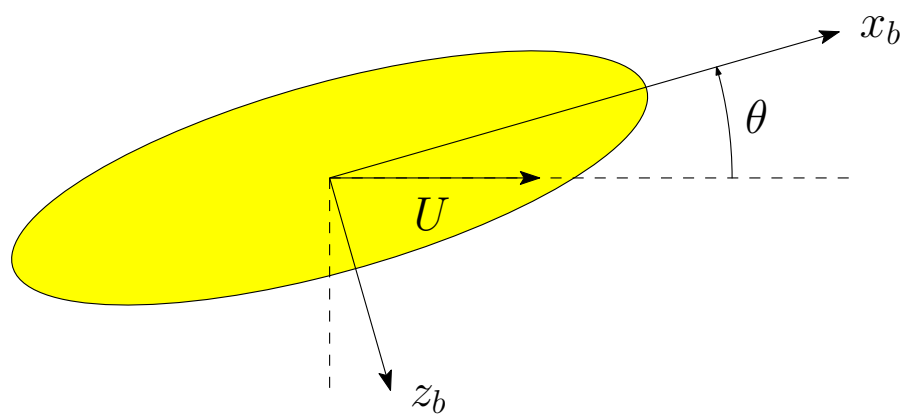

Fig. 2.9 Pitch stability of an AUV-shaped body moving at speed U. The pitch angle is θ.

in vector form. Let

$$\mathbf{x} = \begin{pmatrix} \theta \\ q \end{pmatrix},$$

then

$$\dot{\mathbf{x}} = \begin{pmatrix} q \\ -\dfrac{U^2}{2}\sin(2\theta)\left[\dfrac{Z_{\dot{w}} - X_{\dot{u}}}{I_y - M_{\dot{q}}}\right] \end{pmatrix} = \mathbf{f}, \tag{2.23}$$

where we have used the trigonometric relation $\sin(2\theta) = 2\sin\theta\cos\theta$. From (2.23), it can be seen that the critical points, where $\dot{\mathbf{x}} = 0$, are located at

$$\mathbf{x}_{e1} = \begin{pmatrix} n\pi \\ 0 \end{pmatrix} \quad \text{and} \quad \mathbf{x}_{e2} = \begin{pmatrix} (2m+1)\pi/2 \\ 0 \end{pmatrix},$$

where $n = \pm\{0,1,2,\ldots\}$ and $m = \pm\{0,1,2,\ldots\}$ are integers.

We can start by examining the critical point $\mathbf{x}_{e1}$ for $n = 0$. The matrix $\mathbf{A}$ in (2.15) can be found by taking the *Jacobian* of $\mathbf{f}$ at $\mathbf{x}_{e1}$

$$\mathbf{A} := \left.\frac{\partial \mathbf{f}}{\partial \mathbf{x}}\right|_{\mathbf{x}_{e1}} = \left.\begin{pmatrix} \dfrac{\partial f_1}{\partial x_1} & \dfrac{\partial f_1}{\partial x_2} \\ \dfrac{\partial f_2}{\partial x_1} & \dfrac{\partial f_2}{\partial x_2} \end{pmatrix}\right|_{\mathbf{x}_{e1}} = \left.\begin{pmatrix} 0 & 1 \\ -U^2\cos(2\theta)\left[\dfrac{Z_{\dot{w}} - X_{\dot{u}}}{I_y - M_{\dot{q}}}\right] & 0 \end{pmatrix}\right|_{\mathbf{x}_{e1}=(0,0)}$$

$$= \begin{pmatrix} 0 & 1 \\ -U^2\left[\dfrac{Z_{\dot{w}} - X_{\dot{u}}}{I_y - M_{\dot{q}}}\right] & 0 \end{pmatrix}.$$

Using (2.19), we can solve for τ and Δ to get $\tau = 0$ and

$$\Delta = U^2\left[\frac{Z_{\dot{w}} - X_{\dot{u}}}{I_y - M_{\dot{q}}}\right] < 0,$$

(recall that $M_{\dot{q}} < 0$, $Z_{\dot{w}}$, and $X_{\dot{u}}$). Based on Fig. 2.7a, we expect $\mathbf{x}_{e1}$ to be a saddle point.

Using (2.20), we see that the eigenvalues are

$$\lambda_{1,2} = \pm U\sqrt{-\frac{Z_{\dot{w}} - X_{\dot{u}}}{I_y - M_{\dot{q}}}}.$$

The eigenvectors must satisfy (2.17), which can be rewritten as $(\mathbf{A} - \lambda\mathbf{1})\mathbf{v} = 0$, for each eigenvalue. Thus, we can solve the system

$$\begin{pmatrix} -\lambda & 1 \\ -U^2\left[\dfrac{Z_{\dot{w}}-X_{\dot{u}}}{I_y-M_{\dot{q}}}\right] & -\lambda \end{pmatrix}\begin{pmatrix} v_1 \\ v_2 \end{pmatrix} = \begin{pmatrix} 0 \\ 0 \end{pmatrix},$$

to find the eigenvector corresponding to each eigenvalue. Let λ_1 be the positive eigenvector, which gives

$$\begin{pmatrix} -U\sqrt{-\dfrac{Z_{\dot{w}}-X_{\dot{u}}}{I_y-M_{\dot{q}}}} & 1 \\ -U^2\left[\dfrac{Z_{\dot{w}}-X_{\dot{u}}}{I_y-M_{\dot{q}}}\right] & -U\sqrt{-\dfrac{Z_{\dot{w}}-X_{\dot{u}}}{I_y-M_{\dot{q}}}} \end{pmatrix}\begin{pmatrix} v_1 \\ v_2 \end{pmatrix} = \begin{pmatrix} 0 \\ 0 \end{pmatrix}.$$

A non–trivial solution for $\mathbf{v}_1$ is

$$\mathbf{v}_1 = \begin{pmatrix} v_1 \\ v_2 \end{pmatrix} = \begin{pmatrix} 1 \\ U\sqrt{-\dfrac{Z_{\dot{w}}-X_{\dot{u}}}{I_y-M_{\dot{q}}}} \end{pmatrix}.$$

Similarly, a solution for the other, negative, eigenvector λ_2 is

$$\mathbf{v}_2 = \begin{pmatrix} v_1 \\ v_2 \end{pmatrix} = \begin{pmatrix} 1 \\ -U\sqrt{-\dfrac{Z_{\dot{w}}-X_{\dot{u}}}{I_y-M_{\dot{q}}}} \end{pmatrix}.$$

Thus, the solution to the system (2.23) linearized near $\mathbf{x}_{e1} = [0,0]^T$ is

$$\mathbf{x} = c_1\begin{pmatrix} 1 \\ U\sqrt{-\dfrac{Z_{\dot{w}}-X_{\dot{u}}}{I_y-M_{\dot{q}}}} \end{pmatrix} e^{\lambda_1 t} + c_2\begin{pmatrix} 1 \\ -U\sqrt{-\dfrac{Z_{\dot{w}}-X_{\dot{u}}}{I_y-M_{\dot{q}}}} \end{pmatrix} e^{\lambda_2 t},$$

where c_1 and c_2 are constants, which can be determined using an initial condition for $\mathbf{x}$. As the part of the solution containing λ_1 is unstable in time, trajectories depart from the critical point along the corresponding eigenvector $\mathbf{v}_1$; the converse is true for trajectories lying along the eigenvector corresponding to λ_2, $\mathbf{v}_2$.

Turning now to the critical point corresponding to $m = 0$, $\mathbf{x}_{e2} = [0, \pi/2]^T$, we repeat the process above to find that $\tau = 0$ and

$$\Delta = -U^2\left[\frac{Z_{\dot{w}}-X_{\dot{u}}}{I_y-M_{\dot{q}}}\right] > 0.$$

Based on Figs. 2.7a–b, we expect $\mathbf{x}_{e2}$ to be a center. Using (2.20), we see that the eigenvalues are

$$\lambda_{1,2} = \pm jU\sqrt{-\frac{Z_{\dot{w}} - X_{\dot{u}}}{I_y - M_{\dot{q}}}},$$

where $j = \sqrt{-1}$ is the imaginary number. A phase diagram of the unstabilized AUV is shown in Fig. 2.10. Owing to the trajectory associated with the positive eigenvalue of the saddle point at $\theta = 0$, the pitch angle is unstable there. Small pitch disturbances or initial conditions with $|\theta| \neq 0$ will grow and exhibit oscillations about $\theta = \pm\pi/2$. The critical point topology is periodic and repeats at other values of n and m. Note that the phase portrait is actually best represented on a cylindrical manifold, and simply wraps around the manifold for the other values of n and m.

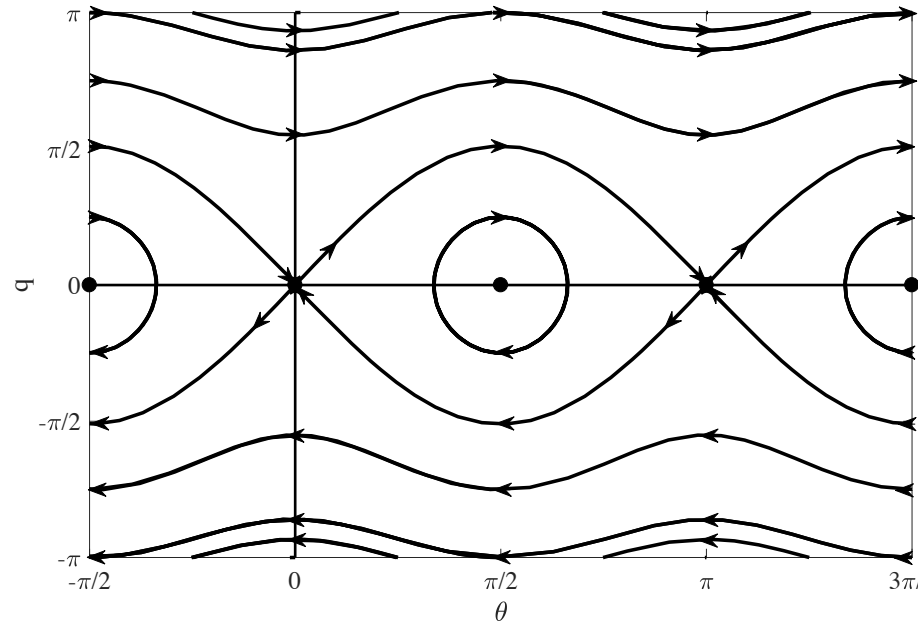

Fig. 2.10 Pitch angle phase portrait for a AUV with unstabilized Munk moment. Critical points at $(\theta, q) = (n\pi, 0)$, integer $n = \pm\{0, 1, 2, 3, \ldots\}$ are saddle points and critical points at $(\theta, q) = ((2m+1)\pi/2, 0)$, integer $m = \pm\{0, 1, 2, 3, \ldots\}$ are centers.

At low speeds, passive design features can be used to create a stabilizing moment when $\theta \neq 0$. For example, by designing the AUV so that its center of buoyancy lies along the z_b axis directly above its center of gravity a stabilizing moment is passively generated when $\theta \neq 0$. Another design strategy is to use fins near the stern of the vehicle. The lift forces generated by the fins when $\theta \neq 0$ will passively generate moments that stabilize the vehicle towards $\theta = 0$. The pitch stability obtained with these approaches is explored in Problem **??**.

Next, we will explore the use of active control to stabilize pitch. As shown in Problem 1.3, a vectored thruster can be used to generate pitch moments by pivoting the propeller so that its thrust has a component in the z_b direction at the stern (see Fig. 2.11). First, we will explore the use of a controller that produces a restoring

torque $-k_p\theta$, which is linearly proportional to the pitch angle, where $k_p > 0$ is a constant. This type of a controller is known as a proportional (P) controller. A P-controller tends to act like a spring that pushes the response of a system towards a desired equilibrium.

The governing equation for pitch becomes

$$(I_y - M_{\dot{q}})\ddot{\theta} = (I_y - M_{\dot{q}})\dot{q} = -U^2 \sin\theta\cos\theta(Z_{\dot{w}} - X_{\dot{u}}) - k_p\theta,$$

so that

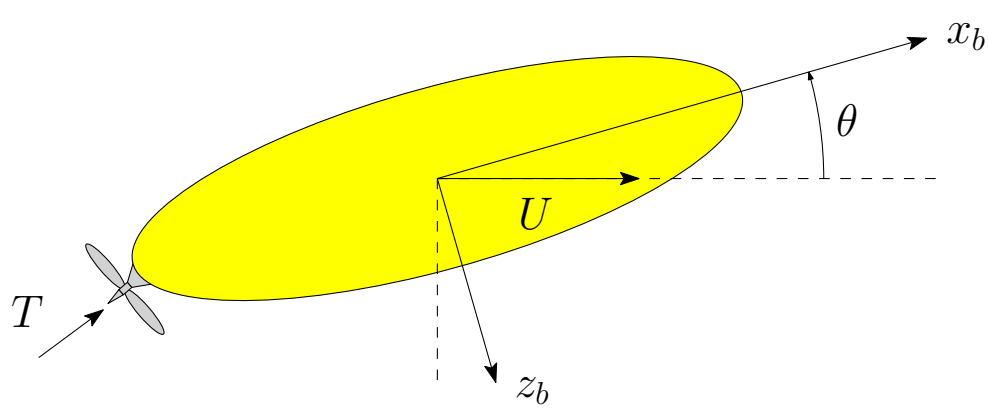

Fig. 2.11 Pivoting the propeller to generate a pitching moment by tilting the thrust vector.

$$\dot{\mathbf{x}} = \begin{pmatrix} q \\ -\dfrac{U^2}{2}\sin(2\theta)\left[\dfrac{Z_{\dot{w}} - X_{\dot{u}}}{I_y - M_{\dot{q}}}\right] - \dfrac{k_p}{I_y - M_{\dot{q}}}\theta \end{pmatrix} = \mathbf{f}. \tag{2.24}$$

An inspection of (2.24) shows that an equilibrium point of the system will be at $\mathbf{x}_e = [0,0]^T$. The Jacobian evaluated at this critical point is

$$\mathbf{A} = \begin{pmatrix} 0 & 1 \\ -U^2\left[\dfrac{Z_{\dot{w}} - X_{\dot{u}}}{I_y - M_{\dot{q}}}\right] - \dfrac{k_p}{I_y - M_{\dot{q}}} & 0 \end{pmatrix}$$

so that $\tau = 0$ and

$$\Delta = \frac{k_p + U^2(Z_{\dot{w}} - X_{\dot{u}})}{I_y - M_{\dot{q}}}.$$

From Fig. 2.7a, it can be seen that to prevent the phase portrait from containing saddle points (which have unstable trajectories), we require $\Delta > 0$, so that

$$k_p > -U^2(Z_{\dot{w}} - X_{\dot{u}}). \tag{2.25}$$

For small angles, when $\sin(\theta) \approx \theta$, a second possible critical point could be located at

$$\mathbf{x} = \begin{bmatrix} \cos^{-1}\left(-\dfrac{k_p}{U^2(Z_{\dot{w}} - X_{\dot{u}})}\right) \\ 0 \end{bmatrix}.$$

However, the constraint (2.25) would make the argument of the $\cos^{-1}(\cdot)$ term above would be greater than 1, so that a second critical point cannot exist.

As shown in Fig. 2.12, the phase portrait will consist of a center at $\theta = 0$. If an initial pitch angle is small, the vehicle will exhibit small pitch oscillations within this small initial angle. While this behavior is an improvement over the uncontrolled case, it could be unsuitable for many applications, such as using the AUV to acoustically map a section of the seafloor using a sidescan sonar. The pitch angle time

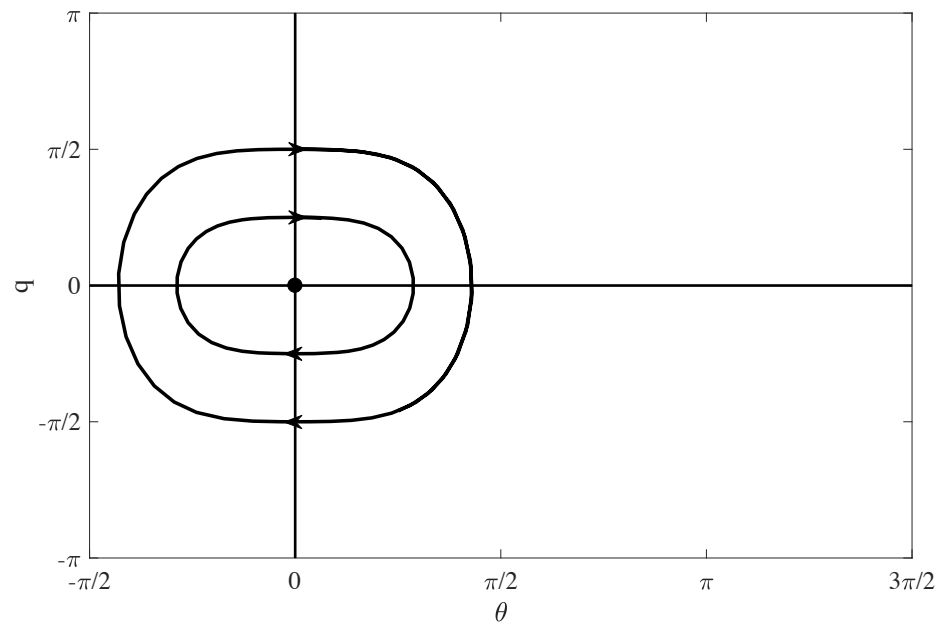

Fig. 2.12 Pitch angle phase portrait for an AUV with unstable Munk moment counteracted by a proportional controller. Critical points occur at $(\theta, q) = (n\pi, 0)$ and are centers. For initial pitch angles $0 < |\theta| < \pi/2$ solution trajectories oscillate around $\theta = 0$.

response for a typical AUV with an initial (large) pitch angle of $\pi/3$ is shown in Fig. 2.13. As can be seen, the oscillations persist and would likely be unsuitable in practice.

Lastly, we explore the effectiveness of adding a second feedback term, which is linearly proportional to the derivative of the pitch angle, to the existing controller so that the total control signal is $-k_p\theta - k_d\dot{\theta}$. This type of a controller is known as a proportional derivative controller. The derivative term tends to act like a damping

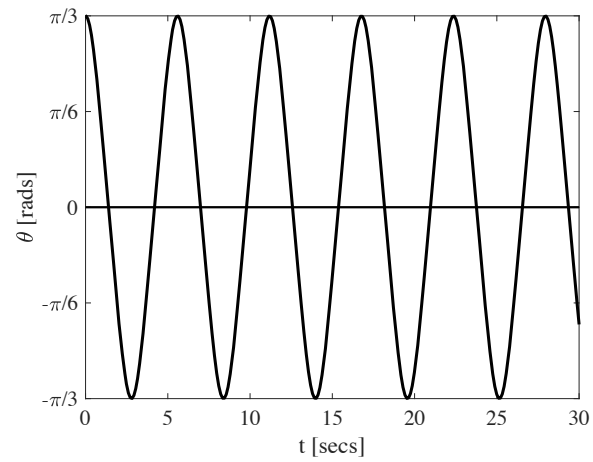

Fig. 2.13 Example pitch angle time response for an AUV with unstable Munk moment counteracted by a proportional controller.

factor. In a situation such as this, it could help to reduce the persistent oscillations observed when using only the k_p term.

The governing equation for pitch becomes

$$(I_y - M_{\dot{q}})\ddot{\theta} = (I_y - M_{\dot{q}})\dot{q} = -U^2 \sin\theta\cos\theta(Z_{\dot{w}} - X_{\dot{u}}) - k_p\theta - k_d\dot{\theta},$$

so that

$$\dot{\mathbf{x}} = \begin{pmatrix} q \\ -\dfrac{U^2}{2}\sin(2\theta)\left[\dfrac{Z_{\dot{w}} - X_{\dot{u}}}{I_y - M_{\dot{q}}}\right] - \dfrac{k_p\theta + k_d\dot{\theta}}{I_y - M_{\dot{q}}} \end{pmatrix} = \mathbf{f}. \tag{2.26}$$

An inspection of (2.26) shows that the equilibrium point of the system will be at $\mathbf{x}_e = [0,0]^T$. The Jacobian matrix at this critical point is

$$\mathbf{A} = \begin{pmatrix} 0 & 1 \\ -U^2\left[\dfrac{Z_{\dot{w}} - X_{\dot{u}}}{I_y - M_{\dot{q}}}\right] - \dfrac{k_p}{I_y - M_{\dot{q}}} & -\dfrac{k_d}{I_y - M_{\dot{q}}} \end{pmatrix}$$

so that

$$\tau = \frac{k_d}{I_y - M_{\dot{q}}}$$

and

$$\Delta = \frac{k_p + U^2(Z_{\dot{w}} - X_{\dot{u}})}{I_y - M_{\dot{q}}}.$$

From Fig. 2.7a, it can be seen that if we select $k_d > 0$ and

$$k_p > -U^2(Z_{\dot{w}} - X_{\dot{u}})$$

the phase portrait will be a stable focus centered at the critical point $\mathbf{x}_e = [0,0]^T$ (see Fig. 2.14). The effect of the additional feedback term is to dampen the pitch oscillations.

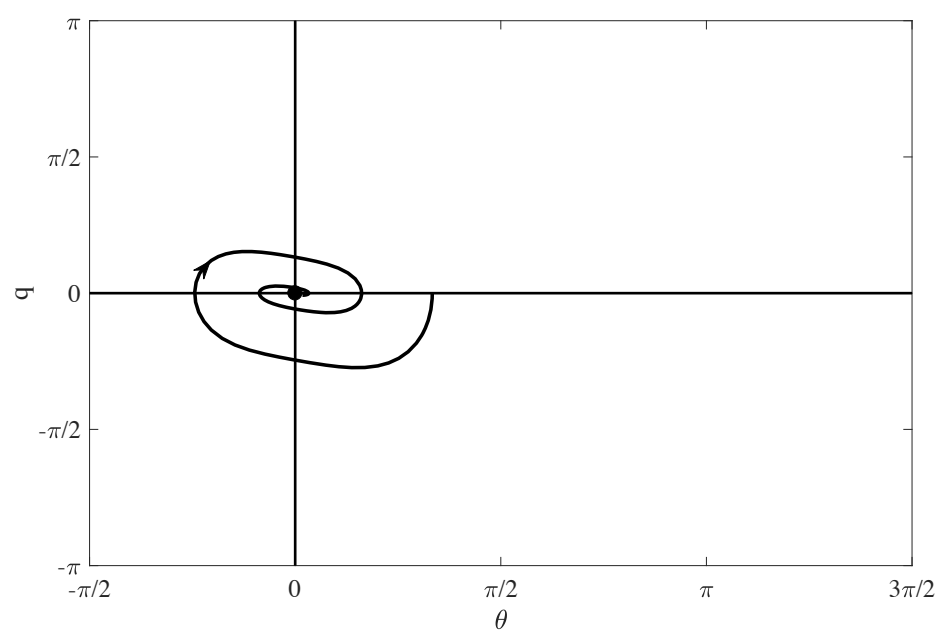

Fig. 2.14 Pitch angle phase portrait for an AUV with unstable Munk moment counteracted by a proportional-derivative controller. Critical points occur at $(\theta, q) = (n\pi, 0)$ and are stable foci. For initial pitch angles $0 < |\theta| < \pi/2$ solution trajectories approach $\theta = 0$.

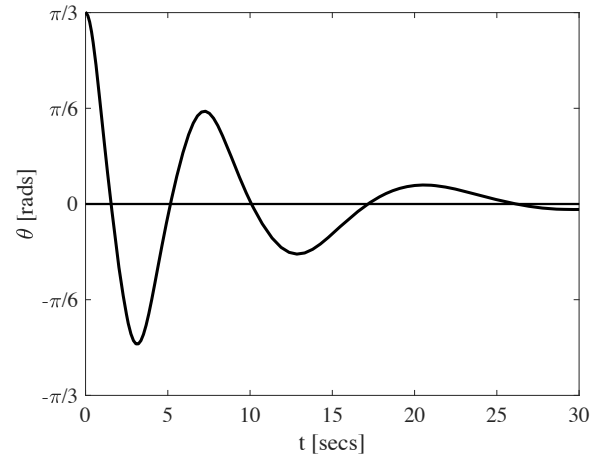

Fig. 2.15 Example pitch angle time response for an AUV with unstable Munk moment counteracted by a proportional-derivative controller. For the values of k_p and k_d selected the pitch oscillations are damped out after a couple of oscillation cycles.

Note that the main objective of this example is to demonstrate the link between stability and control. As will be seen in the following chapters, many methods exist for designing automatic controllers in order to meet specfic performance objectives. The controller gains k_p and k_d are design parameters that could be tuned to produce a desired performance. In this example their values have only been selected to explore some basic stability concepts.

□

2.5 Introduction of Nonlinear Stability Methods

The techniques required for the stability analysis of nonlinear systems are quite different from those of linear systems, as some of the familiar tools, such as Laplace and Fourier Transforms, cannot be easily applied. The analysis of controlled nonlinear systems is most often performed using concepts of Lyapunov stability. We will mostly focus on Lyapunov's Direct (Second) Method, which can be used to show the boundedness of a closed loop system, even when the system has no equilibrium points.

Generally, nonlinear stability theory consists of three main components: 1) *definitions* of the different kinds of stability, which provide insight into the behavior of a closed loop system; 2) the different *conditions* that a closed loop system must satisfy in order to possess a certain type of stability; and 3) *criteria* that enable one to check whether or not the required conditions hold, without having to explicitly compute the solution of the differential equations describing the time evolution of the closed loop system. The *conditions* and *criteria* required to establish the various types of stability are often presented in the form of mathematical theorems.

An engineering student encountering this approach of using a series of mathematical definitions and theorems to characterize the nonlinear stability of a system for the first time may find it daunting. However, a significant advantage of the approach is that such a series of mathematical statements can be used somewhat like a lookup table, allowing one to fairly quickly isolate and characterize the stability properties of a given nonlinear system by matching the criteria and conditions to the specific problem at hand.

2.6 Stability of Time–Invariant Nonlinear Systems

Here we restrict our attention to time–invariant systems of the form

$$\begin{aligned} \dot{\mathbf{x}} &= \mathbf{f}(\mathbf{x},\mathbf{u}), \quad \mathbf{x} \in \mathbb{R}^n, \mathbf{u} \in \mathbb{R}^p \\ \mathbf{y} &= \mathbf{h}(\mathbf{x}), \quad \mathbf{y} \in \mathbb{R}^q, \end{aligned} \tag{2.27}$$

where $\mathbf{f}$ is a locally Lipschitz continuous function. Generally, the control input will be a function of the state so that $\mathbf{u} = \mathbf{u}(\mathbf{x})$ and one could also simply write $\dot{\mathbf{x}} = \mathbf{f}(\mathbf{x})$ to represent the dynamics of a closed loop system. In this text, the notation $\mathbf{f} : \mathbb{R}^n \to \mathbb{R}^n$ will be used to indicate that the vector function $\mathbf{f}$ maps an n-dimensional vector, i.e. $\mathbf{x} \in \mathbb{R}^n$, into another n-dimensional vector, in this case $\dot{\mathbf{x}} \in \mathbb{R}^n$.

Definition 2.1 (Lipschitz Continuous). A function $\mathbf{f}(\mathbf{x})$ is defined to be *Lipschitz continuous* if for some constant $c > 0$,

$$\|\mathbf{f}(\mathbf{x}_2) - \mathbf{f}(\mathbf{x}_1)\| < c\|\mathbf{x}_2 - \mathbf{x}_1\|, \quad \forall\, \mathbf{x}_1, \mathbf{x}_2,$$

where $\| \bullet \|$ denotes the 2-norm (Euclidean norm) of a vector. A sufficient condition for a function to be Lipshitz continuous is that its Jacobian

$$\mathbf{A} = \frac{\partial \mathbf{f}}{\partial \mathbf{x}}$$

is uniformly bounded for all $\mathbf{x}$. When a function is *Lipschitz Continuous*, sometimes we simply say "the function is *Lipschitz*". The constant c is referred to as the *Lipschitz constant*.

The existence and uniqueness of a solution to (2.27) is guaranteed when $\mathbf{f}(\mathbf{x}, \mathbf{u})$ is Lipschitz. The following sections summarize the basics of nonlinear stability. Excellent, detailed references on these topics, which focus on control theory, include [10, 7, 8].

2.6.1 Stability Definitions

Recall from Section 2.4 that equilibrium points correspond to fixed points, or stationary points, where $\dot{\mathbf{x}} = 0$.

Definition 2.2 (Equilibrium Point). A state $\mathbf{x}_e \in \mathbb{R}^n$ is an *equilibrium point* of system (2.27), if $\mathbf{x}(t) = \mathbf{x}_e$ for all t.

Therefore, at an equilibrium point

$$\dot{\mathbf{x}}(t) = \mathbf{f}(\mathbf{x}_e) = 0.$$

Remark 2.1. A linear system, e.g. $\dot{\mathbf{x}} = \mathbf{A}\mathbf{x}$ has an isolated equilibrium point at $\mathbf{x} = 0$ if all of the eigenvalues of $\mathbf{A}$ are nonzero (i.e. $\det(\mathbf{A}) \neq 0$). Otherwise, a linear system will have a continuum of equilibrium points. On the other hand, a nonlinear system can have multiple isolated equilibrium points.

Remark 2.2. For the purposes of conducting stability analysis for control design, it is often more convenient to identify a new variable $\tilde{\mathbf{x}} := (\mathbf{x} - \mathbf{x}_e)$ when $\mathbf{x}_e \neq 0$ and to rewrite the dynamics of the system (2.27) in the form

$$\dot{\tilde{\mathbf{x}}} = \mathbf{f}(\tilde{\mathbf{x}}), \quad \tilde{\mathbf{x}} \in \mathbb{R}^n \tag{2.28}$$

so that the equilibrium point is $\tilde{\mathbf{x}} = 0$, than it is to use the original system (2.27) and state variable $\mathbf{x}$. In this context the new state variable $\tilde{\mathbf{x}}$ is very often also simply referred to as the *state*. Alternatively, it is also sometimes called the *state error*, an *error surface*, or for tracking problems, i.e. when $\mathbf{x}_e = \mathbf{x}_e(t)$, as the *tracking error*.

Definition 2.3 (Stable). Let the parameters δ and ε, where $\varepsilon > \delta > 0$, be the radii of two concentric n-dimensional "balls" (e.g. circles in two dimensions, spheres in three dimensions, etc.), where n is the dimension of the state $\mathbf{x} \in \mathbb{R}^n$. In the sense of Lyapuov, a point $\mathbf{x}_e$ is a *stable equilibrium point* of the system (2.28), if for a given initial condition $\mathbf{x}_0 = \mathbf{x}(t_0)$, where $\|\mathbf{x}_0 - \mathbf{x}_e\| = \|\tilde{\mathbf{x}}_0\| < \delta$, the solution trajectories of $\mathbf{x}(t)$ remain in the region ε for all $t > t_0$, i.e. such that $\|\mathbf{x}(t) - \mathbf{x}_e\| = \|\tilde{\mathbf{x}}\| < \varepsilon$, $\forall t > t_0$ (Fig. 2.16). In this case we will also simply say that the system (2.28) is *stable*.

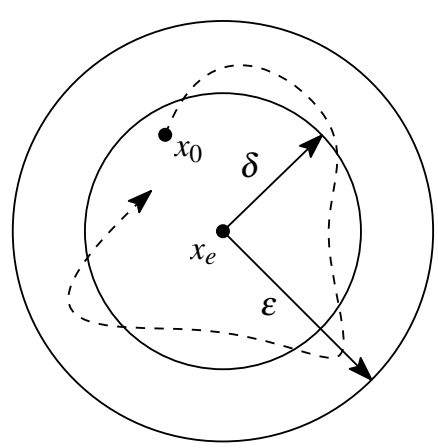

Fig. 2.16 A graphical illustration of Lyapunov stability. The dashed curve represents the trajectory of $\mathbf{x}(t)$ when $\tilde{\mathbf{x}}$ is a solution of (2.28).

Definition 2.4 (Unstable). A system is *unstable* if it is not stable.

Note that stability is a property of equilibrium points. A given system may have both stable and unstable equilibrium points. Also note that the Lyapunov definition of the stability of an equilibrium point does not require the solution trajectories of the system to converge to $\mathbf{x}_e$.

Definition 2.5 (Asymptotically Stable). The system (2.28) is *asymptotically stable* if, 1) it is stable and 2) the solution trajectories of the state $\mathbf{x}$ converge to $\mathbf{x}_e$ for initial conditions sufficiently close to $\mathbf{x}_e$, i.e. a δ can be chosen so that

$$\|\mathbf{x}_0 - \mathbf{x}_e\| = \|\tilde{\mathbf{x}}_0\| < \delta \Rightarrow \lim_{t\to\infty} \|\mathbf{x}(t) - \mathbf{x}_e\| = \lim_{t\to\infty} \|\tilde{\mathbf{x}}(t)\| = 0.$$

Definition 2.6 (Region of Attraction). The set of all initial states $\mathbf{x}_0 = \mathbf{x}(t_0)$ from which the trajectories converge to an equilibrium point $\mathbf{x}_e$ is called the equilibrium point's *region of attraction*.

Definition 2.7 (Compact Set). A set of real numbers $\mathcal{B}_\delta = \{\mathbf{x} \in \mathbb{R} : \|\mathbf{x}\| \leq \delta\}$ is a *compact set* if every sequence in $\mathcal{B}_\delta$ (such as a time dependent trajectory) has a sub-sequence that converges to an element, which is again contained in $\mathcal{B}_\delta$.

Definition 2.8 (Locally Attractive). If the system is not necessarily stable, but has the property that all solutions with initial conditions $\mathbf{x}_0 = \mathbf{x}(t_0)$ that lie within some radius δ of the equilibrium point $\mathbf{x}_e$ converge to $\mathbf{x}_e$, then it is *locally attractive*. If $\|\mathbf{x}_0 - \mathbf{x}_e\| = \|\tilde{\mathbf{x}}_0\| > \delta$, the solution trajectories of $\mathbf{x}(t)$ might not converge to $\mathbf{x}_e$, or even diverge.

Definition 2.9 (Exponentially Stable). An equilibrium point $\mathbf{x}_e$ is *exponentially stable* if there exist positive constants δ, k and λ such that all solutions of (2.28) with $\|\mathbf{x}_0 - \mathbf{x}_e\| = \|\tilde{\mathbf{x}}_0\| \leq \delta$ satisfy the inequality

$$\|\tilde{\mathbf{x}}(t)\| \leq k\|\tilde{\mathbf{x}}_0\|e^{-\lambda t}, \quad \forall t \geq t_0. \tag{2.29}$$

The constant λ in (2.29) is often referred to as the *convergence rate*.

Remark 2.3. Exponential stability implies asymptotic stability, whereas asymptotic stability does not imply exponential stability.

Definition 2.10 (Globally Attractive). Generally, the asymptotic stability and exponential stability of an equilibrium point are local properties of a system. However, when the region of attraction of an equilibrium point includes the entire space of $\mathbb{R}^n$, i.e. $\delta \to \infty$, the equilibrium point is *globally attractive*.

Definition 2.11 (Globally Asymptotically Stable). An equilibrium point $\mathbf{x}_e$ is *globally asymptotically stable* (GAS) if it is stable and the state $\mathbf{x}(t)$ converges to $\mathbf{x}_e$ ($\lim_{t\to\infty} \|\tilde{\mathbf{x}}\| \to 0$) from any initial state $\mathbf{x}_0$.

Definition 2.12 (Globally Exponentially Stable). An equilibrium point $\mathbf{x}_e$ is *globally exponentially stable* (GES) if the state $\mathbf{x}(t)$ converges exponentially to $\mathbf{x}_e$ ($\lim_{t\to\infty} \|\tilde{\mathbf{x}}\| \to 0$) from any initial state $\mathbf{x}_0$.

2.6.2 Lyapunov's Second (Direct) Method

Consider the nonlinear time-invariant system (2.28),

$$\dot{\tilde{\mathbf{x}}} = \mathbf{f}(\tilde{\mathbf{x}}), \quad (\mathbf{x} - \mathbf{x}_e) := \tilde{\mathbf{x}} \in \mathbb{R}^n$$

with a local equilibrium point $\mathbf{x}_e$, such that $\mathbf{f}(\tilde{\mathbf{x}} = 0) = 0$.

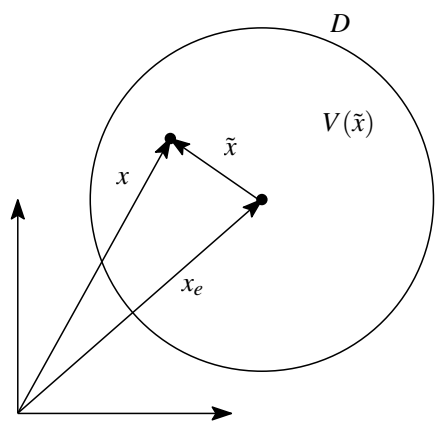

Fig. 2.17 A spherical neighborhood D of $\mathbf{x}_e$.

Definition 2.13 (Class $\mathbb{C}^k$ functions). Let k be a non-negative integer, i.e. $k \in \mathbb{Z}_{\geq 0}$. A function V is a class $\mathbb{C}^k$ function if the derivatives $V', V'', \ldots, V^{(k)}$ exist and are continuous.

In the following definitions we will take $V : \mathbb{R}^n \to \mathbb{R}$ be a $\mathbb{C}^1$ function and explore the properties of V within a neighborhood D of $\mathbf{x}_e$ (Fig. 2.17).

Definition 2.14 (Positive Definite). The function $V(\tilde{\mathbf{x}})$ is *positive definite* (PD) in D if a) $V(\tilde{\mathbf{x}} = 0) = 0$ and b) $V(\tilde{\mathbf{x}}) > 0$ for all $\mathbf{x} \in D$, $\mathbf{x} \neq \mathbf{x}_e$.

Definition 2.15 (Negative Definite). Similarly, the function $V(\tilde{\mathbf{x}})$ is *negative definite* (ND) in D if a) $V(\tilde{\mathbf{x}} = 0) = 0$ and b) $V(\tilde{\mathbf{x}}) < 0$ for all $\mathbf{x} \in D$, $\mathbf{x} \neq \mathbf{x}_e$.

Definition 2.16 (Positive Semidefinite). The function $V(\tilde{\mathbf{x}})$ is *positive semidefinite* (PSD) in D if a) $V(\tilde{\mathbf{x}} = 0) = 0$ and b) $V(\tilde{\mathbf{x}}) \geq 0$ for all $\mathbf{x} \in D$, $\mathbf{x} \neq \mathbf{x}_e$. I.e. $V(\tilde{\mathbf{x}})$ can be zero at points other than $\mathbf{x} = \mathbf{x}_e$.

Definition 2.17 (Negative Semidefinite). The function $V(\tilde{\mathbf{x}})$ is *negative semidefinite* (NSD) in D if a) $V(\tilde{\mathbf{x}} = 0) = 0$ and b) $V(\tilde{\mathbf{x}}) \leq 0$ for all $\mathbf{x} \in D$, $\mathbf{x} \neq \mathbf{x}_e$. Here, $V(\tilde{\mathbf{x}})$ can be zero at points other than $\mathbf{x} = \mathbf{x}_e$.

Definition 2.18 (Radially Unbounded). The function $V(\tilde{\mathbf{x}})$ is *radially unbounded* if

$$\lim_{\|\mathbf{x}\| \to \infty} V(\tilde{\mathbf{x}}) \to \infty.$$

A *Lyapunov function* V, is an energy-like function that can be used to determine the stability of a system. If we can find a non-negative function that always decreases along trajectories of the system, we can conclude that the minimum of the function is a locally stable equilibrium point. Let $V(\tilde{\mathbf{x}})$ be radially unbounded and assume that there exist two class $\mathcal{K}_\infty$ functions α_1, α_2, such that V satisfies

$$\alpha_1(\|\tilde{\mathbf{x}}\|) \leq V(\tilde{\mathbf{x}}) \leq \alpha_2(\|\tilde{\mathbf{x}}\|), \quad \forall \mathbf{x} \in D. \tag{2.30}$$

For time-invariant systems $V(\tilde{\mathbf{x}})$ is an implicit function of time t, such that the time derivative of V, $\dot{V}$ is given by the derivative of V along the solution trajectories of (2.28), i.e.,

$$\frac{\mathrm{d}V}{\mathrm{d}t} = \dot{V}(\tilde{\mathbf{x}}) = \frac{\partial V}{\partial \tilde{\mathbf{x}}}\mathbf{f}(\tilde{\mathbf{x}}). \tag{2.31}$$

The main result of Lyapunov's stability theory is expressed in the following statement.

Theorem 2.1 (Lyapunov Stability). *Suppose that there exists a* $\mathbb{C}^1$ *function* $V : \mathbb{R}^n \to \mathbb{R}$ *which is positive definite in a neighborhood of an equilibrium point* $\mathbf{x}_e$*,*

$$V(\tilde{\mathbf{x}}) > 0, \forall \mathbf{x} \in D, \mathbf{x} \neq \mathbf{x}_e, \tag{2.32}$$

whose time derivative along solutions of the system (2.28) is negative semidefinite, i.e.

$$\dot{V}(\tilde{\mathbf{x}}) \leq 0, \quad \forall \mathbf{x} \in D, \tag{2.33}$$

then the system (2.28) is stable. If the time derivative of $V(\tilde{\mathbf{x}})$ *is negative definite,*

$$\dot{V}(\tilde{\mathbf{x}}) < 0, \quad \forall \mathbf{x} \in D, \mathbf{x} \neq \mathbf{x}_e, \tag{2.34}$$

then (2.28) is asymptotically stable. If, in the latter case, $V(\tilde{\mathbf{x}})$ *is also radially unbounded, then (2.28) is globally asymptotically stable.*

Definition 2.19 (Weak Lyapunov Function). The function V is a *weak Lyapunov function* if it satisfies (2.33).

Definition 2.20 (Lyapunov Function). The function V is a *Lyapunov function* if it satisfies(2.34).

Theorem 2.1 is valid when V is merely continuous and not necessarily $\mathbb{C}^1$, provided that (2.33) and (2.34) are replaced by the conditions that V is nonincreasing and strictly decreasing along nonzero solutions, respectively.

A graphical illustration of Theorem 2.1 is shown in Fig. 2.18. Assume (2.33) holds. Consider the ball around the equilibrium point of radius $\varepsilon > 0$. Pick a positive number $b < \min_{\|\tilde{\mathbf{x}}\|=\varepsilon} V(\tilde{\mathbf{x}})$. Let δ be the radius of some ball around $\mathbf{x}_e$, which is inside the set $\{\mathbf{x} : V(\tilde{\mathbf{x}}) \leq b\}$. Since $\dot{V}(\tilde{\mathbf{x}}) \leq 0$, V is nonincreasing along the solution trajectories of $\tilde{\mathbf{x}}(t)$. Each solution starting in the smaller ball of radius δ satisfies $V(\tilde{\mathbf{x}}(t)) \leq b$, hence it remains inside the bigger ball of radius ε.

From a geometric standpoint, the stronger condition that $\dot{V}(\tilde{\mathbf{x}}) < 0$ in (2.34) means that solution trajectories move to smaller and smaller values of V (Fig. 2.19). If $\dot{V}(\tilde{\mathbf{x}})$ is negative definite, $\lim_{t\to\infty} \|\tilde{\mathbf{x}}\| \to 0$ so that

$$\lim_{t\to\infty} \mathbf{x}(t) \to \mathbf{x}_e.$$

Definition 2.21 (Candidate Lyapunov Functions). In order to apply Theorem 2.1 we must first choose a suitable Lyapunov function. In many cases a suitable function

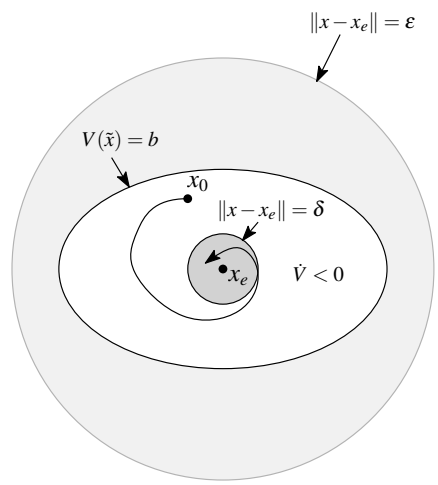

Fig. 2.18 Lyapunov stability.

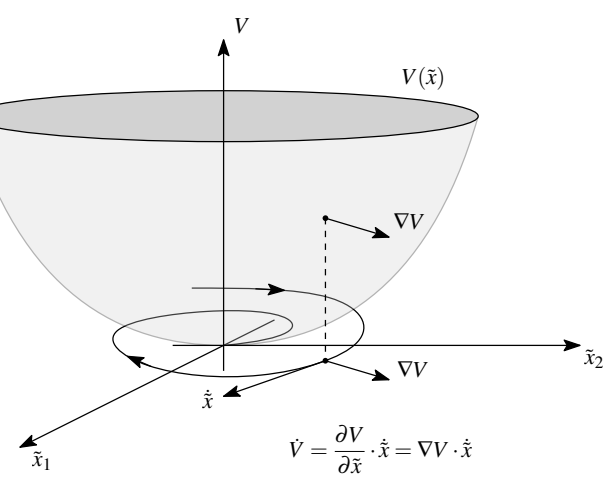

Fig. 2.19 Geometric illustration of Lyapunov's Stability Theorem for time-invariant systems. When $\dot{V}(\tilde{\mathbf{x}}) < 0$, $V(\tilde{\mathbf{x}})$ decreases along the trajectory.

is not known ahead of time and one may try one or more different possible functions. In such cases, the trial functions are often referred to as *Candidate Lyapunov Functions*.

Using Theorem 2.1 to examine the stability of a system in the form of (2.27) about an equilibrium point $\mathbf{x}_e$ is generally performed as follows:

1) A change of coordinates from $\mathbf{x}(t)$ to $\tilde{\mathbf{x}} := (\mathbf{x}(t) - \mathbf{x}_e)$ is used to transform the system (2.27) into the form (2.28).
2) A candidate Lyapunov function $V(\tilde{\mathbf{x}})$, which is PD in a neighborhood of $\tilde{\mathbf{x}} = 0$, is identified.
3) The time derivative of the candidate Lyapunov function, $\dot{V}(\tilde{\mathbf{x}})$, is computed along system trajectories and checked to see if it is NSD or ND in the same neighborhood.

4) If the candidate Lyapunov function satisfies (2.32) and, either (2.33) or (2.34), $\tilde{\mathbf{x}} = 0$ is a stable equilibrium point. Otherwise, no conclusion can be drawn about the equilibrium point's stability. However, the process can be repeated to see if a different candidate Lyapunov function will work.

Remark 2.4. If a Lyapunov function $V(\tilde{\mathbf{x}})$ is known to be admitted by a system, additional functions can be generated using the relation

$$\bar{V}(\tilde{\mathbf{x}}) = \beta V^{\gamma}(\tilde{\mathbf{x}}), \quad \beta > 0, \gamma > 1. \tag{2.35}$$

2.7 Invariant Set Theorem

In many cases, it is preferable to know that the state of a marine vehicle can be controlled so that the closed loop control system approaches a desired equilibrium point, i.e. that the closed loop system is asymptotically stable. However, for nonlinear systems, it is sometimes difficult to find a positive definite function $V(\tilde{\mathbf{x}})$ whose derivative is strictly negative definite. When applying Lyapunov's Direct Method, one may find that the time derivative of the chosen Lyapunov function $\dot{V}(\tilde{\mathbf{x}})$ is only negative semi definite (2.33), rather than negative definite. When this happens, one can infer the stability of the closed loop system, but not the asymptotic stability of the system to $\tilde{\mathbf{x}} = 0$. In such a situation, the Invariant Set Theorem may allow one to analyze the stability of the system in more detail, without needing to identify a different Lyapunov function. Thus, the Invariant Set Theorem enables us to conclude the asymptotic stability of an equilibrium point under less restrictive conditions, which are easier to construct.

Definition 2.22 (Invariant Set). A set of states, which form a subset $G \subseteq \mathbb{R}^n$ of the state space, is an *invariant set* of (2.28) if any trajectory starting from a point $\tilde{\mathbf{x}}_0 \in G$ always stays in G, i.e. if $\tilde{\mathbf{x}}(t) \in G$ for all $t \geq t_0$.

Recall that a state $\mathbf{x}_e \in \mathbb{R}^n$ is an equilibrium point, if $\mathbf{x}(t) = \mathbf{x}_e$ for all t. Thus, the notion of an invariant set is essentially a generalization of the concept of an equilibrium point. Examples of invariant sets include equilibrium points and the basin of attraction of an asymptotically stable equilibrium point.

The basic idea is that if $V(\tilde{\mathbf{x}}) > 0$ (PD) and $\dot{V}(\tilde{\mathbf{x}}) \leq 0$ (NSD) in a neighborhood of $\tilde{\mathbf{x}} = 0$, then if $V(\tilde{\mathbf{x}})$ approaches a limit value, then $\dot{V}(\tilde{\mathbf{x}}) \to 0$, at least under certain conditions.

Theorem 2.2 (LaSalle's Local Invariant Set Theorem). *For time-invariant system* (2.28)*, assume there exists a function $V(\tilde{\mathbf{x}}) \in \mathbb{C}^1$ such that*

1. *the region $\Omega_\alpha = \{\tilde{\mathbf{x}} \in \mathbb{R}^n : V(\tilde{\mathbf{x}}) \leq \alpha\}$ is bounded for some $\alpha > 0$, and*
2. *$\dot{V}(\tilde{\mathbf{x}}) \leq 0$ in α*

and define P, the set of points in Ω_α where $\dot{V}(\tilde{\mathbf{x}}) = 0$, then any trajectory of the system that starts in Ω_α asymptotically approaches M, the largest invariant set

contained in P. A geometric interpretation of LaSalle's Invariant Set Theorem is illustrated in Fig. 2.20.

An immediate consequence of the theorem is the following corollary.

Corollary 2.1 (Local Asymptotic Stability). *An equilibrium point of* (2.28) *is locally asymptotically stable if there exists a function* $V(\tilde{\mathbf{x}}) \in C^1$ *such that*

1) $V(\tilde{\mathbf{x}})$ *is PD in a set D that contains* $\tilde{\mathbf{x}} = 0$,
2) $\dot{V}(\tilde{\mathbf{x}})$ *is NSD in the same set,*
3) the largest invariant set M in P (the subset of D where $\dot{V} = 0$*) consists of* $\tilde{\mathbf{x}} = 0$ *only.*

In addition, if the largest region defined by $V(\tilde{\mathbf{x}}) \leq \alpha$, $\alpha > 0$ *and contained in D is denoted as* Ω_α, Ω_α *is an estimate of the basin of attraction of* $\tilde{\mathbf{x}} = 0$.

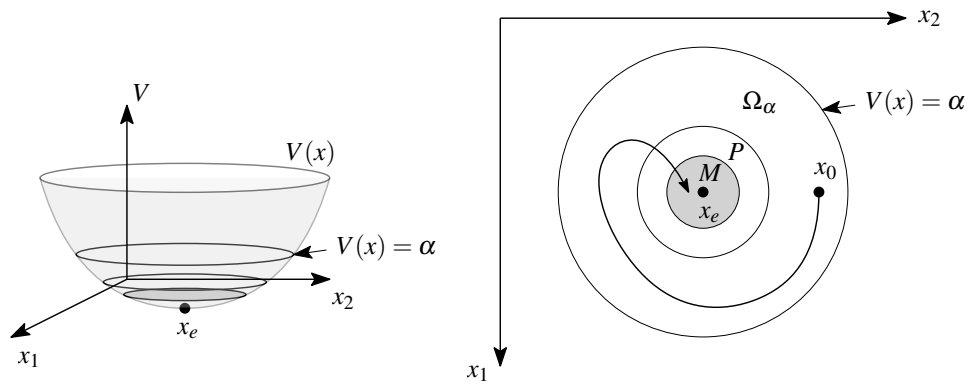

Fig. 2.20 Geometric interpretation of Theorem 2.2 drawn in the original state coordinates of (2.27).

Theorem 2.3 (LaSalle's Global Invariant Set Theorem). *For system* (2.28)*, assume there exists a function* $V(\tilde{\mathbf{x}}) \in \mathbb{C}^1$ *such that*

1. $V(\tilde{\mathbf{x}})$ *is radially unbounded, and*
2. $\dot{V}(\tilde{\mathbf{x}}) \leq 0$ *in* $\mathbb{R}^n$,

then any trajectory of the system asymptotically approaches the set M, the largest invariant set in P, the set of points of Ω_α *where* $\dot{V} = 0$.

Remark 2.5. The radial unboundedness of $V(\tilde{\mathbf{x}})$ guarantees that any region $\Omega_\alpha = \{\tilde{\mathbf{x}} \in \mathbb{R}^n : V(\tilde{\mathbf{x}}) < \alpha\}$, $\alpha > 0$ is bounded.

There is also an additional corollary associated with Theorem 2.3.

Corollary 2.2 (Global Asymptotic Stability). *An equilibrium point* $\tilde{\mathbf{x}} = 0$ *of* (2.28) *is globally asymptotically stable if there exists a function* $V(\tilde{\mathbf{x}}) \in C^1$ *such that*

1. $V(\tilde{\mathbf{x}})$ *is PD in any neighborhood of* $\tilde{\mathbf{x}} = 0$ *and radially unbounded*

2. *$\dot{V}(\tilde{\mathbf{x}})$ is NSD in any neighborhood of $\tilde{\mathbf{x}} = 0$*
3. *the largest invariant set M in P (the subset of D where $\dot{V} = 0$) consists of $\tilde{\mathbf{x}} = 0$ only.*

Example 2.5. Let's re-examine the problem in Example 2.4 of using a vectored thruster to actively stabilize the pitch moment of an AUV (Fig. 2.21). Previously, we explored the stability of the linearized system, i.e. its linear stability, near a desired pitch angle of $\theta = 0$. Here, we will explore the nonlinear stability of the system. Adding a control input u to (2.23), the closed loop equations of motion can be written in the simplified form

$$\begin{aligned} \dot{\theta} &= q, \\ \dot{q} &= c_0 \sin(2\theta) + u, \end{aligned} \tag{2.36}$$

where θ is the pitch angle, $q := \dot{\theta}$ is the pitch rate and $c_0 > 0$ is a constant. When $u = 0$, the open loop system has an unstable equilibrium point at $\theta = q = 0$. A nonlinear controller of the form

$$u = -c_0 \sin(2\theta) - k_p\theta - k_d q, \tag{2.37}$$

where the constants $k_p > 0$ and $k_d > 0$ are control gains, can be used to stabilize the AUV at the origin $\tilde{\mathbf{x}} = [\theta \ q]^T = [0 \ 0]^T$. To explore the closed loop stability of the system, consider the following candidate Lyapunov function

$$V(\tilde{\mathbf{x}}) = \frac{1}{2}\theta^2 + \frac{1}{2}q^2.$$

Note that since $\theta = \theta + 2\pi k$, where $k \in \mathbb{Z}$ is an integer, this Lyapunov function is not radially unbounded. Thus, we will explore local stability for $|\theta| < \pi/2$.

The time derivative of $V(\mathbf{x})$ is

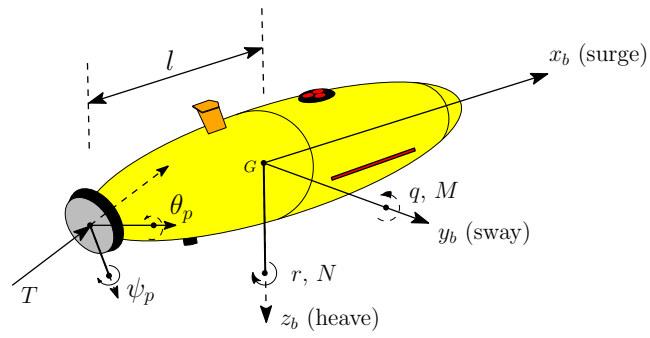

Fig. 2.21 Use of a vectored thruster to control the pitch of an AUV.

$$\begin{aligned}\dot{V} &= \theta\dot{\theta} + q\dot{q} \\ &= q\theta + q[c_0 \sin(2\theta) + u] \\ &= -(k_p - 1)\theta q - k_d q^2.\end{aligned} \tag{2.38}$$

The second term of (2.38), $-k_d q^2$, is ND for any q. However, for $k_p > 1$ first term becomes positive when either $\theta < 0$ and $q > 0$, or $\theta > 0$ and $q < 0$. One could select $k_p = 1$, but it would then not be necessary for both $q = 0$ and $\theta = 0$ to obtain $\dot{V} = 0$. Therefore, we cannot conclude the asymptotic stability of the closed loop system to $\tilde{\mathbf{x}} = 0$ using Theorem 2.1 (recall the similar situation encountered in Example **??** above).

However, if we restrict our analysis to a small neighborhood of the origin Ω_α, $\alpha \ll \pi/2$, then we can define

$$M := \{(\theta, q) \in \Omega_\alpha : q = 0\}$$

and we can compute the largest invariant set inside M. For a trajectory to remain in this set we must have $q = 0$, $\forall t$ and hence $\dot{q} = 0$ as well. Using (2.36) and (2.37) we can write the closed loop dynamics of the system as

$$\begin{aligned}\dot{\theta} &= q \\ \dot{q} &= -k_p\theta - k_d q,\end{aligned} \tag{2.39}$$

so that $q(t) = 0$ and $\dot{q} = 0$ also implies both $\theta = 0$ and $\dot{\theta} = 0$. Hence the largest invariant set inside M is $\tilde{\mathbf{x}} = [\theta\ q]^T = [0\ 0]^T$ and we can use LaSalle's Local Invariant Set Theorem (Theorem 2.2) to conclude that the origin is locally asymptotically stable. A phase portrait of the closed loop system response is shown in Fig. 2.22 for $k_p = 2$, $k_d = 2$ and $\mathbf{x}_0 = [\pi\ \ 0]^T$.

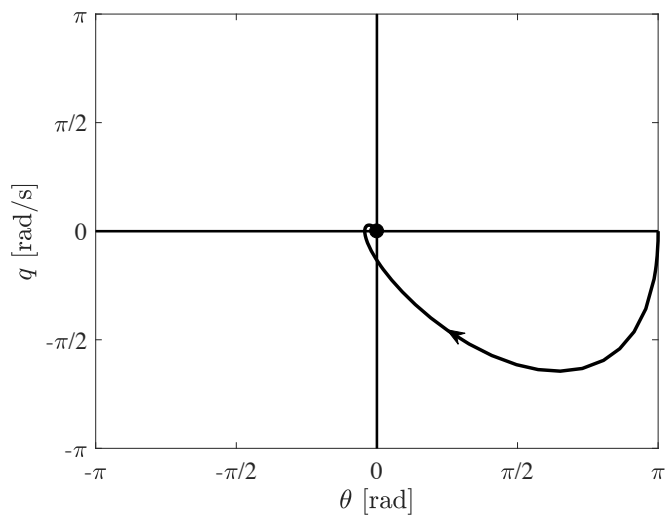

Fig. 2.22 Phase portrait of the stabilized AUV pitch angle.

□

2.8 Stability of Time–Varying Nonlinear Systems

Invariant set theorems only apply to time-invariant systems. Additional tools must be used to determine the stability of a nonlinear time-varying system, e.g. an adaptive control system, or a system with exogenous (externally-generated) time-varying disturbances.

Consider a time-varying differential equation of the form

$$\dot{\mathbf{x}} = \mathbf{f}(\mathbf{x}, t), \tag{2.40}$$

where $\mathbf{f} : \mathbb{R}^n \times \mathbb{R}_{\geq 0} \to \mathbb{R}^n$.

Remark 2.6. As with nonlinear time-invariant systems, it is often convenient when performing stability analyses of time-varying nonlinear systems to transform the coordinates of the state variable $\tilde{\mathbf{x}} := (\mathbf{x} - \mathbf{x}_e)$ and to rewrite the dynamics of the system (2.40) in the form

$$\dot{\tilde{\mathbf{x}}} = \mathbf{f}(\tilde{\mathbf{x}}, t), \quad \tilde{\mathbf{x}} \in \mathbb{R}^n \tag{2.41}$$

so that the equilibrium point of the transformed system is $\tilde{\mathbf{x}} = 0$.

Assumption 2.1. Let the origin $\tilde{\mathbf{x}} = 0$ be an equilibrium point of system (2.41) *and $D \subseteq \mathbb{R}^n$ be a domain containing $\tilde{\mathbf{x}} = 0$. Assume that $\mathbf{f}(\tilde{\mathbf{x}}, t)$ is piecewise continuous in t and locally Lipschitz in $\tilde{\mathbf{x}}$ (see Definition 2.1), for all $t \geq 0$ and $\tilde{\mathbf{x}} \in D$.*

When analyzing the stability of time-varying systems, the solution $\mathbf{x}(t)$ is dependent on both time t and on the initial condition $\mathbf{x}_0 = \mathbf{x}(t_0)$. Comparison functions can be used to formulate the stability definitions so that they hold uniformly in the initial time t_0 [7]. An additional advantage to using comparison functions is that they permit the stability definitions to be written in a compact way.

Definition 2.23 (Class $\mathcal{K}$ Functions). A function $\alpha : [0, a) \to [0, \infty)$ is of class $\mathcal{K}$ if it is continuous, strictly increasing, and $\alpha(0) = 0$.

Definition 2.24 (Class $\mathcal{K}_\infty$ Functions). If

$$\lim_{r \to \infty} \alpha(r) \to \infty, \tag{2.42}$$

then α is a class $\mathcal{K}_\infty$ function.

Definition 2.25 (Class $\mathcal{KL}$ Functions). A continuous function $\beta : [0, a) \times [0, \infty) \to [0, \infty)$ is of class $\mathcal{KL}$ if $\beta(r, t)$ is of class $\mathcal{K}$ with respect to r for each fixed $t \geq t_0$ and, if for each fixed $r \geq 0$, $\beta(r, t)$ decreases with respect to t and

$$\lim_{t \to \infty} \beta(r, t) \to 0. \tag{2.43}$$

We will write $\alpha \in \mathcal{K}_\infty, \beta \in \mathcal{KL}$ to indicate that α is a class $\mathcal{K}_\infty$ function and β is a class $\mathcal{KL}$ function, respectively. Note that the arguments of both functions $\alpha(r)$ and $\beta(r,t)$ are scalar.

Definitions for nonlinear time-varying systems, which are analogous to Definitions 2.3, 2.5, 2.11 and 2.12 above for nonlinear time-invariant systems, can be written using comparison functions.

Definition 2.26 (Uniformly Stable). The equilibrium point $\tilde{\mathbf{x}} = 0$ of system (2.41) is *uniformly stable* (US) if there exists a class $\mathcal{K}$ function α and a constant $\delta > 0$, independent of the initial time t_0, such that

$$\|\tilde{\mathbf{x}}(t)\| \leq \alpha(\|\tilde{\mathbf{x}}_0\|), \quad \forall t \geq t_0 \geq 0, \quad \forall \|\tilde{\mathbf{x}}_0\| < \delta. \tag{2.44}$$

Definition 2.27 (Uniformly Asymptotically Stable). The equilibrium point $\tilde{\mathbf{x}} = 0$ of system (2.41) is *uniformly asymptotically stable* (UAS) if there exists a class $\mathcal{KL}$ function β and a constant $\delta > 0$, independent of the initial time t_0, such that

$$\|\tilde{\mathbf{x}}(t)\| \leq \beta(\|\tilde{\mathbf{x}}_0\|, t - t_0), \quad \forall t \geq t_0 \geq 0, \quad \forall \|\tilde{\mathbf{x}}_0\| < \delta. \tag{2.45}$$

Definition 2.28 (Uniformly Globally Asymptotically Stable). The equilibrium point $\tilde{\mathbf{x}} = 0$ of system (2.41) is *uniformly globally asymptotically stable* (UGAS) if a class $\mathcal{KL}$ function β exists such that inequality (2.45) holds for any initial state, i.e.

$$\|\tilde{\mathbf{x}}(t)\| \leq \beta(\|\tilde{\mathbf{x}}_0\|, t - t_0), \quad \forall t \geq t_0 \geq 0, \quad \forall \|\tilde{\mathbf{x}}_0\|. \tag{2.46}$$

Definition 2.29 (Exponentially Stable). The equilibrium point $\tilde{\mathbf{x}} = 0$ of system (2.41) is *exponentially stable* (ES) if a class $\mathcal{KL}$ function β with the form $\beta(r,s) = kre^{-\lambda s}$ exists for some constants $k > 0$, $\lambda > 0$ and $\delta > 0$, such that

$$\|\tilde{\mathbf{x}}(t)\| \leq k\|\tilde{\mathbf{x}}_0\| \mathrm{e}^{-\lambda(t-t_0)}, \quad \forall t \geq t_0 \geq 0, \quad \forall \|\tilde{\mathbf{x}}_0\| < \delta. \tag{2.47}$$

Definition 2.30 (Globally Exponentially Stable). The equilibrium point $\tilde{\mathbf{x}} = 0$ of system (2.41) is *globally exponentially stable* (GES) if inequality (2.47) holds for any initial state, i.e.

$$\|\tilde{\mathbf{x}}(t)\| \leq k\|\tilde{\mathbf{x}}_0\| \mathrm{e}^{-\lambda(t-t_0)}, \quad \forall t \geq t_0 \geq 0, \quad \forall \|\tilde{\mathbf{x}}_0\|. \tag{2.48}$$

Theorem 2.4 (Uniformly Stable). *Let $\tilde{\mathbf{x}} = 0$ be an equilibrium point of system* (2.41) *and $V(t,\tilde{\mathbf{x}})$ be a continuously differentiable function such that*

$$W_1(\tilde{\mathbf{x}}) \leq V(\tilde{\mathbf{x}}, t) \leq W_2(\tilde{\mathbf{x}})$$

and

$$\frac{\partial V}{\partial t}+\frac{\partial V}{\partial \tilde{\mathbf{x}}}\mathbf{f}(\tilde{\mathbf{x}},t)\leq 0$$

for all $t\geq 0$ and $\tilde{\mathbf{x}}\in D$, where $W_1(\tilde{\mathbf{x}})$ and $W_2(\tilde{\mathbf{x}})$ are continuous positive definite functions in D. Then, under Assumption 2.1, the equilibrium point $\tilde{\mathbf{x}}=0$ is uniformly stable.

The following definition will be subsequently used to characterize the stability of nonlinear time-varying systems.

Definition 2.31 (Ball). A closed ball of radius δ in $\mathbb{R}^n$ centered at $\tilde{\mathbf{x}}=0$ is denoted by $\mathcal{B}_\delta$, i.e.

$$\mathcal{B}_\delta:=\{\tilde{\mathbf{x}}\in\mathbb{R}^n:\|\tilde{\mathbf{x}}\|\leq\delta\}.$$

Theorem 2.5 (Uniformly Asymptotically Stable). *Let $\tilde{\mathbf{x}}=0$ be an equilibrium point of system* (2.41) *and $V(t,\tilde{\mathbf{x}})$ be a continuously differentiable function such that*

$$W_1(\tilde{\mathbf{x}})\leq V(\tilde{\mathbf{x}},t)\leq W_2(\tilde{\mathbf{x}})$$

and

$$\frac{\partial V}{\partial t}+\frac{\partial V}{\partial \tilde{\mathbf{x}}}\mathbf{f}(\tilde{\mathbf{x}},t)\leq -W_3(\tilde{\mathbf{x}})$$

for all $t\geq 0$ and $\tilde{\mathbf{x}}\in D$, where $W_1(\tilde{\mathbf{x}})$, $W_2(\tilde{\mathbf{x}})$ and $W_3(\tilde{\mathbf{x}})$ are continuous positive definite functions in D. Then, under Assumption 2.1, the equilibrium point $\tilde{\mathbf{x}}=0$ is uniformly asymptotically stable.

Further, if there exist two positive constants δ and c, such that the ball $\mathcal{B}_\delta=\{\|\tilde{\mathbf{x}}_0\|\in\mathbb{R}^n:\|\tilde{\mathbf{x}}_0\|\leq\delta\}\subset D$ and $c<\min_{\|x\|=\delta}W_1(\tilde{\mathbf{x}})$, then every solution trajectory starting in $\{\tilde{\mathbf{x}}\in\mathcal{B}_\delta:W_2(\tilde{\mathbf{x}})\leq c\}$ satisfies

$$\|\tilde{\mathbf{x}}(t)\|\leq\beta(\|\tilde{\mathbf{x}}_0\|,t-t_0),\quad\forall t\geq t_0\geq 0$$

for some class $\mathcal{KL}$ function β.

Theorem 2.6 (Uniformly Globally Asymptotically Stable). *If the assumptions of Theorem 2.5 above hold for any initial state $\tilde{\mathbf{x}}_0\in\mathbb{R}^n$, $\|\tilde{\mathbf{x}}_0\|\to\infty$, the equilibrium point $\tilde{\mathbf{x}}=0$ of system* (2.41) *is uniformly globally asymptotically stable (UGAS).*

Theorem 2.7 (Exponentially Stable). *If the assumptions of Theorem 2.5 above are satisfied with*

$$k_1\|\tilde{\mathbf{x}}\|^p\leq V(\tilde{\mathbf{x}},t)\leq k_2\|\tilde{\mathbf{x}}\|^p$$

and

$$\frac{\partial V}{\partial t}+\frac{\partial V}{\partial \tilde{\mathbf{x}}}\mathbf{f}(\tilde{\mathbf{x}},t)\leq -k_3\|\tilde{\mathbf{x}}\|^p$$

for all $t\geq 0$ and $\tilde{\mathbf{x}}\in D$, where k_1, k_2, k_3 and p are positive constants. Then, the equilibrium point $\tilde{\mathbf{x}}=0$ of system (2.41) *is exponentially stable.*

Theorem 2.8 (Globally Exponentially Stable). *If the assumptions of Theorem 2.7 above hold for any initial state* $\tilde{\mathbf{x}}_0 \in \mathbb{R}^n$, $\|\tilde{\mathbf{x}}_0\| \to \infty$, *the equilibrium point* $\tilde{\mathbf{x}} = 0$ *of system* (2.41) *is globally exponentially stable.*

2.9 Input-to-State Stability

The development of automatic controllers for marine systems can be challenging because of the broad range of environmental conditions that they must operate within and the parametric uncertainty in dynamic models for them that arises because of changes in their configuration. Therefore, it is of important to extend stability concepts to include disturbance inputs. In the linear case, which can be represented by the system

$$\dot{\mathbf{x}} = \mathbf{A}\mathbf{x} + \mathbf{B}\mathbf{w}_d,$$

if the matrix $\mathbf{A}$ is Hurwitz, i.e., if the unforced system $\dot{\mathbf{x}} = \mathbf{A}\mathbf{x}$ is asymptotically stable, then bounded inputs $\mathbf{w}_d$ lead to bounded states, while inputs converging to zero produce states converging to zero. Now, consider a nonlinear system of the form

$$\dot{\mathbf{x}} = \mathbf{f}(\mathbf{x}, \mathbf{w}_d) \tag{2.49}$$

where $\mathbf{w}_d$ is a measureable, locally bounded disturbance input. In general, global asymptotic stability of the unforced system $\dot{\mathbf{x}} = \mathbf{f}(\mathbf{x}, 0)$ does not guarantee input-to-state properties of the kind mentioned above. For example, the scalar system

$$\dot{x} = -x + xw_d \tag{2.50}$$

has unbounded trajectories under the bounded input $w_d = 2$. This motivates the following important concept, introduced by Sontag & Wang [12].

The system (2.49) is called input-to-state stable (ISS) with respect to $\mathbf{w}_d$ if for some functions $\gamma \in \mathcal{K}_\infty$ and $\beta \in \mathcal{KL}$, for every initial state $\mathbf{x}_0$, and every input $\mathbf{w}_d$ the corresponding solution of (2.49) satisfies the inequality

$$\|\mathbf{x}(t)\| \leq \beta(\|\mathbf{x}_0\|, t) + \gamma(\|\mathbf{w}_d\|_{[0,t]}) \quad \forall t \geq 0 \tag{2.51}$$

where $\|\mathbf{w}_d\|_{[0,t]} := \text{ess sup}\{|\mathbf{w}_d(s)| \,:\, s \in [0,t]\}$ (supremum norm on [0, t] except for a set of measure zero). Since the system (2.49) is time-invariant, the same property results if we write

$$\|\mathbf{x}(t)\| \leq \beta(\|\mathbf{x}_0)\|, t - t_0) + \gamma(\|\mathbf{w}_d\|_{[t_0,t]}) \quad \forall t \geq t_0 \geq 0.$$

The ISS property admits the following Lyapunov-like equivalent characterization: the system (2.49) is ISS if and only if there exists a positive definite radially unbounded $\mathbb{C}^1$ function $V \,:\, \mathbb{R}^n \to \mathbb{R}$ such that for some class $\mathcal{K}_\infty$ functions α and χ we have

$$\frac{\partial V}{\partial \mathbf{x}} \mathbf{f}(\mathbf{x}, \mathbf{w}_d) \leq -\alpha(\|\mathbf{x}\|) + \chi(\|\mathbf{w}_d\|) \quad \forall \mathbf{x}, \mathbf{w}_d.$$

This is in turn equivalent to the following "gain margin" condition:

$$\|\mathbf{x}\| > \rho(\|\mathbf{w}_d\|) \quad \Rightarrow \quad \frac{\partial V}{\partial \mathbf{x}}\mathbf{f}(\mathbf{x},\mathbf{w}_d) \leq -\bar{\alpha}(\|\mathbf{x}\|)$$

where $\bar{\alpha}$, $\rho \in \mathcal{K}_\infty$. Such functions V are called *ISS-Lyapunov functions*.

The system (2.49) is *locally input-to-state stable* (locally ISS) if the bound (2.51) is valid for solutions with sufficiently small initial conditions and inputs, i.e., if there exists a $\delta > 0$ such that (2.51) is satisfied whenever $\|x_0\| \leq \delta$ and $\|u\|_{[0,t]} \leq \delta$. It turns out (local) asymptotic stability of the unforced system $\dot{x} = f(x,0)$ implies local ISS.

For systems with outputs, it is natural to consider the following notion which is dual to ISS. A system

$$\begin{aligned} \dot{\mathbf{x}} &= \mathbf{f}(\mathbf{x}) \\ \mathbf{y} &= \mathbf{h}(\mathbf{x}) \end{aligned} \tag{2.52}$$

is called *output-to-state stable* if for some functions $\gamma \in \mathcal{K}_\infty$ and $\beta \in \mathcal{KL}$ and every initial state $\mathbf{x}_0$ the corresponding solution of (2.52) satisfies the inequality

$$\|\mathbf{x}(t)\| \leq \beta(\|\mathbf{x}_0\|,t) + \gamma(\|\mathbf{y}\|_{[0,t]})$$

as long as it is defined. While ISS is to be viewed as a generalization of stability, OSS can be thought of as a generalization of observability; it does inded reduce to the standard observability property in the linear case. Given a system with both inputs and outputs

$$\begin{aligned} \dot{\mathbf{x}} &= \mathbf{f}(\mathbf{x},\mathbf{w}_d) \\ \mathbf{y} &= \mathbf{h}(\mathbf{x}) \end{aligned} \tag{2.53}$$

one calls it *input/output-to-state stable* (IOSS) if for some functions $\gamma_1, \gamma_2 \in \mathcal{K}_\infty$ and $\beta \in \mathcal{KL}$, for every initial state $\mathbf{x}_0$, and every input $\mathbf{w}_d$ the corresponding solution of (2.53) satisfies the inequality

$$\|\mathbf{x}(t)\| \leq \beta(\|\mathbf{x}_0\|,t) + \gamma_1(\|\mathbf{w}_d\|_{[0,t]}) + \gamma_2(\|\mathbf{y}\|_{[0,t]})$$

as long as it exists.

2.10 Ultimate Boundedness

Even when an equilibrium point $\tilde{\mathbf{x}} = 0$ of system (2.41) does not exist, a Lyapunov-like stability analysis can be used to show whether or not system state trajectories $\tilde{\mathbf{x}}(t)$ remain bounded within a region of the state space. We begin with a motivating example, which illustrates the concept of *uniform ultimate boundedness* (UUB). When a system is uniformly ultimately bounded the solution trajectories of the the state do not necessarily approach an equilibrium point, but instead converge to, and remain, within some neighborhood of $\tilde{\mathbf{x}} = 0$ after a sufficiently long time.

Example 2.6. Consider a surge speed-tracking controller for an unmanned surface vessel operating under the influence of time-varying exogenous disturbances (e.g. wind or waves). The equation of motion of the system is

$$m\dot{u} = -c_d u|u| - \tau + w_d(t), \tag{2.54}$$

where m is the mass (including added mass) of the vessel, u is the surge speed, c_d is the drag coefficient, τ is the control input (thruster force), and $w_d(t)$ is the disturbance.

Assume that the magnitude of the disturbance can be upper-bounded by a known positive constant $w_{d0} > 0$, such that

$$|w_d(t)| < w_{d0}, \quad \forall t. \tag{2.55}$$

It is desired that the surge speed-controller track a time-dependent speed $u_d(t)$, which is assumed to be continuously differentiable.

Let the control input be

$$\tau = m\dot{u}_d + c_d u|u| - k_p\tilde{u}, \tag{2.56}$$

where $\tilde{u} := u - u_d$ is the speed tracking error and $k_p > 0$ is a control gain. Then the closed loop equation of motion is given by

$$m\dot{\tilde{u}} = -k_p\tilde{u} + w_d(t). \tag{2.57}$$

Using the concept of flow along a line (Section 2.3), it can be seen that when $w_d(t) = 0$ the closed loop system has an equilibrium point at $\tilde{u} = 0$. However, the equilibrium point at $\tilde{u} = 0$ no longer exists when $w_d(t) \neq 0$.

To investigate the stability, consider the Lyapunov function

$$V = \frac{1}{2}\tilde{u}^2, \tag{2.58}$$

which is radially unbounded. Then, taking the derivative along system trajectories using (2.57) gives

$$\begin{aligned} \dot{V} &= \tilde{u}\dot{\tilde{u}} = \tilde{u}\left[-k_p\tilde{u} + w_d(t)\right], \\ &= -k_p\tilde{u}^2 + \tilde{u}w_d(t), \\ &\leq -k_p\tilde{u}^2 + \|\tilde{u}\|w_{d0}, \\ &\leq -\|\tilde{u}\|\left[k_p\|\tilde{u}\| - w_{d0}\right], \end{aligned} \tag{2.59}$$

where the upper bound is obtained with (2.55).

It therefore follows that

$$\dot{V} < 0, \quad \text{for all } \|\tilde{u}\| > \delta := \frac{w_{d0}}{k_p}. \tag{2.60}$$

In other words, $\dot{V} < 0$ when $\tilde{u}$ is outside the compact set $\mathcal{B}_\delta = \{\tilde{u} \in \mathbb{R} : \|\tilde{u}\| \leq \delta\}$ (see Definition 2.7). This implies that all of the solution trajectories $\tilde{u}(t)$ of (2.57) that start outside of $\mathcal{B}_\delta$ will tend towards $\mathcal{B}_\delta$.

We can show that the system is *uniformly bounded*, meaning that the final (*ultimate*) bound of $\tilde{u}$ is independent of the value of $\tilde{u}$ at the initial time t_0. Let $0 < \delta < \Delta$, then all solution trajectories $\tilde{u}(t)$ of (2.57) that start in the set

$$\mathcal{B}_\Delta := \{\tilde{u} \in \mathbb{R} : \|\tilde{u}\| \leq \Delta\}$$

will remain within $\mathcal{B}_\Delta$ for all $t \geq t_0$, where $\mathcal{B}_\delta \subset \mathcal{B}_\Delta$, since $\dot{V} < 0, \forall\ \|\tilde{u}\| > \delta$, see (2.60).

An estimate for the value of the *ultimate bound* can also be determined. Let ζ be a positive constant defined so that $\delta < \zeta < \Delta$. Since $\delta < \|\tilde{u}\| < \Delta$, V can be bounded as

$$\frac{1}{2}\delta^2 < \frac{1}{2}\tilde{u}^2 < \frac{1}{2}\Delta^2.$$

Inside the annular set $(\mathcal{B}_\Delta - \mathcal{B}_\delta)$, $\dot{V} < 0$ so that V decreases monotonically in time until $|\tilde{u}(t)| \leq \zeta$. Denote the earliest time when $|\tilde{u}(t)| \leq \zeta$ as $t = (t_0 + T_\zeta)$, where T_ζ is the elapsed time, and define the compact set $\mathcal{B}_\zeta := \{\tilde{u} \in \mathbb{R} : \|\tilde{u}\| \leq \zeta, \delta < \zeta\}$. For any time $t \geq t_0 + T_\zeta$ the trajectory of $\tilde{u}(t)$ remains inside $\mathcal{B}_\zeta$ because $\dot{V} < 0$ outside $\mathcal{B}_\zeta$ and on its boundary. Thus, using (2.60), we can conclude that the state trajectories of the closed loop system are *uniformly ultimately bounded* (UUB) with the ultimate bound $|\tilde{u}(t_0 + T_\zeta)| = \zeta > w_{d0}/k_p$. Note that the size of the compact set $\mathcal{B}_\zeta$ can be reduced by increasing the control gain k_p.

A simulation of the closed loop USV surge speed control system (2.57) is shown in Fig. 2.24 using a model of the small vehicle shown in Fig. 2.23. The USV has an overall length of 1.7 m, a mass of $m = 15$ kg and is simulated operating in the presence of deep water waves with a wavelength of 1.5 m (wave period of about

Fig. 2.23 A small lightweight USV [5].

1.0 sec). The control gain is set to $k_p = 5$. The desired speed u_d follows a step-like pattern in time. The wave-induced disturbance force has an amplitude of 4.5 N. In Fig. 2.24a it can be seen that the magnitude of the surge speed error decreases rapidly after the simulation starts, and oscillates about $\tilde{u} = 0$ with an amplitude of slightly less than 0.05 m/s. If we bound the anticipated magnitude of the disturbance as $w_{d0} = 4.5$ N, the UUB analysis above gives a very conservative estimate for the bounds of the error as

$$\|\tilde{u}\| > \frac{w_{d0}}{k_p} = 0.9 \text{ m/s}.$$

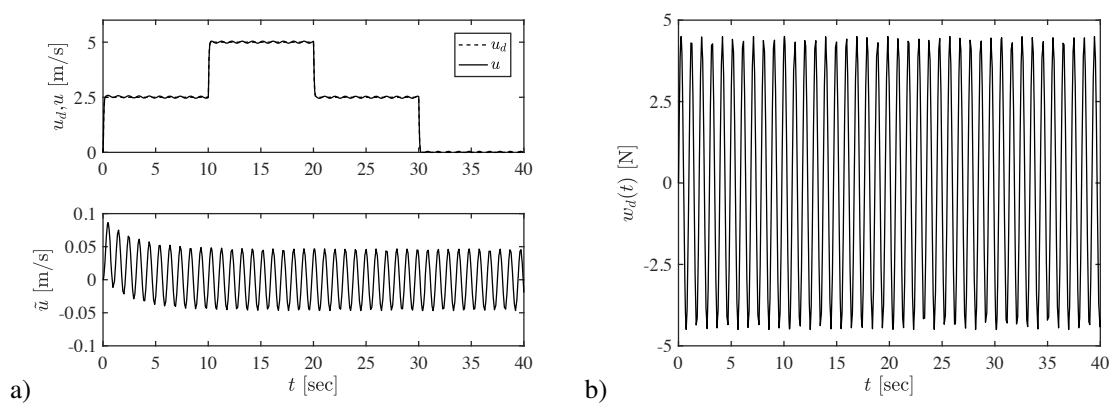

Fig. 2.24 Time response of a surge speed tracking USV: a) desired speed u_d, output speed u, and speed tracking error $\tilde{u}$, b) wave disturbance forces $w_d(t)$.

□

Definition 2.32 (Uniformly Bounded). The solution trajectories $\tilde{\mathbf{x}}(t)$ of (2.41) are *uniformly bounded* (UB) if there exist constants δ and ε, where $0 < \delta < \varepsilon$, and a function $\alpha(\delta) > 0$ such that

$$\|\tilde{\mathbf{x}}_0\| \leq \delta \Rightarrow \|\tilde{\mathbf{x}}(t)\| \leq \alpha(\delta), \quad \forall t \geq t_0 \geq 0. \tag{2.61}$$

Comparing the definition of UB to Definitions 2.3 and 2.44, it can be seen that while UB is similar, it is defined only with reference to the boundedness of solution trajectories, rather than with reference to the position of an equilibrium point.

Definition 2.33 (Uniformly Globally Bounded). The solution trajectories $\tilde{\mathbf{x}}(t)$ of (2.41) are *uniformly globally bounded* (UGB) if (2.61) holds for $\delta \to \infty$.

Definition 2.34 (Uniformly Ultimately Bounded). The solution trajectories $\tilde{\mathbf{x}}(t)$ of (2.41) are *uniformly ultimately bounded* (UUB), with ultimate bound ζ, if there exist constants δ, ζ and ε, where for every $0 < \delta < \varepsilon$, there exists an elapsed time $T = T(\delta, \zeta) \geq 0$ such that

$$\|\tilde{\mathbf{x}}_0\| < \delta \Rightarrow \|\tilde{\mathbf{x}}(t)\| \leq \zeta, \quad \forall t \geq t_0 + T. \tag{2.62}$$

Definition 2.35 (Uniformly Globally Ultimately Bounded). The solution trajectories $\tilde{\mathbf{x}}(t)$ of (2.41) are *uniformly globally ultimately bounded* (UGUB) if (2.62) holds for $\delta \to \infty$.

In Definitions 2.32–2.35 above, the term *uniform* means that the ultimate bound ζ does not depend on the initial time t_0. The term *ultimate* indicates that boundedness holds after an elapsed time T. The constant ε defines a neighborhood of the origin, which is independent of t_0, so that all trajectories starting within the neighborhood remain bounded. If ε can be chosen arbitrarily large then the system then the UUB is global.

Remark 2.7. Lyapunov stability Definitions 2.26–2.30 require that solution state trajectories $\tilde{\mathbf{x}}(t)$ remain arbitrarily close to the system equilibrium point $\tilde{\mathbf{x}} = 0$ by starting sufficiently close to it. In general, this requirement is too strong to achieve in practice, as real systems are usually affected by the presence of unknown disturbances. Further, the UUB bound ζ cannot be made arbitrarily small by starting closer to $\tilde{\mathbf{x}} = 0$. In practical systems, ζ depends on both the disturbances and system uncertainties.

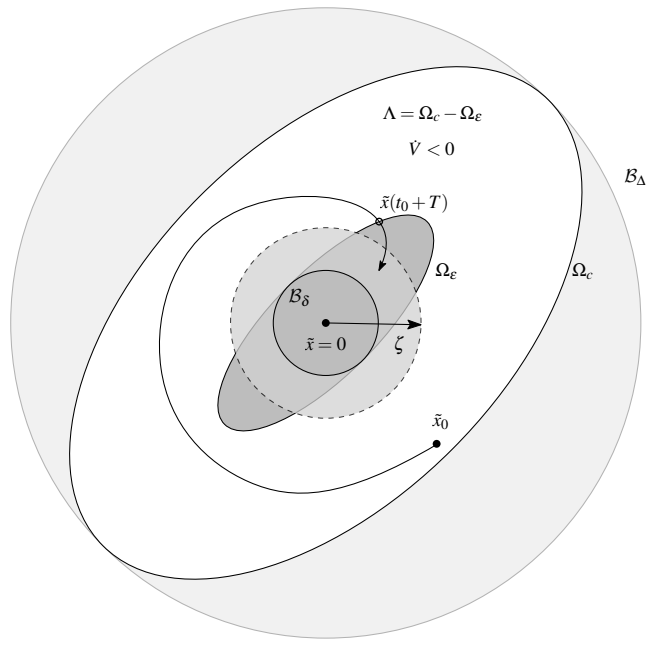

Fig. 2.25 Geometric interpretation of uniform ultimate boundedness.

To understand how a Lyapunov-like analysis can be used to study UUB, consider a continuously differentiable, positive definite function $V : \mathbb{R}^n \to \mathbb{R}$ and suppose that the sets

$$\Omega_c := \{\tilde{\mathbf{x}} \in \mathbb{R}^n : V(\tilde{\mathbf{x}}) \leq c\} \quad \text{and} \quad \Omega_\varepsilon := \{\tilde{\mathbf{x}} \in \mathbb{R}^n : V(\tilde{\mathbf{x}}) \leq \varepsilon\}$$

are compact and invariant from some $0 < \varepsilon < c$ (see Fig. 2.25). Let $\Lambda := \Omega_c - \Omega_\varepsilon = \{\tilde{\mathbf{x}} \in \mathbb{R}^n : \varepsilon \leq V(\tilde{\mathbf{x}}) \leq c\}$ and suppose that the time derivative along the solution trajectories $\tilde{\mathbf{x}}(t)$ of (2.41) is given by

$$\dot{V}(\tilde{\mathbf{x}},t) = \frac{\partial V}{\partial \tilde{\mathbf{x}}}\mathbf{f}(\tilde{\mathbf{x}}) \leq -W_3(\tilde{\mathbf{x}}), \quad \forall \tilde{\mathbf{x}} \in \Lambda, \quad \forall t \geq 0,$$

where $W_3(\tilde{\mathbf{x}})$ is a continuous positive definite function. Since $\dot{V}(\tilde{\mathbf{x}},t) < 0$ for all $\tilde{\mathbf{x}} \in \Lambda$ a trajectory $\tilde{\mathbf{x}}(t)$ starting in the set Λ must move in the direction of decreasing $V(\tilde{\mathbf{x}})$. Thus, $V(\tilde{\mathbf{x}})$ will decrease until the trajectory enters the set Ω_ε, and once inside Ω_ε the trajectory will remain inside Ω_ε for all future times.

Define

$$k := \min_{\tilde{\mathbf{x}} \in \Lambda} W_3(\tilde{\mathbf{x}}) > 0,$$

then

$$\dot{V}(\tilde{\mathbf{x}},t) \leq -k, \quad \forall \tilde{\mathbf{x}} \in \Lambda, \quad \forall t \geq t_0 \geq 0,$$

so that

$$V(\tilde{\mathbf{x}}(t)) \leq V(\tilde{\mathbf{x}}_0) - k(t - t_0) = V_0 - k(t - t_0).$$

Thus, a state starting at the position $\tilde{\mathbf{x}}_0$ at time $t = t_0$ will arrive at the boundary of the compact set $V = \Omega_\varepsilon$ after the elapsed time $T = (V_0 - \varepsilon)/k + t_0$.

In order to find an estimate of the ultimate bound, we define the balls (Definition 2.31)

$$\mathcal{B}_\delta := \{\tilde{\mathbf{x}} \in \mathbb{R}^n : \|\tilde{\mathbf{x}}(t)\| \leq \delta\} \quad \text{and} \quad \mathcal{B}_\Delta := \{\tilde{\mathbf{x}} \in \mathbb{R}^n : \|\tilde{\mathbf{x}}(t)\| \leq \Delta\},$$

such that the compact set Λ occurs in a subset of the region of the state space where $\delta \leq \|\tilde{\mathbf{x}}\| \leq \Delta$ (see Fig. 2.25) and

$$\dot{V}(\tilde{\mathbf{x}},t) \leq -W_3(\tilde{\mathbf{x}}), \quad \forall \delta \leq \|\tilde{\mathbf{x}}\| \leq \Delta, \quad \forall t \geq t_0 \geq 0.$$

Let α_1 and α_2 be class $\mathcal{K}$ functions, such that

$$\alpha_1(\|\tilde{\mathbf{x}}\|) \leq V(\tilde{\mathbf{x}}) \leq \alpha_2(\|\tilde{\mathbf{x}}\|). \tag{2.63}$$

Referring to Fig. 2.25, it can be seen that $c = \alpha_2(\Delta)$ where the boundaries of $\mathcal{B}_\Delta$ and Ω_c touch. Thus, inside the compact set Ω_c, $V(\tilde{\mathbf{x}}) \leq \alpha_2(\Delta)$, so that $\Omega_c \subseteq \mathcal{B}_\Delta$. Since the maximum value of $V(\tilde{\mathbf{x}})$ in the set Ω_ε occurs at its boundary, we have $\varepsilon = \alpha_2(\delta)$ where the surfaces of Ω_ε and $\mathcal{B}_\delta$ touch. However, inside of Ω_ε, $\alpha_1(\|\tilde{\mathbf{x}}\|) \leq V(\tilde{\mathbf{x}})$, so that the relation $\alpha_1(\|\tilde{\mathbf{x}}\|) \leq \varepsilon = \alpha_2(\delta)$ holds. Taking the inverse of this latter inequality provides an estimate of the ultimate bound

$$\|\tilde{\mathbf{x}}\| \leq \alpha_1^{-1}\left[\alpha_2(\delta)\right]. \tag{2.64}$$

Remark 2.8. The ultimate bound is independent of the initial state $\tilde{\mathbf{x}}_0 \in \Omega_c$ and is a class $\mathcal{K}$ function of δ. As a consequence, the smaller the value of δ, the smaller the ultimate bound.

Theorem 2.9 (Uniformly Ultimately Bounded). *Suppose that*

$$\alpha_1(\|\tilde{\mathbf{x}}\|) \leq V(\tilde{\mathbf{x}}) \leq \alpha_2(\|\tilde{\mathbf{x}}\|),$$

$$\dot{V}(\tilde{\mathbf{x}},t) = \frac{\partial V}{\partial \tilde{\mathbf{x}}}\mathbf{f}(\tilde{\mathbf{x}}) \leq -W_3(\tilde{\mathbf{x}}), \quad \forall \|\tilde{\mathbf{x}}\| \geq \delta > 0, \quad \forall t \geq 0,$$

and $\|\tilde{\mathbf{x}}\| \leq \Delta$*, where* $\alpha_1, \alpha_2 \in \mathcal{K}$*,* $W_3(\tilde{\mathbf{x}}) > 0$ *is continuous, and* $\delta < \alpha_2^{-1}[\alpha_1(\Delta)]$*. Then, for every initial state* $\tilde{\mathbf{x}}_0 \in \{\|\tilde{\mathbf{x}}\| \leq \alpha_2^{-1}[\alpha_1(\Delta)]\}$*, there exists an elapsed time* $T = T(\tilde{\mathbf{x}}_0, \delta) \geq 0$*, such that*

$$\|\tilde{\mathbf{x}}(t)\| \leq \alpha_1^{-1}[\alpha_2(\delta)], \quad \forall t \geq t_0 + T.$$

If the conditions hold for $\Delta \to \infty$ *and* $\alpha_1 \in \mathcal{K}_\infty$*, then the conclusions are valid for every initial state* $\tilde{\mathbf{x}}_0$ *and the system is uniformly globally ultimately bounded.*

2.11 Practical Stability

Thus far, we have mostly considered the stability of nonlinear time-varying systems when no external disturbances are acting on them and when there is no uncertainty in the dynamics of the system. However, most marine vehicles operate in uncertain environments and with inaccurate dynamic models. Thus, it is important to understand how disturbances and model uncertainty can affect the stability of the system. This is especially true for systems that operate near the upper limits of the capabilities of their actuators.

As discussed in Example 2.6, when systems operate in the presence of time-varying disturbances, an equilibrium point $\tilde{\mathbf{x}} = 0$ no longer exists. However, the solution trajectories of the state $\tilde{\mathbf{x}}(t)$ may be ultimately bounded within a finite region. In some cases, as in the example, the size of the bounded region can be decreased by tuning the control gains. This stability property is often referred to as *practical stability*.

When the region of attraction of the state trajectories of a system consists of the entire state space, the region is *globally attractive*, see Definitions 2.28, 2.30 and 2.35, for example. Instead, when the region of attraction of a closed loop system can be arbitrarily enlarged by tuning a set of control gains, the region is called *semiglobally attractive*.

In Section 2.7 it is seen that invariant sets can be thought of as a generalization of the concept of an equilibrium point. In a similar way, we will consider the stability of state trajectories towards closed *balls* (Definition 2.31) in state space as a similar generalization of the idea of an equilibrium point when characterizing the stability of nonlinear systems in the presence of disturbances. The following stability defi-

nitions, theorems and notation are developed in [1, 2, 6]. Additional details can be found in these references.

However, before proceeding, we will generalize the notion of uniform asymptotic stability (UAS) about an equilibrium point given in Definition 2.27 and Theorem 2.5 above to the UAS of a ball. To do this, define a bound for the shortest distance between a point $\tilde{\mathbf{z}}$ on the surface of the ball $\mathcal{B}_\delta$ and the point $\tilde{\mathbf{x}}$, as

$$\|\tilde{\mathbf{x}}\|_\delta := \inf_{\tilde{\mathbf{z}} \in \mathcal{B}_\delta} \|\tilde{\mathbf{x}} - \tilde{\mathbf{z}}\| \tag{2.65}$$

and let $\Delta > \delta > 0$ be two non-negative numbers.

Definition 2.36 (Uniform Asymptotic Stability of a Ball). The ball $\mathcal{B}_\delta$ is *uniformly asymptotically stable* (UAS) on $\mathcal{B}_\Delta$ for the system (2.41), if and only if there exists a class $\mathcal{KL}$ function β, such that for all initial states $\tilde{\mathbf{x}}_0 \in \mathcal{B}_\Delta$ and all initial times $t_0 \geq 0$, the solution of (2.41) satisfies

$$\|\tilde{\mathbf{x}}(t)\|_\delta \leq \beta(\|\tilde{\mathbf{x}}_0\|, t - t_0), \quad \forall t \geq t_0. \tag{2.66}$$

Definition 2.37 (Uniform Global Asymptotic Stability of a Ball). The ball $\mathcal{B}_\delta$ is *uniformly globally asymptotically stable* (UGAS) if (2.66) holds for any initial condition $\tilde{\mathbf{x}}_0$, i.e. $\Delta \to \infty$.

While the UAS and the UGAS of a ball imply the property of ultimate boundedness (with any $\zeta > \delta$ as the ultimate bound), they are stronger properties, as they guarantee that sufficiently small transients remain arbitrarily near $\mathcal{B}_\delta$. Thus, the definition of the stability of a system about a ball, is similar to the definition of stability about an equilibrium point, e.g. compare Definition 2.36 to Definition 2.5. Ultimate boundedness is really a notion of convergence, which does not necessary imply stability to perturbations.

Consider a nonlinear, time-varying system of the form

$$\dot{\tilde{\mathbf{x}}} = \mathbf{f}(\tilde{\mathbf{x}}, t, \theta), \quad \tilde{\mathbf{x}} \in \mathbb{R}^n, \quad t \geq 0, \tag{2.67}$$

where $\theta \in \mathbb{R}^m$ is a vector of constant parameters, and $f : \mathbb{R}^n \times \mathbb{R} \times \mathbb{R}^m$ is locally Lipschitz in $\tilde{\mathbf{x}}$ and piecewise continuous in t. System (2.67) is representative of closed loop control systems, where θ would typically contain control gains, but could represent other parameters.

In the following definitions, let $\Theta \subset \mathbb{R}^m$ be a set of parameters.

Definition 2.38 (Uniform Global Practical Asymptotic Stability). The system (2.67) is *uniformly globally practically asymptotically stable* (UGPAS) on Θ, if for any $\delta > 0$ there exists a $\theta^\star(\delta) \in \Theta$, such that $\mathcal{B}_\delta$ is UGAS for system (2.67) when $\theta = \theta^\star$.

Thus, (2.67) is UGPAS if the ball $\mathcal{B}_\delta$, which is UGAS, can be arbitrarily diminished by a convenient choice of θ.

Definition 2.39 (Uniform Semiglobal Practical Asymptotic Stability). The system (2.67) is *uniformly semiglobally practically asymptotically stable* (USPAS) on Θ, if for any $\Delta > \delta > 0$ there exists a $\theta^\star(\delta,\Delta) \in \Theta$, such that $\mathcal{B}_\delta$ is UAS on $\mathcal{B}_\Delta$ for system (2.67) when $\theta = \theta^\star$.

In this case, (2.67) is USPAS if the estimate of the domain of attraction $\mathcal{B}_\Delta$ and the ball $\mathcal{B}_\delta$, which is UAS, can be arbitrarily enlarged and diminished, respectively, by tuning the parameter θ.

Definition 2.40 (Uniform Global Practical Exponential Stability). System (2.67) is *uniformly globally practically exponentially stable* (UGPES) on Θ, if for any $\delta > 0$ there exists a $\theta^\star(\delta) \in \Theta$, and positive constants $k(\delta)$ and $\gamma(\delta)$, such that for any initial state $\tilde{\mathbf{x}}_0 \in \mathbb{R}^n$ and for any time $t \geq t_0 \geq 0$ the solution trajectories of (2.67) satisfy

$$\|\tilde{\mathbf{x}}(t,\theta^\star)\| \leq \delta + k(\delta)\|\tilde{\mathbf{x}}_0\| \mathrm{e}^{-\gamma(\delta)(t-t_0)}, \quad \forall t \geq t_0.$$

Definition 2.41 (Uniform Semiglobal Practical Exponential Stability). System (2.67) is *uniformly semiglobally practically exponentially stable* (USPES) on Θ, if for any $\Delta > \delta > 0$ there exists a $\theta^\star(\delta,\Delta) \in \Theta$, and positive constants $k(\delta,\Delta)$ and $\gamma(\delta,\Delta)$, such that for any initial state $\tilde{\mathbf{x}}_0 \in \mathcal{B}_\Delta$ and for any time $t \geq t_0 \geq 0$ the solution trajectories of (2.67) satisfy

$$\|\tilde{\mathbf{x}}(t,\theta^\star)\| \leq \delta + k(\delta,\Delta)\|\tilde{\mathbf{x}}_0\| \mathrm{e}^{-\gamma(\delta,\Delta)(t-t_0)}, \quad \forall t \geq t_0.$$

Theorem 2.10 (UGPAS). *Suppose that given any $\delta > 0$ there exist a parameter $\theta^\star(\delta) \in \Theta$, a continuously differentiable function $V : \mathbb{R}^n \times \mathbb{R}_{\geq 0} \to \mathbb{R}_{\geq 0}$, and three class $\mathcal{K}_\infty$ functions α_1, α_2 and α_3, such that for all $\tilde{\mathbf{x}} \in \mathbb{R}^n \backslash \mathcal{B}_\delta$ (i.e. all points $\tilde{\mathbf{x}}$ that are not inside $\mathcal{B}_\delta$) and for all $t \geq 0$*

$$\alpha_1(\|\tilde{\mathbf{x}}\|) \leq V(\tilde{\mathbf{x}},t) \leq \alpha_2(\|\tilde{\mathbf{x}}\|),$$

$$\frac{\partial V}{\partial t} + \frac{\partial V}{\partial \tilde{\mathbf{x}}}\mathbf{f}(\tilde{\mathbf{x}},t) \leq -\alpha_3(\|\tilde{\mathbf{x}}\|),$$

and

$$\lim_{\delta \to 0} \alpha_1^{-1}[\alpha_2(\delta)] = 0. \tag{2.68}$$

Then, (2.67) *is UGPAS on the parameter set Θ.*

The first two conditions of Theorem 2.10 can often be verified using a Lyapunov function that establishes the UGAS of the system (Theorem 2.6) when the disturbances and uncertainties are assumed to be zero [1]. The Lyapunov function may depend on the tuning parameter θ, and so on the radius δ. Hence, (2.68) is required to links the bounds on the Lyapunov function.

Theorem 2.11 (USPAS). *Suppose that given any $\Delta > \delta > 0$ there exist a parameter $\theta^\star(\delta,\Delta) \in \Theta$, a continuously differentiable function $V : \mathbb{R}^n \times \mathbb{R}_{\geq 0} \to \mathbb{R}_{\geq 0}$, and three class $\mathcal{K}_\infty$ functions α_1, α_2 and α_3, such that for all $\delta < \|\tilde{\mathbf{x}}\| < \Delta$ and for all $t \geq 0$*

$$\alpha_1(\|\tilde{\mathbf{x}}\|) \leq V(\tilde{\mathbf{x}},t) \leq \alpha_2(\|\tilde{\mathbf{x}}\|),$$

and

$$\frac{\partial V}{\partial t} + \frac{\partial V}{\partial \tilde{\mathbf{x}}}\mathbf{f}(\tilde{\mathbf{x}},t) \leq -\alpha_3(\|\tilde{\mathbf{x}}\|).$$

Assume further that for any constants $0 < \delta^\star < \Delta^\star$, there exist $0 < \delta < \Delta$ such that

$$\alpha_1^{-1}[\alpha_2(\delta)] \leq \delta^\star \quad \text{and} \quad \alpha_2^{-1}[\alpha_1(\Delta)] \geq \Delta^\star. \tag{2.69}$$

Then, (2.67) *is USPAS on the parameter set Θ.*

Since the Lyapunov function $V(\tilde{\mathbf{x}},t)$ is not required to be the same for all δ and all Δ, the conditions in (2.69) must be imposed to ensure that the estimate of the domain of attraction $\mathcal{B}_\Delta$ and the set $\mathcal{B}_\delta$, which is UAS, can be arbitrarily enlarged and diminished, respectively [2].

Theorem 2.12 (UGPES). *Suppose that for any $\delta > 0$ there exist a parameter $\theta^\star(\delta) \in \Theta$, a continuously differentiable function $V : \mathbb{R}^n \times \mathbb{R}_{\geq 0} \to \mathbb{R}_{\geq 0}$, and positive constants $k_1(\delta)$, $k_2(\delta)$ and $k_3(\delta)$, such that for all $\tilde{\mathbf{x}} \in \mathbb{R}^n \backslash \mathcal{B}_\delta$ (i.e. all points $\tilde{\mathbf{x}}$ that are not inside $\mathcal{B}_\delta$) and for all $t \geq 0$*

$$k_1(\delta)\|\tilde{\mathbf{x}}\|^p \leq V(\tilde{\mathbf{x}},t) \leq k_2(\delta)\|\tilde{\mathbf{x}}\|^p,$$

$$\frac{\partial V}{\partial t} + \frac{\partial V}{\partial \tilde{\mathbf{x}}}\mathbf{f}(\tilde{\mathbf{x}},t) \leq -k_3(\delta)\|\tilde{\mathbf{x}}\|^p,$$

where $p > 0$ is a constant and

$$\lim_{\delta \to 0} \frac{k_2(\delta)\delta^p}{k_1(\delta)} = 0. \tag{2.70}$$

Then, (2.67) *is UGPES on the parameter set Θ.*

Theorem 2.13 (USPES). *Suppose that for any $\Delta > \delta > 0$ there exist a parameter $\theta^\star(\delta,\Delta) \in \Theta$, a continuously differentiable function $V : \mathbb{R}^n \times \mathbb{R}_{\geq 0} \to \mathbb{R}_{\geq 0}$, and positive constants $k_1(\delta,\Delta)$, $k_2(\delta,\Delta)$ and $k_3(\delta,\Delta)$, such that for all $\tilde{\mathbf{x}} \in \mathcal{B}_\Delta \backslash \mathcal{B}_\delta$ (i.e. all points $\tilde{\mathbf{x}}$ in $\mathcal{B}_\Delta$ that are not inside $\mathcal{B}_\delta$) and for all $t \geq 0$*

$$k_1(\delta,\Delta)\|\tilde{\mathbf{x}}\|^p \leq V(\tilde{\mathbf{x}},t) \leq k_2(\delta,\Delta)\|\tilde{\mathbf{x}}\|^p,$$

$$\frac{\partial V}{\partial t} + \frac{\partial V}{\partial \tilde{\mathbf{x}}}\mathbf{f}(\tilde{\mathbf{x}},t) \leq -k_3(\delta,\Delta)\|\tilde{\mathbf{x}}\|^p,$$

where $p > 0$ is a constant. Assume further that for any constants $0 < \delta^\star < \Delta^\star$, there exist $0 < \delta < \Delta$ such that

$$\frac{k_2(\delta,\Delta)\delta^p}{k_1(\delta,\Delta)} \leq \delta^\star \quad \text{and} \quad \frac{k_1(\delta,\Delta)\Delta^p}{k_2(\delta,\Delta)} \geq \Delta^\star. \tag{2.71}$$

Then, (2.67) *is USPES on the parameter set* Θ.

The following inequalities can be very useful for simplifying the stability analysis of nonlinear systems.

Theorem 2.14 (Young's Inequality). *Assume that* $a \in \mathbb{R}$, $b \in \mathbb{R}$ *and* $\varepsilon > 0$. *Then*

$$ab \leq \frac{a^2}{2\varepsilon} + \frac{\varepsilon b^2}{2}. \tag{2.72}$$

This can also be expressed in vector form as

$$\|\mathbf{a}^T\mathbf{b}\| \leq \frac{\|\mathbf{a}\|^2}{2\varepsilon} + \frac{\varepsilon\|\mathbf{b}\|^2}{2}, \quad \forall \mathbf{a},\mathbf{b} \in \mathbb{R}^n. \tag{2.73}$$

Theorem 2.15 (Triangle Inequality). *Assume that* $\|\mathbf{a}\|$ *and* $\|\mathbf{b}\|$ *are two vectors. Then*

$$\|\mathbf{a}+\mathbf{b}\| \leq \|\mathbf{a}\| + \|\mathbf{b}\|, \quad \forall \mathbf{a},\mathbf{b} \in \mathbb{R}^n. \tag{2.74}$$

Theorem 2.16 (Cauchy-Schwarz Inequality). *Assume that* $\|\mathbf{a}\|$ *and* $\|\mathbf{b}\|$ *are two vectors. Then*

$$\|\mathbf{a}^T\mathbf{b}\| \leq \|\mathbf{a}\|\|\mathbf{b}\|, \quad \forall \mathbf{a},\mathbf{b} \in \mathbb{R}^n. \tag{2.75}$$

Example 2.7. Let us return to Example 2.6 where we considered the surge speed-tracking control of an unmanned surface vessel operating under the influence of a time-varying exogenous disturbance. It can be seen that the term $-k_p\tilde{u}^2$ in (2.59) is ND. How to handle the second term may be unclear, as it depends on the unknown disturbance. Fortunately, even though we don't know the value of $w_d(t)$ at any given time, we can use the known upper bound on the magnitude of the disturbance $|w_d(t)| < w_{d0}, \quad \forall t$ to find an upper bound for $\dot{V}$.

Applying Young's Inequality (Theorem 2.14) with $\varepsilon = 1$ to (2.59) and using $w_d(t)^2 < w_{d0}^2$ gives

$$\begin{aligned} \dot{V} &\leq -k_p\tilde{u}^2 + \frac{\tilde{u}^2}{2} + \frac{w_d(t)^2}{2}, \\ &\leq -\frac{(2k_p-1)}{2}\tilde{u}^2 + \frac{w_{d0}^2}{2}. \end{aligned} \tag{2.76}$$

From (2.58) we have

$$-\frac{(2k_p-1)}{2}\tilde{u}^2 = -(2k_p-1)V \tag{2.77}$$

so that

$$\dot{V} \leq -(2k_p - 1)V + \frac{w_{d0}^2}{2}. \tag{2.78}$$

For $k_p > 1/2$, V will decrease until $\dot{V} = 0$. Thus, $\dot{V}$ is NSD because we can have $\dot{V} = 0$ even though $\tilde{u} \neq 0$. Since $w_d = w_d(t)$ the system is not time-invariant, so LaSalle's Invariant Set Theorem (Theorem 2.3) cannot be used to analyze its stability.

However, note that integrating (2.78) gives

$$V \leq \left[V_0 - \frac{w_{d0}^2}{2(2k_p - 1)} \right] \mathrm{e}^{-(2k_p-1)(t-t_0)} + \frac{w_{d0}^2}{2(2k_p - 1)}, \tag{2.79}$$

where V_0 is the value of V at the initial time $t = t_0$. Thus, it can be seen that the value of V decreases to its equilibrium value (when $\dot{V} = 0$) exponentially in time.

Using (2.58), we can solve for the bounds of $\|\tilde{u}\|$ from the bounds of V to get

$$\|\tilde{u}\| \leq \sqrt{\left[\tilde{u}_0^2 - \frac{w_{d0}^2}{(2k_p - 1)} \right] \mathrm{e}^{-(2k_p-1)(t-t_0)} + \frac{w_{d0}^2}{(2k_p - 1)}}. \tag{2.80}$$

This can be simplified into the form of a USPES system (Definition 2.41), using the Triangle Inequality (Theorem 2.15), to get

$$\begin{aligned} \|\tilde{u}\| &\leq \sqrt{\tilde{u}_0^2 - \frac{w_{d0}^2}{(2k_p - 1)}}\, \mathrm{e}^{-(k_p-1/2)(t-t_0)} + \frac{w_{d0}}{\sqrt{2k_p - 1}}, \\ &\leq \frac{w_{d0}}{\sqrt{2k_p - 1}} + \|\tilde{u}_0\| \sqrt{1 - \frac{w_{d0}^2}{\tilde{u}_0^2(2k_p - 1)}}\, \mathrm{e}^{-(k_p-1/2)(t-t_0)}, \\ &\leq \delta + k(\delta, \Delta)\|\tilde{u}_0\| \mathrm{e}^{-\gamma(t-t_0)}, \end{aligned} \tag{2.81}$$

where $\delta := w_{d0}/\sqrt{2k_p - 1}$, $\Delta := \|\tilde{u}_0\|$,

$$k(\delta, \Delta) := \sqrt{1 - \frac{w_{d0}^2}{\tilde{u}_0^2(2k_p - 1)}} = \sqrt{1 - \frac{\delta^2}{\Delta^2}},$$

and $\gamma(\delta, \Delta) := (k_p - 1/2)$.

Note that with (2.81) it can be seen that

$$\lim_{t \to \infty} = \|\tilde{u}\| = \frac{w_{d0}}{\sqrt{2k_p - 1}}.$$

Thus, the size of the bounded region into which the trajectories of $\tilde{u}(t)$ converge in time can be decreased by increasing the control gain k_p. As discussed above, this type of stability is known as *practical stability*.

In order to actually prove that the system is USPES, we need to confirm that it satisfies the three conditions given in Theorem 2.13.

Note that simultaneously satisfying both the first and third conditions of Theorem 2.13 effectively provides an upper and lower bounds for V. These bounds depend on the relative sizes of δ and Δ. Using the numerical values provided in Example 2.6 above, we have $w_{d0} = 4.5$ N, $k_p = 5$ (this gain would effectively have units of kg/s) and $\|\tilde{u}_0\| = 2.5$ m/s (the maximum initial surge speed error occurring in the problem), so that $\delta = 1.5$ m/s and $\Delta = 2.5$ m/s.

With $\Delta^* > \delta^* > 0$ the third condition of Theorem 2.13 can also be expressed as $k_1\Delta/\delta > k_2 > 0$. Combining this with the first condition of Theorem 2.13 we can also write this as $k_1\Delta/\delta > k_2 > k_1$, which places an upper and lower bounds on the range of k_2 with respect to k_1. For this example, the numerical range of possible values for k_1 and k_2 is $5k_1/3 > k_2 > k_1$ and $k_1 < 1/2$ (because of the first condition and the fact that $V = \|\tilde{u}\|^2/2$). Thus, by selecting $k_1 = 1/4$ and $k_2 = 3/8$ both the first and third conditions of Theorem 2.13 are satisfied.

In order to show that the closed loop system is USPES, it only remains to prove that the second condition of Theorem 2.13 is also satisfied. Using (2.79) in (2.78) gives

$$\begin{aligned}
\dot{V} &\leq -(2k_p-1)\left[V_0 - \frac{w_{d0}^2}{2(2k_p-1)}\right]\mathrm{e}^{-(2k_p-1)(t-t_0)}, \\
&\leq -\frac{(2k_p-1)}{2}\left[\tilde{u}_0^2 - \frac{w_{d0}^2}{(2k_p-1)}\right]\mathrm{e}^{-(2k_p-1)(t-t_0)} + \frac{w_{d0}^2}{2}, \\
&\leq -\frac{(2k_p-1)}{2}\left\{\left[\tilde{u}_0^2 - \frac{w_{d0}^2}{(2k_p-1)}\right]\mathrm{e}^{-(2k_p-1)(t-t_0)} + \frac{w_{d0}^2}{(2k_p-1)}\right\}.
\end{aligned}$$

Comparing this result with (2.80), it can be seen that

$$\dot{V} \leq -k_3\|\tilde{u}\|^2,$$

where $k_3 := (k_p - 1/2)$ so that the second condition of Theorem 2.13 is also satisfied.

Thus, as the closed loop system has been shown to satisfy all three conditions of of Theorem 2.13, it is guaranteed to be uniformly semiglobally exponentially stable.

□

2.12 Barbalat's Lemma

When using Lyapunov Theory to solve adaptive control problems, $\mathrm{d}V/\mathrm{d}t$ is often only negative semidefinite and additional conditions must be imposed on the system, in such cases the following lemma can be useful.

Lemma 2.1 (Barbalat's Lemma). *For a time-invariant nonlinear system* $\dot{\mathbf{x}} = \mathbf{f}(\mathbf{x},t)$. *Consider a function* $V(\mathbf{x},t) \in \mathbb{C}^1$. *If*

1) $V(\mathbf{x},t)$ *is lower bounded,*

2) $\dot{V}(\mathbf{x},t) \leq 0$*, and*
3) $\dot{V}(\mathbf{x},t)$ *is uniformly continuous,*

then $\dot{V}(\mathbf{x},t) \leq 0$ *converges to zero along the trajectories of the system.*

Remark 2.9. The third condition of Barbalat's Lemma is often replaced by the stronger condition $\ddot{V}(\mathbf{x},t)$ is bounded. In general, Barbalat's Lemma relaxes some conditions, e.g. V is not required to be PD.

Example 2.8 (Stability of MIMO adaptive control for marine systems). The Lyapunov function for a MIMO marine system using adaptive control via feedback linearization will have the form

$$V = \frac{1}{2}\tilde{\eta}^T \mathbf{K}_p \tilde{\eta} + \frac{1}{2}\mathbf{s}^T \mathbf{M}_\eta(\eta)\mathbf{s} + \frac{1}{2}\tilde{\theta}^T \Gamma^{-1}\tilde{\theta},$$

where $\tilde{\theta} := (\hat{\theta} - \theta)$ is the parameter estimation error, $\mathbf{M}_\eta(\eta) = \mathbf{M}_\eta^T(\eta) > 0$ is the inertia tensor in the NED frame, $\mathbf{K}_p > 0$ is a diagonal control design matrix, $\Gamma = \Gamma^T > 0$ is a weighting matrix, and both $\tilde{\eta} := (\eta - \eta_d)$ and $\mathbf{s} := \dot{\tilde{\eta}} + \Lambda\tilde{\eta}$ are measures of the tracking error [4, 15], . The parameter $\Lambda > 0$ in $\mathbf{s}$ is also a diagonal control design matrix.

Here we show that in order for the closed loop system to be stable, the conditions of Lemma 2.1 must be satisfied.

The time derivative of V is

$$\dot{V} = -\tilde{\eta}^T \mathbf{K}_p \Lambda \tilde{\eta} - \mathbf{s}^T \left[\mathbf{D}_\eta(\mathbf{v},\eta) + \mathbf{K}_d\right]\mathbf{s} + \tilde{\theta}^T \Gamma^{-1}\left[\dot{\hat{\theta}} + \Gamma \Phi^T \mathbf{J}^{-1}(\eta)\mathbf{s}\right], \quad (2.82)$$

where $\mathbf{D}_\eta(\mathbf{v},\eta) = \mathbf{D}_\eta^T(\mathbf{v},\eta) > 0$ is the drag (dissipation) tensor in the NED frame and $\mathbf{K}_d > 0$ is a diagonal control design matrix. The first two terms in the above equation are negative definite for all $\mathbf{s} \neq 0$ and for all $\tilde{\eta} \neq 0$. To obtain $\dot{V} \leq 0$, the *parameter update law* is selected as

$$\dot{\hat{\theta}} = -\Gamma \Phi^T \mathbf{J}^{-1}(\eta)s.$$

However, it can be seen that $\dot{V}$ is still only negative semidefinite, not negative definite, because it does not contain any terms that are negative definite in $\tilde{\theta}$. As shown in [13], using the parameter update law, equation (2.82) can be written in the form

$$\dot{V} = -\tilde{\eta}^T \mathbf{K}_p \Lambda \tilde{\eta} - \mathbf{s}^T \left[\mathbf{D}_\eta(\mathbf{v},\eta) + \mathbf{K}_d\right]\mathbf{s} = -\mathbf{e}^T \mathbf{Q}\mathbf{e}, \quad (2.83)$$

where $\mathbf{Q} = \mathbf{Q}^T$ and $\mathbf{e} = [\tilde{\eta} \quad \dot{\tilde{\eta}}]^T$ is a vector of tracking errors. Since $\dot{V} \leq 0$, V is always less than or equal to its initial value V_0, so that $\tilde{\eta}$, $\dot{\tilde{\eta}}$, $\mathbf{s}$ and $\tilde{\theta}$ are necessarily bounded, if V_0 is finite.

If $\dot{V}$ is continuous in time, i.e. if $\ddot{V}$ is bounded in time (see Remark 2.9), then $\dot{V}$ will be integrable. If this condition is met, (2.83) can be integrated to obtain

$$V - V_0 = -\int_0^t \mathbf{e}^T \mathbf{Q}\mathbf{e}\, \mathrm{d}t < \infty, \quad (2.84)$$

which implies that $\mathbf{e}$ is a square integrable function and that $\mathbf{e} \to 0$ as $t \to \infty$ [13]. Note that, the condition that $\dot{V}$ is continuous requires $\dot{\tilde{\eta}}$ to also be continuous (it is a component of $\mathbf{e}$). In turn, this requires both $\ddot{\eta}$ and $\ddot{\eta}_d$ to be bounded. The equations of motion (1.35)–(1.36) can be used to verify that $\ddot{\eta}$ is bounded and restricting the permissible reference trajectories $\ddot{\eta}_d$ will ensure that $\dot{\tilde{\eta}}$ is continuous. Provided these latter conditions are satisfied, the velocity error also converges to zero $\dot{\tilde{\eta}} \to 0$. □

Problems

2.1. A CTD (conductivity-temperature-depth) sensor is an oceanographic instrument commonly used to measure profiles of the salinity and temperature of seawater vs. depth. A thermistor, a type of resistor whose resistance is dependent on temperature, is often used on CTDs as the temperature sensing element. The temperature response of a thermister is given by the relation

$$R = R_0 e^{-0.1T},$$

where R is resistance, T is temperature in $^\circ$C and $R_0 = 10 \times 10^3 \Omega$. Find a linear model of the thermister operating at $T = 20^\circ$C for a small range of temperature variations about this operating condition.

2.2. Use linear stability analysis to classify the fixed points, as either stable or unstable, for the following systems. If linear stability analysis fails because $f'(x) = 0$, use a graphical argument to determine the stability.

(a) $\dot{x} = x(2-x)$
(b) $\dot{x} = x(2-x)(4-x)$

2.3. Analyze the following equations graphically. In each case, sketch the vector field on the real line, find all of the fixed points, classify their stability (as either stable or unstable), and sketch the graph of $x(t)$ for different initial conditions.

(a) $\dot{x} = 2x^2 - 8$
(b) $\dot{x} = 2 + \cos x$

2.4. Analyze the stability of the dynamics (corresponding to a mass sinking in a viscous liquid)

$$\dot{u} + 2a|u|u + bu = c, \quad a > 0,\ b > 0.$$

2.5. Consider the heave motion of a spar buoy with the dynamics

$$m\ddot{z} + c\dot{z} + kz = 0.$$

A natural candidate for a Lyapunov function is the total energy of the system, given by

$$V = \frac{1}{2}m\dot{w}^2 + \frac{1}{2}kz^2,$$

where z is the vertical displacement of the buoy from its equilibrium position and $w = \dot{z}$ is the velocity in the heave direction. Use LaSalle's Invariance Principle to show that the system is asymptotically stable.

2.6. As shown in Example 2.4, the pitch angle θ of an AUV is governed by an equation of the form

$$\ddot{\theta} = \frac{c}{2}\sin(2\theta),$$

where $c > 0$ is a physical constant based on a model of the AUV. The use of a nonlinear control input $u = -k(V_0 - V)\dot{\theta}\cos^2(2\theta)$ is proposed to control the pitch, where

$$V(\theta, \dot{\theta}) = \frac{c}{4}\cos(2\theta) - 1 + \frac{1}{2}\dot{\theta}^2$$

is a Lyapunov function and V_0 is an estimate for the initial value of V. In practice, one might take V_0 to be an upper bound for the largest value of V.

With this controller, the closed loop equation of motion is

$$\ddot{\theta} = \frac{c}{2}\sin(2\theta) - k(V_0 - V)\dot{\theta}\cos^2(2\theta).$$

Show that the controller stabilizes the pitch angle of the AUV to $\theta = 0$.

2.7. The kinetic energy of a marine vehicle V_k is often included as one of the terms in a candidate Lyapunov functions used for control design. Let

$$V_k = \frac{1}{2}\mathbf{v}^T\mathbf{M}\mathbf{v},$$

where, in body-fixed coordinates, $\mathbf{M}$ is the inertial tensor and $\mathbf{v}$ is the velocity.

a) Show that the upper and lower bounds for V_k can be written as

$$\frac{1}{2}\lambda_{\min}(\mathbf{M})\|\mathbf{v}\|^2 \leq \frac{1}{2}\mathbf{v}^T\mathbf{M}\mathbf{v} \leq \frac{1}{2}\lambda_{\max}(\mathbf{M})\|\mathbf{v}\|^2.$$

Recall from Section 1.4.2 that $\mathbf{M} = \mathbf{M}^T > 0$.

b) When performing Lyapunov stability analysis one must typically show that $\dot{V} < 0$, which involves showing that each of the individual terms in the time derivative of the candidate Lyapunov function are negative definite. Use the inequality above to find an upper bound for $-\|\mathbf{v}\|^2$ (note that this is a negative value).

References

1. Antoine Chaillet and Antonio Loría. Uniform global practical asymptotic stability for time-varying cascaded systems. *European Journal of Control*, 12(6):595–605, 2006.
2. Antoine Chaillet and Antonio Loría. Uniform semiglobal practical asymptotic stability for non-autonomous cascaded systems and applications. *Automatica*, 44(2):337–347, 2008.
3. Odd M Faltinsen. *Hydrodynamics of high-speed marine vehicles*. Cambridge University Press, 2005.
4. Thor I Fossen. *Handbook of marine craft hydrodynamics and motion control*. John Wiley & Sons, 2011.
5. Thomas C Furfaro, Jeff E Dusek, and Karl D von Ellenrieder. Design, construction, and initial testing of an autonomous surface vehicle for riverine and coastal reconnaissance. In *OCEANS 2009*, pages 1–6. IEEE, 2009.

6. Esten Ingar Grotli, Antoine Chaillet, and Jan Tommy Gravdahl. Output control of spacecraft in leader follower formation. In *2008 47th IEEE Conference on Decision and Control*, pages 1030–1035. IEEE, 2008.
7. Hassan K Khalil. *Nonlinear systems*. Prentice Hall Englewood Cliffs, NJ, 3 edition, 2002.
8. Daniel Liberzon. *Switching in systems and control*. Springer Science & Business Media, 2012.
9. AE Perry and MS Chong. A description of eddying motions and flow patterns using critical-point concepts. *Annual Review of Fluid Mechanics*, 19:125–155, 1987.
10. Jean-Jacques E Slotine and Weiping Li. *Applied nonlinear control*. Prentice-Hall Englewood Cliffs, NJ, 1991.
11. SNAME. Nomenclature for treating the motion of a submerged body through a fluid: Report of the American Towing Tank Conference. Technical and Research Bulletin 1–5, Society of Naval Architects and Marine Engineers, 1950.
12. Eduardo D Sontag and Yuan Wang. On characterizations of the input-to-state stability property. *Systems & Control Letters*, 24(5):351–359, 1995.
13. Mark W Spong, Seth Hutchinson, and Mathukumalli Vidyasagar. *Robot modeling and control*. Wiley, 2006.
14. Steven H Strogatz. *Nonlinear dynamics and chaos: with applications to physics, biology, chemistry, and engineering*. Westview Press Boulder, CO, 2 edition, 2014.
15. Karl Dietrich von Ellenrieder. *Control of marine vehicles*. Springer, 2021.

Lecture 3
Control of Underactuated Marine Vehicles

Abstract The kinematics and dynamics of underactuated marine vehicles must be taken into account during control design, significantly more so than when developing controllers for fully-actuated vehicles. Here, we first present some of the specialized terminology used to define the main features of underactuated systems, the types of constraints (e.g. velocity and acceleration constraints) that make a vehicle underactuated, and the dynamics of underactuated marine vehicles. Then techniques for the trajectory tracking control of nonholonomic surface vessels are introduced.

3.1 Introduction

When designing motion control systems for marine vehicles, it is important to distinguish between under-actuated vehicles and fully-actuated vehicles. Underactuated systems cannot be arbitrarily moved from some initial pose to some final pose because they cannot generate control forces/moments along every degree of freedom (missing actuators), or because actuator magnitude constraints, or rate limits, restrict their ability to accelerate in a certain direction. It is generally easier to control a fully-actuated vehicle, while under-actuation puts limitations on the control objectives that can be satisfied. Unfortunately, full-actuation is often impractical, because of considerations involving cost, weight or energy consumption, and so most marine vehicles are under-actuated. Here, we will consider the trajectory tracking control of underactuated surface vessels.

In *trajectory tracking control* a marine vehicle must track a desired, time varying pose $\eta_d(t)$. If a fully-actuated vehicle does not have any actuator constraints, it can track any arbitrary time-dependent trajectory. However, even when a vehicle possesses actuators that can produce forces in any desired direction, when the forces required to maintain the speed or acceleration required to catch up to and track a rapidly varying pose exceed the capabilities of the actuators, the vehicle is considered to be underactuated. Here, we will focus on the case when a marine vehicle is missing an actuator along one of the desired directions of motion and explore the

use of its kinematics and dynamics to generate a dynamically feasible trajectory, which can then be tracked using a standard control approach.

A common philosophy for the design of controllers for underactuated systems is that, whenever possible, it is better to incorporate the natural open loop dynamics of an underactuated system into the control design, rather than trying to overcome them with a controller, because doing so requires fewer actuators and a lower control effort.

Lastly, it should be noted that a broad range of powerful control design techniques exists for the control of fully-actuated systems, including optimal control, robust control and adaptive control. The use of these techniques is possible because the structure of the dynamic equations, which govern fully-actuated vehicles, possesses special mathematical properties that facilitate the control design, such as feedback linearizeability, passivity, matching conditions, and linear parameterizeability. The application of one or more of these special mathematical properties is often not possible when a system is underactuated. In addition, undesirable mathematical characteristics, such as higher relative degree and nonminimum phase behavior are typically present in underactuated systems.

3.2 The terminology of underactuated vehicles

In order to analyze the motion and control of underactuated vehicles, knowledge of the following basic notation and terminology is needed.

Definition 3.1 (Configuration Space). The configuration of a marine vehicle specifies the location of every point on the vehicle. The n-dimensional *configuration space* is the set of all configurations, i.e the set of all possible positions and orientations that a vehicle can have, possibly subject to external constraints.

Definition 3.2 (Degrees of Freedom – DOF). A marine vehicle is said to have n *degrees of freedom* if its configuration can be minimally specified by n parameters. Therefore, the number of DOF is the same as the number of dimensions of the configuration space. The set of DOF is the set of independent displacements and rotations that completely specify the displaced position and orientation of the vehicle. A rigid body, such as a marine vehicle, that can freely move in three dimensions has six DOF: three translational DOF (linear displacements) and three rotational DOF (angular displacements).

When simulating the motion of a vehicle with 6 DOF, a system of 12 first-order, ordinary differential equations are needed — 6 for the kinematic relations and 6 for the kinetic equations of motion. The *order of a system* of the system of equations required to model a vehicle's motion is two times the number of its degrees of freedom n.

Definition 3.3 (Number of Independent Control Inputs). The *number of independent control inputs r* is the number of *independently controlled directions* in which a vehicle's actuators can generate forces/moments.

Definition 3.4 (Underactuated Marine Vehicles). A marine vehicle is *underactuated* if it has fewer control inputs than generalized coordinates $(r < n)$.

Definition 3.5 (Fully Actuated Marine Vehicles). A marine vehicle is *fully actuated* if the number of control inputs is equal to, or greater than, the number of generalized coordinates $(r \geq n)$.

Definition 3.6 (Workspace). An underactuated vehicle can only produce independent control forces in $r < n$ directions. Therefore, when developing a controller, it makes sense to explore whether or not a space of fewer dimensions $m < n$ might exist in which the vehicle can be suitably controlled. Following [4], we define the workspace as the reduced space of dimension $m < n$ in which the control objective is defined.

In the parlance of feedback linearization, the processes of stabilization, path following control and trajectory tracking generally involve input–output linearization. For these processes, the controlled outputs are the pose or velocity of a vehicle. Underactuated vehicles have more states in their configuration space n than independent control inputs r. Because of this, some vehicle states are uncontrollable (unreachable). Thus, while it is possible to design a motion control system for an underactuated marine vehicle when its workspace is fully-actuated $m = r$, one must ensure that the zero dynamics of the closed loop system are stable when the dimension of the configuration space is reduced to that of the workspace. The uncontrolled equations of motion will appear as k dynamic constraints that must have bounded solutions in order to prevent the system from becoming unstable.

3.3 Motion Constraints

In general, the constraints affecting a system can arise from both input and state constraints. Examples of dynamic constraints include missing actuators, but could also be caused by the magnitude or rate limitations of those actuators which are present. Constraints can also arise because of a physical barrier in the environment, e.g. a ship is generally constrained to move along the free surface of the water.

Constraints, which depend on both vehicle state and inputs can be expressed in the form

$$h(\boldsymbol{\eta}, \mathbf{u}, t) \geq 0. \tag{3.1}$$

Often the constraints are separated into those that depend only on the input (e.g. actuator constraints, also called *input constraints*) $h(\mathbf{u}) \geq 0$ and those that depend on the vehicle pose $h(\boldsymbol{\eta}) \geq 0$, which are known as *state constraints*. As $\boldsymbol{\eta}$ is an n-dimensional vector, if k geometric constraints exist,

$$h_i(\boldsymbol{\eta}) \geq 0, \quad i = 1, \ldots, k \tag{3.2}$$

the possible motions of the vehicle are restricted to an $(n-k)$-dimensional submanifold (space). Thus, the state constraints reduce the dimensionality of the system's available state space.

When the constraints have the form

$$h_i(\eta) = 0, \quad i = 1, \ldots, k < n, \tag{3.3}$$

they are known as *holonomic constraints*.

System constraints that depend on both the pose and its first time derivative are *first order constraints*

$$h_i(\eta, \dot{\eta}) = 0, \quad i = 1, \ldots, k < n, \tag{3.4}$$

and are also called *kinematic constraints*, or *velocity constraints*. First order kinematic constraints limit the possible motions of a vehicle by restricting the set of velocities $\dot{\eta}$ that can be obtained in a given configuration. These constraints are usually encountered in the form

$$\mathbf{A}^T(\eta)\dot{\eta} = 0. \tag{3.5}$$

Holonomic constraints of the form (3.3) imply kinematic constraints of the form

$$\nabla h \cdot \dot{\eta} = 0. \tag{3.6}$$

However, the converse is not true. Kinematic constraints of the form (3.5) cannot always be integrated to obtain constraints of the form (3.3). When this is true, the constraints (and the system) are *nonholonomic*.

Note that (3.4) is a first order constraint. However, in many underactuated systems, including marine systems, the nonholonomic (non integrable) constraints are usually of second order and involve the acceleration of the system. They can be represented in the form

$$h_i(\eta, \dot{\eta}, \ddot{\eta}) = 0, \quad i = 1, \ldots, k < n. \tag{3.7}$$

Nonholonomic constraints limit the mobility of a system in a completely different way from holonomic constraints. A nonholonomic constraint does not restrain the possible configurations of the system, but rather how those configurations can be reached. While nonholonomic constraints confine the velocity or acceleration of a system to an $m = (n-k)$ dimensional subspace (the workspace), the entire n dimensional configuration space of the system can still be reached. Instead, each holonomic constraint reduces the number of degrees of freedom of a system by one, so that the motion of a holonomic system with k constraints is constrained to an $(n-k)$ dimensional subset of the full n dimensional configuration space [3].

3.4 The dynamics of underactuated surface vessels

In three DOF, the kinematic equations are

$$\dot{\eta} = \mathbf{R}(\psi)\mathbf{v}, \tag{3.8}$$

where ψ is the heading angle of the vehicle, $\mathbf{R}(\psi)$ is the transformation matrix from the body-fixed system to the a North-East-Down (NED) inertial coordinate system, which is given by

$$\mathbf{R}(\psi) := \begin{bmatrix} \cos\psi & -\sin\psi & 0 \\ \sin\psi & \cos\psi & 0 \\ 0 & 0 & 1 \end{bmatrix} \in SO(3), \tag{3.9}$$

and

$$\eta := \begin{bmatrix} x_n \\ y_n \\ \psi \end{bmatrix} \in \mathbb{R}^2 \times \mathcal{S}, \quad \text{and} \quad \mathbf{v} := \begin{bmatrix} u \\ v \\ r \end{bmatrix} \in \mathbb{R}^3 \tag{3.10}$$

are the position and orientation (pose) vector and velocity vector (in body-fixed coordinates), respectively (see Fig. 3.1). The variables appearing in (3.10) include position Northward x_n, position Eastward y_n, surge speed u, sway speed v and yaw rate r.

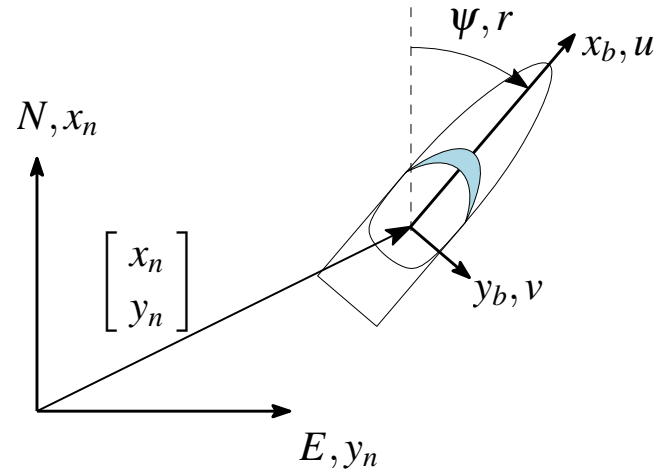

Fig. 3.1 3 DOF maneuvering coordinate system definitions.

Consider the kinetic equation of motion

$$\mathbf{M}\dot{\mathbf{v}} + \mathbf{C}(\mathbf{v})\mathbf{v} + \mathbf{D}(\mathbf{v})\mathbf{v} = \tau. \tag{3.11}$$

Assuming that the origin of the body-fixed coordinate system is the located at the center of mass of the vessel and the vehicle is moving through still water,

$$\mathbf{M} := \begin{bmatrix} m - X_{\dot{u}} & 0 & 0 \\ 0 & m - Y_{\dot{v}} & -Y_{\dot{r}} \\ 0 & -N_{\dot{v}} & I_z - N_{\dot{r}} \end{bmatrix} = \begin{bmatrix} m_{11} & 0 & 0 \\ 0 & m_{22} & m_{23} \\ 0 & m_{32} & m_{33} \end{bmatrix}, \tag{3.12}$$

$$\mathbf{C}(\mathbf{v}) := \begin{bmatrix} 0 & 0 & -m_{22}v - \dfrac{(m_{23}+m_{32})}{2}r \\ 0 & 0 & m_{11}u \\ m_{22}v + \dfrac{(m_{23}+m_{32})}{2}r & -m_{11}u & 0 \end{bmatrix}, \tag{3.13}$$

$$\mathbf{D}_{nl}(\mathbf{v}) := -\begin{bmatrix} X_{u|u|}|u| & 0 & 0 \\ 0 & Y_{v|v|}|v| + Y_{v|r|}|r| & Y_{r|v|}|v| + Y_{r|r|}|r| \\ 0 & N_{v|v|}|v| + N_{v|r|}|r| & N_{r|v|}|v| + N_{r|r|}|r| \end{bmatrix}, \tag{3.14}$$

$$\mathbf{D}_l := -\begin{bmatrix} X_u & 0 & 0 \\ 0 & Y_v & Y_r \\ 0 & N_v & N_r \end{bmatrix}. \tag{3.15}$$

where m is the mass of the vehicle, I_z is the mass moment of inertia about the z_b axis of the vehicle, and $X_{u|u|} < 0$ is the drag coefficient along the longitudinal axis of the vehicle.

Here, the Society of Naval Architects and Marine Engineers (SNAME) [5] nomenclature is used to represent the hydrodynamic coefficients (added mass and drag), which give rise to the forces and moments on the vessel in the body-fixed frame. The X coefficients give rise to forces in the surge direction, the Y coefficients give rise to forces in the sway direction and the N coefficients give rise to moments about the yaw axis. The subscript(s) on each coefficient correspond to the velocities of the vessel in the body-fixed frame, and denote(s) the motion which gives rise to the corresponding force/moment. For example, the coefficient $X_{\dot{u}}$ characterizes the surge force arising from acceleration in the surge direction (i.e. it is an *added mass* term).

The total drag $\mathbf{D}(\mathbf{v})\mathbf{v}$ is obtained by combining the nonlinear drag $\mathbf{D}_{nl}(\mathbf{v})\mathbf{v}$ with the linear drag $\mathbf{D}_l\mathbf{v}$, as

$$\mathbf{D}(\mathbf{v})\mathbf{v} = [\mathbf{D}_{nl}(\mathbf{v}) + \mathbf{D}_l]\,\mathbf{v} = \begin{bmatrix} d_x \\ d_y \\ d_\psi \end{bmatrix}. \tag{3.16}$$

Then, expanding terms, the equations of motion can be rewritten component-wise as

$$m_{11}\dot{u} - m_{22}vr - \left(\frac{m_{23}+m_{32}}{2}\right)r^2 + d_x = \tau_x, \tag{3.17}$$

$$m_{22}\dot{v} + m_{23}\dot{r} + m_{11}ur + d_y = 0, \tag{3.18}$$

$$m_{32}\dot{v} + m_{33}\dot{r} + (m_{22}-m_{11})uv + \left(\frac{m_{23}+m_{32}}{2}\right)ur + d_\psi = \tau_\psi. \tag{3.19}$$

Let $\mathbf{x} := [x_n \;\; y_n \;\; \psi \;\; u \;\; v \;\; r]^T$. We express the combined kinematic and dynamic equations vectorially by first solving for $\dot{u}$, $\dot{v}$ and $\dot{r}$ from (3.17)–(3.19) and then assembling the resulting equations into vector form. From (3.17) we have

$$\begin{aligned}\dot{u} &= \frac{1}{m_{11}}\left[m_{22}vr + \left(\frac{m_{23}+m_{32}}{2}\right)r^2 - d_x\right] + \frac{\tau_x}{m_{11}}. \\ &= f_x + \frac{\tau_x}{m_{11}}.\end{aligned} \tag{3.20}$$

Dividing (3.18) by m_{22} and (3.19) by m_{33}, they can be written as

$$\begin{aligned}\dot{v} + \frac{m_{23}}{m_{22}}\dot{r} &= -\frac{1}{m_{22}}\left[m_{11}ur + d_y\right], \\ &= f'_y,\end{aligned} \tag{3.21}$$

and

$$\begin{aligned}\frac{m_{32}}{m_{33}}\dot{v} + \dot{r} &= -\frac{1}{m_{33}}\left[(m_{22}-m_{11})uv + \left(\frac{m_{23}+m_{32}}{2}\right)ur + d_\psi\right] + \frac{\tau_\psi}{m_{33}}, \\ &= f'_\psi + \frac{\tau_\psi}{m_{33}},\end{aligned} \tag{3.22}$$

respectively.

These latter two equations can be decoupled by multiplying (3.21) by m_{23}/m_{22}, subtracting the result from (3.22) and solving for $\dot{v}$. Similarly, one can find the decoupled differential equation for $\dot{r}$ by multiplying (3.22) by m_{32}/m_{33}, subtracting the result from (3.21) and solving for $\dot{r}$. The decoupled equations are

$$\begin{aligned}\dot{v} &= a_\psi\left[f'_y - \frac{m_{23}}{m_{22}}f'_\psi\right] + a_y\frac{\tau_\psi}{m_{33}}, \\ &= f_y + a_y\frac{\tau_\psi}{m_{33}},\end{aligned} \tag{3.23}$$

and

$$\begin{aligned}\dot{r} &= a_\psi\left[f'_\psi - \frac{m_{32}}{m_{33}}f'_y\right] + a_\psi\frac{\tau_\psi}{m_{33}}, \\ &= f_\psi + a_\psi\frac{\tau_\psi}{m_{33}},\end{aligned} \tag{3.24}$$

where

$$a_\psi = \frac{m_{22}m_{33}}{m_{22}m_{33} - m_{23}m_{32}} \quad \text{and} \quad a_y = -\frac{m_{23}}{m_{22}}a_\psi. \tag{3.25}$$

Then, from (3.8)–(3.10), (3.20) and (3.23)–(3.25) we have

$$\dot{\mathbf{x}} = \begin{bmatrix} u\cos\psi - v\sin\psi \\ u\sin\psi + v\cos\psi \\ r \\ f_x \\ f_y \\ f_\psi \end{bmatrix} + \begin{bmatrix} 0 \\ 0 \\ 0 \\ \dfrac{1}{m_{11}} \\ 0 \\ 0 \end{bmatrix} \tau_x + \begin{bmatrix} 0 \\ 0 \\ 0 \\ 0 \\ \dfrac{a_y}{m_{33}} \\ \dfrac{a_\psi}{m_{33}} \end{bmatrix} \tau_\psi, \tag{3.26}$$

which has the form

$$\dot{\mathbf{x}} = \mathbf{f}(\mathbf{x}) + \mathbf{g}_1\tau_x + \mathbf{g}_2\tau_\psi.$$

We will first explore the problem of stabilizing nonholonomic systems, as it provides the underlying rationale for the commonly used strategy of separating the control of underactuated vehicles into a motion planning problem and a feedback control problem, and then proceed to investigate the path following control and trajectory tracking of underactuated surface vessels.

3.5 Trajectory tracking for underactuated surface vessels

When planning a trajectory for an underactuated surface vessel, two important considerations must be taken into account.

1) The trajectory should be *dynamically feasible*. The dynamics of many surface vessels must satisfy second order nonholonomic acceleration constraints. By taking the dynamics of the vehicle into account (in particular its inertial and drag properties, as well as any unactuated directions) when planning a trajectory between a start point $(x(t_0), y(t_0)) = (x_0, y_0)$ and an endpoint $(x(t_f), y(t_f)) = (x_f, y_f)$, where t_0 is the time when the vehicle is located at the start point and t_f is the time the vehicle is located at the end point, one can be more certain that the closed loop system will be capable of tracking the planned trajectory.
2) Some control design methods include second order or higher order time derivatives of the desired trajectory in the control input. To ensure that the associated control inputs are bounded, one must plan trajectories which have smooth higher order derivatives in time.

Here, the approach for computing the dynamically feasible heading proposed in [1] is presented. An advantage of the method is that it can also be used to compute the surge force and yaw moment required to achieve the dynamically feasible heading,

which can be used for either open loop control of an underactuated vessel, or as feedforward control inputs in a two degree of freedom controller.

3.5.1 Desired heading and feedforward control inputs

Once we have a time-dependent set of $x_d(t), y_d(t)$ positions that we would like to follow, we need to determine the corresponding values of $\psi(t)$ that are dynamically feasible. To do this, we start by using the kinematic equations of motion to determine what the corresponding sway acceleration $\dot{v}_d$ at each instant in time would be. While an underactuated vehicle cannot directly apply a force in the sway direction, for most marine vehicles the kinetic equations of motion for sway and yaw are coupled via the added mass terms occurring in their inertia tensors. We take advantage of this coupling to find a virtual control input relating the time derivative of the yaw rate $\dot{r}$ to $\dot{v}_d$. The method shown here was developed by [1].

From (3.8) and (3.9), the velocity of the vessel in the body-fixed frame can be related to its velocity in the inertial (NED) frame, as

$$\mathbf{v} = \mathbf{R}^{-1}(\psi)\dot{\eta} = \mathbf{R}^{T}(\psi)\dot{\eta}.$$

From this, one can obtain an expression of the sway speed v in terms of the velocities in the NED frame as

$$v = -\dot{x}_n \sin\psi + \dot{y}_n \cos\psi.$$

Let $(x_d(t), y_d(t))$ be a sufficiently smooth trajectory designed using a point-to-point planning method represented in the NED reference frame. Then, the desired sway speed $v_d(t)$ is given by

$$v_d(t) = -\dot{x}_d \sin\psi + \dot{y}_d \cos\psi.$$

Taking the time derivative of this gives the desired sway acceleration

$$\dot{v}_d(t) = -\ddot{x}_d \sin\psi - \dot{x}_d r\cos\psi + \ddot{y}_d \cos\psi - \dot{y}_d r\sin\psi. \tag{3.27}$$

Next we turn to the kinetic equations of motion to find the relationship between $\dot{r}$ and $\dot{v}_d$. Using (3.24), we can eliminate τ_ψ in (3.23) to get

$$\dot{v} = f_y + \frac{a_y}{a_\psi}\left[\dot{r} - f_\psi\right]. \tag{3.28}$$

To find the virtual control input $\dot{r}_d$ that gives the heading angle required for a dynamically feasible trajectory, define the sway acceleration error as $\tilde{\dot{v}} := \dot{v} - \dot{v}_d$, where $\dot{v}_d$ is given by (3.27). Then, using (3.28) we have

$$\tilde{\dot{v}} = f_y + \frac{a_y}{a_\psi}\left[\dot{r} - f_\psi\right] - \dot{v}_d,$$

so that the virtual control input $\dot{r}_d$ that makes $\dot{\tilde{v}} = 0$ is given by

$$\dot{r}_d = \frac{a_\psi}{a_y}\left[\dot{v}_d - f_y\right] + f_\psi. \tag{3.29}$$

Thus, given a desired trajectory $(x_d(t), y_d(t))$ one can completely specify the dynamically feasible time-dependent pose $\eta_d(t) = [x_d \;\; y_d \;\; \psi_d]^T$ of an underactuated surface vessel using the associated sway acceleration $\dot{v}_d(t)$ from (3.27) and integrating (3.29) twice to obtain the desired heading angle $\psi_d(t)$, subject to the initial conditions $\psi_d(t = t_0)$ and $\dot{\psi}_d(t = t_0)$.

Further, (3.20) and (3.24) can be used to find a set of feedforward control inputs that can be used in a two degree of freedom control system architecture for trajectory tracking. To do this, use (3.9) to obtain an expression for the desired surge speed u_d in terms of the desired velocities in the NED frame, as

$$u_d = \dot{x}_d \cos\psi + \dot{y}_d \sin\psi.$$

The desired surge acceleration is then

$$\dot{u}_d = \ddot{x}_d \cos\psi - \dot{x}_d r \sin\psi + \ddot{y}_d \sin\psi + \dot{y}_d r \cos\psi.$$

Replacing $\dot{u}$ with $\dot{u}_d$ in (3.20) gives the feedforward surge control input

$$\tau_x = m_{11}\left(\dot{u}_d - f_x\right), \tag{3.30}$$

and similarly replacing $\dot{r}$ with $\dot{r}_d$ in (3.24) gives the feedforward yaw moment control input

$$\tau_\psi = \frac{m_{33}}{a_\psi}\left(\dot{r}_d - f_\psi\right), \tag{3.31}$$

that will produce the desired dynamically feasible trajectory in the absence of disturbances. A separate feedback controller can be used to ensure that the system is robust to disturbances and modeling uncertainties.

Example 3.1 (USV trajectory planning). Consider the problem of constructing dynamically feasible trajectories for a USV with the following inertial properties

$$M = \begin{bmatrix} 189.0 & 0.0 & 0.0 \\ 0.0 & 1036.4 & -543.5 \\ 0.0 & -543.5 & 2411.1 \end{bmatrix}.$$

The drag is assumed to be linear and is modeled with the following coefficients

$$D = \begin{bmatrix} 50.0 & 0.0 & 0.0 \\ 0.0 & 948.2 & 385.4 \\ 0.0 & 385.4 & 1926.9 \end{bmatrix}.$$

Using these values in (3.25) a_y and a_ψ are found to be

$$a_y = 0.595 \quad \text{and} \quad a_\psi = 1.134.$$

Here we will examine three cases:

a) The vehicle moves in a straight line from an initial point $(x_0, y_0) = (0,0)$ at $t_0 = 0$ to a final point $(x_f, y_f) = (-30,-30)$ at $t_f = 50$ secs, where the (x,y) coordinates are specified in meters. The initial velocity of the USV is 1 m/s in the northward (x) direction. Here, the trajectory is designed using a cubic polynomial.
b) The vehicle moves in a straight line from an initial point $(x_0, y_0) = (0,0)$ at $t_0 = 0$ to a final point $(x_f, y_f) = (-30,0)$ at $t_f = 50$ secs, where the (x,y) coordinates are specified in meters. The initial velocity of the USV is 1 m/s in the northward (x) direction. Here, the trajectory will designed using a quintic (5^{th} order) polynomial.
c) The vehicle follows a circular trajectory of radius $R = 10$ m in the clockwise direction, starting from $(x_0, y_0) = (0,0)$ at $t_0 = 0$ and finishing at the same position $(x_f, y_f) = (0,0)$ at $t_f = 50$ secs, where the (x,y) coordinates are specified in meters. The center of the circle is located at the point $(x_c, y_c) = (0,10)$.

Case a: In the first case, a cubic polynomial is selected to represent the trajectory. The $x_d(t)$ and $y_d(t)$ positions along the trajectory are given by

$$x_d(t) = t - 0.076t^2 + 8.8 \times 10^{-4} t^3,$$
$$y_d(t) = -0.036t^2 + 4.8 \times 10^{-4} t^3.$$

These $x_d(t)$ and $y_d(t)$ positions and the corresponding desired heading angle $\psi_d(t)$ are shown in Fig. 3.2. Since the USV has an initial heading and speed northward, it must rotate counterclockwise to reach $(x_f, y_f) = (-30,-30)$. As can be seen in Fig. 3.3 the vehicle dynamics predict that the vehicle will have a sway speed as it executes the turn to the southwest and that there will be some oscillation in both the surge speed and yaw rate. The corresponding control inputs oscillate during the turn. As a cubic polynomial is used for trajectory planning, even though the desired surge speed is zero at (x_f, y_f), the control input is nonzero at the end of the trajectory. This will result in a jerk at the end of the trajectory.

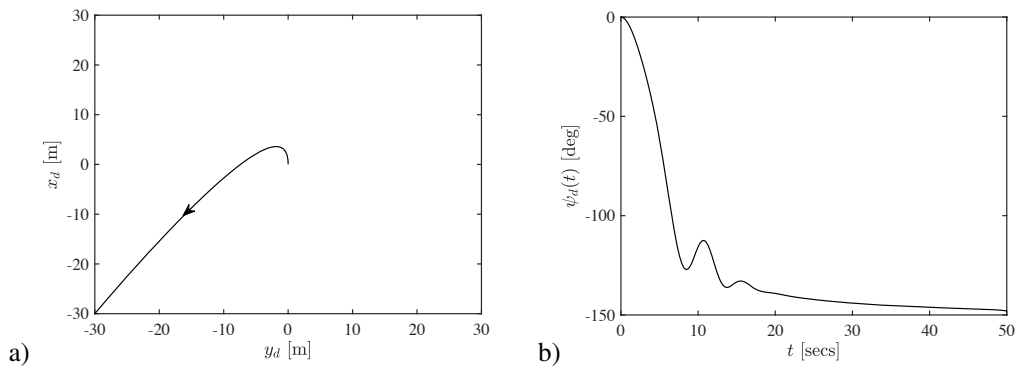

Fig. 3.2 Case a: a) trajectory and b) desired heading angle.

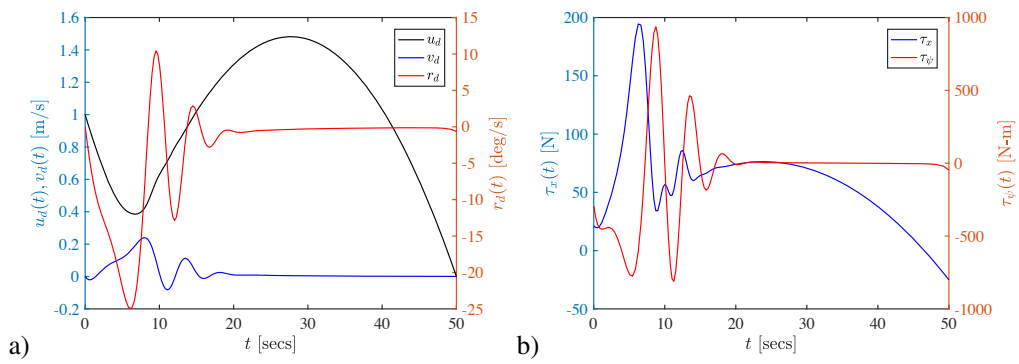

Fig. 3.3 Case a: a) desired body-fixed velocities and b) control inputs.

Case b: In the second case, a 5$^{\text{th}}$ order polynomial of the form

$$x(t) = a_0 + a_1 t + a_2 t^2 + a_3 t^3 + a_4 t^4 + a_5 t^5 \tag{3.32}$$

is used to represent the trajectory. The coefficients are determined writing a system of equations describing the endpoint constraints in matrix form and solving for the coefficients as a vector [6]. The resulting desired trajectory is

$$\begin{aligned} x_d(t) &= t - 4.80 \times 10^{-3} t^3 + 1.36 \times 10^{-4} t^4 - 1.06 \times 10^{-6} t^5, \\ y_d(t) &= 0. \end{aligned}$$

As can be seen in Figs. 3.4–3.5, the vehicle does not need to turn to perform this maneuver and $\psi_d(t) = 0$ throughout the trajectory. Since the $x_d(t)$ and $y_d(t)$ positions determined using the polynomial require the vehicle to move forward for several seconds, the τ_x control input remains positive for about 10 seconds, before reversing to drive the vehicle backwards towards the final point at $(x_f, y_f) = (-30, 0)$. Note that the desired surge speed and the surge control input both smoothly approach zero as the vehicle approaches the end of the trajectory.

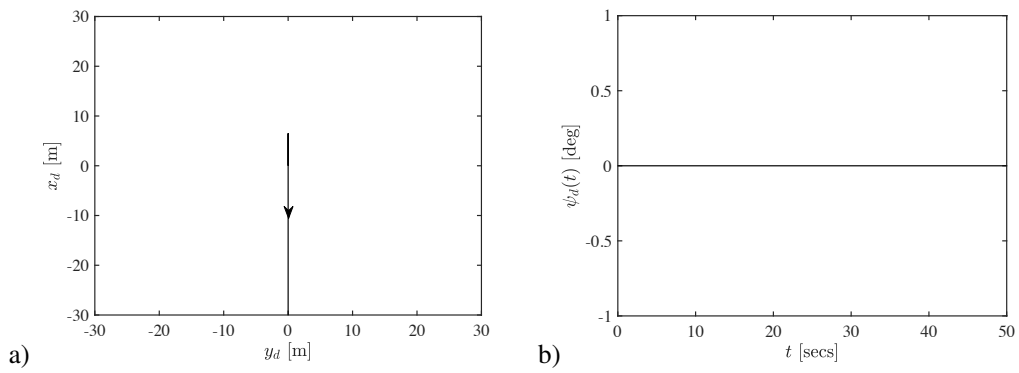

Fig. 3.4 Case b: a) trajectory and b) desired heading angle.

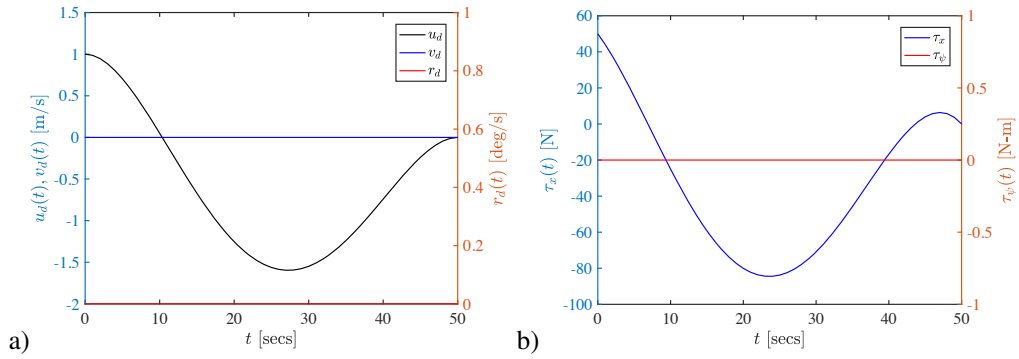

Fig. 3.5 Case b: a) desired body-fixed velocities and b) control inputs.

Case c: In the third case, the trajectory is given by

$$x_d(t) = R\sin(\omega_d t),$$
$$y_d(t) = R[1-\cos(\omega_d t)],$$

where $\omega_d = 2\pi/t_f$. After a small initial transient, the desired yaw rate becomes constant so that $r_d = \omega_d$ (see Figs. 3.6–3.7). In order to maintain the turn, vehicle has a small desired sway speed v_d yaw moment control input τ_ψ throughout the trajectory.

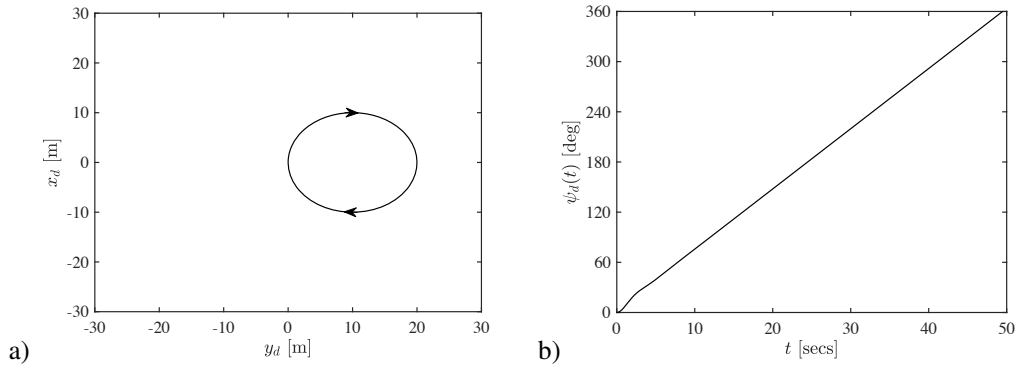

Fig. 3.6 Case c: a) trajectory and b) desired heading angle.

□

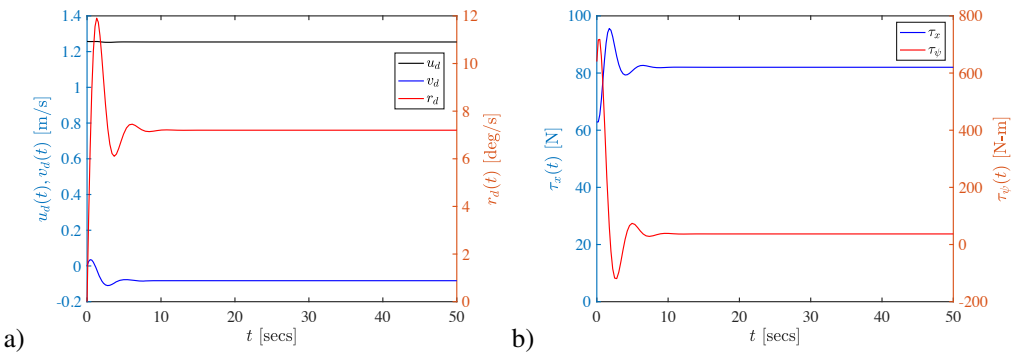

Fig. 3.7 Case c: a) desired body-fixed velocities and b) control inputs.

Problems

3.1. A USV is propelled using a pair of small thrusters, which are positioned at the locations

$$\mathbf{r}_p := -l_t\hat{i} - \frac{b_t}{2}\hat{j},$$

$$\mathbf{r}_s := -l_t\hat{i} + \frac{b_t}{2}\hat{j},$$

where l_t is the distance aft of the center of gravity and b_t is the transverse distance between the thrusters (see Fig. 3.8). Each thruster is oriented so that the thrust produced is parallel to the surge axis of the vehicle, i.e. $\mathbf{T}_p = T_p\hat{i}$ and $\mathbf{T}_s = T_s\hat{i}$. Write the three component vector of control forces $\tau = [\tau_x \;\; \tau_y \;\; \tau_\psi]^T$.

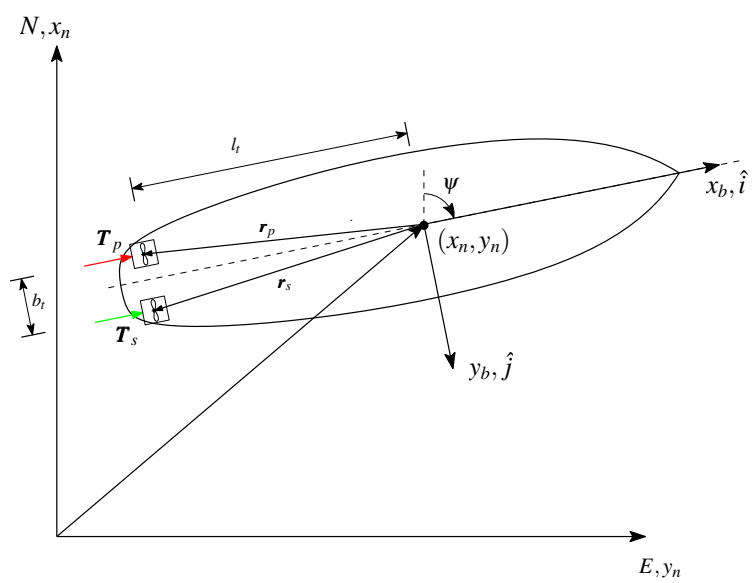

Fig. 3.8 USV thruster configuration (view from top).

3.2. An AUV operates in 6 DOF.

a) What is the dimension of its configuration space n?
b) Write the generalized position (pose) η as a column vector, showing each of its components.
c) Write the body-fixed velocity $\mathbf{v}$ as a column vector, showing each of its components.
d) What is the order of the system of equations needed to describe the AUV's motion?
e) Suppose the AUV employs a set of 4 independently controlled fore-aft tunnel thrusters that produce forces in the heave and sway directions, a moving mass system to produce a torque about its roll axis and a propeller at its stern to produce thrust along its surge axis (Fig. 3.9a). What is the number of independent control inputs r? Is the vehicle fully-actuated or underactuated?
f) Suppose the stern of the AUV has a propeller, a set of elevator planes that move in unison (i.e. they are connected by a rigid shaft and are constrained to by the same amount in the same direction), and a set of rudder planes that move in unison (Fig. 3.9b). What is the number of independent control inputs r? Is the vehicle fully-actuated or underactuated?

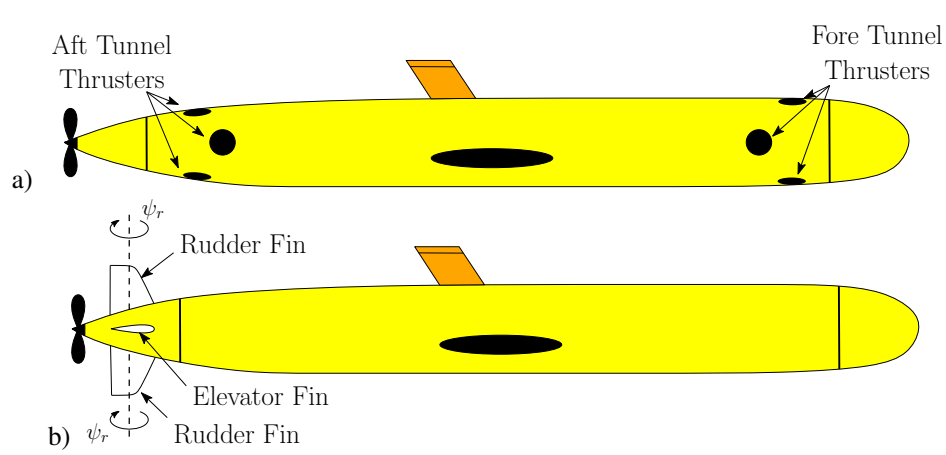

Fig. 3.9 An AUV steered using a) fore-aft tunnel thrusters and b) rudder and elevator planes (fins) at the stern.

3.3. A surface vessel restricted to operate in the horizontal plane (surge, sway and yaw).

a) What is the dimension of its configuration space n?
b) Write the generalized position (pose) η as a column vector, showing each of its components.
c) Write the body-fixed velocity $\mathbf{v}$ as a column vector, showing each of its components.
d) What is the order of the system of equations needed to describe the surface vessel's motion?

e) Suppose that the surface vessel uses two fixed thrusters at its stern, like that shown in Fig. 3.8. What is the number of independent control inputs r? Is the vehicle fully-actuated or underactuated?
f) Suppose the surface vessel uses two azimuthing thrusters at its stern, like that shown in Fig. 3.10. What is the number of independent control inputs r? Is the vehicle fully-actuated or underactuated?

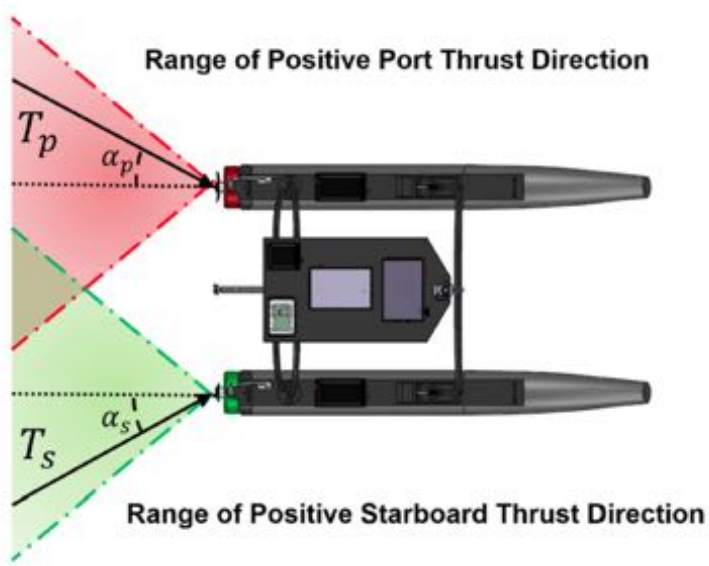

Fig. 3.10 Top view of a surface vessel with azimuthing thrusters (from [2]).

3.4. You are designing a trajectory tracking controller for an underactuated surface vessel, as shown in Fig. 3.11. The desired trajectory is a circle of constant radius. Is it possible to control the vehicle so that the desired heading $\psi_d(t)$ is always tangent to the circle? Explain your reasoning.

[Hint: you may want to consider the results in Case c of Example 3.1 and Figs. 3.6–3.7 while formulating your response.]

References

1. Hashem Ashrafiuon, Sergey Nersesov, and Garrett Clayton. Trajectory tracking control of planar underactuated vehicles. *IEEE Trans Autom Control*, 62(4):1959–1965, 2017.
2. I. Bertaska and K. von Ellenrieder. Experimental evaluation of supervisory switching control for unmanned surface vehicles. *IEEE J. Oceanic Eng.*, 44(1):7–28, 2019.
3. Alessandro De Luca and Giuseppe Oriolo. Modelling and control of nonholonomic mechanical systems. In *Kinematics and dynamics of multi-body systems*, pages 277–342. Springer, 1995.
4. Thor I Fossen. *Handbook of marine craft hydrodynamics and motion control*. John Wiley & Sons, 2011.

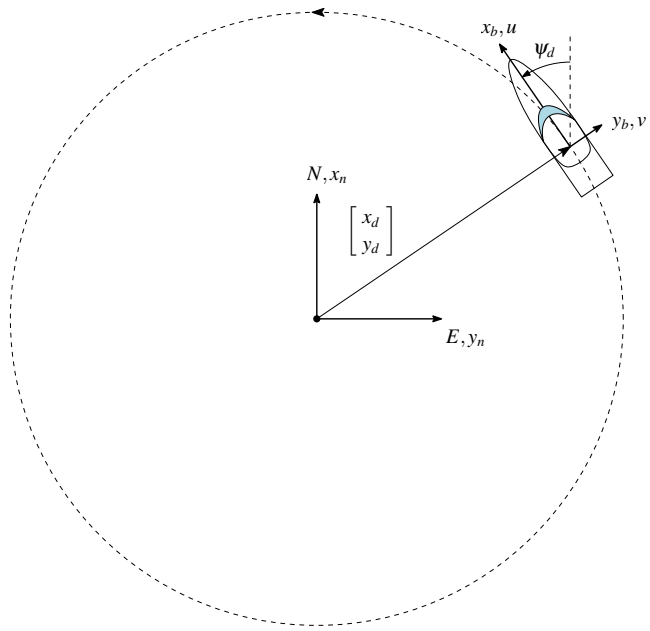

Fig. 3.11 A surface vessel tracking a circular trajectory.

5. SNAME. Nomenclature for treating the motion of a submerged body through a fluid: Report of the American Towing Tank Conference. Technical and Research Bulletin 1–5, Society of Naval Architects and Marine Engineers, 1950.
6. Karl Dietrich von Ellenrieder. *Control of marine vehicles*. Springer, 2021.

Lecture 4
Feedback Linearization & Backstepping

Abstract The method of feedback linearization via inverse dynamics is presented. The concepts involved in the use of integrator backstepping techniques are introduced starting with a simple single input, single output system and then examining multiple input multiple output vectorial integrator backstepping for marine systems. Backstepping methods are fairly complex and there are several related implementation issues, such as the required smoothness of desired trajectories and how to perform the real-time differentiation of stabilizing functions. Methods for handling these issues are briefly discussed.

4.1 Introduction

Feedback linearization can be used to transform the nonlinear dynamics of a vehicle into a linear system upon which conventional linear control techniques can be applied. Provided that the full state of a system can be measured, and that a general observability condition holds, it may be possible to identify nonlinear transformations that leave the transformed system linear. A linear controller is then designed for the transformed model and the control input signal from the linear controller is transformed back into a nonlinear signal before being passed to the actuators/plant. In this way, knowledge of the nonlinearities in the system are built into the controller. Feedback linearization is very different from simply linearizing a nonlinear system about one or more operating points, using a Taylor's series expansion for example, and then designing a controller for the linearized system. Instead, feedback linearization is accomplished by an exact state transformation and feedback.

Nonlinear backstepping is a recursive design procedure for constructing feedback control laws and their associated Lyapunov functions. The approach is systematic, flexible and can be applied in vectorial form to MIMO systems. Backstepping can permit a control designer to exploit "good" nonlinearities, while "bad" nonlinearities can be dominated by adding nonlinear damping, for instance. Hence, it is often possible to obtain additional robustness to model uncertainty and exogenous

(externally-generated) disturbances, which is important for the control of marine vehicles because it is typically difficult to obtain precise models in practice. The most basic form of backstepping generally leads to proportional-derivative-like controllers. Because of its versatility, backstepping is often combined with other control methods, such as optimal control and adaptive control. The backstepping methodology also makes it fairly straightforward to handle actuator constraints. Lastly, a significant advantage of backstepping controllers is that they have globally bounded tracking errors. Because of these advantages, backstepping is one of the most widely used type of control for marine vehicles.

However, a serious drawback is that the implementation of a backstepping controller often involves an *explosion of complexity*, whereby differentiation of the plant model requires that a very large number of terms be included in the computation of the control law.

4.2 Inverse Dynamics

Inverse dynamics is a special case of input-output feedback linearization. For marine vehicles, inverse dynamics can be separated into velocity control in the body-fixed frame and position and attitude (pose) control in the NED frame [1].

4.2.1 Body-fixed Frame Inverse Dynamics

Consider the kinetic equation of motion for a marine vehicle,

$$\mathbf{M}\dot{\mathbf{v}} + \mathbf{C}(\mathbf{v})\mathbf{v} + \mathbf{D}(\mathbf{v})\mathbf{v} + \mathbf{g}(\eta) = \tau.$$

A control input

$$\tau = \mathbf{f}(\eta, \mathbf{v}, t)$$

that linearizes the closed loop system is sought. By inspection, it can be seen that if a control input of the form

$$\tau = \mathbf{M}\mathbf{a}_b + \mathbf{C}(\mathbf{v})\mathbf{v} + \mathbf{D}(\mathbf{v})\mathbf{v} + \mathbf{g}(\eta)$$

can be found, the equation of motion reduces to

$$\dot{\mathbf{v}} = \mathbf{a}_b,$$

where $\mathbf{a}_b$ can be thought of as the commanded acceleration of the vehicle in the body-fixed frame. This new system is linear. Further, if the input $\mathbf{a}_b$ is designed so that each of its components are decoupled, i.e. so that a_{bi} is only a function of η_i and v_i for $i = 1, \ldots, n$, the closed loop system is also decoupled. A simple approach

is to design a linear proportional integral derivative control law of the form

$$\mathbf{a}_b = \dot{\mathbf{v}}_d - \mathbf{K}_p\tilde{\mathbf{v}} - \mathbf{K}_i\int_0^t \tilde{\mathbf{v}}(\tau)\mathrm{d}\tau - \mathbf{K}_d\dot{\tilde{\mathbf{v}}},$$

where $\mathbf{v}_d = \mathbf{v}_d(t)$ is the desired velocity, $\tilde{\mathbf{v}} := \mathbf{v} - \mathbf{v}_d$ is the velocity error, and $\mathbf{K}_p > 0$, $\mathbf{K}_i > 0$ and $\mathbf{K}_d > 0$ are diagonal proportional, integral and derivative gain matrices, respectively. Note that the first term of $\mathbf{a}_b$, $\dot{\mathbf{v}}_d$, functions as a feedforward term for the desired acceleration.

4.2.2 NED Frame Inverse Dynamics

Next, consider the full equations of motion for a marine vehicle

$$\dot{\eta} = \mathbf{J}(\eta)\mathbf{v},$$

$$\mathbf{M}\dot{\mathbf{v}} = -\mathbf{C}(\mathbf{v})\mathbf{v} - \mathbf{D}(\mathbf{v})\mathbf{v} - \mathbf{g}(\eta) + \tau.$$

Position and orientation trajectory tracking can be accomplished by commanding an acceleration $\mathbf{a}_n$ (measured with respect to an Earth-fixed inertial reference frame) of the form

$$\ddot{\eta} = \mathbf{a}_n$$

that linearizes the closed loop system. Taking the time derivative of the first term in the vehicle equations of motion gives

$$\ddot{\eta} = \frac{\mathrm{d}\left[\mathbf{J}(\eta)\right]}{\mathrm{d}t}\mathbf{v} + \mathbf{J}(\eta)\dot{\mathbf{v}}.$$

Solving for $\dot{\mathbf{v}}$ gives

$$\dot{\mathbf{v}} = \mathbf{J}^{-1}(\eta)\left\{\ddot{\eta} - \frac{\mathrm{d}\left[\mathbf{J}(\eta)\right]}{\mathrm{d}t}\mathbf{v}\right\}.$$

Substituting this into the equations of motion yields

$$\mathbf{M}\mathbf{J}^{-1}(\eta)\left\{\ddot{\eta} - \frac{\mathrm{d}\left[\mathbf{J}(\eta)\right]}{\mathrm{d}t}\mathbf{v}\right\} = -\mathbf{C}(\mathbf{v})\mathbf{v} - \mathbf{D}(\mathbf{v})\mathbf{v} - \mathbf{g}(\eta) + \tau.$$

If τ is selected as

$$\tau = \mathbf{M}\mathbf{J}^{-1}(\eta)\left\{\mathbf{a}_n - \frac{\mathrm{d}\left[\mathbf{J}(\eta)\right]}{\mathrm{d}t}\mathbf{v}\right\} + \mathbf{C}(\mathbf{v})\mathbf{v} + \mathbf{D}(\mathbf{v})\mathbf{v} + \mathbf{g}(\eta)$$

the closed loop system becomes

$$\ddot{\eta} = \mathbf{a}_n.$$

As above, a linear proportional integral derivative control law can now be designed as

$$\mathbf{a}_n = \ddot{\eta}_d - \mathbf{K}_p\tilde{\eta} - \mathbf{K}_i\int_0^t \tilde{\eta}(\sigma)\mathrm{d}\sigma - \mathbf{K}_d\dot{\tilde{\eta}},$$

where σ is used as an integration variable, $\eta_d = \eta_d(t)$ is the desired position and orientation of the vehicle, $\tilde{\eta} := \eta - \eta_d$ is the pose error, and $\mathbf{K}_p > 0$, $\mathbf{K}_i > 0$ and $\mathbf{K}_d > 0$ are diagonal proportional, integral and derivative gain matrices, respectively. As above, the first term of $\mathbf{a}_n$, $\ddot{\eta}_d$, functions as a feedforward term. Note that the transformation matrix $\mathbf{J}(\eta)$ must be nonsingular to use this approach, which limits the magnitude of the pitch angle of the vehicle to the range $-\pi/2 < \theta < \pi/2$.

4.2.3 Fundamental Concepts in Feedback Linearization

The use of inverse dynamics to design a nonlinear controller, is a special case of feedback linearization. It can be seen that the use of inverse dynamics essentially splits the controller into two parts, an inner loop that exactly linearizes the nonlinear system, and an outer loop, which can be designed using linear techniques according to tracking or disturbance rejection performance requirements (Fig. 4.1). The more general process of feedback linearization works in the same way, except that the outer-loop process of linearizing the nonlinear system may also involve a transformation of the state variable into a new set of coordinates. While inverse dynamics can be sufficient for many problems involving the control of marine vessels, the use of the more general form of feedback linearization may be needed when solving marine vehicle control problems that must take actuator dynamics or underactuation into account [9].

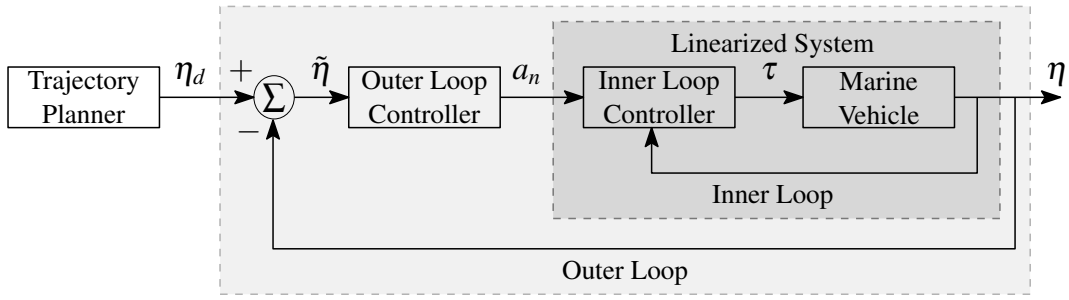

Fig. 4.1 Block diagram of a controller designed using feedback linearization. The system consists of an inner loop, which uses $\mathbf{a}_n$, as well as the states $\mathbf{v}$ and η, to compute a control input τ that compensates for nonlinearities in the plant model. The outer-loop consists of a trajectory tracking linear controller, which can be designed based on the decoupled linear plant model.

4.3 Integrator Backstepping

Consider the dynamic equations of a marine vehicle in body-fixed coordinates

$$\dot{\eta} = \mathbf{J}(\eta)\mathbf{v},$$

$$\mathbf{M}\dot{\mathbf{v}} = -\mathbf{C}(\mathbf{v})\mathbf{v} - \mathbf{D}(\mathbf{v})\mathbf{v} - \mathbf{g}(\eta) + \tau + \mathbf{w}_d.$$

Note the structure of the equations. The terms η and $\mathbf{v}$ are state variables. The equations are coupled and there are functions of the state variables (i.e. $\mathbf{J}(\eta)$, $\mathbf{C}(\mathbf{v})$, and $\mathbf{D}(\mathbf{v})$) that are multiplied by the state variable $\mathbf{v}$. The coupling created by the products of nonlinear functions of the state variables multiplying the state variables makes it difficult to identify a control input that can be used to stabilize the system around a desired equilibrium point. Backstepping techniques provide means of decoupling the dynamic equations so that they can be stabilized.

Backstepping concepts are introduced gradually here. First we examine a the backstepping procedure applied to a simple two-state SISO system and then a vectorial form of backstepping that can be used for marine vehicle control.

4.3.1 A simple 2-state SISO system

Consider the single-input single-output (SISO) system

$$\dot{x}_1 = f_1(x_1) + g_1(x_1)x_2, \tag{4.1}$$

$$\dot{x}_2 = u, \tag{4.2}$$

$$y = x_1,$$

where $f_1(x_1)$ and $g_1(x_1)$ are known functions. It is assumed that $g_1(x_1) \neq 0$ for all x_1 in the domain of interest. The control objective is to design a state feedback control law that tracks a desired output $y_d(t)$.

The system can be viewed as a cascade connection of two components. The first component (4.1) can be thought of as having the state x_2 as a *virtual control input* and the second component (4.2) is an integrator with u as input (see Fig. 4.2). Since there are two states x_1 and x_2, the design will be conducted recursively in 2 steps.

Suppose that we can find a smooth *stabilizing function* $\alpha_1(x_1)$ that permits us to decouple the system by driving $x_2 \to \alpha_1$. To see how this can work, let us add and subtract $g_1(x_1)\alpha_1(x_1)$ to the right hand side of (4.1) to obtain a new system

$$\dot{x}_1 = [f_1(x_1) + g_1(x_1)\alpha_1(x_1)] + g_1(x_1)[x_2 - \alpha_1(x_1)] \tag{4.3}$$

$$\dot{x}_2 = u. \tag{4.4}$$

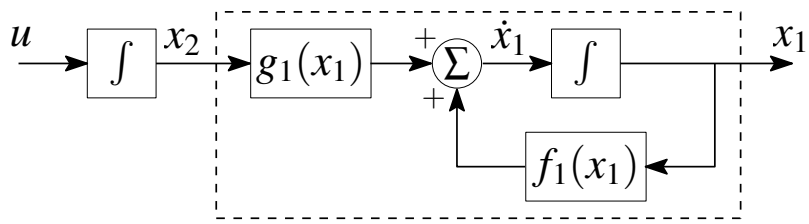

Fig. 4.2 Block diagram of system (4.1)–(4.2).

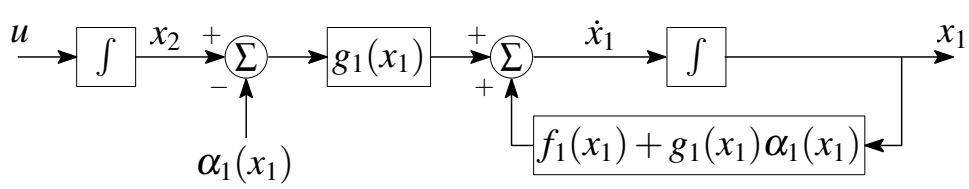

Fig. 4.3 Block diagram of system (4.3)–(4.4). The stabilizing function $\alpha_1(x_1)$ is introduced to stabilize the x_1 system (4.3) at $x_1 = 0$.

Define the stabilization errors as

$$z_1 := y - y_d = x_1 - y_d \tag{4.5}$$

and

$$z_2 := x_2 - \alpha_1 . \tag{4.6}$$

Then (4.1) and (4.2) can be rewritten in terms of the stabilizations errors as

$$\dot{z}_1 = \dot{x}_1 - \dot{y}_d = [f_1(x_1) + g_1(x_1)\alpha_1] + g_1(x_1)z_2 - \dot{y}_d, \tag{4.7}$$

$$\dot{z}_2 = u - \dot{\alpha}_1 = v. \tag{4.8}$$

From (4.7), it can be seen that when $x_2 \to \alpha_1$, so that $z2 \to 0$, the resulting subsystem $\dot{z}_1 = f_1(x_1) + g_1(x_1)\alpha_1(x_1) - \dot{y}_d$ can be stabilized independently of z_2. The stabilizing function needed to achieve this will be determined as the first step of the backstepping control design process. As can be seen by comparing Fig. 4.4 with Fig. 4.2, the new system (4.7)–(4.8) is similar to the one we started with (4.1)–(4.2). However, when the input of this new system is $v = 0$, it can be asymptotically stabilized to its origin $(z_1 = 0, z_2 = 0)$.

Also note that by comparing Fig. 4.4 with Fig. 4.3, we can see that in the process of stabilizing the x_2 function we are stepping $\alpha_1(x_1)$ back through an integrator block to compute $v = u - \dot{\alpha}_1$. This is why this control design technique is known as *integrator backstepping*.

The stabilizing function α_1 and the control input u will be determined by selecting a suitable *control Lyapunov function* (CLF) $V(z_1, z_2, u)$. Recall from Sec-

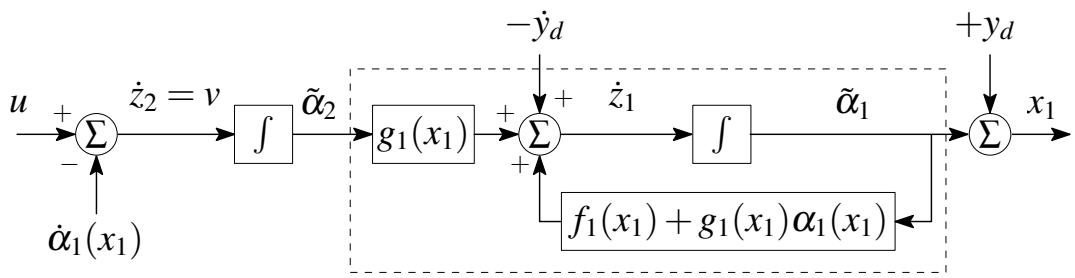

Fig. 4.4 Block diagram of system (4.7)–(4.8). The control input u is selected to stabilize the x_2 system.

tion 2.6.2 that a *Lyapunov function* V, is an energy-like function that can be used to determine the stability of a system. If we can find a positive definite $V > 0$ that always decreases along trajectories of the system, e.g.

$$\dot{V} = \frac{\partial V}{\partial z_1}\dot{z}_1 + \frac{\partial V}{\partial z_2}\dot{z}_2 \ < 0 \quad \forall z_1, z_2 \neq 0,$$

we can conclude that the minimum of the function is a stable equilibrium point. Lyapunov functions can be used to test whether a dynamical system is *stable*, e.g. whether the system will remain within some domain D when it starts at some initial state $[z_1(0) \quad z_2(0)]^T \in D$, or whether a system is *asymptotically stable*, meaning that when it starts at some initial state $[z_1(0) \quad z_2(0)]^T$, $\lim_{t\to\infty}[z_1(t) \quad z_2(t)]^T \to \mathbf{0}$. Similarly, CLFs are used to test whether a closed loop system can be feedback stabilized — e.g. whether or not a control input $u(z_1, z_2, t)$ exists that can drive the system from any initial state $[z_1(0) \quad z_2(0)]^T$ to $[z_1(t) \quad z_2(t)]^T = 0$.

Here, we explore use of the candidate CLF

$$V = \frac{1}{2}z_1^2 + \frac{1}{2}z_2^2. \tag{4.9}$$

Taking its time derivative gives

$$\begin{aligned} \dot{V} &= z_1\dot{z}_1 + z_2\dot{z}_2, \\ &= z_1\left[f_1(x_1) + g_1(x_1)\alpha_1 + g_1(x_1)z_2 - \dot{y}_d\right] + z_2(u - \dot{\alpha}_1). \end{aligned} \tag{4.10}$$

Noting that $z_1 g_1(x_1) z_2 = z_2 g_1(x_1) z_1$, this term can be moved from the first expression in square brackets to the second one so that the first one is a function of x_1 only, so that (4.10) can be rewritten as

$$\dot{V} = z_1\left[f_1(x_1) + g_1(x_1)\alpha_1 - \dot{y}_d\right] + z_2[u - \dot{\alpha}_1 + g_1(x_1)z_1]. \tag{4.11}$$

Step 1: With our assumption that $g_1(x_1) \neq 0$ in our domain of interest, select α_1 as

$$\alpha_1 = \frac{1}{g_1(x_1)}\left[-k_1 z_1 + \dot{y}_d - f_1(x_1)\right], \tag{4.12}$$

where $k_1 > 0$. Then, using (4.11), (4.7) and (4.8) gives

$$\dot{V} = -k_1 z_1^2 + z_2[u - \dot{\alpha}_1 + g_1(x_1)z_1]. \tag{4.13}$$

As the first term on the right hand side of this equation is negative definite, the z_1 subsystem is stabilized with our choice of α_1.

Step 2: Next, the control input u is selected to stabilize the z_2 system by making the remaining terms in (4.13) negative definite. Let

$$u = -k_2 z_2 + \dot{\alpha}_1 - g_1(x_1)z_1 \tag{4.14}$$

with $k_2 > 0$, then

$$\dot{V} = -k_1 z_1^2 - k_2 z_2^2 < 0 \quad \forall z_1, z_2 \neq 0. \tag{4.15}$$

As $\dot{V}$ is negative definite $\forall z_1, z_2 \neq 0$, the full system is now stabilized. Further, using (4.9) and (4.15) it can be seen that

$$\dot{V} \leq -2\mu V \tag{4.16}$$

where $\mu := \min\{k_1, k_2\}$. Let the value of V at time $t = 0$ be V_0, then integrating (4.15) gives

$$V \leq V_0 \mathrm{e}^{-2\mu t}, \tag{4.17}$$

where

$$V_0 := \frac{1}{2}\left[z_1(0)^2 + z_2(0)^2\right].$$

Thus, using (4.17) and (4.9), we find that both $z_1(t)$ and $z_2(t)$ decrease exponentially in time and that the controller is globally exponentially stable.

In terms of the states x_1, x_2 and the desired time-dependent trajectory $y_d(t)$, the final control law can be rewritten as

$$u = -k_2(x_2 - \alpha_1) + \dot{\alpha}_1 - g_1(x_1)\left[x_1 - y_d\right], \tag{4.18}$$

where

$$\alpha_1 = -\frac{1}{g_1(x_1)}\left[f_1(x_1) + k_1(x_1 - y_d) - \dot{y}_d\right]. \tag{4.19}$$

The computation of the control input u requires one to take the time derivative of the stabilizing function, $\dot{\alpha}_1$. There are two important implementation issues associated with this:

1) **The Explosion of Complexity:** The computation of $\dot{\alpha}_1$ involves taking time derivatives of the states and plant model, which in turn can lead to a situation sometimes called an *explosion of complexity* [8, 7], where the number of terms required to compute the time derivative of the stabilizing function becomes very large. In general, one should avoid taking the time derivatives of the states directly, instead using the original state equation whenever possible. For example, $\dot{\alpha}_1$ can be computed as

$$\dot{\alpha}_1 = \frac{\partial \alpha_1}{\partial x_1}\dot{x}_1 = \frac{\partial \alpha_1}{\partial x_1}[f_1(x_1) + g_1(x_1)x_2]. \tag{4.20}$$

The Dynamic Surface Control Technique [8, 7, 9] is an approach developed to avoid this problem.

2) As can be seen from (4.19), the computation of $\dot{\alpha}_1$ also involves the second derivative in time of the desired trajectory. In order for the control input to be bounded, the desired trajectory must be smooth and continuous to second order. In practice, it is common to pass the desired trajectory through a linear filter to ensure the smoothness of $\ddot{y}_d(t)$.

Example 4.1. A buoyancy-driven automatic profiler is used to collect data by vertically traversing the water column in the open ocean (Fig. 4.5). Careful regulation of the profiler's vertical speed is desired to ensure the effectiveness of the sampling instrumentation, which could be a conductivity-temperature-depth (CTD) sensor, for example. The vertical ascent/descent rate is controlled using a piston to regulate the system's buoyancy by changing the volume of an oil-filled bladder. The equation of motion of the system is

$$\dot{x}_1 = -\frac{\rho A C_d}{2m}x_1|x_1| + \frac{g(\rho - \rho_f)}{m}x_2 \tag{4.21}$$

where x_1 is the ascent/descent rate of the profiler, m is the mass and added mass, A is the frontal area, C_d is the drag coefficient, x_2 is the change in piston volume, g is gravity, ρ is the density of seawater and ρ_f is the density of the oil. The control input is the piston's rate of volume change (the product of the piston velocity and the circular cross sectional area of the piston head),

$$\dot{x}_2 = u. \tag{4.22}$$

The system output is the ascent/descent rate $y = x_1$. Comparing (4.21) and (4.22) to (4.1) and (4.2), we see that

$$f_1(x_1) = -\frac{\rho A C_d}{2m}x_1|x_1|, \quad \text{and} \quad g_1(x_1) = \frac{g(\rho - \rho_f)}{m}.$$

From (4.19) we have

$$\alpha_1 = -\frac{m}{g(\rho - \rho_f)}\left[-\frac{\rho A C_d}{2m}x_1|x_1| + k_1(x_1 - y_d) - \dot{y}_d\right]$$

$$= -\frac{m}{g(\rho - \rho_f)}\left[-\frac{\rho A C_d}{2m}x_1^2\mathrm{sgn}(x_1) + k_1(x_1 - y_d) - \dot{y}_d\right]$$

and from (4.20)

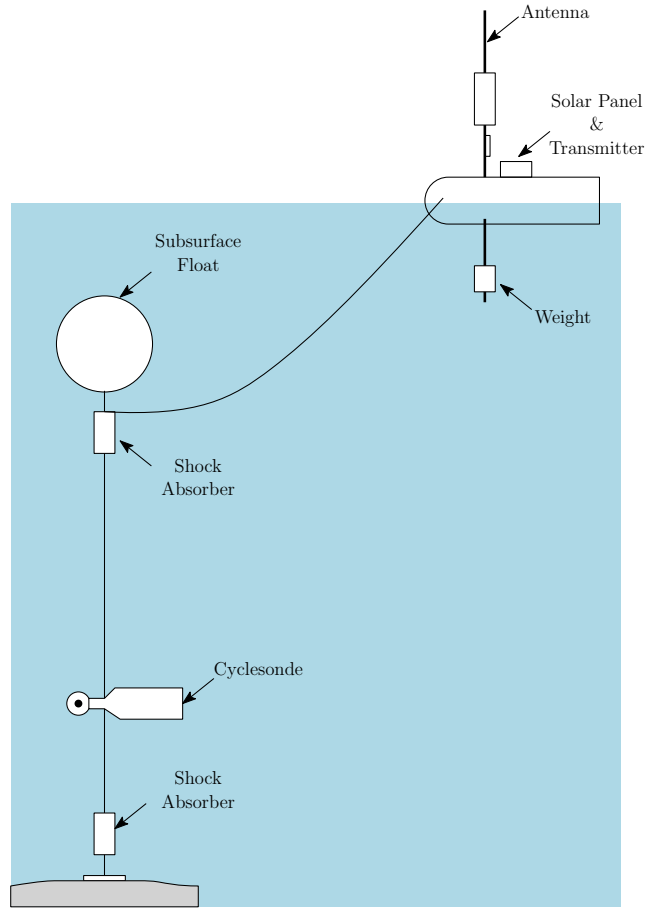

Fig. 4.5 The *cyclesonde*, an example of a buoyancy-controlled automatic profiler [3].

$$\dot{\alpha}_1 = \frac{\partial \alpha_1}{\partial x_1}\dot{x}_1,$$

$$= -\frac{m}{g(\rho-\rho_f)}\left\{-\frac{\rho A C_d}{2m}\frac{\partial}{\partial x_1}\left[x_1^2 \mathrm{sgn}(x_1)\right]+k_1\right\}\dot{x}_1,$$

$$= -\frac{m}{g(\rho-\rho_f)}\left\{-\frac{\rho A C_d}{2m}\left[2x_1\mathrm{sgn}(x_1)+2x_1^2\delta(x_1)\right]+k_1\right\}\dot{x}_1,$$

$$= -\frac{m}{g(\rho-\rho_f)}\left[-\frac{\rho A C_d}{m}|x_1|+k_1\right]\dot{x}_1,$$

Then from (4.18) the control input is

$$u = -k_2(x_2-\alpha_1)+\dot{\alpha}_1-\frac{g(\rho-\rho_f)}{m}\left[x_1-y_d\right].$$

Let the control gains be $k_1 = 1$ and $k_2 = 1$. The physical characteristics of the profiler and the other constants used are $m = 4320$ kg, $A = 1$ m^2, $C_d = 1.0$, $g = 9.81$ m/s^2, $\rho = 1025.9$ kg/m^3 and $\rho_f = 850$ kg/m^3. The ascent/descent rate of the closed loop system is shown for a time varying $y_d(t)$ in Fig. 4.6.

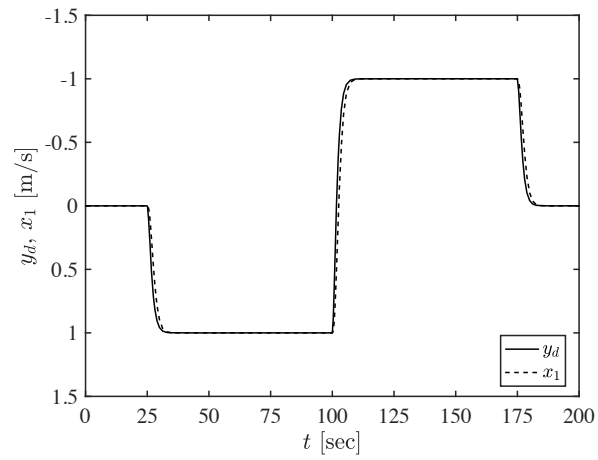

Fig. 4.6 Vertical ascent/descent rate x_1 of the buoyancy-driven profiler when tracking a desired time-dependent input $y_d(t)$. The vertical axis of the plot is reversed, as the downward direction (increasing depth) is usually taken to be positive for marine vehicles.

□

4.4 Backstepping for Trajectory Tracking Marine Vehicles

Recall the equations of motion for a marine vehicle

$$\dot{\eta} = \mathbf{J}(\eta)\mathbf{v}$$

and

$$\mathbf{M}\dot{\mathbf{v}} + \mathbf{C}(\mathbf{v})\mathbf{v} + \mathbf{D}(\mathbf{v})\mathbf{v} + \mathbf{g}(\eta) = \tau$$

in body-fixed coordinates [1]. For the time being, any actuator constraints and the effects of external disturbances are neglected.

In the following formulation, the coordinate transformation matrix $\mathbf{J}(\eta)$, which is used to convert the representation of vectors between a body-fixed coordinate system and an Earth-fixed North-East-Down coordinate system, is based on the use of Euler angles. The transformation matrix $\mathbf{J}(\eta)$ has singularities at pitch angles of $\theta = \pm\pi/2$. Here, it is assumed that $|\theta| < \pi/2$.

Note that the singularities at $\theta = \pm\pi/2$ are not generally a problem for unmanned ground vehicles or unmanned surface vessels. However, unmanned aerial vehicles and underwater vehicles may occassionally approach these singularities if

performing extreme maneuvers. In such cases, as suggested in [1], the kinematic equations could be described by two Euler angle representations with different singularities and the singular points can be avoided by switching between the representations.

The control objective is to make the system track a desired trajectory η_d. The trajectory η_d and its derivatives $\eta_d^{(3)}$, $\ddot{\eta}_d$, and $\dot{\eta}_d$ are assumed to be smooth and bounded.

Two approaches, often used for backstepping control design in marine vehicles, are presented here. The first approach uses a straight-forward implementation of vectorial backstepping. The second approach presented relies upon the definition of a virtual reference velocity and requires that the equations of motion be reformulated in a NED, Earth-fixed inertial reference frame where the inertia tensor becomes a function of vehicle orientation $\mathbf{M}(\eta)$. This second approach is similar to that often used for designing controllers for robotic manipulators and is based on the concept of passivity [5, 6]. The passivity approach is slightly more complicated, but has advantages when using backstepping for adaptive or robust control. Further, the passivity approach permits one to more heavily weight either position tracking or velocity tracking, as desired. On the other hand, with the straight-forward vectorial backstepping approach the identification of a control law is simpler. Both approaches ensure the global exponential stability of the closed loop system in the absence of model uncertainty and disturbance.

4.4.1 Straight-forward backstepping

Let

$$\tilde{\eta} := \eta - \eta_d, \quad \tilde{\eta} \in \mathbb{R}^n \tag{4.23}$$

be the Earth-fixed tracking surface error and define the body-fixed velocity surface error vector as

$$\tilde{\mathbf{v}} := \mathbf{v} - \alpha_1, \quad \tilde{\mathbf{v}} \in \mathbb{R}^n \tag{4.24}$$

Using (4.23) and (4.24), the kinematic and kinetic equations of motion can be rewritten as

$$\begin{aligned} \dot{\tilde{\eta}} &= \mathbf{J}(\eta)\mathbf{v} - \dot{\eta}_d = \mathbf{J}(\eta)\tilde{\mathbf{v}} + \mathbf{J}(\eta)\alpha_1 - \dot{\eta}_d, \\ \mathbf{M}\dot{\tilde{\mathbf{v}}} &= -\mathbf{C}(\mathbf{v})\mathbf{v} - \mathbf{D}(\mathbf{v})\mathbf{v} - \mathbf{g}(\eta) + \tau - \mathbf{M}\dot{\alpha}_1. \end{aligned} \tag{4.25}$$

Consider the candidate Lyapunov function

$$V = \frac{1}{2}\tilde{\eta}^T\tilde{\eta} + \frac{1}{2}\tilde{\mathbf{v}}^T\mathbf{M}\tilde{\mathbf{v}}. \tag{4.26}$$

Taking the time derivative gives

$$\dot{V} = \tilde{\eta}^T\dot{\tilde{\eta}} + \tilde{\mathbf{v}}^T\mathbf{M}\dot{\tilde{\mathbf{v}}}, \tag{4.27}$$

where it is assumed that $\mathbf{M} = \mathbf{M}^T > 0$. Using (4.25), $\dot{V}$ can be written as

$$\begin{aligned} \dot{V} &= \tilde{\eta}^T \left[\mathbf{J}\tilde{\mathbf{v}} + \mathbf{J}\alpha_1 - \dot{\eta}_d\right] + \tilde{\mathbf{v}}^T \left[-\mathbf{C}\mathbf{v} - \mathbf{D}\mathbf{v} - \mathbf{g} + \tau - \mathbf{M}\dot{\alpha}_1\right], \\ &= \tilde{\eta}^T \left[\mathbf{J}\alpha_1 - \dot{\eta}_d\right] + \tilde{\mathbf{v}}^T \left[\mathbf{J}^T\tilde{\eta} - \mathbf{C}\mathbf{v} - \mathbf{D}\mathbf{v} - \mathbf{g} + \tau - \mathbf{M}\dot{\alpha}_1\right]. \end{aligned} \tag{4.28}$$

The stabilizing function α_1 and control input τ can be selected so that

$$\dot{V} = -\tilde{\eta}^T \mathbf{K}_p \tilde{\eta} - \tilde{\mathbf{v}}^T \mathbf{K}_d \tilde{\mathbf{v}} < 0, \tag{4.29}$$

where $\mathbf{K}_p = \mathbf{K}_p^T > 0 \in \mathbb{R}^{n\times n}$ and $\mathbf{K}_d = \mathbf{K}_d^T > 0 \in \mathbb{R}^{n\times n}$ are positive definite matrices of control gains. To accomplish this take

$$\mathbf{J}\alpha_1 - \dot{\eta}_d = -\mathbf{K}_p\tilde{\eta}$$

so that

$$\alpha_1 := \mathbf{J}^{-1}\left[-\mathbf{K}_p\tilde{\eta} + \dot{\eta}_d\right] \tag{4.30}$$

and

$$\mathbf{J}^T\tilde{\eta} - \mathbf{C}\mathbf{v} - \mathbf{D}\mathbf{v} - \mathbf{g} + \tau - \mathbf{M}\dot{\alpha}_1 = -\mathbf{K}_d\tilde{\mathbf{v}},$$

which gives

$$\tau := -\mathbf{K}_d\tilde{\mathbf{v}} + \mathbf{M}\dot{\alpha}_1 + \mathbf{C}\mathbf{v} + \mathbf{D}\mathbf{v} + \mathbf{g} - \mathbf{J}^T\tilde{\eta}. \tag{4.31}$$

The closed loop error dynamics can be obtained using (4.25), (4.30) and (4.31) to get

$$\begin{aligned} \dot{\tilde{\eta}} &= -\mathbf{K}_p\tilde{\eta} + \mathbf{J}\tilde{\mathbf{v}}, \\ \mathbf{M}\dot{\tilde{\mathbf{v}}} &= -\mathbf{K}_d\tilde{\mathbf{v}} - \mathbf{J}^T\tilde{\eta}, \end{aligned} \tag{4.32}$$

which has a stable equilibrium point at $(\tilde{\eta}, \tilde{\mathbf{v}}) = (0,0)$.

From (4.29), it can be seen that

$$\dot{V} \leq -\Lambda_{\min}(\mathbf{K}_p)\tilde{\eta}^T\tilde{\eta} - \Lambda_{\min}(\mathbf{K}_d)\tilde{\mathbf{v}}^T\tilde{\mathbf{v}},$$

where $\Lambda_{\min}(\mathbf{K})$ denotes the minimum eigenvalue of matrix $\mathbf{K}$. Noting that $\mathbf{M} = \mathbf{M}^T > 0$ implies that $\tilde{\mathbf{v}}^T\tilde{\mathbf{v}} \leq \tilde{\mathbf{v}}^T\mathbf{M}\tilde{\mathbf{v}}$ so that

$$\dot{V} \leq -\Lambda_{\min}(\mathbf{K}_p)\tilde{\eta}^T\tilde{\eta} - \Lambda_{\min}(\mathbf{K}_d)\tilde{\mathbf{v}}^T\mathbf{M}\tilde{\mathbf{v}} \leq -2\mu V,$$

where $\mu = \min\{\Lambda_{\min}(\mathbf{K}_p), \Lambda_{\min}(\mathbf{K}_d)\}$. Taking V_0 to be the value of V at time $t = 0$, V can therefore be expressed as

$$V = V_0 e^{-2\mu t}.$$

Since V is radially unbounded (i.e. $V \to \infty$ if $\tilde{\eta} \to \infty$ or $\tilde{\mathbf{v}} \to \infty$) and exponentially decaying with a stable equilibrium point at the origin, the closed loop system is globally exponentially stable.

4.4.2 Passivity-based backstepping

Let

$$\tilde{\eta} := \eta - \eta_d \tag{4.33}$$

be the Earth-fixed tracking error. Then define an Earth-fixed *reference velocity* [5], also called a *virtual reference trajectory* [1], as

$$\dot{\eta}_r := \dot{\eta}_d - \Lambda \tilde{\eta}, \tag{4.34}$$

where $\Lambda > 0$ is a diagonal control design matrix. In body-fixed (NED-fixed) coordinates the reference velocity is

$$\mathbf{v}_r := \mathbf{J}^{-1}(\eta)\dot{\eta}_r. \tag{4.35}$$

Let $\mathbf{s}$ be a *measure of tracking* [4, 2] (also referred to as a *velocity error* [5]) defined as

$$\mathbf{s} := \dot{\eta} - \dot{\eta}_r = \dot{\tilde{\eta}} + \Lambda \tilde{\eta}. \tag{4.36}$$

As shown in [1], the equations of motion (both kinematic and kinetic) can be rewritten in the combined form

$$\mathbf{M}_\eta(\eta)\ddot{\eta} + \mathbf{C}_\eta(\mathbf{v},\eta)\dot{\eta} + \mathbf{D}_\eta(\mathbf{v},\eta)\dot{\eta} + \mathbf{g}_\eta(\eta) = \mathbf{J}^{-T}(\eta)\tau, \tag{4.37}$$

where

$$\begin{aligned} &\mathbf{M}_\eta(\eta) = \mathbf{M}_\eta^T(\eta) > 0, \\ &\mathbf{s}^T\left[\frac{1}{2}\dot{\mathbf{M}}_\eta(\eta) - \mathbf{C}_\eta(\mathbf{v},\eta)\right]\mathbf{s} = 0, \quad \forall \mathbf{v},\eta,\mathbf{s} \\ &\mathbf{D}_\eta(\mathbf{v},\eta) > 0, \end{aligned} \tag{4.38}$$

and the relationships between the terms $\mathbf{M}$, $\mathbf{C}(\mathbf{v})$, $\mathbf{D}(\mathbf{v})$ and $\mathbf{g}(\eta)$ in the body-fixed coordinate system and $\mathbf{M}_\eta(\eta)$, $\mathbf{C}_\eta(\mathbf{v},\eta)$, $\mathbf{D}_\eta(\mathbf{v},\eta)$ and $\mathbf{g}_\eta(\eta)$ in the Earth-fixed coordinate system are provided in Table 4.1 below. Note that the second property in (4.38) results from the fact that $\left[\frac{1}{2}\dot{\mathbf{M}}_\eta(\eta) - \mathbf{C}_\eta(\mathbf{v},\eta)\right]$ is skew symmetric. The skew-symmetry of this term can be viewed as an expression of the conservation of energy [5].

Remark 4.1. As shown in (4.38), the drag tensor $\mathbf{D}(\mathbf{v})$ is strictly positive, such that

$$\mathbf{D}(\mathbf{v}) > 0 \Rightarrow \frac{1}{2}\mathbf{x}^T[\mathbf{D}(\mathbf{v}) + \mathbf{D}^T(\mathbf{v})]\mathbf{x} > 0, \forall \mathbf{x} \neq 0.$$

This assumption implies that $\mathbf{D}_\eta$ is also strictly positive. We can see this by examining the symmetric part of $\mathbf{D}_\eta$,

Table 4.1 Relations between the inertia tensor, Coriolis/centripetal acceleration tensor, drag tensor and hydrostatic force vector in Earth-fixed and body-fixed coordinate systems.

$\mathbf{M}_\eta(\eta) := \mathbf{J}^{-T}(\eta)\mathbf{M}\mathbf{J}^{-1}(\eta)$
$\mathbf{C}_\eta(\mathbf{v},\eta) := \mathbf{J}^{-T}(\eta)[\mathbf{C}(\mathbf{v}) - \mathbf{M}\mathbf{J}^{-1}(\eta)\dot{\mathbf{J}}(\eta)]\mathbf{J}^{-1}(\eta)$
$\mathbf{D}_\eta(\mathbf{v},\eta) := \mathbf{J}^{-T}(\eta)\mathbf{D}(\mathbf{v})\mathbf{J}^{-1}(\eta)$
$\mathbf{g}_\eta(\eta) := \mathbf{J}^{-T}(\eta)\mathbf{g}(\eta)$

$$\begin{aligned}\tfrac{1}{2}\mathbf{x}^T\left[\mathbf{D}_\eta + \mathbf{D}_\eta^T\right]\mathbf{x} &= \tfrac{1}{2}\mathbf{x}^T\left\{\mathbf{J}^{-T}(\eta)\mathbf{D}(\mathbf{v})\mathbf{J}^{-1}(\eta) + \left[\mathbf{J}^{-T}(\eta)\mathbf{D}(\mathbf{v})\mathbf{J}^{-1}(\eta)\right]^T\right\}\mathbf{x},\\ &= \tfrac{1}{2}\mathbf{x}^T\left[\mathbf{J}^{-T}(\eta)\mathbf{D}(\mathbf{v})\mathbf{J}^{-1}(\eta) + \mathbf{J}^{-T}(\eta)\mathbf{D}^T(\mathbf{v})\mathbf{J}^{-1}(\eta)\right]\mathbf{x},\\ &= \tfrac{1}{2}\mathbf{x}^T\mathbf{J}^{-T}(\eta)\left[\mathbf{D}(\mathbf{v}) + \mathbf{D}^T(\mathbf{v})\right]\mathbf{J}^{-1}(\eta)\mathbf{x},\end{aligned}$$

Let $\bar{\mathbf{x}}^T := \mathbf{x}^T\mathbf{J}^{-T}(\eta)$, then $\bar{\mathbf{x}} = \mathbf{J}^{-1}(\eta)\mathbf{x}$, which implies

$$\frac{1}{2}\mathbf{x}^T\left[\mathbf{D}_\eta + \mathbf{D}_\eta^T\right]\mathbf{x} = \frac{1}{2}\bar{\mathbf{x}}^T\left[\mathbf{D}(\mathbf{v}) + \mathbf{D}^T(\mathbf{v})\right]\bar{\mathbf{x}} > 0, \forall\bar{\mathbf{x}} \neq 0,$$

so that $\mathbf{D}_\eta(\mathbf{v},\eta)$ is also strictly positive. This result will be used in the stability analysis below.

The product $\mathbf{M}_\eta(\eta)\dot{\mathbf{s}}$ is an important quantity that will be used in the controller derivation. It can be written as

$$\begin{aligned}\mathbf{M}_\eta(\eta)\dot{\mathbf{s}} = &-\mathbf{C}_\eta(\mathbf{v},\eta)\mathbf{s} - \mathbf{D}_\eta(\mathbf{v},\eta)\mathbf{s}\\ &+\mathbf{J}^{-T}(\eta)\left[\tau - \mathbf{M}\dot{\mathbf{v}}_r - \mathbf{C}(\mathbf{v})\mathbf{v}_r - \mathbf{D}(\mathbf{v})\mathbf{v}_r - \mathbf{g}(\eta)\right],\end{aligned} \tag{4.39}$$

where $\dot{\mathbf{v}}_r = \dot{\mathbf{J}}^{-1}(\eta)\dot{\eta}_r + \mathbf{J}^{-1}(\eta)\ddot{\eta}_r = \dot{\mathbf{J}}^{-1}(\eta)\dot{\eta}_r + \mathbf{J}^{-1}(\eta)\left[\ddot{\eta}_d - \Lambda\left(\dot{\eta} - \dot{\eta}_d\right)\right]$.

Step 1: Define the virtual control signal

$$\dot{\eta} = \mathbf{J}(\eta)\mathbf{v} := \mathbf{s} + \alpha_1, \tag{4.40}$$

where α_1 is a smoothly continuous function that stabilizes the system at the origin, which can be chosen as

$$\alpha_1 = \dot{\eta}_r = \dot{\eta}_d - \Lambda\tilde{\eta}. \tag{4.41}$$

Then, (4.40) can be written as

$$\dot{\tilde{\eta}} = -\Lambda\tilde{\eta} + \mathbf{s}. \tag{4.42}$$

Next, consider the Lyapunov function candidate

$$V_1 = \frac{1}{2}\tilde{\eta}^T \mathbf{K}_p \tilde{\eta}. \tag{4.43}$$

Its time derivative is

$$\dot{V}_1 = \tilde{\eta}^T \mathbf{K}_p \dot{\tilde{\eta}} = -\tilde{\eta}^T \mathbf{K}_p \Lambda \tilde{\eta} + \tilde{\eta}^T \mathbf{K}_p \mathbf{s} \tag{4.44}$$

where $\mathbf{K}_p = \mathbf{K}_p^T > 0$ is a design matrix.

Step 2: Consider the Lyapunov function candidate

$$V_2 = V_1 + \frac{1}{2}\mathbf{s}^T \mathbf{M}_\eta(\eta)\mathbf{s}. \tag{4.45}$$

Its time derivative is

$$\dot{V}_2 = -\tilde{\eta}^T \mathbf{K}_p \Lambda \tilde{\eta} + \mathbf{s}^T \left[\mathbf{K}_p \tilde{\eta} + \mathbf{M}_\eta(\eta)\dot{\mathbf{s}} + \frac{1}{2}\dot{\mathbf{M}}_\eta(\eta)\mathbf{s} \right]. \tag{4.46}$$

Using (4.39) and then applying the skew symmetry property of $\left[\frac{1}{2}\dot{\mathbf{M}}_\eta(\eta) - \mathbf{C}_\eta(\mathbf{v},\eta)\right]$ in (4.38), $\dot{V}_2$ can be rewritten as

$$\begin{aligned} \dot{V}_2 = & -\tilde{\eta}^T \mathbf{K}_p \Lambda \tilde{\eta} - \mathbf{s}^T \mathbf{D}_\eta(\mathbf{v},\eta)\mathbf{s} \\ & + \mathbf{s}^T \mathbf{J}^{-T}(\eta) \left[\mathbf{J}^T(\eta)\mathbf{K}_p \tilde{\eta} + \tau - \mathbf{M}\dot{\mathbf{v}}_r - \mathbf{C}(\mathbf{v})\mathbf{v}_r - \mathbf{D}(\mathbf{v})\mathbf{v}_r - \mathbf{g}(\eta) \right]. \end{aligned} \tag{4.47}$$

Select the control law to be

$$\tau = \mathbf{M}\dot{\mathbf{v}}_r + \mathbf{C}(\mathbf{v})\mathbf{v}_r + \mathbf{D}(\mathbf{v})\mathbf{v}_r + \mathbf{g}(\eta) - \mathbf{J}^T(\eta)\mathbf{K}_d \mathbf{s} - \mathbf{J}^T(\eta)\mathbf{K}_p \tilde{\eta}. \tag{4.48}$$

Then $\dot{V}_2$ becomes

$$\dot{V}_2 = -\tilde{\eta}^T \mathbf{K}_p \Lambda \tilde{\eta} - \mathbf{s}^T \left[\mathbf{D}_\eta(\mathbf{v},\eta) + \mathbf{K}_d \right] \mathbf{s}. \tag{4.49}$$

Since $\Lambda > 0$, $\mathbf{K}_p > 0$ and $\mathbf{D}_\eta(\mathbf{v},\eta) > 0$, $\dot{V}_2 < 0,\ \forall \mathbf{v}, \eta, \mathbf{s} \neq 0$. Note that the closed loop error system is given by

$$\dot{\tilde{\eta}} = -\Lambda \tilde{\eta} + \mathbf{s},$$

$$\mathbf{M}_\eta(\eta)\dot{\mathbf{s}} = -\mathbf{C}_\eta(\mathbf{v},\eta)\mathbf{s} - \mathbf{D}_\eta(\mathbf{v},\eta)\mathbf{s} - \mathbf{K}_d \mathbf{s} - \mathbf{K}_p \Lambda \tilde{\eta}.$$

Thus, it can be seen that the use of passivity does not lead to a linear closed loop error system, as straight-forward backstepping does in (4.32). However, the trajectory tracking control law developed with the use of the passivity (4.48) can be shown to render the closed loop system globally exponentially stable (see [1]).

4.4.3 Backstepping implementation issues

The first two implementation issues are associated with the computation of the time derivatives of the stabilizing functions α_i. Both of these issues become more complicated as the order of the system n increases.

(1) Computing the time derivatives of the stabilizing functions α_i involves taking time derivatives of the state variables, which appear in the dynamic model of the system. These computations can involve a very large number of terms, leading to the *explosion of complexity* problem discussed in Section 4.3.1.

(2) Computing the time derivatives of the stabilizing functions α_i also requires taking higher order time derivatives of the desired trajectory. Generally, these time derivatives must be smooth and bounded to at an order corresponding to at least the number of integrators in the dynamic system in order to ensure that the stabilizing functions and control input are bounded.
If a desired trajectory is not smooth to the required order, a simple approach for using backstepping is to generate an approximate trajectory by passing the desired trajectory through a low pass linear filter [1]. For example, the square wave like trajectory used in Example 4.1 above was generated by passing a square wave trajectory through a second order linear filter.
To ensure that the smoothed trajectory is feasible, the choice of filter parameters should be based on the dynamics of the vehicle, taking into account speed and acceleration limits, as well as actuator constraints. The bandwidth of the filter used to generate the reference trajectory should be lower than the bandwidth of the motion control system.
Let $r(t)$ be the unfiltered trajectory. The approximate desired trajectory $y_d(t)$ to be used for backstepping control can be determined as

$$y_d(t) = G_f(s)R(s) \tag{4.50}$$

where s is the Laplace transform variable and $G_f(s)$ is the low pass filter transfer function. A convenient filter function that can be used for marine vessels is the canonical form of a second order system

$$G_f(s) = \frac{\omega_n^2}{s^2 + 2\zeta\omega_n s + \omega_n^2}, \tag{4.51}$$

where the natural frequency ω_n and damping ratio ζ can be tuned to specify the phase lag and overshoot between the desired and approximate trajectories. They should also be tuned bearing in mind the physical capabilities of the vehicle to be controlled, as discussed above. If needed, higher order filters can be obtained by taking powers of $G_f(s)$. For example a fourth order filter can be constructed with

$$G_4(s) = G_f(s) \cdot G_f(s) = \frac{\omega_n^4}{[s^2 + 2\zeta\omega_n s + \omega_n^2]^2}. \tag{4.52}$$

During computational implementation, it is often convenient to express these filters in state space form. For example, the second order differential equation corresponding to the application of (4.51) to a nonsmooth input trajectory $r(t)$ to produce an approximate trajectory $y_d(t)$ is given by

$$\ddot{y}_d + 2\zeta\omega_n\dot{y}_d + \omega_n^2 y_d = \omega_n^2 r, \tag{4.53}$$

so that

$$\ddot{y}_d = -2\zeta\omega_n\dot{y}_d - \omega_n^2 y_d + \omega_n^2 r.$$

Let $y_{d1} = y_d$, $y_{d2} = \dot{y}_d$ and $\mathbf{y}_d = [y_{d1} \quad y_{d2}]^T$, then

$$\dot{\mathbf{y}}_d = \begin{bmatrix} 0 & 1 \\ -\omega_n^2 & -2\zeta\omega_n \end{bmatrix} \mathbf{y}_d + \begin{bmatrix} 0 \\ \omega_n^2 \end{bmatrix} r. \tag{4.54}$$

With this system, given a nonsmooth $r(t)$ one can solve for a smooth $y_d(t)$ and $\dot{y}_d(t)$ (note that $\ddot{y}_d(t)$ will not be smooth because it has $r(t)$ as an input).

Remark 4.2 (Numerical differentiation of a signal). Note that linear state space filtering of a signal of the form shown in (4.54) can be used to compute the time derivative of any input signal and can be extended to compute higher order derivatives by using the state space representation of higher order filters, such as the 4^{th} order filter given by (4.52). This can be useful in many practical circumstances, for example when it is necessary to compute the time derivative of a signal measured by a feedback sensor, or the time derivative of a stabilizing function. By formulating the state space equations as a set of finite difference equations, it is fairly easy to implement such a differentiator on a control computer (e.g. a microcontroller or single board computer). Normally, the highest order time derivatives will contain the most noise, so the order of the filter should be higher than the order of the desired derivative. Note that some phase lag and attenuation of the filtered signal and its time derivatives will occur, depending on the values of ζ and ω_n. These values should be selected based on knowledge of how fast the input signal tends to fluctuate.

(3) In the computation of the stabilizing functions and control input it is implicitly assumed that the terms $\mathbf{f}_i(\mathbf{x}_i)$ and $\mathbf{G}_i(\mathbf{x}_i)$ are precisely known. However, there will generally be some uncertainty associated with the dynamical model of any physical system. By including the linear terms $-k_i z_i$, where z_i is the state error as in (4.15), in the stabilizing functions and control input, it can be ensured that the control Lyapunov function of the closed loop system is positive definite and that its derivative is negative definite when model uncertainties are small. The terms $-k_i z_i$ can be thought of as linear damping terms. However, owing to the nonlinearity of most systems, model uncertainty can adversely affect the

stability of the system when it is operated away from its closed loop equilibrium point $\tilde{\alpha}_i = 0$. The nonlinearities associated with model uncertainty are often referred to as *bad nonlinearities*.

With backstepping it is relatively straightforward to make the closed loop system more robust to model uncertainty by including additional *nonlinear damping* terms in the definitions of the stabilizing functions and control input, e.g. of the form $-k_i z_i^3$, etc.. Such nonlinear damping is intended to dominate any "bad nonlinearities". By suitable selection of the control gains multiplying these nonlinear damping terms, it is (in principle) possible to ensure that the system is stable.

Since it can be difficult to characterize the bad nonlinearities, an obvious drawback to the use of nonlinear damping is that the control effort used may be more than is actually required. An approach to mitigating this problem is the use of nonlinear disturbance observer based control [9].

Problems

4.1. Consider the longitudinal motion of an underwater vehicle. The equation of motion is

$$m\dot{u} = -c|u|u + \tau,$$

where m is the mass of the vehicle, c is the drag coefficient, u is the surge speed and τ is the control input (thrust force generated by a propeller). Let $x_2 = \dot{x}_1 = u$ and $\mathbf{x} = [x_1 \;\; x_2]^T$.

a) Use the inverse dynamics approach (Section 4.2.2) to find a linearizing PID control input τ to track a desired time dependent position $x_d(t)$.
b) Take $m = 40$ kg and $c = 1.25$ kg/m. Create a numerical simulation using your result from part a) to follow the trajectory

$$x_d(t) = \begin{cases} 5 \text{ m}, & 0 < t \leq 20 \text{ secs}, \\ 15 \text{ m}, & 20 < t \leq 60 \text{ secs}, \\ 0 \text{ m}, & 60 < t \leq 120 \text{ secs}. \end{cases}$$

Assume that the vehicle starts from rest, i.e. $x_1(0) = x_2(0) = 0$. Experiment with different proportional, derivative and integral gains to see how the response varies.
c) Repeat part b) when the model of the system is uncertain. I.e., let the value of the drag coefficient in the control input c_τ be slightly different from what it is in the system model c. How do the simulations vary when $c_\tau = \{0.5c, 0.75c, 1.25c, 1.5c\}$?

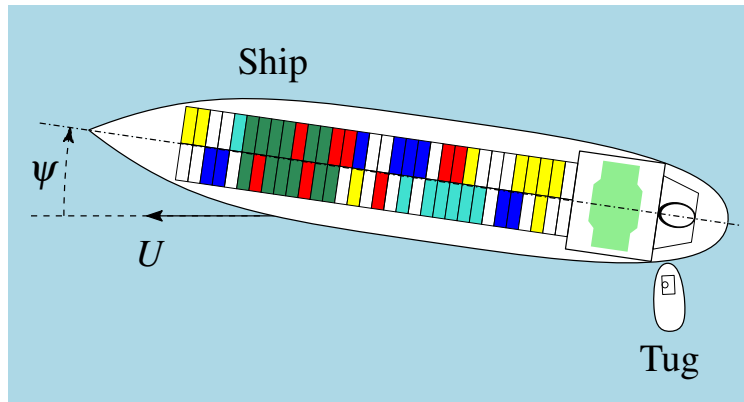

Fig. 4.7 Tugboat aligning a cargo ship.

4.2. Consider the situation shown in Fig. 4.7 in which a tugboat is used to guide the path of a cargo ship coming into port. Modeling the hull of the cargo ship as being symmetrical about the vertical centerline plane and ignoring any air or wave drag, we will take the yaw response of the ship to result from a combination of the

hydrodynamic Munk moment and the moment applied by the tugboat. The equations of motion are given by

$$\begin{aligned}\dot{x}_1 &= x_2,\\ \dot{x}_2 &= \sin(x_1)\cos(x_1) + u\cos(x_1),\\ y &= x_1,\end{aligned}$$

where $x_1 := \psi$ and $x_2 := r$ are the yaw angle and yaw rate of the cargo ship. The control objective is to stabilize the system at $\mathbf{x} = [\psi \;\; r]^T = 0$. Design a backstepping controller.

a) Define suitable error surfaces z_1 and z_2.
b) Rewrite the equations of motion in terms of the error surfaces.
c) Using the candidate Lyapunov function

$$V = \frac{1}{2}z_1^2 + \frac{1}{2}z_2^2,$$

find the stabilizing function and control input that stabilize the system.

4.3. A CTD is a device used to obtain profiles of the conductivity, temperature, density and sound speed versus depth. CTDs are often lowered and raised from the side of a boat using a davit (small crane) with a cable reel to let out and pull in the CTD cable. CTDs are often designed to be used with profiling speeds in the range $0.5 \leq |v| \leq 2$ m/s, with speeds of about 1 m/s generally being the best compromise between data quality and profile resolution. A tachometer is used as a feedback sensor for measuring the cable speed. The rate of change of the radius of the reel r is

$$\frac{\mathrm{d}r}{\mathrm{d}t} = -\frac{d_c^2\omega}{2\pi w},$$

where d_c is the diameter of the cable, w is the width of the reel and ω is the angular velocity of the reel.

The relation between reel angular velocity and the input torque from the controller τ is

$$I\frac{\mathrm{d}\omega}{\mathrm{d}t} = \tau.$$

The inertia I changes when the cable is wound or unwound. The equation $I = 50r^4 - 0.1$ can be used to account for the changing inertia.

Rather than writing out all of the terms involved, the analysis can be simplified by expressing the dynamics of the system in the following form

$$\begin{aligned}\dot{r} &= -a\omega,\\ \dot{\omega} &= i(r)\tau,\\ y &= r\omega,\end{aligned}$$

where the output y is the profiling speed of the CTD, the constant $a := d_c^2/(2\pi w)$, and the function $i(r) := 1/I = 1/(50r^4 - 0.1)$. Use the backstepping controller design technique to find a suitable control input.

References

1. Thor I Fossen. *Handbook of marine craft hydrodynamics and motion control*. John Wiley & Sons, 2011.
2. Thor I Fossen and Jan P Strand. Tutorial on nonlinear backstepping: Applications to ship control. 1999.
3. Walter R Johnson, John C Van Leer, and Christopher NK Mooers. A cyclesonde view of coastal upwelling. *Journal of Physical Oceanography*, 6(4):556–574, 1976.
4. J-J Slotine and Weiping Li. Adaptive strategies in constrained manipulation. In *Proc. 1987 IEEE International Conference on Robotics and Automation*, volume 4, pages 595–601. IEEE, 1987.
5. Jean-Jacques E Slotine and Weiping Li. *Applied nonlinear control*. Prentice-Hall Englewood Cliffs, NJ, 1991.
6. Mark W Spong, Seth Hutchinson, and Mathukumalli Vidyasagar. *Robot modeling and control*. Wiley, 2006.
7. D Swaroop, J Karl Hedrick, Patrick P Yip, and J Christian Gerdes. Dynamic surface control for a class of nonlinear systems. *IEEE transactions on automatic control*, 45(10):1893–1899, 2000.
8. DVAHG Swaroop, JC Gerdes, P Patrick Yip, and J Karl Hedrick. Dynamic surface control of nonlinear systems. In *American Control Conference, 1997. Proceedings of the 1997*, volume 5, pages 3028–3034. IEEE, 1997.
9. Karl Dietrich von Ellenrieder. *Control of marine vehicles*. Springer, 2021.

Lecture 5
Adaptive Control

Abstract The basic principles of adaptive control are presented, including model reference adaptive control, adaptive feedback linearization of single input, single output systems and adaptive feedback linearization for multiple input, multiple out systems.

5.1 Introduction

The dynamics of a marine vehicle are generally almost always uncertain. In the first place, it can be very difficult to accurately measure the inertial characteristics (e.g. the exact center of mass, distribution of mass, etc.) and damping (which can depend on temperature and loading) of a marine vehicle (parametric uncertainties). Secondly, even if these characteristics could be measured with high precision, they would likely vary over time as the vehicle is used, or because the system is reconfigured slightly to accommodate specific task requirements.

Marine vehicles are often used to transport loads (e.g. payloads, actuators, manipulators) of various sizes, weights, and inertial distributions. It is very restrictive to assume that the inertial parameters of such loads are well-known and static. If controllers with constant gains are used and the load parameters are not accurately known, the vehicle motion can be inaccurate or unstable.

Marine vehicles are often automatically steered to follow a path or trajectory. However, the dynamic characteristics of the vehicle strongly depend on many uncertain parameters, such as the frictional characteristics of the ground surface (e.g. snow, sand, ice, mud, grass, gravel, uneven ground), loading, wind conditions and even the operational speed of the vehicle. Adaptive control can be used to achieve good control performance under varying operating conditions, as well as to avoid energy loss due to excessive actuation.

In some cases, the parameter uncertainty must be gradually reduced on-line by an adaptation or estimation mechanism, or it may cause inaccuracy or instability of the controlled marine vehicle. Without the continuous ”redesign” of the controller, an

initially appropriate controller design may not be able to control the changing plant well. Generally, the basic objective of adaptive control is to maintain consistent performance of a system in the presence of uncertainty or unknown variation in plant parameters.

Note that ordinary feedback control with a constant gain controller can also reduce the effects of parameter uncertainty. However, a constant gain feedback controller is not an adaptive controller. Here, as in [1], we will take the attitude that an adaptive controller is a controller with adjustable parameters and a mechanism which adjusts those parameters online.

Adaptive control is an approach to the control of systems with constant or slowly-varying uncertain parameters. Adaptive controllers can be thought of as having two loops, an inner feedback loop consisting of the vehicle and controller, and an outer loop which adjusts the control parameters. The basic idea is to estimate uncertain parameters on-line using available state measurements, and to use the estimated parameters in the control law. Here, we will assume that the unknown plant parameters are constant. In practice, adaptive control is often used to handle time-varying unknown parameters. In order for the analysis results to be applicable to these practical cases, the time-varying plant parameters must vary considerably slower than the parameter adaptation. Fortunately, this is often satisfied in practice.

5.2 Model Reference Adaptive Control

With *model reference adaptive control* (MRAC) techniques, a control system is generally composed of four blocks, as shown in Fig. 5.1: a) the marine vehicle, b) a reference model, which specifies the desired output of the system, c) a feedback control law containing the adjustable parameters, and d) an adaptation law, which updates the adjustable parameters in the controller.

The structure of the dynamic equations governing the motion of the marine vehicle are assumed to be known, although the exact values of the parameters in the equations may be uncertain (e.g. the inertial and drag terms).

A *reference model* is used to specify the ideal response of the adaptive control system to the reference command $r(t)$. It provides the desired ideal plant response that the adaptation mechanism drives the system toward when adjusting the parameters. The selection of an appropriate reference model is part of the control system design and must satisfy two requirements: a) it should have the desired performance characteristics to perform the given control task, e.g. rise time, settling time, overshoot, etc. b) the ideal reference behavior should be achievable for the adaptive control system, i.e., it must have the correct order and relative degree for the assumed structure of the plant model.

The controller is parameterized by a number of adjustable terms. When the plant parameters are exactly known, the corresponding controller parameters should make the plant output identical to that of the reference model. When the plant parameters are not known, the adaptation mechanism will adjust the controller parameters so

that perfect tracking is can be achieved. If the control law is linear in terms of the adjustable parameters, it is said to be a *linearly parameterized control law*. Existing adaptive control designs normally require linear parameterization of the controller in order to obtain adaptation mechanisms with guaranteed stability and tracking convergence.

An *adaptation mechanism* is used to adjust the parameters in the control law until the response of the plant under adaptive control becomes the same as that of the reference model. As the objective of the adaptation mechanism is to make the tracking error converge to zero, the adjustable parameters will not necessary converge to the plant parameters. The basic ideas of MRAC are next illustrated using an example in which a single parameter is adjusted.

Example 5.1. Consider the use of MRAC for the vertical position tracking of an unmanned aerial vehicle (UAV). Let the mass of the vehicle be m, the vertical force input from the propellers be τ and g be gravity, the dynamics of the UAV in the vertical direction are

$$m\ddot{z} = mg + \tau. \tag{5.1}$$

The UAV is required to carry a small load, such as a camera, with an unknown weight (Fig. 5.2). The control objective is to track a desired time-dependent height $z_d(t)$.

Suppose that we would like the UAV to have the response of an ideal linear second order system with the form

$$\ddot{z}_m + 2\zeta\omega_n\dot{z}_m + \omega_n^2 z_m = \omega_n^2 z_d(t), \tag{5.2}$$

where z_m is the position of the reference model, and the damping ratio ζ and the natural frequency ω_n are selected to satisfy a set of desired performance characteristics, such as maximum overshoot

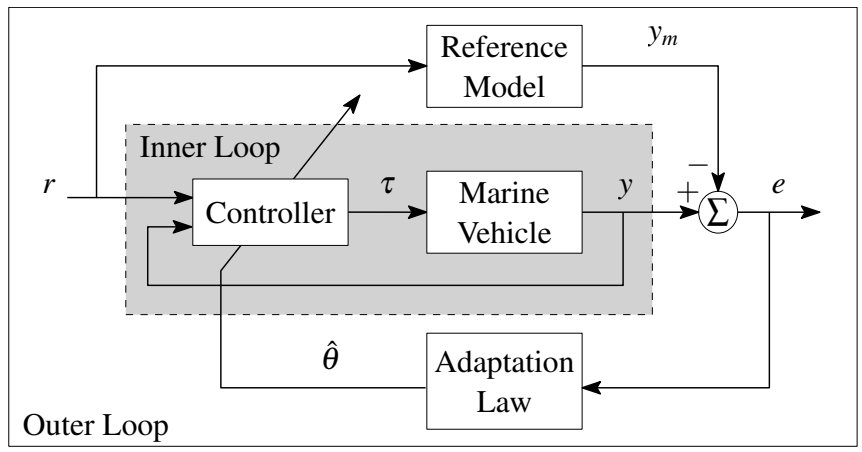

Fig. 5.1 A model reference adaptive control system. The arrow drawn across the controller indicates that the control parameters are adjusted. The system can be thought of as having an inner loop for control and an outer loop for parameter estimation.

Fig. 5.2 An unmanned aerial vehicle configured to carry a camera.

$$M_p = \mathrm{e}^{-\pi\zeta/\sqrt{1-\zeta^2}}, \quad 0 < \zeta \leq 1$$

and 2% settling time

$$t_s = \frac{4.0}{\zeta\,\omega_n}.$$

First, let us assume that the mass of the UAV and its load are precisely known. Take the control input to be $\tau = m\left(-g + \ddot{z}_m - 2\lambda\dot{\tilde{z}} - \lambda^2\tilde{z}\right)$, where $\tilde{z} := z(t) - z_m(t)$ is the tracking error and $\lambda > 0$ is a constant control gain, gives the closed loop error dynamics

$$\begin{aligned} \dot{\tilde{z}}_1 &= \tilde{z}_2 \\ \dot{\tilde{z}}_2 &= -2\lambda\tilde{z}_2 - \lambda^2\tilde{z}_1, \end{aligned} \tag{5.3}$$

where $\tilde{z}_1 := \tilde{z}$ and $\tilde{z}_2 := \dot{\tilde{z}}$. This system can be shown to be exponentially stable with an equilibrium point at $\tilde{z}_2 = \tilde{z}_1 = 0$ (perfect tracking).

Now let us assume that the mass is not precisely known, but that we have an estimate of it $\hat{m}$, which we will use in the control law as $\tau = \hat{m}\left(-g + \ddot{z}_m - 2\lambda\dot{\tilde{z}} - \lambda^2\tilde{z}\right)$. Then, (5.1) becomes

$$m\ddot{z} = \tilde{m}g - \hat{m}\left(-\ddot{z}_m + 2\lambda\tilde{z}_2 + \lambda^2\tilde{z}_1\right), \tag{5.4}$$

where $\tilde{m} := m - \hat{m}$. Following the approach in [2], we will define a new "combined error variable" variable

$$s := \tilde{z}_2 + \lambda\tilde{z}_1. \tag{5.5}$$

If we compute $\dot{s} + \lambda s$ and simplify the result using (5.4), we get the following combined expression for the closed loop tracking errors

$$\begin{aligned} m(\dot{s}+\lambda s) &= m\left(\dddot{\tilde{z}}_2+2\lambda\ddot{\tilde{z}}_2+\lambda^2\dot{\tilde{z}}_1\right), \\ &= m\ddot{z}+m\left(-\dddot{z}_m+2\lambda\ddot{\tilde{z}}_2+\lambda^2\dot{\tilde{z}}_1\right), \\ &= \tilde{m}g-\hat{m}\left(-\dddot{z}_m+2\lambda\ddot{\tilde{z}}_2+\lambda^2\dot{\tilde{z}}_1\right)+m\left(-\dddot{z}_m+2\lambda\ddot{\tilde{z}}_2+\lambda^2\dot{\tilde{z}}_1\right), \\ &= \tilde{m}\left(-\dddot{z}_m+2\lambda\ddot{\tilde{z}}_2+\lambda^2\dot{\tilde{z}}_1+g\right), \\ &= \tilde{m}\nu. \end{aligned} \tag{5.6}$$

Consider the following candidate Lyapunov function

$$V=\frac{1}{2}ms^2+\frac{1}{2\gamma}\tilde{m}^2, \tag{5.7}$$

where $\gamma>0$ is an adaption gain. Taking the derivative of this along trajectories of the closed loop system gives

$$\dot{V}=sm\dot{s}+\frac{1}{\gamma}\tilde{m}\dot{\tilde{m}}=sm\dot{s}-\frac{1}{\gamma}\tilde{m}\dot{\hat{m}}, \tag{5.8}$$

where it is assumed that $\dot{\tilde{m}}\approx-\dot{\hat{m}}$ because the value of the uncertain mass is either constant or very slowly varying in time (compared to its estimate, which can be updated much more rapidly). Using (5.6), this can be simplified to

$$\begin{aligned} \dot{V} &= s\left[-m\lambda s+\tilde{m}\nu\right]-\frac{1}{\gamma}\tilde{m}\dot{\hat{m}}, \\ &= -m\lambda s^2+\tilde{m}\left[s\nu-\frac{1}{\gamma}\dot{\hat{m}}\right]. \end{aligned} \tag{5.9}$$

We can ensure that $\dot{V}<0,\forall s\neq 0$ by selecting an update law for the mass estimate to be

$$\dot{\hat{m}}=\gamma s\nu=\gamma s\left(-\dddot{z}_m+2\lambda\ddot{\tilde{z}}_2+\lambda^2\dot{\tilde{z}}_1+g\right) \tag{5.10}$$

Using Barbalat's Lemma, one can show that s converges to zero. Thus, from (5.5) it can be seen that both the position tracking error $\tilde{z}_1$ and the velocity tracking error $\tilde{z}_2$ converge to zero.

Consider the use of an adaptive controller that permits a UAV to track a desired vertical position containing step-like jumps of ± 2.5 m (Fig. 5.3). Simulation results are shown in Figs. 5.4. For comparison, the same controller with the adaptation mechanism disabled is also shown. The unloaded mass of the UAV is $m=15$ kg. The UAV is carrying a payload (for example a camera) with a mass of $m_p=1.5$ kg, but the control law is implemented without knowledge of the payload mass. The reference model is taken to be an ideal second order system (5.2). The control design specifications are that for each step-like jump the peak overshoot and settling time of the UAV should be $M_p\leq 0.05$ and $t_s\leq 1.8$ secs, respectively. These design criteria can be satisfied using $\zeta=1/\sqrt{2}$ and $\omega_n=\pi$. It is also assumed that the UAV can only generate thrust in the downward direction and that the maximum thrust is

limited to twice the weight of the UAV. The gain of the parameter update law is $\gamma = 1$ and the control gain $\lambda = 10$.

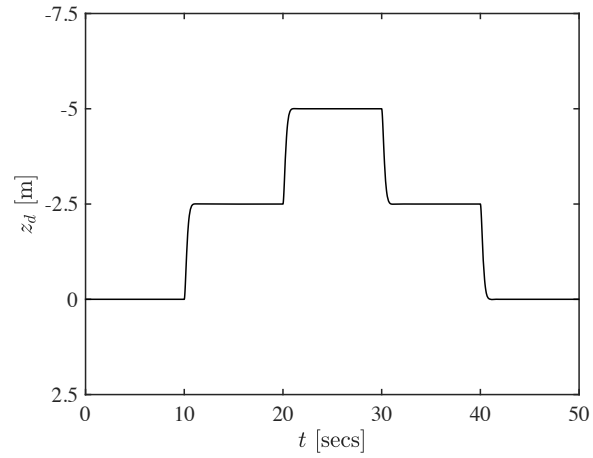

Fig. 5.3 Desired position $z_d(t)$ of the UAV. The trajectory is plotted in the NED frame, where upwards is in the negative direction.

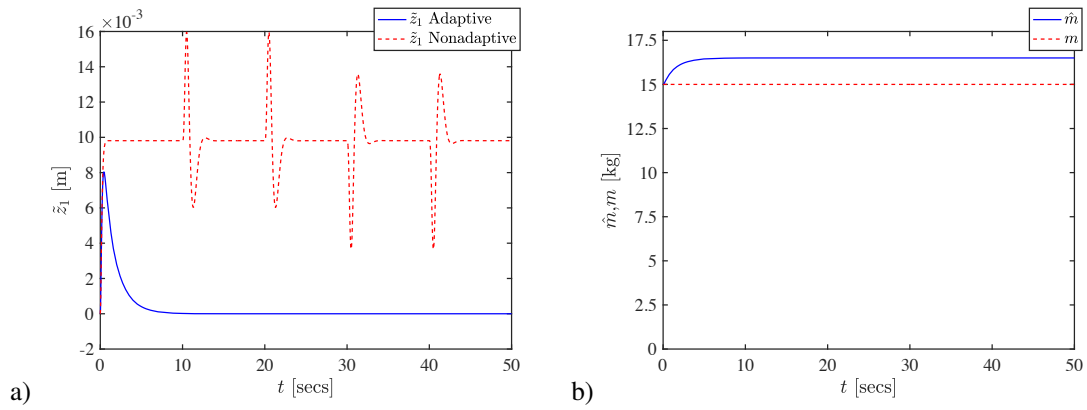

Fig. 5.4 a) Vertical position error of the UAV, and 2) mass estimate $\hat{m}$ from the adaptive controller versus actual mass m. The initial estimate of the total mass at $t = 0$ is taken to be $\hat{m} = 15$ kg. The solid blue lines correspond to the adaptive controller and the dashed red line corresponds to the corresponding non adaptive controller.

□

5.3 Adaptive SISO Control via Feedback Linearization

Next we explore the use of adaptive control via feedback linearization for single-input single-output systems, with multiple uncertain parameters. Consider an n^{th}

order nonlinear system in the form

$$mx^{(n)} + \sum_{i=1}^{n} \theta_i f_i(\mathbf{x}, t) = \tau, \tag{5.11}$$

where $\mathbf{x} = [x\ \dot{x}\ \cdots\ x^{(n-1)}]^T$ is the state vector,

$$x^{(n)} = \frac{\mathrm{d}^n x}{\mathrm{d}t^n}, \quad \forall n,$$

the $f_i(\mathbf{x},t)$ are known nonlinear functions, and the parameters θ_i and m are uncertain constants. Take the output of the system to be $y(t) = x(t)$. Assume that the full state vector $\mathbf{x}$ is measured.

The control objective is to make the output asymptotically track a desired, time-dependent, trajectory $y_d(t)$, despite an uncertain knowledge of the parameters.

As in Example 5.1, a combined error variable s can be defined for the system as

$$s := e^{(n-1)} + \lambda_{n-2} e^{(n-2)} + \cdots + \lambda_0 e, \tag{5.12}$$

where $e := (y - y_d) = (x - x_d)$ is the output tracking error and $\lambda_i > 0$ for all $i \in \{0, \ldots, (n-2)\}$. Let $x_r^{(n-1)} := x_d^{(n-1)} - \lambda_{n-2} e^{(n-1)} - \cdots - \lambda_0 e$ so that s can be rewritten as

$$s := x^{(n-1)} - x_r^{(n-1)}. \tag{5.13}$$

Take the control law to be

$$\tau = m x_r^{(n)} - ks + \sum_{i=1}^{n} \theta_i f_i(\mathbf{x}, t), \tag{5.14}$$

where k is a constant of the same sign as m and $x_r^{(n)}$ is the derivative of $x_r^{(n-1)}$ so that

$$x_r^{(n)} := x_d^{(n)} - \lambda_{n-2} e^{(n-1)} - \cdots - \lambda_0 \dot{e}. \tag{5.15}$$

If the parameters were all well-known, the tracking error dynamics would be

$$m\dot{s} = -ks, \tag{5.16}$$

which would give the exponential convergence of s, and by extension the exponential convergence of e.

However, since the model parameters are not known, the control law is given by

$$\tau = \hat{m} x_r^{(n)} - ks + \sum_{i=1}^{n} \hat{\theta}_i f_i(\mathbf{x}, t), \tag{5.17}$$

where $\hat{m}$ and $\hat{\theta}_i$ are the estimated values of m and the θ_i, respectively. Then, the closed loop tracking error is given by

$$m\dot{s} = -ks + \tilde{m}x_r^{(n)} + \sum_{i=1}^{n} \tilde{\theta}_i f_i(\mathbf{x},t), \tag{5.18}$$

where $\tilde{m} := \hat{m} - m$ and $\tilde{\theta}_i := \hat{\theta}_i - \theta_i$ are the parameter estimation errors. Consider the candidate Lyapunov function

$$V = |m|s^2 + \gamma^{-1}\left[\tilde{m}^2 + \sum_{i=1}^{n} \tilde{\theta}_i^2\right]. \tag{5.19}$$

Its time derivative is

$$\dot{V} = 2|m|s\dot{s} + 2\gamma^{-1}\left[\tilde{m}\dot{\hat{m}} + \sum_{i=1}^{n} \tilde{\theta}_i\dot{\hat{\theta}}_i\right]. \tag{5.20}$$

Using $m\dot{s} = |m|\text{sgn}(m)\dot{s}$ in (5.18), $\dot{V}$ can be rewritten as

$$\begin{aligned}
\dot{V} &= [2\text{sgn}(m)s]\,|m|\text{sgn}(m)\dot{s} + 2\gamma^{-1}\left[\tilde{m}\dot{\hat{m}} + \sum_{i=1}^{n} \tilde{\theta}_i\dot{\hat{\theta}}_i\right], \\
&= 2\text{sgn}(m)s\left[-ks + \tilde{m}x_r^{(n)} + \sum_{i=1}^{n} \tilde{\theta}_i f_i(\mathbf{x},t)\right] + 2\gamma^{-1}\left[\tilde{m}\dot{\hat{m}} + \sum_{i=1}^{n} \tilde{\theta}_i\dot{\hat{\theta}}_i\right], \\
&= -2\text{sgn}(m)ks^2 + 2\tilde{m}\left[\text{sgn}(m)sx_r^{(n)} + \gamma^{-1}\dot{\hat{m}}\right] \\
&\qquad + 2\sum_{i=1}^{n} \tilde{\theta}_i\left[\text{sgn}(m)sf_i(\mathbf{x},t) + \gamma^{-1}\dot{\hat{\theta}}_i\right].
\end{aligned} \tag{5.21}$$

With the assumption above that m and k have the same sign, $\dot{V}$ can be reduced to

$$\dot{V} = -2|k|s^2, \tag{5.22}$$

which is negative definite for every $s \neq 0$, by selecting the parameter update laws to be

$$\begin{aligned}
\dot{\hat{m}} &= -\gamma\text{sgn}(m)sx_r^{(n)}, \\
\dot{\hat{\theta}}_i &= -\gamma\text{sgn}(m)sf_i(\mathbf{x},t).
\end{aligned} \tag{5.23}$$

By using Barbalat's Lemma one can show that the system is globally asymptotically stable, so that the tracking errors converge to zero. It can also be shown that global tracking convergence is preserved if a different adaptation gain γ_i is used for each unknown parameter [2], i.e.

$$\begin{aligned}
\dot{\hat{m}} &= -\gamma_0\,\text{sgn}(m)sx_r^{(n)}, \\
\dot{\hat{\theta}}_i &= -\gamma_i\,\text{sgn}(m)sf_i(\mathbf{x},t).
\end{aligned}$$

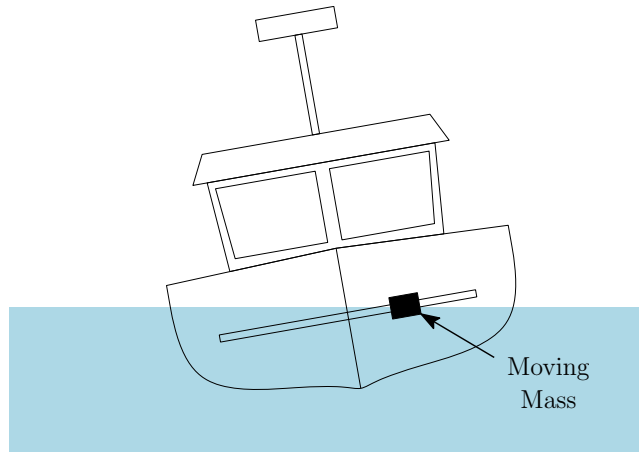

Fig. 5.5 Use of a moving mass system to stabilize the roll axis of a USV in waves.

Example 5.2. A classic example of (5.11) is the nonlinear equation for the rolling motion of an unmanned surface vehicle about its surge axis

$$m\ddot{\phi} + c_d|\dot{\phi}|\dot{\phi} + k_s\phi = \tau, \tag{5.24}$$

where m is the mass moment of inertia (including added mass) about the roll axis, c is a damping coefficient and k is a spring constant related to the buoyancy-induced righting moment. We will assume that m, c_d and k_s are unknown and use an adaptive controller to stabilize the USV at $\phi = 0$. For example, consider the use of a moving mass system to stabilize the roll axis of the vehicle in waves (Fig. 5.5).

Comparing (5.11) and (5.24), it can be seen that $\theta_1 = c_d$, $\theta_2 = k_s$, $f_1 = |\dot{\phi}|\dot{\phi}$ and $f_2 = \phi$. The system is second order so that $n = 2$. Taking the state variable to be $x = \phi$ and $\phi_d = \dot{\phi}_d = \ddot{\phi}_d = 0$, we get $e = \phi$, $\ddot{x}_r = -\lambda_0\dot{\phi}$ and $s = \dot{\phi} + \lambda_0\phi$. Thus, the control law (5.17) is given by

$$\tau = \hat{m}\ddot{x}_r - ks + \hat{\theta}_1|\dot{\phi}|\dot{\phi} + \hat{\theta}_2\phi.$$

The parameters estimates are found using the update laws

$$\begin{aligned} \dot{\hat{m}} &= -\gamma_0 s\ddot{x}_r, \\ \dot{\hat{\theta}}_1 &= -\gamma_1 s|\dot{\phi}|\dot{\phi}, \\ \dot{\hat{\theta}}_2 &= -\gamma_2 s\phi. \end{aligned} \tag{5.25}$$

The roll response of the USV is shown in Fig. 5.6 when the system is uncontrolled, and controlled with adaptive control and controlled with non adaptive control. The true values of the system are $m = 100$ kg-m^2, $c_d = 8.4$ kg-m^2 and $k_s = 17.5$ N-m. The control gains used are $\lambda_0 = 2$, $\gamma_0 = 10$, $\gamma_1 = 10$, $\gamma_2 = 1$, and $k = 5$. □

As can be seen in Example 5.2, the adaptation mechanism does not necessarily estimate the unknown parameters exactly, but simply generates values that permit a

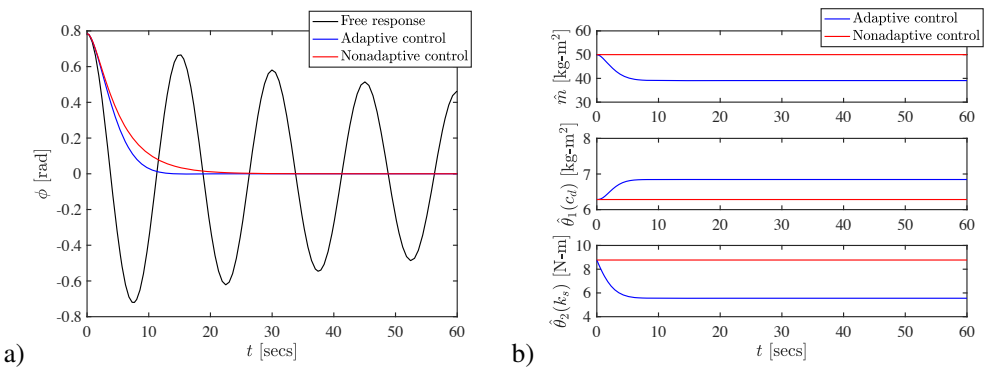

Fig. 5.6 a) Roll response of the USV when $\phi = \pi/4$ at time $t = 0$ when the USV is uncontrolled, and with adaptive controller and non adaptive controllers. The response with the adaptive controller settles to within $\phi = 0.02$ rad in about 10.6 secs, whereas for the non adaptive controller it takes about 17.5 secs. b) Parameter estimates for the adaptive controller and non adaptive controllers. The initial values of the estimates are $\hat{m} = 0.5m$, $\hat{\theta}_1 = 0.75c_d$ and $\hat{\theta}_2 = 0.5k_s$.

desired task to be achieved. The practical relevance is that physical effects, such as inertial loading and drag can still be accounted for.

Problems

5.1. Most propellers used on marine vehicles are rate-limited. The time response of the thrust generated can be modeled as a first order system of the form

$$T_d \dot{u} = -u + u_c,$$

where u_c is the commanded thrust, u is the output thrust and T_d is a time constant. In general, T_d is an uncertain parameter, as it can be difficult to measure experimentally, varies with the speed of the vessel and can change over time (e.g. from propeller blade damage caused by unintentional grounding). Use an adaptive control input to provide an estimate of $\hat{T}_d$ via the feedback linearization approach. Let the error variable be $s = u - u_d$, where $u_d(t)$ is the desired thrust, and take the control input to be $u_c = -ks + \hat{T}_d \dot{u}_d + u$.

a) Take the candidate Lyapunov function to be

$$V = \frac{1}{2}s^2 + \frac{1}{2\gamma}\tilde{T}_d^2,$$

with $\tilde{T}_d = \hat{T}_d - T_d$. Show that the resulting parameter update law is given by

$$\dot{\hat{T}}_d = -\gamma \dot{u}_d s,$$

where $\gamma > 0$ is a constant adaptation gain.

b) What variables must be measured in order for use of this approach to work? Explain the pros and cons of implementing this approach in practice (i.e. on a real marine vessel).

5.2. A station-keeping controller for a lightweight unmanned surface vehicle (USV) with a low draft and a large windage area is being developed. The vehicle will be outfitted with an anemometer to measure the apparent wind velocity. The anemometer measurements will be used as an input to a model for estimating the wind forces acting on the above-surface portions of the USV. The estimated wind drag is fed-forward as a negative term in the control input to counteract the wind drag. As the USV is frequently reconfigured between missions, the coefficients in the wind drag model are highly uncertain.

Here, we'll focus on only the surge axis of the vehicle. The equation of motion are given by

$$\begin{aligned} \dot{x}_1 &= x_2, \\ \dot{x}_2 &= -c_0 x_2 |x_2| - c_w u_a |u_a| + \tau, \end{aligned}$$

where x_1 is the vehicle position along the surge direction, x_2 is the speed of the USV along the surge axis, c_0 is a drag coefficient (for the underwater portion of the hull), c_w is a drag coefficient for the wind, u_a is the apparent wind velocity along the longitudinal axis of the vehicle ($u_a > 0$ when the USV is in a headwind) and τ is the control input (the equation for the dynamics has been normalized by the mass of

the USV). For station-keeping the control objective is to keep the USV at the origin $(x_1, x_2) = 0$.

Use adaptive feedback linearization to design a station-keeping controller for the USV. Take the control input to be

$$\tau = -ks + \hat{c}_0 x_2 |x_2| + \hat{c}_w u_a |u_a| + \dot{x}_r$$

and define appropriate expressions for the error variable s, x_r, and the candidate Lyapunov function V. What are the resulting update laws for $\hat{c}_0$ and $\hat{c}_w$.

5.3. Consider the surge speed tracking control of an unmanned surface vehicle. The equation of motion is

$$m\dot{u} = -C_d u|u| + \tau,$$

where m is the vehicle mass, C_d is the drag coefficient and τ is the thrust from a propeller. The control objective is for the vehicle to track a time-dependent trajectory $u_d(t)$ when C_d and m are uncertain and possibly slowly varying in time. Using model reference adaptive control, take the reference model to be the first order equation

$$\dot{u}_m = -\frac{u_m - u_d}{T_d},$$

where T_d is a time constant. Define the surge-speed velocity tracking error to be $\tilde{u} := u - u_m$. Using partial feedback linearization, the control input is taken to be

$$\tau = \hat{C}_d u|u| + \hat{m}\dot{u}_m - k_p \tilde{u},$$

where $\hat{C}_d$ and $\hat{m}$ are estimates of C_d and m, respectively.

a) Assuming that we have a perfect model of the vehicle, such that $C_d = C_d$ and $\hat{m} = m$, substitute the control input τ into the equation of motion to show that the closed loop system has a stable equilibrium point at $\tilde{u} = 0$.
b) If we no longer have a perfect model of the vehicle, such that $\hat{C}_d \neq C_d$ and $\hat{m} \neq m$, substitute the control input τ into the equation of motion to show that the closed loop system is given by

$$m\dot{\tilde{u}} = -\tilde{C}_d u|u| - \tilde{m}\dot{u}_m - k_p \tilde{u},$$

where $\tilde{C}_d := C_d - \hat{C}_d$ and $\tilde{m} := m - \hat{m}$ are the estimation errors.
c) Take the combined error variable to be $s = \tilde{u}$ and consider the candidate Lyapunov function

$$V = \frac{1}{2}ms^2 + \frac{1}{2\gamma_m}\tilde{m}^2 + \frac{1}{2\gamma_d}\tilde{C}_d^2.$$

d) Using the result from part b) above and the definitions of $\tilde{m}$ and $\tilde{C}_d$, show that the time derivative of $\dot{V}$ can be written as

$$\dot{V} = -k_p\tilde{u}^2 - \tilde{m}\left[\frac{1}{\gamma_m}\dot{\hat{m}} + \dot{u}_m\tilde{u}\right] - \tilde{C}_d\left[\frac{1}{\gamma_d}\dot{\hat{C}}_d + u|u|\tilde{u}\right].$$

e) What are the parameter update laws for $\dot{\hat{m}}$ and $\dot{\hat{C}}_d$ that render $\dot{V} \leq 0$ for all $\tilde{u} \neq 0$.

5.4. Let us revisit Problem 5.3. Create a Simulink model of the model reference adaptive control system using user defined blocks for the controller, vehicle model (plant) and update mechanism. The reference model can be constructed from either a subsystem composed of simple blocks, or a user defined function. Use the parameter values $m = 35$ kg, $C_d = 0.5$, $\gamma_d = 10$, $\gamma_m = 10$, $T_d = 1$ secs and $kp = 20$. Let the initial values of the parameter estimates be $\hat{C}_d = 0$ and $\hat{m} = 0$.

a) Take $u_d = 2$ m/s (constant). Show that the controlled system achieves the desired velocity.
b) Now, let the desired velocity be a $u_d(t) = 2 + 0.5\cos(2\pi t/20)$ m/s. Show that the controlled system is able to track the desired velocity.
c) Next, let the desired velocity once again be $u_d = 2$ m/s (constant). However, now assume that a constant disturbance of $w_d = 50$ N is acting on the vehicle and change the Simulink model accordingly. Show that the output now has a steady state error. What is its magnitude?
d) We will add integral control to see if the steady state error can be removed. Define the combined error variable to be

$$s = \tilde{u} + \lambda \int_0^t \tilde{u} \mathrm{d}t$$

and let the control input be

$$\tau = \hat{C}_d u|u| + \hat{m}\left(\dot{u}_m - \lambda \tilde{u}\right) - k_p s.$$

As before, let the candidate Lyapunov function be

$$V = \frac{1}{2} m s^2 + \frac{1}{2}\gamma_m \tilde{m}^2 + \frac{1}{2}\gamma_d \tilde{C}_d^2.$$

Show that the time derivative of $\dot{V}$ can now be written as

$$\dot{V} = -k_p s^2 - \tilde{m}\left[\gamma_m \dot{\hat{m}} + \left(\dot{u}_m - \lambda \tilde{u}\right) s\right] - \tilde{C}_d\left[\gamma_d \dot{\hat{C}}_d + u|u|s\right].$$

What are the parameter update laws for $\dot{\hat{m}}$ and $\dot{\hat{C}}_d$ that render $\dot{V} < 0$ for all $\tilde{u} \neq 0$ (negative definite)?
e) Revise your simulation using the new control law and parameter update rule for $\dot{\hat{m}}$. Set $\lambda = 2$ and leave the values of all the other coefficients the same. Show that the steady state error is now driven to zero.

5.5. Consider the automatic launch and recovery of an AUV from a USV. After the AUV is launched, the USV must accurately track a desired trajectory so that it can rendezvous with the AUV at the correct time and place for recovery. When the AUV is launched, the mass of the above surface system changes substantially so that the draft of the USV, and the associated drag and added mass characteristics change.

Explore the use of adaptive control for the trajectory tracking of a USV performing an automatic launch. For simplicity, focus on the surge motion of the USV.

The equations of motion are

$$\dot{x} = u,$$
$$m\dot{u} = -c_o u|u| + \tau,$$

where x is the surge position, u is the surge velocity, τ is the control input, m is the uncertain/changing mass, and c_0 is the drag coefficient.

The mass of the AUV is 40 kg, the mass of the USV is 150 kg (without AUV) and the drag coefficient of the USV is $c_0 = 8.5$ kg/m when carrying the AUV, and $c_0 = 6.0$ kg/m after the AUV has been launched.

A short launch and recovery test sequence is performed in which the system is at zero speed during both the launch and the recovery. The AUV is launched at time $t = 0$ at the position $x(0) = 0$ and recovered at time $t = t_f = 300$ seconds at the location $x(t_f) = x_f = 600$ m. The desired trajectory is given by

$$x_d(t) = 3x_f \left(\frac{t}{t_f}\right)^2 - 2x_f \left(\frac{t}{t_f}\right)^3.$$

Define the tracking error to be $e = x - x_d$.

a) Use inverse dynamics feedback linearization to design the control input, by selecting

$$\tau = c_o u|u| + m\ddot{x}_d - k_1 e - k_2 \dot{e}.$$

   i) Select k_1 and k_2 to obtain good performance when m corresponds to the mass of the entire system (USV with AUV) and c_0 corresponds to the drag coefficient when the USV is carrying the AUV.
   ii) Create a Simulink simulation and confirm the expected performance of the system when the USV carries the AUV.
   iii) Modify the simulation so that at $t = t_l = 60$ secs the AUV is suddenly dropped. The parameters c_0, m and the control gains in the controller τ should remain fixed, but the mass and drag in the vehicle model should change step-wise at time t_l. How well is the controller able to cope with the sudden changes?

b) Use adaptive feedback linearization to design the control input.

   i) What are the parameter update laws for $\hat{c}_0$ and $\hat{m}$?
   ii) Create a new Simulink simulation with the adaptive update law and tune the control parameters to obtain good performance when the AUV is suddenly dropped at $t = t_l = 60$ secs. How well does the adaptive controller handle the sudden changes?
   iii) Plot the tracking error and the parameters estimates $\hat{\theta}$ to show their convergence.

References

1. Karl J Astrom and Björn Wittenmark. *Adaptive control*. Dover Publications, Inc. New York, NY, 2 edition, 2008.
2. Jean-Jacques E Slotine and Weiping Li. *Applied nonlinear control*. Prentice-Hall Englewood Cliffs, NJ, 1991.

Lecture 6
Sliding Mode Control

Abstract The fundamental principles of first and second order sliding mode control are presented. It is shown that first order sliding mode control is robust to exogenous disturbances, but involves the use of a discontinuous control signal that may lead to a chattering effect in which the control input rapidly fluctuates. Chattering is generally undesirable, as it can damage actuators, but in some cases it is possible to alleviate it by approximating the discontinuous term with a continuous function. It is shown that the control input generated when using second order sliding mode control is smooth, but still robust to exogenous disturbances and model uncertainty.

6.1 Introduction

Consider the dynamic equations of a marine vehicle (Fig. 6.1) in body-fixed coordinates

$$\dot{\eta} = \mathbf{J}(\eta)\mathbf{v},$$

$$\mathbf{M}\dot{\mathbf{v}} = -\mathbf{C}(\mathbf{v})\mathbf{v} - \mathbf{D}(\mathbf{v})\mathbf{v} - \mathbf{g}(\eta) + \tau + \mathbf{w}_d.$$

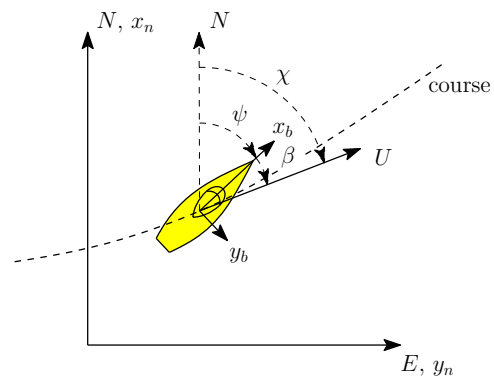

Fig. 6.1 3 DOF maneuvering coordinate system definitions.

It should be noted that dynamic models of marine vehicles generally tend to be fairly uncertain. The drag properties $\mathbf{D}(\mathbf{v})$ and actuator capabilities (in generating τ) may change if the vehicle is operated at off-design speeds, or from the wear and tear that occurs with normal usage. Further, the vehicle may have been designed to operate in one configuration, but a user may later add or remove components of the system, significantly changing the inertial properties represented by $\mathbf{M}$ and $\mathbf{C}(\mathbf{v})$, as well as the drag term $\mathbf{D}(\mathbf{v})$. Lastly, there are often unpredictable exogenous (externally-generated) disturbances that affect the vehicle's performance, which are unknown, but can be bounded. Here, the disturbances and model uncertainty will be combined and represented in the equations of motion (6.1) as the vector $\mathbf{w}_d$.

From (6.1) it can be seen that the dynamics of a marine vehicle tend to be non-linear. Model uncertainties and exogenous disturbances, tend to strongly affect non-linear systems, thus it is important to find control approaches that are *robust* to these uncertainties. Sliding mode control is an important robust control technique. The main advantages of sliding mode control include:

1) robustness to uncertain plant model parameters, unmodeled dynamics and exogenous disturbances,
2) finite-time convergence, and
3) reduced order dynamics.

Several marine vehicle trajectory tracking control designs are based on the use of sliding mode control (SMC) to provide a fast response and to guarantee that tracking errors are bounded and robust to unmodeled dynamics and exogenous disturbances. SMC is generally based upon maintaining a sliding surface constraint through the use of high frequency switching, which is usually accomplished by injecting a non-linear discontinuous term into the control input.

The order of a sliding mode controller is categorized according to the relative degree r_s between the sliding surface $s = 0$ and the injected discontinuous term. For example, a first order sliding mode controller (standard SMC) has $r_s = 1$, such that the discontinuous control input explicitly appears in the first total time derivative $\dot{s}$.

A potential problem with first order SMC designs is that, while the discontinuous control input enables the system to reject disturbances and improves robustness to model uncertainty, it can lead to an undesirable chattering effect, even with the use of some of the standard chattering mitigation techniques that are presented below.

The use of higher order sliding mode (HOSM) control design techniques, where $(r_s \geq 2)$, can be used to alleviate the chattering problem. In addition, HOSM techniques can also be used for the design of real-time differentiators (for example, to take the time derivatives of a measured signal or of a backstepping virtual control input) and observers (for estimating system states or disturbances) [6, 7, 11]. Higher order sliding mode controllers have convergence and robustness properties similar to those of first order sliding mode controllers, but they produce a continuous control signal (without chatter). Effectively, the approach still uses a non-linear discontinuous term, as is done in first order sliding mode techniques, but the relative degree r_s between s and the discontinuous term is increased, so that the control signal is continuous. HOSM controllers are often used in combination with HOSM differen-

tiators/observers, as computation of the control input can require knowledge of state derivatives and disturbances.

Note that since the highest order terms in a sliding mode system are discontinuous, modified forms of the nonlinear Lyapunov stability analysis methods can be applied in some limited cases, i.e. when $r_s = 2$ [9, 8], but more generally the stability of such systems must be understood in the sense of Filippov [3]. Such analyses are beyond the scope of these lecture notes. Here the focus is only the basics, so the main conditions required for the stability of the given sliding mode systems will only be stated. Interested readers can refer to the citations provided to more fully study the stability of sliding mode systems.

6.2 Linear feedback control under the influence of disturbances

Let us start by exploring the effects of uncertainty and external disturbance on a linear controller.

Example 6.1. Consider depth control of a Lagrangian float. Let the depth be represented by $x_1 = z$ and the vertical descent/ascent rate be $x_2 = \dot{z}$. Then the equations of motion can be written as

$$\begin{aligned} \dot{x}_1 &= x_2, \\ \dot{x}_2 &= \tau + w_d(x_1, x_2, t), \end{aligned} \tag{6.1}$$

where τ is the control input and w_d is a bounded disturbance (e.g. from a current), with bounds $L \geq |w_d|$, where $L > 0$ is a positive constant.

The control objective is to design a feedback control law that drives $x_1 \to 0$ and $x_2 \to 0$ asymptotically. Achieving asymptotic convergence in the presence of the unknown disturbance is challenging. For example, consider a linear control law of the form $\tau = -k_1 x_1 - k_2 x_2$. When $w_d = 0$, the closed loop system can be written in the state space form

$$\dot{\mathbf{x}} = \frac{\mathrm{d}}{\mathrm{d}t} \begin{bmatrix} x_1 \\ x_2 \end{bmatrix} = \begin{bmatrix} 0 & 1 \\ -k_1 & -k_2 \end{bmatrix} \begin{bmatrix} x_1 \\ x_2 \end{bmatrix} = \mathbf{A}\mathbf{x}. \tag{6.2}$$

The closed loop system is stable when the matrix $\mathbf{A}$ is Hurwitz (when the real part of all eigenvalues of $\mathbf{A} < 0$). The eigenvalues of $\mathbf{A}$ can be computed by solving the equation

$$\det(\lambda \mathbf{1} - \mathbf{A}) = \begin{vmatrix} \lambda & -1 \\ k_1 & \lambda + k_2 \end{vmatrix} = \lambda(\lambda + k_2) + k_1 = 0, \tag{6.3}$$

for λ, where $\mathbf{1}$ is the identity matrix and $\det(\cdot)$ is the determinant. Solving (6.3) gives the two eigenvalues

$$\lambda_{1,2} = -\frac{k_2}{2} \pm \frac{1}{2}\sqrt{k_2^2 - 4k_1}. \tag{6.4}$$

In order for both eigenvalues to have negative real parts, we require $k_2 > 0$ and $k_1 > k_2^2/4$. A plot of the solution trajectories of (6.1) with $w_d = 0$ in the state space of the system is shown in Fig. 6.2a. When $w_d \neq 0$, the solution trajectories are

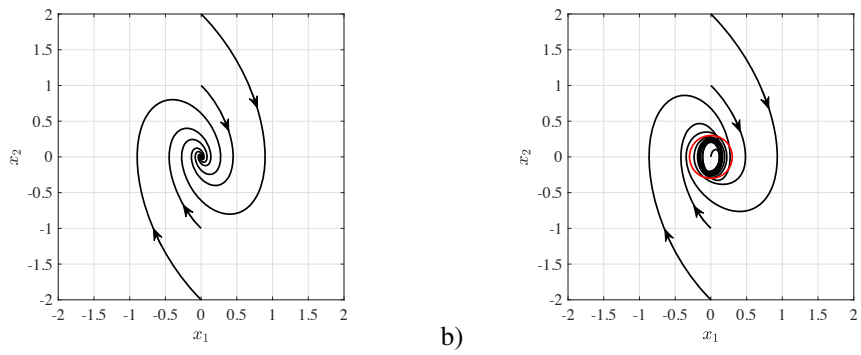

Fig. 6.2 Phase portrait of multiple solution trajectories of (6.1) for $k_1 = 2$ and $k_2 = 1$ when a) $w_d = 0$ and b) $w_d = 0.25\sin(1.5t)$. When $w_d = 0$, the controller asymptotically drives the closed loop system to the origin of its state space. Instead, when $w_d \neq 0$ the controller drives the states to a bounded region of convergence (represented approximately by the red circle).

ultimately bounded, that is they do not necessary approach the origin, but instead converge to a region, or "ball", of radius δ near the origin (Fig. 6.2b).

□

Here, we will examine the stability of the closed loop systems. Recall that Lyapunov functions are continuously differentiable, non-negative energy-like functions that always decrease along the solution trajectories of the system. We start by identifying a candidate Lyapunov function (CLF) $V(x_1, x_2)$, where

(a) V is a radially unbounded function of the state variables, i.e.

$$\lim_{|x_1|,|x_2|\to\infty} V(x_1, x_2) \to \infty, \tag{6.5}$$

and

(b) the time derivative of V is negative definite,

$$\dot{V} < 0, \forall x_1, x_2 \neq 0. \tag{6.6}$$

Example 6.2. Let explore the closed loop stability of (6.1) with linear control input $\tau = -k_1 x_1 - k_2 x_2$ using the CLF

$$V = \frac{1}{2}x_1^2 + \frac{1}{2}x_2^2. \tag{6.7}$$

From (6.7), it can be seen that this function is radially unbounded, i.e. that

$$\lim_{|x_1|,|x_2|\to\infty} V \to \infty.$$

Taking the time derivative of (6.7), we will see that control gains can be selected so that $\dot{V} < 0, \forall x_1, x_2 \neq 0$. First, we see that

$$\begin{aligned} \dot{V} &= x_1\dot{x}_1 + x_2\dot{x}_2, \\ &= x_1x_2 - x_2(-k_1x_1 - k_2x_2 + w_d), \\ &= (1-k_1)x_1x_2 - k_2x_2^2 + x_2w_d. \end{aligned} \tag{6.8}$$

This can be further simplified as

$$\begin{aligned} \dot{V} &\leq (1-k_1)\left[\frac{1}{2}x_1^2 + \frac{1}{2}x_2^2\right] - k_2x_2^2 + \left[\frac{1}{2}x_2^2 + \frac{1}{2}w_d^2\right], \\ &\leq -\frac{(k_1-1)}{2}x_1^2 - \left[\frac{(k_1-1)+2k_2-1}{2}\right]x_2^2 + \frac{1}{2}w_d^2, \end{aligned} \tag{6.9}$$

by using Young's Inequality.

Let

$$\mu_1 := \frac{(k_1-1)}{2} \quad \text{and} \quad \mu_2 := \left[\frac{(k_1-1)+2k_2-1}{2}\right] \tag{6.10}$$

where we take $\mu_1 > 0$ and $\mu_2 > 0$ to ensure stability. Then define

$$\mu := \min\{\mu_1, \mu_2\} \tag{6.11}$$

and

$$C_d := \sup_{\{x_1, x_2, t\}} \left|\frac{1}{2}w_d^2\right|. \tag{6.12}$$

With these definitions, (6.9) becomes

$$\dot{V} \leq -\mu_1x_1^2 - \mu_2x_2^2 + C_d. \tag{6.13}$$

It can be shown that $\dot{V}$ is upper-bounded by $-2\mu V + C_d$ when μ is either μ_1 or μ_2. For example, let $\mu = \mu_1$. Then (6.13) becomes

$$\dot{V} \leq -\mu_1\left(x_1^2 + \frac{\mu_2}{\mu_1}x_2^2\right) + C_d = -\mu\left(x_1^2 + \frac{\mu_2}{\mu}x_2^2\right) + C_d. \tag{6.14}$$

Using the definition of V in (6.7), and noting that $\mu_2/\mu > 1$, gives

$$\mu\left(x_1^2 + \frac{\mu_2}{\mu}x_2^2\right) > \mu\left(x_1^2 + x_2^2\right) = 2\mu V. \tag{6.15}$$

Therefore,

$$-\mu\left(x_1^2 + \frac{\mu_2}{\mu}x_2^2\right) + C_d < -2\mu V + C_d, \tag{6.16}$$

so that

$$\dot{V} \leq -2\mu V + C_d. \tag{6.17}$$

The same can be shown to be true when $\mu = \mu_2 = \min\{\mu_1, \mu_2\}$.

Equation (6.17) can be integrated to show that

$$V \leq \left(V_0 - \frac{C_d}{2\mu}\right) \mathrm{e}^{-2\mu t} + \frac{C_d}{2\mu}, \tag{6.18}$$

where V_0 is the value of V at time $t = 0$. The stability of this system can be classified as uniformly globally practically exponentially stable (USPES), see [13].

□

6.3 First Order Sliding Mode Control

We have seen that when exogenous disturbances and uncertainties are present, the closed loop trajectories of the system do not reach a specific equilibrium point, but instead asymptotically approach a finite region (ball) in the state space. Let's see if we can *reverse engineer* the desired closed loop dynamics of our system (6.1) in order to drive it to a desired equilibrium point when $w_d \neq 0$, instead.

When no disturbances are present, a stable linear controller for the state x_1 would have the form

$$\dot{x}_1 = -\lambda x_1, \quad \lambda > 0. \tag{6.19}$$

Since, $x_2 := \dot{x}_1$, the general solution of (6.19) is

$$\begin{aligned} x_1(t) &= x_1(0)\mathrm{e}^{-\lambda t}, \\ x_2(t) &= \dot{x}_1(t) = -\lambda x_1(0)\mathrm{e}^{-\lambda t}, \end{aligned} \tag{6.20}$$

where both $x_1(t)$ and $x_2(t)$ exponentially converge to zero. Ideally, nonzero disturbances $w_d(x_1, x_2, t) \neq 0$ will not affect our desired solution.

To design a controller that can achieve this desired solution we can introduce a new variable s in the state space of the system as

$$s = x_2 + \lambda x_1, \quad \lambda > 0. \tag{6.21}$$

We seek a control input τ that can drive s to zero in finite time. To find this control, we take the time derivative of (6.21), and use (6.1) to introduce the control input from the dynamics of the closed loop system into the resulting equation

$$\dot{s} = \dot{x}_2 + \lambda \dot{x}_1 = \tau + w_d(x_1, x_2, t) + \lambda x_2. \tag{6.22}$$

This expression can then be used to identify a suitable (CLF) to stabilize the closed loop system. Let

$$V = \frac{1}{2} s^2. \tag{6.23}$$

In order to ensure that the closed loop system converges to its equilibrium point in finite time, we also require the CLF to also (simultaneously) satisfy the inequality

$$\dot{V} \leq -\alpha V^{1/2}, \quad \alpha > 0. \tag{6.24}$$

The inequality can be solved using separation of variables, so that

$$\begin{aligned} \int_{V_0}^{V} \frac{\mathrm{d}V}{V^{1/2}} &\leq -\int_0^t \alpha \mathrm{d}t, \\ 2\left[V^{1/2} - V_0^{1/2}\right] &\leq -\alpha t, \\ V^{1/2} &\leq -\frac{\alpha t}{2} + V_0^{1/2}, \end{aligned} \tag{6.25}$$

where, as above, V_0 is the value of V at time $t = 0$. The Lyapunov function $V = V(x_1(t), x_2(t))$ becomes zero in the finite time t_r, which is bounded by

$$t_r \leq \frac{2V_0^{1/2}}{\alpha}. \tag{6.26}$$

Differentiating (6.23) we can find a control input τ so that $\dot{V} \leq 0$,

$$\dot{V} = s\dot{s} = s\left[\lambda x_2 + w_d(x_1, x_2, t) + \tau\right] \tag{6.27}$$

by taking $\tau = -\lambda x_2 + \nu$ to get

$$\dot{V} = s\left[\nu + w_d(x_1, x_2, t)\right] = s\nu + s w_d(x_1, x_2, t) \leq |s|L + s\nu. \tag{6.28}$$

Let $\nu = -\rho \mathrm{sgn}(s), \rho > 0$, where

$$\mathrm{sgn}(s) := \begin{cases} +1, & s > 0, \\ -1, & s < 0. \end{cases} \tag{6.29}$$

Note that strictly speaking one can take

$$\mathrm{sgn}(0) \in [-1, 1], \tag{6.30}$$

(see [11]). However, it is common in engineering practice to use $\mathrm{sgn}(0) = 0$, as in [4].

Then, noting that $\mathrm{sgn}(s)s = |s|$, (6.28) can be rewritten as

$$\dot{V} \leq L|s| - \rho \mathrm{sgn}(s)s = (L - \rho)|s|, \tag{6.31}$$

where L is an upper bound for the magnitude of the disturbance. Using (6.23) and (6.24), $\dot{V}$ can also be written as

$$\dot{V} \leq -\frac{\alpha}{\sqrt{2}}|s|. \tag{6.32}$$

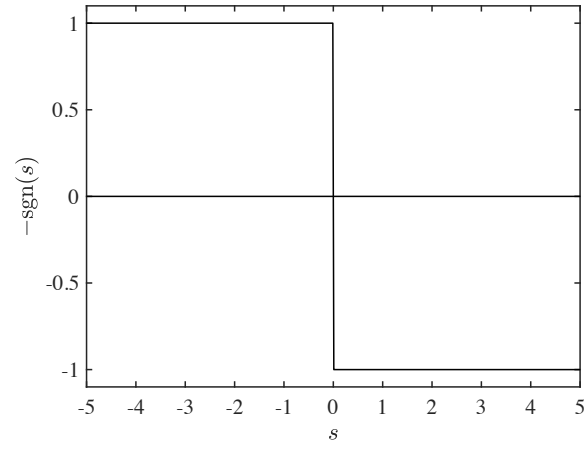

Fig. 6.3 A plot of the function $-\mathrm{sgn}(s)$.

Matching the right hand sides of inequalities (6.31) and (6.32) gives

$$(L-\rho) = -\frac{\alpha}{\sqrt{2}}, \tag{6.33}$$

so that the control gain can be selected as

$$\rho = L + \frac{\alpha}{\sqrt{2}}, \tag{6.34}$$

where the first component L compensates for the bounded disturbance and the second component determines the sliding surface reaching time t_r, which increases as α increases. The resulting control law is

$$\tau = -\lambda x_2 - \rho\,\mathrm{sgn}(s). \tag{6.35}$$

Remark 6.1. The surface $s = 0$ (which is the straight line $x_2 + \lambda x_1 = 0$ in two dimensions) is called a *sliding surface*. Equation (6.24), which is equivalent to

$$s\dot{s} \leq -\frac{\alpha}{\sqrt{2}}|s|, \tag{6.36}$$

is called a *reaching condition*. When the reaching condition is met, the solution trajectory of the closed loop system is driven towards the sliding surface and remains on it for all subsequent times.

Definition 6.1 (sliding mode controller). A control law that drives the state variables to the sliding surface in finite time t_r and keeps them on the surface thereafter in the presence of a bounded disturbance is called a sliding mode controller. An ideal sliding mode is taking place when $t > t_r$.

Example 6.3. Let us revisit control of the Lagrangian float discussed in Example 6.1. Consider the response of system (6.1) when the control input is instead taken to be $\tau = -\lambda x_2 - \rho \text{sgn}(s)$ with $\lambda = 1.5$, $\rho = 2$ and $w_d(x_1, x_2, t) = 0.25\sin(1.5t)$ and initial conditions $x_1(0) = 0$, $x_2(0) = 2$. From equation (6.23) it can be seen that

$$V_0 = \frac{1}{2}\left[x_2(0) + \lambda x_1(0)\right]^2 = 2. \tag{6.37}$$

If we take $L = 0.25$, then from (6.33) we have

$$\alpha = \sqrt{2}(\rho - L) = 2.475. \tag{6.38}$$

From (6.26), we see that the estimated *reaching time* is

$$t_r \leq \frac{2V_0^{1/2}}{\alpha} = \frac{2\sqrt{2}}{2.475} = 1.143 \text{ secs}. \tag{6.39}$$

The time responses of x_1, x_2 and s are plotted in Fig. 6.4a. It can be seen that for times between $t = 0$ and slightly earlier than $t = t_r$, the sliding surface $s \neq 0$, so that the closed loop system is in its reaching phase. At just before $t = t_r$ the value of x_2 changes discontinuously as $s \to 0$ and the system enters the sliding phase. It can be seen that both x_1 and x_2 are driven to zero. The corresponding phase portrait of the system is shown in Fig. 6.4b. By comparing Figs. 6.4a & b it can be seen that the curved branch of the trajectory in the phase plane corresponds to the reaching phase and the straight line portion (which moves along the line $x_2 = -1.5x_1$) corresponds to the sliding phase. The solution trajectory of the closed loop system reaches the desired equilibrium point $(x_1, x_2) = (0, 0)$, despite the nonzero disturbance acting upon it.

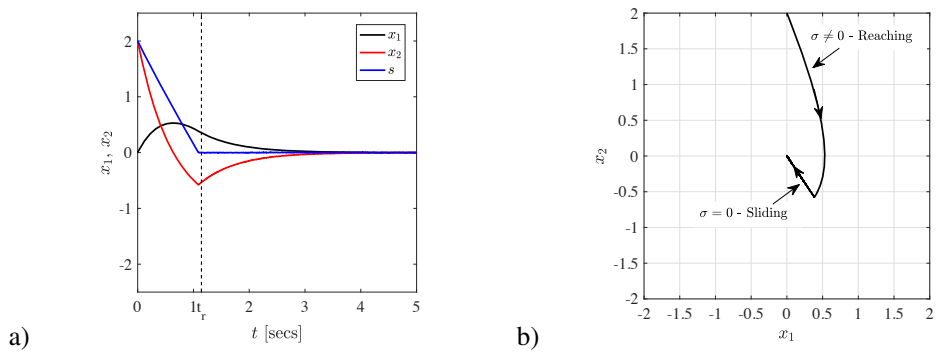

Fig. 6.4 a) Time response and b) phase portrait of the system in (6.1) when the control input is taken to be $\tau = -\lambda x_2 - \rho \text{sgn}(s)$ with $\lambda = 1.5$, $\rho = 2$ and $w_d(x_1, x_2, t) = 0.25\sin(1.5t)$ and initial conditions $x_1(0) = 0$, $x_2(0) = 2$.

For comparison purposes, the phase portrait is shown in Fig. 6.5 for the same initial conditions used in Figs. 6.2a–b.

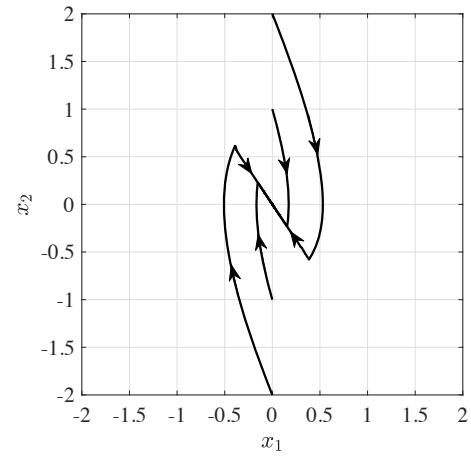

Fig. 6.5 Phase portrait of the sliding mode controller with $\lambda = 1.5$ and $\rho = 2$ and disturbance $w_d = 0.25\sin(1.5t)$.

Thus far, the sliding mode control approach seems fantastic. However, there is a catch. In numerical and practical implementations of the control law (6.35) the $\text{sgn}(s)$ term rapidly switches between $\text{sgn}(s) = +1$ and $\text{sgn}(s) = -1$ as the controller approaches the sliding mode phase, i.e. as $s \to 0$. Owing to the finite size of the time step in numerical simulations and to time delays or other imperfections in switching devices found in real implementations, the sign of s will continue to switch between positive and negative values after the reaching phase, so that the solution trajectory of the system zig-zags across the sliding surface, rather than truly sliding along it, in a condition known as *chattering* (Fig. 6.6a). This is can also be seen in the control input signal, which will also tend to rapidly oscillate in amplitude (Fig. 6.6b). In an ideal sliding mode, the frequency of the zig-zag motion would approach infinity and its amplitude would approach zero. However, in practical implementations this high frequency switching is undesirable, as it can result in low control accuracy, high heat losses in electrical circuits and the rapid wear of moving mechanical parts.

□

6.4 Chattering Mitigation

The chattering problem discussed in the previous section can be overcome by replacing the $\text{sgn}(s)$ function in (6.35) with a continuous approximation $f(s)$. In principle, the approximate function could be any function that is continuous, sigmoidal $\lim_{s\to\pm\infty} f(s) \to \pm 1$, odd $f(-s) = -f(s)$, zero at zero $f(0) = 0$ and strictly increasing. In practice, it is common to use a saturation function [12]

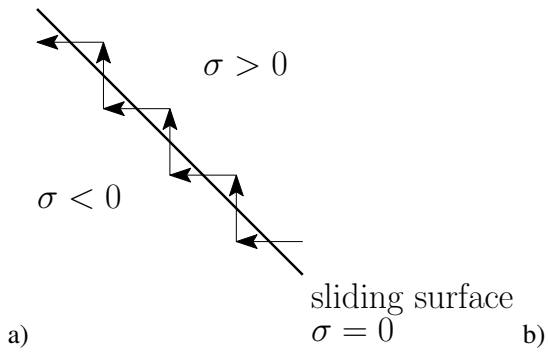

Fig. 6.6 a) Zig-zag motion of the solution trajectory across the sliding surface $s = 0$ exhibited during chattering. b) Chattering of the control input when using the sliding mode controller with $\lambda = 1.5$ and $\rho = 2$ and disturbance $w_d = 0.25\sin(1.5t)$. The inset for times $1.085 \leq t \leq 1.090$ illustrates how the control signal rapidly switches in amplitude during chattering.

$$f(s) = \text{sat}\left(\frac{s}{\Phi}\right) := \begin{cases} \dfrac{s}{\Phi}, & \left|\dfrac{s}{\Phi}\right| < 1, \\ \text{sgn}\left(\dfrac{s}{\Phi}\right), & \left|\dfrac{s}{\Phi}\right| \geq 1, \end{cases} \tag{6.40}$$

a hyperbolic tangent function [4]

$$f(s) = \tanh\left(\frac{s}{\Phi}\right), \tag{6.41}$$

or a simple sigmoidal function [11], such as

$$f(s) = \frac{\dfrac{s}{\Phi}}{\dfrac{|s|}{\Phi} + 1}, \tag{6.42}$$

where $\Phi > 0$ is a parameter that stretches the region along the s direction around the origin $s = 0$ (Fig. 6.7).

In the case of the saturation function (Fig. 6.8), it can be shown that the stretched region $|s| < \Phi$ functions like a boundary layer [12]. From (6.32) it can be seen that $\dot{V} < 0$ for $s \neq 0$ (negative definite) so that the boundary layer region is attractive. At the edges of the boundary layer, $|s| = \Phi$ so that $V_{\text{BL}} = \Phi^2/2$. Thus, modifying (6.25) as

$$\int_{V_0}^{V_{\text{BL}}} \frac{\text{d}V}{V^{1/2}} \leq -\int_0^{t_{\text{BL}}} \alpha \text{d}t \quad \Rightarrow \quad 2\left[V_{\text{BL}}^{1/2} - V_0^{1/2}\right] \leq -\alpha t_{\text{BL}},$$

it can be shown that the boundary layer is reached in the finite time t_{BL},

$$t_{\text{BL}} \leq \frac{\sqrt{2}(s_0 - \Phi)}{\alpha},$$

where, from (6.23), $s_0 = \sqrt{2V_0}$.

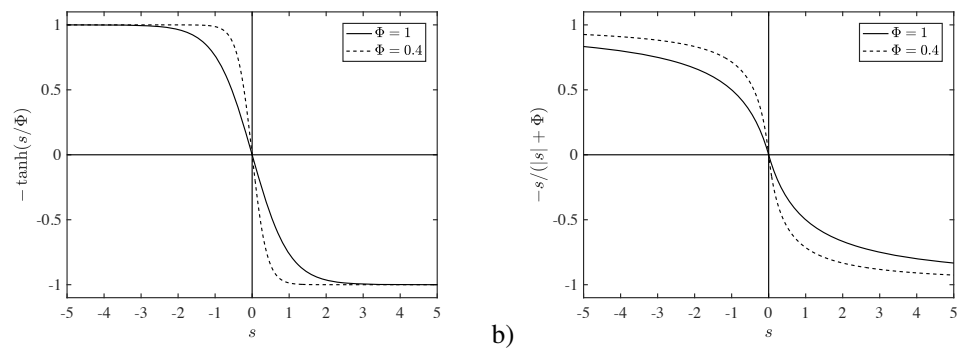

Fig. 6.7 Examples of continuous functions suitable for approximating the $-\text{sgn}(s)$ function in (6.35) with $\Phi = 1$ and $\Phi = 0.4$: a) the hyperbolic tangent function (6.41), and b) the sigmoidal function (6.42). It can be seen that as Φ decreases the output of each function is "squeezed" about $s = 0$.

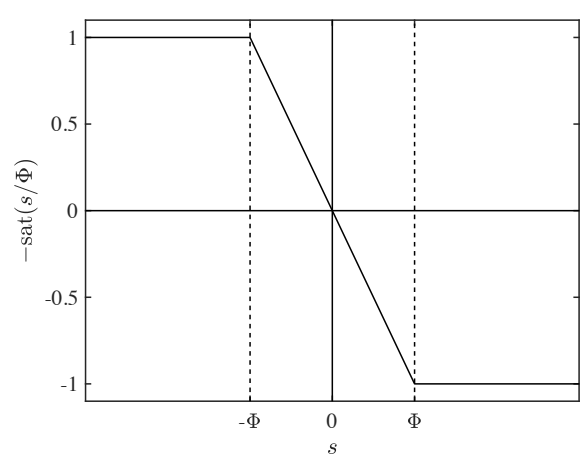

Fig. 6.8 Use of the saturation function (6.40) for approximating the $-\text{sgn}(s)$ function in (6.35). The region from $-\Phi \leq 0 \leq \Phi$ is the boundary layer.

Once inside the boundary layer, the solution trajectories will remain within the region $B = \{\mathbf{x} : |s(\mathbf{x},t)| \leq \Phi\}$ for all future times. However, within the boundary layer it is no longer guaranteed that $s \to 0$ for nonzero disturbances. Instead, the system will reach some bounded region around $s = 0$, the size of which depends upon Φ and λ (see [12]). Although s and the state variables no longer converge to the origin, the performance of the system can be very close to that of a true sliding mode controller.

Example 6.4. Returning to the control of the Lagrangian float discussed in Examples 6.1–6.3 above, we now implement the continuous saturation function (6.40) in the control law as $\tau = -\lambda x_2 - \rho\,\text{sat}(s/\Phi)$, where $\Phi = 0.05$, $\lambda = 1.5$, $\rho = 2$ and $w_d(x_1,x_2,t) = 0.25\sin(1.5t)$ and initial conditions $x_1(0) = 0$, $x_2(0) = 2$, as before. Comparing Fig. 6.9a and Fig. 6.4a, it can be seen that the time response of the system is almost the same. However, while the control input resulting from use of the

discontinuous function exihibits substantial chattering (Fig. 6.6b), the control input obtained with the saturation function is smooth (Fig. 6.9b).

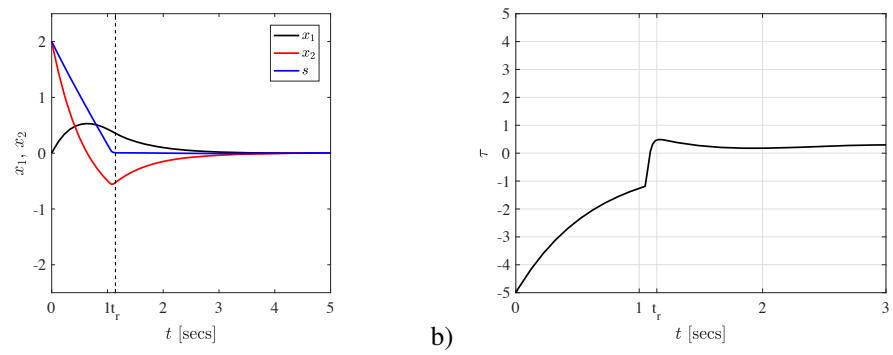

Fig. 6.9 The a) time response and b) control input of system (6.1) when $\tau = -\lambda x_2 - \rho \text{sat}(s/\Phi)$, where $\Phi = 0.05$, $\lambda = 1.5$, $\rho = 2$ and $w_d(x_1, x_2, t) = 0.25\sin(1.5t)$ and initial conditions $x_1(0) = 0$, $x_2(0) = 2$.

□

6.5 Equivalent Control

It is shown above that for times $t \geq t_r$ the trajectory of the closed loop system is on the sliding surface where $s = x_2 + \lambda x_1 = 0$. Once on the sliding surface, the trajectory remains there because of the sliding mode controller, so that $s = \dot{s} = 0$. Let us examine the condition $\dot{s} = 0$ more closely. From (6.27), we see that

$$\dot{s} = \lambda x_2 + w_d(x_1, x_2, t) + \tau = 0, \quad s(t \geq t_r) = 0 \tag{6.43}$$

would be satisfied by a an *equivalent control* input of the form

$$\tau_{\text{eq}} = -\lambda x_2 - w_d(x_1, x_2, t). \tag{6.44}$$

This suggests that the control law, which needs to be applied to ensure that the system remains on the sliding surface after reaching would be given by τ_{eq}. However, it would not be possible to implement this control law in practice, as the term $w_d(x_1, x_2, t)$ represents exogenous disturbances and model uncertainty, which we do not know. Given that the sliding mode control law (6.35) developed in Section 6.3 above is capable of keeping the closed loop system on the sliding surface after the reaching time, one can argue that we have identified a control law that acts like the desired τ_{eq}. Thus, the average effect of the high frequency switching in our sliding mode control law is τ_{eq}. We can approximate τ_{eq} by using a low pass filtered version of our sliding mode control law, which averages the effects of the high frequency switching caused by the $\text{sgn}(s)$ term as

$$\hat{\tau}_{\text{eq}} = -\lambda x_2 - \rho \text{LPF}\left[\text{sgn}(s)\right], \quad t \geq t_r. \tag{6.45}$$

The low pass filter can be implemented as a first order differential equation of the form

$$\begin{aligned} T\dot{z} &= -z + \text{sgn}(s) \\ \hat{\tau}_{\text{eq}} &= -\lambda x_2 - \rho z, \end{aligned} \tag{6.46}$$

where $T \in [0,1)$ is a filter time constant (which should be as small as possible, but larger than the sampling time of the computer). Comparing (6.44) and (6.45), it can be seen that the term $\text{LPF}\left[\text{sgn}(s)\right]$ in (6.45) acts like a disturbance observer, which can be used to provide an estimate of the combined effects of exogenous disturbances and model uncertainty.

6.6 Summary of First Order Sliding Mode Control

Based on our results thus far, we can state the following observations:

1) First Order sliding mode control design consists of two main tasks:
   a) Design of a first order sliding surface $s = 0$.
   b) Design of the control τ, which drives the sliding variable s in (6.21) to zero use the sliding variable dynamics in (6.22).
2) Application of the sliding mode control law (6.35) in (6.1) yields the closed loop system dynamics

$$\begin{aligned} \dot{x}_1 &= x_2, \\ \dot{x}_2 &= -\lambda x_2 - \rho \text{sgn}(s) + w_d(x_1, x_2, t). \end{aligned} \tag{6.47}$$

When the system is in sliding mode ($t \geq t_r$), the closed loop system is driven by its equivalent dynamics (6.44) so that (6.47) becomes

$$\begin{aligned} \dot{x}_1 &= x_2, \\ \dot{x}_2 &= \underbrace{-\lambda x_2 - w_d(x_1, x_2, t)}_{\tau_{\text{eq}}} + w_d(x_1, x_2, t) = -\lambda x_2 = -\lambda \dot{x}_1, \end{aligned} \tag{6.48}$$

which implies that

$$\begin{aligned} \dot{x}_1 &= x_2, \\ x_2 &= -\lambda x_1. \end{aligned}$$

Thus, once the sliding mode condition is reached, the dynamics of the system are first order (6.48), whereas the original system (6.1) is second order. This reduction of order is known as a *partial dynamical collapse*.

3) In the sliding mode the closed loop sytem dynamics do not depend on the disturbance term $w_d(x_1,x_2,t)$. However, the upper limit of w_d must be taken into account when selecting the controller gain.
4) In practical implementations, it may be necessary to use a continuous approximation of the discontinuous function $\text{sgn}(s)$ in the control law to avoid chattering.

6.7 Stabilization vs. Tracking

The problem of designing a control input that drives the closed loop system to an equilibrium point is known as a *stabilization problem*. However, many important marine vehicle control applications require one to design a control law that tracks a desired trajectory y_d, i.e. to design a control input which solves a *tracking problem*.

Let the output of the system be y. To ensure the system is stable, it is important to identify its relative degree. This can be thought of as the number of times r the output must be differentiated before the control input explicitly appears in the input–output relation. For example, if we take $y = x_1$ for system (6.1),

$$\begin{aligned} \dot{x}_1 &= x_2, \\ \dot{x}_2 &= \tau + w_d(x_1,x_2,t), \end{aligned} \tag{6.49}$$

it can be seen that $\ddot{y} = \ddot{x}_1 = \dot{x}_2 = \tau + w_d(x_1,x_2,t)$. Thus, the relative degree of system (6.1) is $r = 2$. When the order of the system is the same as its relative degree, it does not have any (hidden) internal dynamics (e.g. dynamics which cannot be directly controlled using the control input τ). When the relative degree of the system is less than its order, additional analysis is necessary to ensure that the internal dynamics of the system are stable.

Recent work that utilizes one or more first order sliding mode control terms for the trajectory tracking control of marine systems includes [1], [15], [2], [14], [5] and [10]. An example of the use of first order sliding mode control for station keeping is provided in the following example.

6.8 SISO Super–Twisting Sliding Mode Control

Once again, consider the system (6.49), where the output is taken to be $y = x_1$. Here, we will modify our definition of the sliding variable in (6.21) to solve an output tracking problem. Let $\tilde{x}_1 := (y - y_d) = (x_1 - y_d)$ and

$$s := \dot{\tilde{x}}_1 + \lambda\tilde{x}_1 = \tilde{x}_2 + \lambda\tilde{x}_1, \quad \lambda > 0. \tag{6.50}$$

We seek a control input that drives s to $s = 0$ in finite time and keeps it there, such that $\dot{s} = 0$. Taking the time derivative of (6.50) gives

$$\begin{aligned} \dot{s} &= \ddot{\tilde{x}}_1 + \lambda \dot{\tilde{x}}_1, \\ &= \ddot{y} - \ddot{y}_d + \lambda \dot{y} - \lambda \dot{y}_d, \\ &= \dot{x}_2 - \ddot{y}_d + \lambda x_2 - \lambda \dot{y}_d, \end{aligned} \tag{6.51}$$

Using (6.49), this can be reduced to

$$\dot{s} = \underbrace{-\ddot{y}_d - \lambda \dot{y}_d + \lambda x_2 + w_d(x_1, x_2, t)}_{\gamma(x_1, x_2, t)} + \tau = 0, \tag{6.52}$$

where $\gamma(x_1, x_2, t)$ is a *cumulative* disturbance term, which is upper-bounded by a positive constant M, e.g. $|\gamma(x_1, x_2, t)| \leq M$.

When $\gamma(x_1, x_2, t) = 0$ using the control input

$$\tau = -\lambda |s|^{1/2} \text{sgn}(s), \quad \lambda > 0 \tag{6.53}$$

in (6.51) makes compensated dynamics in the sliding mode become

$$\dot{s} = -\lambda |s|^{1/2} \text{sgn}(s), \quad s(0) = s_0. \tag{6.54}$$

This can be integrated to get

$$|s|^{1/2} - |s_0|^{1/2} = -\frac{\lambda}{2} t. \tag{6.55}$$

Taking $s = 0$, we find that the corresponding reaching time would be given by

$$t_r \geq \frac{2}{\lambda} |s_0|^{1/2}. \tag{6.56}$$

Unfortunately, when $\gamma(x_1, x_2, t) \neq 0$, these relations no longer hold. Therefore, we ask if it might be possible to add another term to the controller to cancel the effects of cumulative disturbance.

Assuming that the time derivative of the cumulative error can be upper bounded, i.e. $\dot{\gamma}(x_1, x_2, t) \leq C$, a modified form of the controller above,

$$\begin{aligned} \tau &= -\lambda |s|^{1/2} \text{sgn}(s) + z, \quad \lambda = 1.5\sqrt{C} \\ \dot{z} &= -b \text{sgn}(s), \quad b = 1.1C \end{aligned} \tag{6.57}$$

makes the compensated s-dynamics become

$$\begin{aligned} \dot{s} &= \gamma(x_1, x_2, t) - \lambda |s|^{1/2} \text{sgn}(s) + z, \\ \dot{z} &= -b \text{sgn}(s). \end{aligned} \tag{6.58}$$

The term z acts like an equivalent control term, which produces a low pass filtered estimate of the cumulative disturbance. When it starts following the disturbance

term, the sliding variable dynamics correspond to (6.53) so that the remaining term $\lambda|s|^{1/2}\text{sgn}(s)$ in the control law can drive s to zero in finite time.

Based on these results, we make the following observations about super-twisting sliding mode control

1) From (6.52), it can be seen that, using the definition of s in (6.50), the relative degree between s and τ is 1, but the relative degree between s and the discontinuous injected term $b\text{sgn}(s)$ is $r_s = 2$. Thus, the super twisting control input τ is continuous because both $\lambda|s|^{1/2}\text{sgn}(s)$ and $z = -\int b\text{sgn}(s)\text{d}t$ are continuous. The high frequency switching in the $\text{sgn}(s)$ term is smoothed by the integral.
2) Use of the term z and the augmented system $\dot{z} = -b\text{sgn}(s)$ are mandatory (very important) for ensuring continuity of the control function while simultaneously canceling the effects of the (unknown) cumulative disturbance.
3) Once the cumulative disturbance is canceled, the super-twisting controller uses a nonlinear sliding manifold given by $\dot{s} = -\lambda|s|^{1/2}\text{sgn}(s)$ to drive both drive both $\dot{s}$ and s to zero in finite time. This is different from the conventional sliding mode controller presented in Section 6.3, which uses a linear sliding surface that can only drive s to zero in finite time.

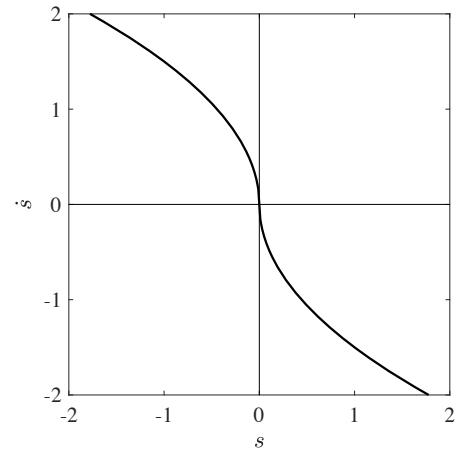

Fig. 6.10 The super-twisting sliding surface given by $\dot{s} = -1.5|s|^{1/2}\text{sgn}(s)$.

4) If we define our state variables to be the output tracking errors $\tilde{x}_1$ and $\tilde{x}_2 := \dot{\tilde{x}}_1$, we can rewrite the sliding variable (6.50) in the form $s = \tilde{x}_2 + \lambda\tilde{x}_1$. The fact that $\dot{s}$ is driven to zero in finite time, implies that $s \to 0$ in finite time, so that when the system is in sliding mode, its compensated dynamics are

$$\begin{aligned} \tilde{x}_2 &= -\lambda\tilde{x}_1 \\ \dot{s} &= 0. \end{aligned} \tag{6.59}$$

Therefore, we have complete dynamical collapse in the sliding mode — the second order uncompensated dynamics of the original system in (6.1) are reduced

to the algebraic equations $\tilde{x}_2 = \tilde{x}_1 = 0$ in finite time. From a control engineering standpoint, this is an important result, as it guarantees that any inner loop dynamics or parasitic dynamics can be eliminated by the control input.

Problems

6.1. Consider the pitch stabilization of an AUV in the presence of exogenous disturbances and unmodeled dynamics. The equations of motion can be written as

$$\dot{\theta} = q,$$
$$\dot{q} = c_0 \sin(2\theta) + \tau + w_d(\theta, q, t),$$

where τ is the control input and $w_d(\theta, q, t)$ represents the effects of unknown exogenous disturbances and unmodeled vehicle dynamics. The magnitude of $w_d(\theta, q, t)$ is upper bounded by a known constant L.

a) First using either inverse dynamics or backstepping to obtain a linearized system, design a first order sliding mode controller to stabilize the pitch angle to $\theta = 0$ in finite time when $w_d = 0.25\sin(2\pi t/10) + 2(\theta/\pi)^2$. Provide an estimate for L. Take the initial condition to be $[\theta_0 \;\; q_0]^T = [\pi/4 \;\; 0]^T$, give an estimate for the reaching time t_r.
b) Create a simulation in Matlab/Simulink and plot the time response of the system (i.e. θ and q versus time) for the conditions given in part a) above. Also plot the control input τ versus time. Is chattering present?
c) Use the nonlinear function $\tanh(s/\Phi)$, where $\Phi > 1$, as an approximation for the sgn function in the control law you designed in part a). Let $\Phi = 10$. Is chattering eliminated? Try one or two other values of Φ — how is the performance of the closed loop system affected?

6.2. Repeat parts a) and b) of Problem 1 above using a super-twisting controller.

References

1. Hashem Ashrafiuon, Sergey Nersesov, and Garrett Clayton. Trajectory tracking control of planar underactuated vehicles. *IEEE Trans Autom Control*, 62(4):1959–1965, 2017.
2. Taha Elmokadem, Mohamed Zribi, and Kamal Youcef-Toumi. Terminal sliding mode control for the trajectory tracking of underactuated autonomous underwater vehicles. *Ocean Engineering*, 129:613–625, jan 2017.
3. Aleksei Fedorovich Filippov. *Differential equations with discontinuous righthand sides: control systems*, volume 18. Springer Science & Business Media, 2013.
4. Thor I Fossen. *Handbook of marine craft hydrodynamics and motion control*. John Wiley & Sons, 2011.
5. Mansour Karkoub, Hsiu-Ming Wu, and Chih-Lyang Hwang. Nonlinear trajectory-tracking control of an autonomous underwater vehicle. *Ocean Engineering*, 145:188–198, 2017.
6. Arie Levant. Higher-order sliding modes, differentiation and output-feedback control. *Int J Control*, 76(9-10):924–941, 2003.
7. Arie Levant. Homogeneity approach to high-order sliding mode design. *Automatica*, 41(5):823–830, 2005.
8. Jaime A Moreno. Lyapunov function for levant's second order differentiator. In *Proc 51th IEEE Conf Decis Control*, pages 6448–6453. IEEE, 2012.

9. Jaime A Moreno and Marisol Osorio. A lyapunov approach to second-order sliding mode controllers and observers. In *Proc 47th IEEE Conf Decis Control*, pages 2856–2861, 2008.
10. Lei Qiao, Bowen Yi, Defeng Wu, and Weidong Zhang. Design of three exponentially convergent robust controllers for the trajectory tracking of autonomous underwater vehicles. *Ocean Engineering*, 134:157–172, 2017.
11. Yuri Shtessel, Christopher Edwards, Leonid Fridman, and Arie Levant. *Sliding mode control and observation*. Springer, 2014.
12. Jean-Jacques E Slotine and Weiping Li. *Applied nonlinear control*. Prentice-Hall Englewood Cliffs, NJ, 1991.
13. Karl Dietrich von Ellenrieder. *Control of marine vehicles*. Springer, 2021.
14. Ning Wang, Shuailin Lv, Weidong Zhang, Zhongzhong Liu, and Meng Joo Er. Finite-time observer based accurate tracking control of a marine vehicle with complex unknowns. *Ocean Engineering*, 145:406–415, 2017.
15. Zheping Yan, Haomiao Yu, Wei Zhang, Benyin Li, and Jiajia Zhou. Globally finite-time stable tracking control of underactuated UUVs. *Ocean Engineering*, 107:132–146, 2015.

Index

Fundamentals of Marine Vehicle Control: Adaptive Control

Karl D. von Ellenrieder

Field Robotics Lab South Tyrol
Facoltà di Scienze e Tecnologie, Libera Università di Bolzano
39100 Bolzano, Italia
Email: karl.vonellenrieder@unibz.it

MTS/IEEE Global OCEANS 2022: Chennai, India

21 February 2022

Introduction: Overview of Tutorial

Basic concepts of:

- Introduction
- Basic Stability
- Control of Underactuated Vehicles
- Feedback Linearization by Dynamic Inversion & Nonlinear Backstepping
- Adaptive Control
- Sliding Mode Control

Background

Marine vehicle dynamics:

$$\dot{\boldsymbol{\eta}} = \boldsymbol{R}(\psi)\boldsymbol{\nu},$$

$$\boldsymbol{M}\dot{\boldsymbol{\nu}} = -\boldsymbol{C}(\boldsymbol{\nu})\boldsymbol{\nu} - \boldsymbol{D}(\boldsymbol{\nu})\boldsymbol{\nu} + \boldsymbol{\tau} + \boldsymbol{d},$$

Control Challenges:

a) $\boldsymbol{M}$, $\boldsymbol{C}$, $\boldsymbol{D}$ and $\boldsymbol{\tau}$ uncertain.
b) $\boldsymbol{d}$ unknown/time-varying (but bounded).
c) Nonlinear $\rightarrow$ exacerbates points a & b

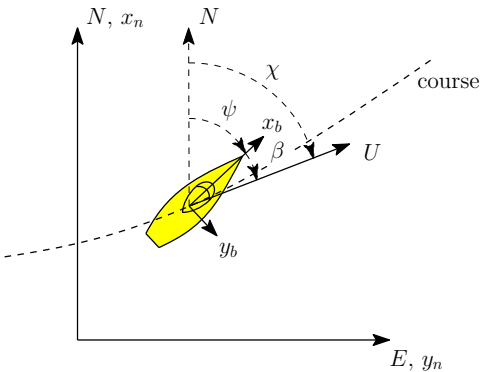

Maneuvering coordinates.

Background

Robust Control:

- Adaptive Control: control parameters adjust online to accommodate uncertainties.
- Disturbance Observer Based Control: include estimate $\hat{\boldsymbol{d}}$ in control signal to cancel real $\boldsymbol{d}$.
- Sliding mode control techniques.

Background

Robust Control:

- Adaptive Control: control parameters adjust online to accommodate uncertainties.
- Disturbance Observer Based Control: include estimate $\hat{\boldsymbol{d}}$ in control signal to cancel real $\boldsymbol{d}$.
- Sliding mode control techniques.

Advantages of adaptive control include:

- can be used to achieve good performance under varying operational conditions;
- well-suited for systems with constant or slowly varying parameters (the usual case in practice).

Background

Basic Ideas:

- Adaptive controller has two loops, an inner feedback loop consisting of the vehicle and controller, and an outer loop which adjusts the control parameters.
- Uncertain parameters are estimated on-line using available state measurements.
- Estimated parameters are used in the control law.
- Time-varying plant parameters vary considerably slower than the parameter adaptation $\rightarrow$ so they are treated as constants in controller design.

Model Reference Adaptive Control (MRAC)

Control system composed of four blocks:

a) the marine vehicle,

b) a reference model, which specifies the desired output of the system,

c) a feedback control law containing the adjustable parameters, and

d) an adaptation law, which updates the adjustable parameters in the controller.

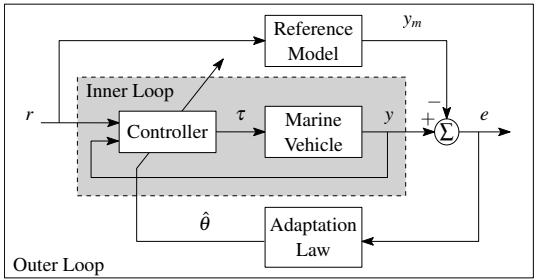

A model reference adaptive control system.

Structure of dynamic equations governing the vehicle assumed to be known, but exact values of parameters may be uncertain (e.g. inertial and drag terms).

Model Reference Adaptive Control (MRAC)

In more detail:

- **Reference model** specifies ideal response of system to a reference command.
  - Selection of reference model part of control design.
  - Two requirements:
    a) it should have desired performance characteristics to perform the given control task, e.g. rise time, settling time, overshoot, etc.
    b) ideal reference behavior should be achievable for the adaptive control system, i.e., correct order and relative degree for the assumed structure of plant model.
- When multiple parameters adpatively updated, may be more than one combination of parameters that achieve desired performance $\rightarrow$ the estimates might not approach the true physical values. OK, as long as plant output identical to that of the reference model.
- Normally, we require control law to be linear in terms of adjustable parameters to guarantee stability and tracking convergence.

Model Reference Adaptive Control (MRAC): Example

Consider vertical position tracking of an unmanned aerial vehicle (UAV). Mass of the vehicle is m, the vertical force input from the propellers is τ and g is gravity. Dynamics of UAV in vertical direction are

$$m\ddot{z} = mg + \tau.$$

UAV carries a small load, such as a camera, with an unknown weight. Control objective is to track desired time-dependent height $z_d(t)$.

An unmanned aerial vehicle configured to carry a camera.

Model Reference Adaptive Control (MRAC): Example

Suppose we want UAV to have response of ideal linear second order system

$$\ddot{z}_m + 2\zeta\omega_n\dot{z}_m + \omega_n^2 z_m = \omega_n^2 z_d(t),$$

where z_m is position of the reference model. Damping ratio ζ and natural frequency ω_n selected to satisfy desired performance characteristics, such as maximum overshoot

$$M_p = \mathrm{e}^{-\pi\zeta/\sqrt{1-\zeta^2}}, \quad 0 < \zeta \leq 1$$

and 2% settling time

$$t_s = \frac{4.0}{\zeta\omega_n}.$$

Model Reference Adaptive Control (MRAC): Example

First, assume mass of UAV and load are precisely known. Let $\tau = m\left(-g + \ddot{z}_m - 2\lambda\dot{\tilde{z}} - \lambda^2\tilde{z}\right)$, where $\tilde{z} := z(t) - z_m(t)$ is tracking error and $\lambda > 0$ is constant control gain, gives the closed loop error dynamics

$$\begin{aligned} \dot{\tilde{z}}_1 &= \tilde{z}_2 \\ \dot{\tilde{z}}_2 &= -2\lambda\tilde{z}_2 - \lambda^2\tilde{z}_1, \end{aligned}$$

where $\tilde{z}_1 := \tilde{z}$ and $\tilde{z}_2 := \dot{\tilde{z}}$.
System is exponentially stable with equilibrium point at $\tilde{z}_2 = \tilde{z}_1 = 0$ (perfect tracking).

Model Reference Adaptive Control (MRAC): Example

Now assume mass not precisely known, but we have an estimate $\hat{m}$, which we use in control law $\tau = \hat{m}\left(-g + \ddot{z}_m - 2\lambda\dot{\tilde{z}} - \lambda^2\tilde{z}\right)$. Then, we have

$$m\ddot{z} = \tilde{m}g - \hat{m}\left(-\ddot{z}_m + 2\lambda\tilde{z}_2 + \lambda^2\tilde{z}_1\right),$$

where $\tilde{m} := m - \hat{m}$. Following the approach in **?**, we define a new "combined error variable" variable

$$s := \tilde{z}_2 + \lambda\tilde{z}_1.$$

Model Reference Adaptive Control (MRAC): Example

If we compute $\dot{s} + \lambda s$ and simplify, the closed loop tracking errors are

$$\begin{aligned} m\left(\dot{s} + \lambda s\right) &= m\left(\dot{\tilde{z}}_2 + 2\lambda\tilde{z}_2 + \lambda^2\tilde{z}_1\right), \\ &= m\ddot{z} + m\left(-\ddot{z}_m + 2\lambda\tilde{z}_2 + \lambda^2\tilde{z}_1\right), \\ &= \tilde{m}g - \hat{m}\left(-\ddot{z}_m + 2\lambda\tilde{z}_2 + \lambda^2\tilde{z}_1\right) + m\left(-\ddot{z}_m + 2\lambda\tilde{z}_2 + \lambda^2\tilde{z}_1\right), \\ &= \tilde{m}\left(-\ddot{z}_m + 2\lambda\tilde{z}_2 + \lambda^2\tilde{z}_1 + g\right), \\ &= \tilde{m}\nu. \end{aligned}$$

Model Reference Adaptive Control (MRAC): Example

Consider the candidate Lyapunov function

$$V = \frac{1}{2} m s^2 + \frac{1}{2\gamma} \tilde{m}^2,$$

where $\gamma > 0$ is an adaption gain. Taking the derivative of this along trajectories of closed loop system gives

$$\dot{V} = sm\dot{s} + \frac{1}{\gamma} \tilde{m} \dot{\tilde{m}} = sm\dot{s} - \frac{1}{\gamma} \tilde{m} \dot{\hat{m}},$$

where we assumed $\dot{\tilde{m}} \approx -\dot{\hat{m}}$ because the uncertain mass is constant or very slowly varying in time (compared to its estimate, which can be updated much more rapidly). Simplifying gives

$$\begin{aligned} \dot{V} &= s\left[-m\lambda s + \tilde{m}\nu\right] - \frac{1}{\gamma} \tilde{m} \dot{\hat{m}}, \\ &= -m\lambda s^2 + \tilde{m}\left[s\nu - \frac{1}{\gamma} \dot{\hat{m}}\right]. \end{aligned}$$

Model Reference Adaptive Control (MRAC): Example

We can ensure $\dot{V} < 0, \forall s \neq 0$ by selecting the update law

$$\dot{\hat{m}} = \gamma s \nu = \gamma s \left(-\ddot{z}_m + 2\lambda \tilde{z}_2 + \lambda^2 \tilde{z}_1 + g \right)$$

Using Barbalat's Lemma, one can show that s converges to zero. Thus, both the position tracking error $\tilde{z}_1$ and the velocity tracking error $\tilde{z}_2$ converge to zero.

Model Reference Adaptive Control (MRAC): Example

Let UAV mass be $m = 15$ kg and payload mass be $m_p = 1.5$ kg.
Control law has no knowledge of payload mass. Use 2^{nd} order reference model with peak overshoot $M_p \leq 0.05$ and and settling time $t_s \leq 1.8$ secs $\Rightarrow \zeta = 1/\sqrt{2}$ and $\omega_n = \pi$. Assume UAV only generates thrust downward and max thrust is twice UAV weight. Update gain is $\gamma = 1$ and control gain is $\lambda = 10$.

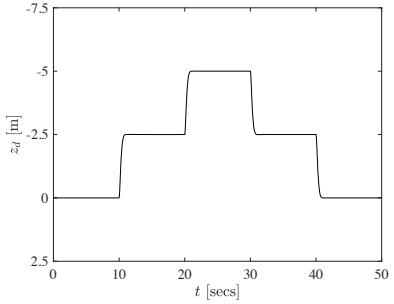

Desired position $z_d(t)$ of the UAV.

Model Reference Adaptive Control (MRAC): Example

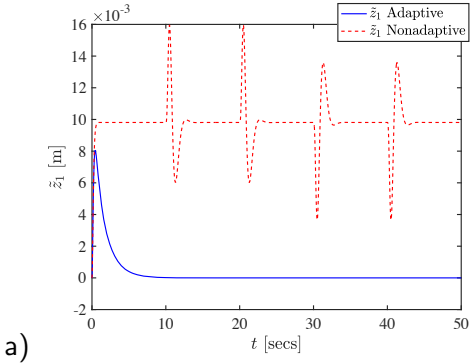

a)

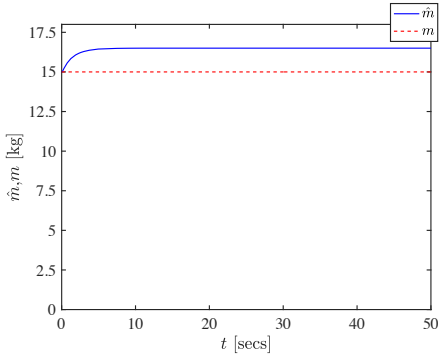

b)

a) Vertical position error of the UAV, and 2) mass estimate $\hat{m}$ from the adaptive controller versus actual mass m. The initial estimate of the total mass at $t = 0$ is taken to be $\hat{m} = 15$ kg. The solid blue lines correspond to the adaptive controller and the dashed red line corresponds to the corresponding non adaptive controller.

Adaptive SISO Control via Feedback Linearization

Adaptive control via feedback linearization for single-input single-output systems, with multiple uncertain parameters.

Consider an n^{th} order nonlinear system in the form

$$m x^{(n)} + \sum_{i=1}^{n} \theta_i f_i(\boldsymbol{x}, t) = \tau,$$

where $\boldsymbol{x} = [x \ \dot{x} \ \cdots \ x^{(n-1)}]^T$ is the state vector,

$$x^{(n)} = \frac{\mathrm{d}^n x}{\mathrm{d}t^n}, \quad \forall n,$$

the $f_i(\boldsymbol{x}, t)$ are known nonlinear functions, and parameters θ_i and m are uncertain constants. Take output of system to be $y(t) = x(t)$. Assume full state vector $\boldsymbol{x}$ measured.

Control objective: make output asymptotically track $y_d(t)$, despite uncertain knowledge of plant parameters.

Adaptive SISO Control via Feedback Linearization

Define combined error variable s

$$s := e^{(n-1)} + \lambda_{n-2} e^{(n-2)} + \cdots + \lambda_0 e,$$

where $e := (y - y_d) = (x - x_d)$ is output tracking error and $\lambda_i > 0$ for all $i \in \{0, \ldots, (n-2)\}$. Let $x_r^{(n-1)} := x_d^{(n-1)} - \lambda_{n-2} e^{(n-1)} - \cdots - \lambda_0 e$ so that s can be rewritten as

$$s := x^{(n-1)} - x_r^{(n-1)}.$$

Take the control law to be

$$\tau = m x_r^{(n)} - ks + \sum_{i=1}^{n} \theta_i f_i(\boldsymbol{x}, t),$$

where k is a constant of the same sign as m and $x_r^{(n)}$ is derivative of $x_r^{(n-1)}$ so that

$$x_r^{(n)} := x_d^{(n)} - \lambda_{n-2} e^{(n-1)} - \cdots - \lambda_0 \dot{e}.$$

Adaptive SISO Control via Feedback Linearization

If the parameters were all well-known, tracking error dynamics would be

$$m\dot{s} = -ks,$$

which would give exponential convergence of s, and thus exponential convergence of e. But model parameters are not known, so control law is

$$\tau = \hat{m}x_r^{(n)} - ks + \sum_{i=1}^{n} \hat{\theta}_i f_i(\boldsymbol{x}, t),$$

where $\hat{m}$ and $\hat{\theta}_i$ are estimated values of m and θ_i, respectively.

Adaptive SISO Control via Feedback Linearization

Then, closed loop tracking error is

$$m\dot{s} = -ks + \tilde{m}x_r^{(n)} + \sum_{i=1}^{n} \tilde{\theta}_i f_i(\boldsymbol{x}, t),$$

where $\tilde{m} := \hat{m} - m$ and $\tilde{\theta}_i := \hat{\theta}_i - \theta_i$ are parameter estimation errors.
Consider candidate Lyapunov function

$$V = |m|s^2 + \gamma^{-1}\left[\tilde{m}^2 + \sum_{i=1}^{n} \tilde{\theta}_i^2\right].$$

Its time derivative is

$$\dot{V} = 2|m|s\dot{s} + 2\gamma^{-1}\left[\tilde{m}\dot{\hat{m}} + \sum_{i=1}^{n} \tilde{\theta}_i\dot{\hat{\theta}}_i\right].$$

Adaptive SISO Control via Feedback Linearization

Using $m\dot{s} = |m|\mathrm{sgn}(m)\dot{s}$, $\dot{V}$ can be rewritten as

$$\begin{aligned}\dot{V} &= -2\mathrm{sgn}(m)ks^2 + 2\tilde{m}\left[\mathrm{sgn}(m)sx_r^{(n)} + \gamma^{-1}\dot{\hat{m}}\right] \\ &\quad + 2\sum_{i=1}^{n}\tilde{\theta}_i\left[\mathrm{sgn}(m)sf_i(\boldsymbol{x},t) + \gamma^{-1}\dot{\hat{\theta}}_i\right].\end{aligned}$$

With the assumption above that m and k have the same sign, $\dot{V}$ can be reduced to

$$\dot{V} = -2|k|s^2,$$

which is negative definite for every $s \neq 0$, by selecting the parameter update laws to be

$$\begin{aligned}\dot{\hat{m}} &= -\gamma\,\mathrm{sgn}(m)sx_r^{(n)}, \\ \dot{\hat{\theta}}_i &= -\gamma\,\mathrm{sgn}(m)sf_i(\boldsymbol{x},t).\end{aligned}$$

Adaptive SISO Control via Feedback Linearization

Using Barbalat's Lemma one can show that system is globally asymptotically stable, so that the tracking errors converge to zero. It can also be shown that global tracking convergence is preserved if a different adaptation gain γ_i is used for each unknown parameter **?**, i.e.

$$\dot{\hat{m}} = -\gamma_0 \operatorname{sgn}(m) s x_r^{(n)},$$

$$\dot{\hat{\theta}}_i = -\gamma_i \operatorname{sgn}(m) s f_i(\boldsymbol{x}, t).$$

Adaptive SISO Control via Feedback Linearization: Example

Consider rolling motion of an unmanned surface vehicle about its surge axis

$$m\ddot{\phi} + c_d|\dot{\phi}|\dot{\phi} + k_s\phi = \tau,$$

where m is mass moment of inertia (including added mass) about roll axis, c is damping coefficient and k_s is spring constant related to buoyancy-induced righting moment.
Assume m, c_d and k_s are unknown and use adaptive control to stabilize USV in waves at $\phi = 0$.

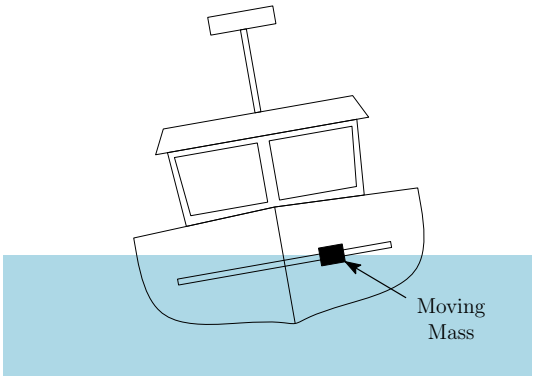

Use of a moving mass system to stabilize the roll axis of a USV in waves.

Adaptive SISO Control via Feedback Linearization: Example

Based on form of dynamics, $\theta_1 = c_d$, $\theta_2 = k_s$, $f_1 = |\dot{\phi}|\dot{\phi}$ and $f_2 = \phi$.

System is 2^{nd} order so $n = 2$. Taking $x = \phi$ and $\phi_d = \dot{\phi}_d = \ddot{\phi}_d = 0$, we get $e = \phi$, $\ddot{x}_r = -\lambda_0 \dot{\phi}$ and $s = \dot{\phi} + \lambda_0 \phi$.

Thus, the control law is

$$\tau = \hat{m}\ddot{x}_r - ks + \hat{\theta}_1 |\dot{\phi}|\dot{\phi} + \hat{\theta}_2 \phi.$$

The parameters estimates are found using the update laws

$$\begin{aligned} \dot{\hat{m}} &= -\gamma_0 \, s\ddot{x}_r, \\ \dot{\hat{\theta}}_1 &= -\gamma_1 \, s|\dot{\phi}|\dot{\phi}, \\ \dot{\hat{\theta}}_2 &= -\gamma_2 \, s\phi. \end{aligned}$$

Adaptive SISO Control via Feedback Linearization: Example

Take $m = 100$ kg-m^2, $c_d = 8.4$ kg-m^2 and $k_s = 17.5$ N-m. Control gains used are $\lambda_0 = 2$, $\gamma_0 = 10$, $\gamma_1 = 10$, $\gamma_2 = 1$, and $k = 5$.

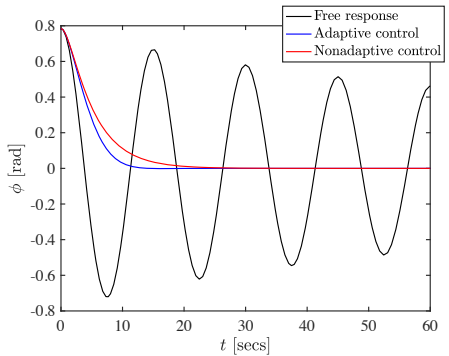

a)

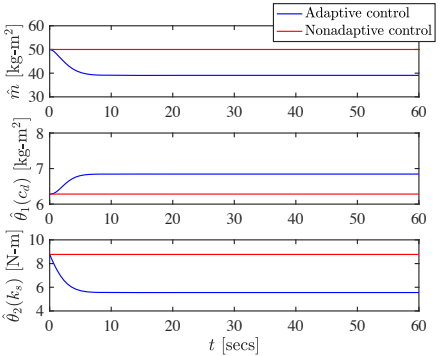

b)

a) Controlled and uncontrolled roll responses. b) Parameter estimates for adaptive and non adaptive controllers.

Fundamentals of Marine Vehicle Control: Feedback Linearization & Backstepping

Karl D. von Ellenrieder

Field Robotics Lab South Tyrol
Facoltà di Scienze e Tecnologie, Libera Università di Bolzano
39100 Bolzano, Italia
Email: karl.vonellenrieder@unibz.it

MTS/IEEE Global OCEANS 2022: Chennai, India

21 February 2022

Introduction: Overview of Tutorial

Basic concepts of:

- Introduction
- Basic Stability
- Control of Underactuated Vehicles
- Feedback Linearization by Dynamic Inversion & Nonlinear Backstepping
- Adaptive Control
- Sliding Mode Control

Feedback Linearization by Dynamic Inversion

Basic Ideas:

- Transform nonlinear dynamics of a vehicle into a linear system upon which conventional linear control techniques can be applied.
- Linear controller designed for transformed model and control input from linear controller transformed back into a nonlinear signal before being passed to the actuators/plant.
- Thus, knowledge of system nonlinearities are built into controller via an exact state transformation and feedback.
- **Note:** Very different from linearizing nonlinear system about an operating point, and designing a controller for linearized system.
- For marine vehicles, inverse dynamics can be separated into velocity control in the body-fixed frame and position and attitude (pose) control in the NED frame Fossen [2011].

Feedback Linearization by Dynamic Inversion: Body-fixed Frame

Consider the kinetic equation of motion for a marine vehicle,

$$\boldsymbol{M}\dot{\boldsymbol{\nu}} + \boldsymbol{C}(\boldsymbol{\nu})\boldsymbol{\nu} + \boldsymbol{D}(\boldsymbol{\nu})\boldsymbol{\nu} + \boldsymbol{g}(\boldsymbol{\eta}) = \boldsymbol{\tau}.$$

A control input

$$\boldsymbol{\tau} = \boldsymbol{f}(\boldsymbol{\eta}, \boldsymbol{\nu}, t)$$

that linearizes the closed loop system is sought. By inspection, it can be seen that if a control input of the form

$$\boldsymbol{\tau} = \boldsymbol{M}\boldsymbol{a}_b + \boldsymbol{C}(\boldsymbol{\nu})\boldsymbol{\nu} + \boldsymbol{D}(\boldsymbol{\nu})\boldsymbol{\nu} + \boldsymbol{g}(\boldsymbol{\eta})$$

can be found, the equation of motion reduces to

$$\dot{\boldsymbol{\nu}} = \boldsymbol{a}_b,$$

where $\boldsymbol{a}_b$ is the commanded acceleration of the vehicle in the body-fixed frame.
The new system linear and if $\boldsymbol{a}_b$ designed so each of its components is decoupled from the others, the closed loop system is also decoupled.

Feedback Linearization by Dynamic Inversion: Body-fixed Frame

Simple approach: to design linear proportional integral derivative controller law of form

$$\boldsymbol{a}_b = \dot{\boldsymbol{v}}_d - \boldsymbol{K}_p\tilde{\boldsymbol{v}} - \boldsymbol{K}_i \int_0^t \tilde{\boldsymbol{v}}(\tau)\mathrm{d}\tau - \boldsymbol{K}_d\dot{\tilde{\boldsymbol{v}}},$$

where $\boldsymbol{v}_d = \boldsymbol{v}_d(t)$ is the desired velocity, $\tilde{\boldsymbol{v}} := \boldsymbol{v} - \boldsymbol{v}_d$ is the velocity error, and $\boldsymbol{K}_p > 0$, $\boldsymbol{K}_i > 0$ and $\boldsymbol{K}_d > 0$ are diagonal proportional, integral and derivative gain matrices, respectively.

Note: the first term of $\boldsymbol{a}_b$, $\dot{\boldsymbol{v}}_d$, acts as feedforward term for desired acceleration.

Feedback Linearization by Dynamic Inversion: NED Frame

Consider full NED fram equations of motion for a marine vehicle

$$\begin{aligned} \dot{\boldsymbol{\eta}} &= \boldsymbol{J}(\boldsymbol{\eta})\boldsymbol{\nu}, \\ \boldsymbol{M}\dot{\boldsymbol{\nu}} &= -\boldsymbol{C}(\boldsymbol{\nu})\boldsymbol{\nu} - \boldsymbol{D}(\boldsymbol{\nu})\boldsymbol{\nu} - \boldsymbol{g}(\boldsymbol{\eta}) + \boldsymbol{\tau}. \end{aligned}$$

Position and orientation trajectory tracking can be accomplished by commanding an acceleration $\boldsymbol{a}_n$ (measured with respect to an Earth-fixed inertial reference frame) of the form

$$\ddot{\boldsymbol{\eta}} = \boldsymbol{a}_n$$

that linearizes the closed loop system. Taking time derivative of first term in vehicle equations of motion gives

$$\ddot{\boldsymbol{\eta}} = \frac{\mathrm{d}\left[\boldsymbol{J}(\boldsymbol{\eta})\right]}{\mathrm{d}t}\boldsymbol{\nu} + \boldsymbol{J}(\boldsymbol{\eta})\dot{\boldsymbol{\nu}}.$$

Solving for $\dot{\boldsymbol{\nu}}$ gives

$$\dot{\boldsymbol{\nu}} = \boldsymbol{J}^{-1}(\boldsymbol{\eta})\left\{\ddot{\boldsymbol{\eta}} - \frac{\mathrm{d}\left[\boldsymbol{J}(\boldsymbol{\eta})\right]}{\mathrm{d}t}\boldsymbol{\nu}\right\}.$$

Feedback Linearization by Dynamic Inversion: NED Frame

Substituting $\dot{\boldsymbol{v}}$ into the equations of motion yields

$$\boldsymbol{M}\boldsymbol{J}^{-1}(\boldsymbol{\eta})\left\{\ddot{\boldsymbol{\eta}} - \frac{\mathrm{d}\left[\boldsymbol{J}(\boldsymbol{\eta})\right]}{\mathrm{d}t}\boldsymbol{v}\right\} = -\boldsymbol{C}(\boldsymbol{v})\boldsymbol{v} - \boldsymbol{D}(\boldsymbol{v})\boldsymbol{v} - \boldsymbol{g}(\boldsymbol{\eta}) + \boldsymbol{\tau}.$$

If $\boldsymbol{\tau}$ selected as

$$\boldsymbol{\tau} = \boldsymbol{M}\boldsymbol{J}^{-1}(\boldsymbol{\eta})\left\{\boldsymbol{a}_n - \frac{\mathrm{d}\left[\boldsymbol{J}(\boldsymbol{\eta})\right]}{\mathrm{d}t}\boldsymbol{v}\right\} + \boldsymbol{C}(\boldsymbol{v})\boldsymbol{v} + \boldsymbol{D}(\boldsymbol{v})\boldsymbol{v} + \boldsymbol{g}(\boldsymbol{\eta})$$

closed loop system becomes

$$\ddot{\boldsymbol{\eta}} = \boldsymbol{a}_n.$$

Feedback Linearization by Dynamic Inversion: NED Frame

As above, a linear proportional integral derivative control law can now be designed as

$$\boldsymbol{a}_n = \ddot{\boldsymbol{\eta}}_d - \boldsymbol{K}_p\tilde{\boldsymbol{\eta}} - \boldsymbol{K}_i \int_0^t \tilde{\boldsymbol{\eta}}(\sigma)\mathrm{d}\sigma - \boldsymbol{K}_d\dot{\tilde{\boldsymbol{\eta}}},$$

where σ is used as an integration variable, $\boldsymbol{\eta}_d = \boldsymbol{\eta}_d(t)$ is the desired position and orientation of the vehicle, $\tilde{\boldsymbol{\eta}} := \boldsymbol{\eta} - \boldsymbol{\eta}_d$ is the pose error, and $\boldsymbol{K}_p > 0$, $\boldsymbol{K}_i > 0$ and $\boldsymbol{K}_d > 0$ are diagonal proportional, integral and derivative gain matrices, respectively.

As above, the first term of $\boldsymbol{a}_n$, $\ddot{\boldsymbol{\eta}}_d$, functions as a feedforward term.

Note: transformation matrix $\boldsymbol{J}(\boldsymbol{\eta})$ must be nonsingular $\Rightarrow$ limits magnitude of pitch angle to $-\pi/2 < \theta < \pi/2$.

General Feedback Linearization

- Inverse dynamics is a special case of feedback linearization.
- Can seen inverse dynamics splits the controller into two parts:
  a) an inner loop that exactly linearizes the nonlinear system, and
  b) an outer loop, which can be designed using linear techniques according to tracking or disturbance rejection performance requirements.

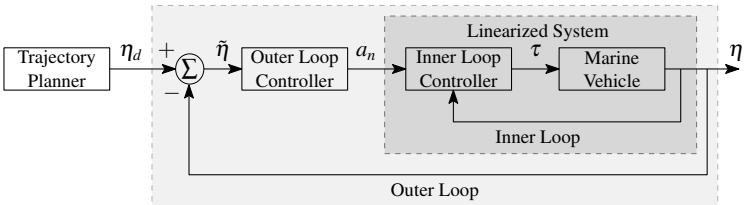

Block diagram of a controller designed using feedback linearization.

General Feedback Linearization

- More general process of feedback linearization works in same way, except the outer-loop process of linearizing the nonlinear system may also involve a transformation of the state variable into a new set of coordinates.
- Inverse dynamics can be sufficient for many problems involving the control of marine vessels, the use of the more general form of feedback linearization may be needed when solving marine vehicle control problems that must take actuator dynamics or underactuation into account.

Nonlinear Backstepping: Introduction

A recursive design procedure to construct feedback control laws and associated Lyapunov functions — very widely used to control marine vehicles..

Pros:

- Systematic, flexible and can be applied in vector form to MIMO systems.
- Robustness: control designer can exploit "good" nonlinearities and suppress "bad" nonlinearities.
- Basic form of backstepping gives PD-like controllers, but can be made PID-like using integrator augmentation.
- Easy to combine with other control methods, e.g. optimal or adaptive control.
- Straightforward to handle actuator constraints.
- Backstepping controllers have globally bounded tracking errors.

Cons:

- Implementation often involves an *explosion of complexity* — differentiation of the plant model, which requires very large number of terms in control law.

Nonlinear Backstepping: Introduction

Consider the dynamic equations of a marine vehicle in body-fixed coordinates

$$\begin{aligned} \dot{\boldsymbol{\eta}} &= \boldsymbol{J}(\boldsymbol{\eta})\boldsymbol{\nu}, \\ \boldsymbol{M}\dot{\boldsymbol{\nu}} &= -\boldsymbol{C}(\boldsymbol{\nu})\boldsymbol{\nu} - \boldsymbol{D}(\boldsymbol{\nu})\boldsymbol{\nu} - \boldsymbol{g}(\boldsymbol{\eta}) + \boldsymbol{\tau} + \boldsymbol{w}_d. \end{aligned}$$

Note structure of equations:

- Equations are coupled with functions of state variables (i.e. $\boldsymbol{J}(\boldsymbol{\eta})$, $\boldsymbol{C}(\boldsymbol{\nu})$, and $\boldsymbol{D}(\boldsymbol{\nu})$) multiplied by state variable $\boldsymbol{\nu}$.
- Coupling makes it hard to find a control input to stabilize the system around desired equilibrium point.
- Backstepping provide a means of decoupling equations so they can be stabilized.
- For many marine vehicle control applications a vector form of backstepping must be used.

To understand the basics, we start with a simple 2-state SISO system, before looking at the vectorial MIMO form of backstepping.

Nonlinear Backstepping: A simple 2-state SISO system

Consider the single-input single-output (SISO) system

$$\begin{aligned} \dot{x}_1 &= f_1(x_1) + g_1(x_1)x_2, \\ \dot{x}_2 &= u, \\ y &= x_1, \end{aligned}$$

where $f_1(x_1)$ and $g_1(x_1)$ are known functions. Assume $g_1(x_1) \neq 0$.

Control objective: design state feedback control input to track desired output $y_d(t)$.

Nonlinear Backstepping: A simple 2-state SISO system

System is cascade connection of 2 components. First component has state x_2 as *virtual control input*; second component is an integrator with u as input. Since there are 2 states, design is conducted recursively in 2 steps.

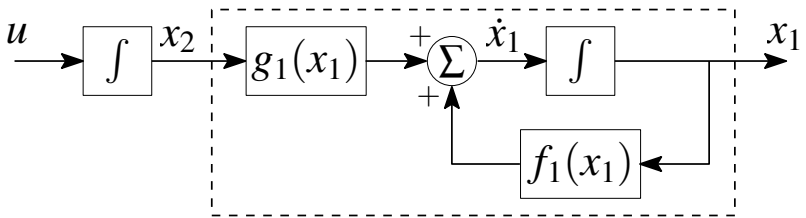

Block diagram of 2-state SISO system.

Nonlinear Backstepping: A simple 2-state SISO system

Suppose we can find a smooth *stabilizing function* $\alpha_1(x_1)$ that permits us to decouple the system by driving $x_2 \to \alpha_1$. To do this add and subtract $g_1(x_1)\alpha_1(x_1)$ to the right hand side of the first equation to get

$$\begin{aligned} \dot{x}_1 &= [f_1(x_1) + g_1(x_1)\alpha_1(x_1)] + g_1(x_1)[x_2 - \alpha_1(x_1)] \\ \dot{x}_2 &= u. \end{aligned}$$

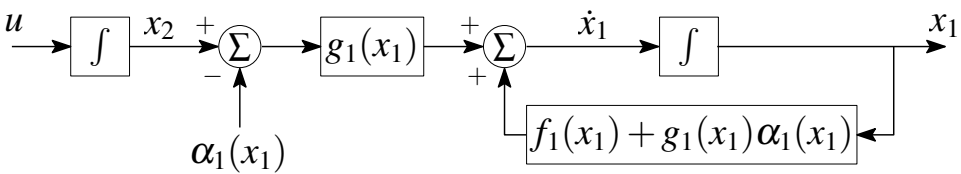

Stabilizing function $\alpha_1(x_1)$ introduced to stabilize the x_1 system at $x_1 = 0$.

Nonlinear Backstepping: A simple 2-state SISO system

Define the stabilization errors as

$$z_1 := y - y_d = x_1 - y_d$$

and

$$z_2 := x_2 - \alpha_1.$$

Then, in terms of the stabilizations errors, system of equations is

$$\dot{z}_1 = \dot{x}_1 - \dot{y}_d = [f_1(x_1) + g_1(x_1)\alpha_1] + g_1(x_1)z_2 - \dot{y}_d,$$

$$\dot{z}_2 = u - \dot{\alpha}_1 = v.$$

When $x_2 \to \alpha_1$, $z_2 \to 0$, so $\dot{z}_1 = f_1(x_1) + g_1(x_1)\alpha_1(x_1) - \dot{y}_d$ can be stabilized independently of z_2.

Stabilizing function α_1 found in first step of backstepping control design process.

Nonlinear Backstepping: A simple 2-state SISO system

The new system similar to initial one, but when input of new system is $v = 0$, it can be asymptotically stabilized to its origin ($z_1 = 0, z_2 = 0$).

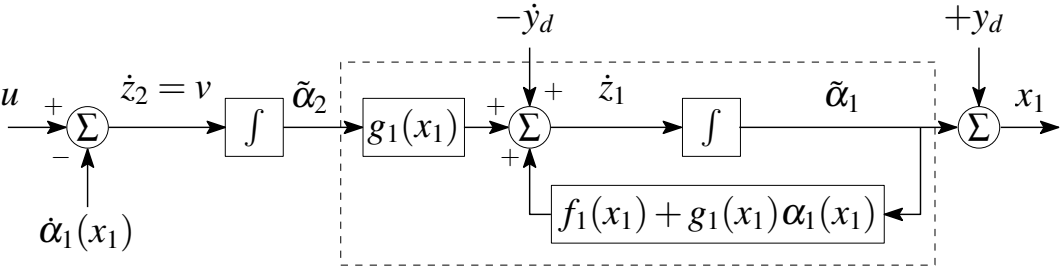

Control input u selected to stabilize the x_2 system.

In stabilizing x_2 we step $\alpha_1(x_1)$ back through an integrator to compute $v = u - \dot{\alpha}_1 \Rightarrow$ this is why control design technique is called *integrator backstepping*.

Nonlinear Backstepping: A simple 2-state SISO system

Stabilizing function α_1 and control input u determined using a suitable *control Lyapunov function* (CLF) $V(z_1, z_2, u)$.
If we can find a $V > 0$ that always decreases along trajectories of the system, e.g.

$$\dot{V} = \frac{\partial V}{\partial z_1}\dot{z}_1 + \frac{\partial V}{\partial z_2}\dot{z}_2 \; < 0 \quad \forall z_1, z_2 \neq 0,$$

we can conclude that the minimum of the function is a stable equilibrium point.
Try the CLF

$$V = \frac{1}{2}z_1^2 + \frac{1}{2}z_2^2.$$

Taking its time derivative gives

$$\begin{aligned} \dot{V} &= z_1\dot{z}_1 + z_2\dot{z}_2, \\ &= z_1\left[f_1(x_1) + g_1(x_1)\alpha_1 + g_1(x_1)z_2 - \dot{y}_d\right] + z_2(u - \dot{\alpha}_1). \end{aligned}$$

Nonlinear Backstepping: A simple 2-state SISO system

Moving the term $z_1 g_1(x_1) z_2 = z_2 g_1(x_1) z_1$ from the first expression to the second one we have

$$\dot{V} = z_1 \left[f_1(x_1) + g_1(x_1)\alpha_1 - \dot{y}_d \right] + z_2 [u - \dot{\alpha}_1 + g_1(x_1) z_1].$$

Step 1: Assuming $g_1(x_1) \neq 0$ select α_1 as

$$\alpha_1 = \frac{1}{g_1(x_1)} \left[-k_1 z_1 + \dot{y}_d - f_1(x_1) \right],$$

where $k_1 > 0$ gives

$$\dot{V} = -k_1 z_1^2 + z_2 [u - \dot{\alpha}_1 + g_1(x_1) z_1].$$

Since first term on r.h.s of equation < 0 for all $z_1 \neq 0$, z_1 subsystem stabilized for our choice of α_1.

Nonlinear Backstepping: A simple 2-state SISO system

Step 2: Next, select u to stabilize z_2 system by making remaining terms negative definite. Let

$$u = -k_2 z_2 + \dot{\alpha}_1 - g_1(x_1) z_1$$

with $k_2 > 0$, then

$$\dot{V} = -k_1 z_1^2 - k_2 z_2^2 < 0 \quad \forall z_1, z_2 \neq 0.$$

Since $\dot{V} < 0$ is negative definite $\forall z_1, z_2 \neq 0$, full system now stabilized. Further,

$$\dot{V} \leq -2\mu V$$

where $\mu := \min\{k_1, k_2\}$. Let value of V at time $t = 0$ be V_0, then

$$V \leq V_0 \mathrm{e}^{-2\mu t},$$

where

$$V_0 := \frac{1}{2}\left[z_1(0)^2 + z_2(0)^2\right].$$

Thus, both $z_1(t)$ and $z_2(t)$ decrease exponentially in time $\Rightarrow$ closed loop system is globally exponentially stable.

Nonlinear Backstepping: A simple 2-state SISO system

In terms of x_1, x_2 and $y_d(t)$, final control law is

$$u = -k_2(x_2 - \alpha_1) + \dot{\alpha}_1 - g_1(x_1)\left[x_1 - y_d\right],$$

where

$$\alpha_1 = -\frac{1}{g_1(x_1)}\left[f_1(x_1) + k_1(x_1 - y_d) - \dot{y}_d\right].$$

Note: Computation of u requires time derivative of $\dot{\alpha}_1$.

Nonlinear Backstepping: A simple 2-state SISO system

Two important implementation issues associated with computing $\dot{\alpha}_1$.

a) **The Explosion of Complexity:** Computation involves taking time derivatives of states and plant model, leads an *explosion of complexity*, where number of terms in control input is very large. Generally, should avoid taking the time derivatives of states directly, instead use original state equation when possible, e.g.

$$\dot{\alpha}_1 = \frac{\partial \alpha_1}{\partial x_1}\dot{x}_1 = \frac{\partial \alpha_1}{\partial x_1}[f_1(x_1) + g_1(x_1)x_2].$$

- Dynamic Surface Control Technique can be used to avoid this problem.

b) Computation of $\dot{\alpha}_1$ requires $\ddot{y}_d$. Thus, $y_d(t)$ must be smooth and continuous to 2^{nd} order. In practice may need low pass filter $y_d(t)$ to ensure continuity and smoothness of $\dot{y}_d(t)$ and $\ddot{y}_d(t)$.

Nonlinear Backstepping: 2-state SISO system Example

Vertical speed regulation of buoyancy-driven automatic profiler. Equation of motion are

$$\begin{aligned} \dot{x}_1 &= -\frac{\rho A C_d}{2m} x_1 |x_1| + \frac{g(\rho - \rho_f)}{m} x_2 \\ \dot{x}_2 &= u \\ y &= x_1, \end{aligned}$$

where x_1 is ascent/descent rate, m is mass/added mass, A is frontal area, C_d is drag coefficient, x_2 is change in piston volume, g is gravity, ρ is density seawater and ρ_f is density of the oil.

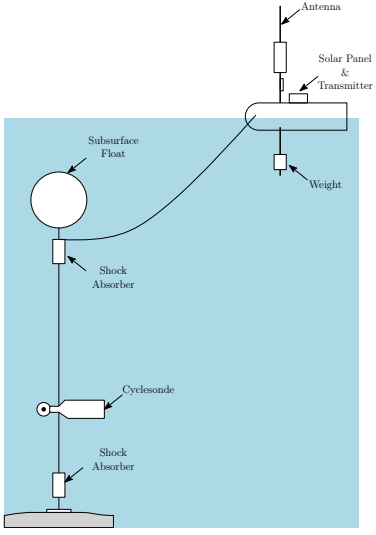

Buoyancy-controlled automatic profiler.

Nonlinear Backstepping: 2-state SISO system Example

We have

$$f_1(x_1) = -\frac{\rho A C_d}{2m} x_1 |x_1|, \quad \text{and} \quad g_1(x_1) = \frac{g(\rho - \rho_f)}{m},$$

so that

$$\alpha_1 = -\frac{m}{g(\rho - \rho_f)} \left[-\frac{\rho A C_d}{2m} x_1^2 \operatorname{sgn}(x_1) + k_1 (x_1 - y_d) - \dot{y}_d \right]$$

and

$$\dot{\alpha}_1 = \frac{\partial \alpha_1}{\partial x_1} \dot{x}_1 = -\frac{m}{g(\rho - \rho_f)} \left[-\frac{\rho A C_d}{m} |x_1| + k_1 \right] \dot{x}_1,$$

Then the control input is

$$u = -k_2 (x_2 - \alpha_1) + \dot{\alpha}_1 - \frac{g(\rho - \rho_f)}{m} [x_1 - y_d].$$

Nonlinear Backstepping: 2-state SISO system Example

Let control gains be $k_1 = 1$ and $k_2 = 1$. The physical characteristics of profiler and other constants used are $m = 4320$ kg, $A = 1$ m^2, $C_d = 1.0$, $g = 9.81$ m/s^2, $\rho = 1025.9$ kg/m^3 and $\rho_f = 850$ kg/m^3.

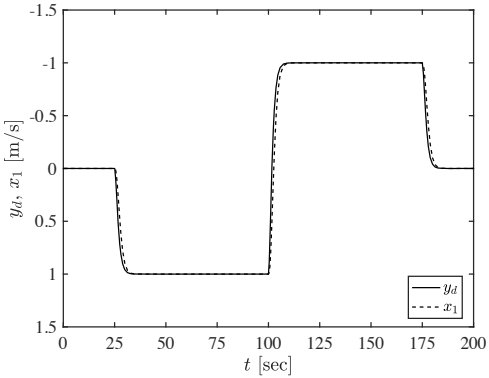

Vertical ascent/descent rate x_1 of buoyancy-driven profiler tracking $y_d(t)$.

Backstepping for Trajectory Tracking Marine Vehicles

Recall equations of motion for a marine vehicle in body-fixed coordinates

$$\dot{\boldsymbol{\eta}} = \boldsymbol{J}(\boldsymbol{\eta})\boldsymbol{\nu}$$

and

$$\boldsymbol{M}\dot{\boldsymbol{\nu}} + \boldsymbol{C}(\boldsymbol{\nu})\boldsymbol{\nu} + \boldsymbol{D}(\boldsymbol{\nu})\boldsymbol{\nu} + \boldsymbol{g}(\boldsymbol{\eta}) = \boldsymbol{\tau}.$$

Neglect actuator constraints and external disturbances.

Coordinate transformation matrix $\boldsymbol{J}(\boldsymbol{\eta})$ has singularities at pitch angles of $\theta = \pm\pi/2$, so assume $|\theta| < \pi/2$.

Control objective: make system track a desired trajectory $\boldsymbol{\eta}_d(t)$, where $\boldsymbol{\eta}_d$, $\boldsymbol{\eta}_d^{(3)}$, $\ddot{\boldsymbol{\eta}}_d$, and $\dot{\boldsymbol{\eta}}_d$ are assumed to be smooth and bounded.

Backstepping for Trajectory Tracking Marine Vehicles

Let

$$\tilde{\boldsymbol{\eta}} := \boldsymbol{\eta} - \boldsymbol{\eta}_d, \quad \tilde{\boldsymbol{\eta}} \in \mathbb{R}^n$$

be the Earth-fixed tracking surface error and define the body-fixed velocity surface error vector as

$$\tilde{\boldsymbol{\nu}} := \boldsymbol{\nu} - \boldsymbol{\alpha}_1, \quad \tilde{\boldsymbol{\nu}} \in \mathbb{R}^n$$

Writing the equations of motion in terms of the tracking errors gives

$$\begin{aligned} \dot{\tilde{\boldsymbol{\eta}}} &= \boldsymbol{J}(\boldsymbol{\eta})\boldsymbol{\nu} - \dot{\boldsymbol{\eta}}_d = \boldsymbol{J}(\boldsymbol{\eta})\tilde{\boldsymbol{\nu}} + \boldsymbol{J}(\boldsymbol{\eta})\boldsymbol{\alpha}_1 - \dot{\boldsymbol{\eta}}_d, \\ \boldsymbol{M}\dot{\tilde{\boldsymbol{\nu}}} &= -\boldsymbol{C}(\boldsymbol{\nu})\boldsymbol{\nu} - \boldsymbol{D}(\boldsymbol{\nu})\boldsymbol{\nu} - \boldsymbol{g}(\boldsymbol{\eta}) + \boldsymbol{\tau} - \boldsymbol{M}\dot{\boldsymbol{\alpha}}_1. \end{aligned}$$

Backstepping for Trajectory Tracking Marine Vehicles

Consider the candidate Lyapunov function

$$V = \frac{1}{2}\tilde{\boldsymbol{\eta}}^T\tilde{\boldsymbol{\eta}} + \frac{1}{2}\tilde{\boldsymbol{\nu}}^T\boldsymbol{M}\tilde{\boldsymbol{\nu}}.$$

Taking the time derivative gives

$$\dot{V} = \tilde{\boldsymbol{\eta}}^T\dot{\tilde{\boldsymbol{\eta}}} + \tilde{\boldsymbol{\nu}}^T\boldsymbol{M}\dot{\tilde{\boldsymbol{\nu}}},$$

where it is assumed that $\boldsymbol{M} = \boldsymbol{M}^T > 0$. Then,

$$\begin{aligned}\dot{V} &= \tilde{\boldsymbol{\eta}}^T\left[\boldsymbol{J}\tilde{\boldsymbol{\nu}} + \boldsymbol{J}\boldsymbol{\alpha}_1 - \dot{\boldsymbol{\eta}}_d\right] + \tilde{\boldsymbol{\nu}}^T\left[-\boldsymbol{C}\boldsymbol{\nu} - \boldsymbol{D}\boldsymbol{\nu} - \boldsymbol{g} + \boldsymbol{\tau} - \boldsymbol{M}\dot{\boldsymbol{\alpha}}_1\right], \\ &= \tilde{\boldsymbol{\eta}}^T\left[\boldsymbol{J}\boldsymbol{\alpha}_1 - \dot{\boldsymbol{\eta}}_d\right] + \tilde{\boldsymbol{\nu}}^T\left[\boldsymbol{J}^T\tilde{\boldsymbol{\eta}} - \boldsymbol{C}\boldsymbol{\nu} - \boldsymbol{D}\boldsymbol{\nu} - \boldsymbol{g} + \boldsymbol{\tau} - \boldsymbol{M}\dot{\boldsymbol{\alpha}}_1\right].\end{aligned}$$

Backstepping for Trajectory Tracking Marine Vehicles

The stabilizing function $\boldsymbol{\alpha}_1$ and control input $\boldsymbol{\tau}$ can be selected so that

$$\dot{V} = -\tilde{\boldsymbol{\eta}}^T \boldsymbol{K}_p \tilde{\boldsymbol{\eta}} - \tilde{\boldsymbol{\nu}}^T \boldsymbol{K}_d \tilde{\boldsymbol{\nu}} < 0,$$

where $\boldsymbol{K}_p = \boldsymbol{K}_p^T > 0 \in \mathbb{R}^{n \times n}$ and $\boldsymbol{K}_d = \boldsymbol{K}_d^T > 0 \in \mathbb{R}^{n \times n}$ are positive definite matrices of control gains. To accomplish this take

$$\boldsymbol{J}\boldsymbol{\alpha}_1 - \dot{\boldsymbol{\eta}}_d = -\boldsymbol{K}_p \tilde{\boldsymbol{\eta}}$$

so that

$$\boldsymbol{\alpha}_1 := \boldsymbol{J}^{-1} \left[-\boldsymbol{K}_p \tilde{\boldsymbol{\eta}} + \dot{\boldsymbol{\eta}}_d \right]$$

and

$$\boldsymbol{J}^T \tilde{\boldsymbol{\eta}} - \boldsymbol{C}\boldsymbol{\nu} - \boldsymbol{D}\boldsymbol{\nu} - \boldsymbol{g} + \boldsymbol{\tau} - \boldsymbol{M}\dot{\boldsymbol{\alpha}}_1 = -\boldsymbol{K}_d \tilde{\boldsymbol{\nu}},$$

which gives

$$\boldsymbol{\tau} := -\boldsymbol{K}_d \tilde{\boldsymbol{\nu}} + \boldsymbol{M}\dot{\boldsymbol{\alpha}}_1 + \boldsymbol{C}\boldsymbol{\nu} + \boldsymbol{D}\boldsymbol{\nu} + \boldsymbol{g} - \boldsymbol{J}^T \tilde{\boldsymbol{\eta}}.$$

Backstepping for Trajectory Tracking Marine Vehicles

Then, the closed loop error dynamics are

$$\begin{aligned} \dot{\tilde{\boldsymbol{\eta}}} &= -\boldsymbol{K}_p\tilde{\boldsymbol{\eta}} + \boldsymbol{J}\tilde{\boldsymbol{\nu}}, \\ \boldsymbol{M}\dot{\tilde{\boldsymbol{\nu}}} &= -\boldsymbol{K}_d\tilde{\boldsymbol{\nu}} - \boldsymbol{J}^T\tilde{\boldsymbol{\eta}}, \end{aligned}$$

which has a stable equilibrium point at $(\tilde{\boldsymbol{\eta}}, \tilde{\boldsymbol{\nu}}) = (0, 0)$. Thus,

$$\dot{V} \leq -\Lambda_{\min}(\boldsymbol{K}_p)\tilde{\boldsymbol{\eta}}^T\tilde{\boldsymbol{\eta}} - \Lambda_{\min}(\boldsymbol{K}_d)\tilde{\boldsymbol{\nu}}^T\tilde{\boldsymbol{\nu}},$$

where $\Lambda_{\min}(\boldsymbol{K})$ is the minimum eigenvalue of $\boldsymbol{K}$. Since $\boldsymbol{M} = \boldsymbol{M}^T > 0$ implies $\tilde{\boldsymbol{\nu}}^T\tilde{\boldsymbol{\nu}} \leq \tilde{\boldsymbol{\nu}}^T\boldsymbol{M}\tilde{\boldsymbol{\nu}}$ we have

$$\dot{V} \leq -\Lambda_{\min}(\boldsymbol{K}_p)\tilde{\boldsymbol{\eta}}^T\tilde{\boldsymbol{\eta}} - \Lambda_{\min}(\boldsymbol{K}_d)\tilde{\boldsymbol{\nu}}^T\boldsymbol{M}\tilde{\boldsymbol{\nu}} \leq -2\mu V,$$

where $\mu = \min\{\Lambda_{\min}(\boldsymbol{K}_p), \Lambda_{\min}(\boldsymbol{K}_d)\}$. Let V_0 be V at $t = t_0$, then

$$V = V_0 e^{-2\mu t}.$$

Since $V \to \infty$ if $\tilde{\boldsymbol{\eta}} \to \infty$ or $\tilde{\boldsymbol{\nu}} \to \infty$ and exponentially decaying with a stable equilibrium point at origin, closed loop system is globally exponentially stable.

Bibliography I

T. I. Fossen. *Handbook of marine craft hydrodynamics and motion control*. John Wiley & Sons, 2011.

Fundamentals of Marine Vehicle Control: Introduction

Karl D. von Ellenrieder

Field Robotics Lab South Tyrol
Facoltà di Scienze e Tecnologie, Libera Università di Bolzano
39100 Bolzano, Italia
Email: karl.vonellenrieder@unibz.it

MTS/IEEE Global OCEANS 2022: Chennai, India

21 February 2022

Introduction: Overview of Tutorial

Basic concepts of:

- Introduction
- Basic Stability
- Control of Underactuated Vehicles
- Feedback Linearization by Dynamic Inversion & Nonlinear Backstepping
- Adaptive Control
- Sliding Mode Control

Introduction: Overview of Tutorial

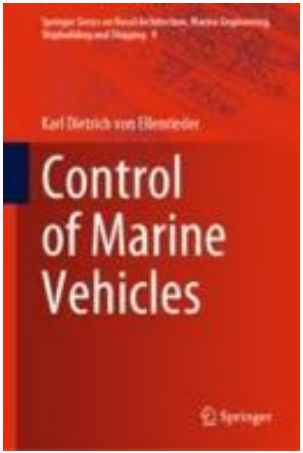

Would like to acknowledge permission of Springer to:

- Reproduce figures/graphics
- Reproduce manuscript form of text for lecture notes
- Reuse selected problems

von Ellenrieder [2021]

https://link.springer.com/book/10.1007/978-3-030-75021-3

Introduction: Background

Sarda et al. [2016]

Marine environments are

- Complex
- Unstructured
- Uncertain
- Disturbances, e.g. wind, waves and currents are
  - time varying
  - unpredictable

Introduction: Background

Dynamics of marine vehicles is usually highly nonlinear, and uncertain e.g.

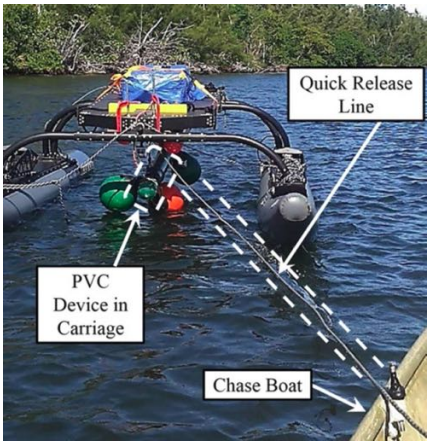

Klinger et al. [2017]

- Wave-making (residuary) resistance of surface vessels
- Trim and draft of surface vessels changes with speed
- Hydrodynamics of main hull and actuators characterized separately $\rightarrow$ uncertainty when combined
- Nonlinear hydrodynamic interactions between actuators and main body of vehicle (e.g. vortex shedding)
- Nonlinear hydrodynamic interactions between sea surface/floor and vehicle
- Operation at off-design conditions

Introduction: Background

Lastly, note that the control of most marine vehicles involves the simultaneous control of multiple states at once, e.g. speed and heading. Such systems are known as *Multiple Input Multiple Output (MIMO)* systems

Motivates use of control design approaches

- that are nonlinear
- Multiple Input Multiple Output
- that are robust to exogeneous disturbances and model uncertainty
- and for which the stability can be well-characterized

Structure of Marine Guidance, Navigation and Control Systems

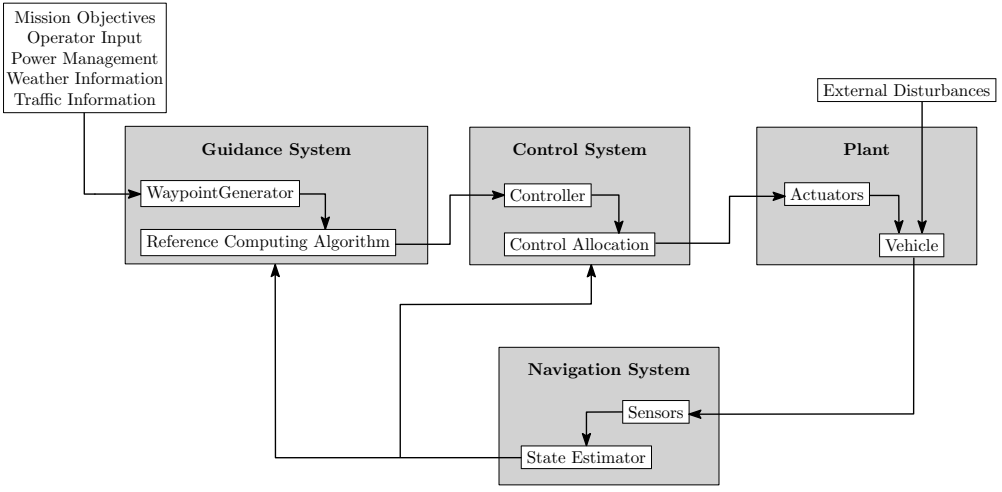

A typical Guidance, Navigation and Control System used for marine vehicles.

Structure of Marine Guidance, Navigation and Control Systems

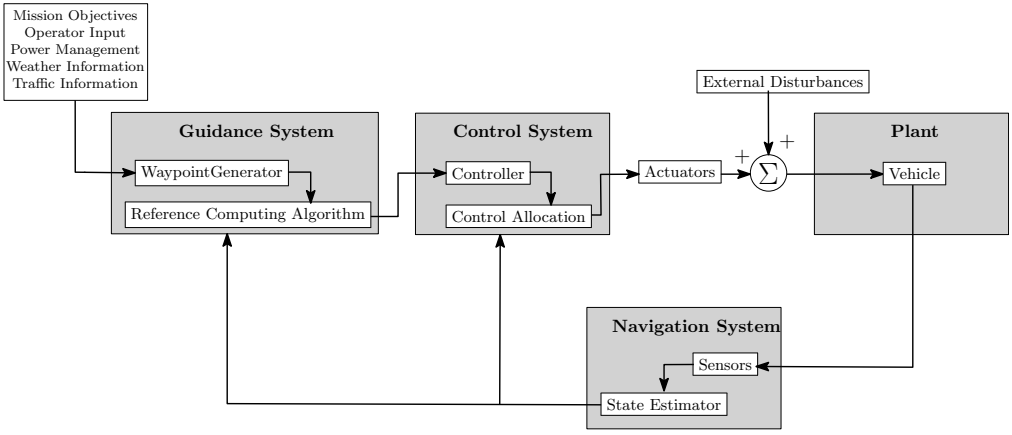

A typical Guidance, Navigation and Control System used for marine vehicles.

Overview of Marine Vehicle Control

Automatic Control: the use of machines, rather than humans, as controllers

- *plant* — the controlled system, e.g. the hull/structure of a marine vehicle
- *actuators* — devices for creating forces, moments that move the plant, e.g. propellers, waterjets, etc.
- *control input* — a signal sent to an actuator, which is turned into a force/moment that acts on a plant
- *system output* — the response of a plant
- *disturbances* — unknown, forces or moments that act on a plant, e.g. from the environment
- *model uncertainty*
  - *structural uncertainty* — uncertainty about the functional form of a system model
  - *parametric uncertainty* — functional form of a system model assumed to be correct, but values of parameters in model are not well known

Overview of Marine Vehicle Control

Basic functions required for a marine vehicle to operate in real-world:

1. Localization — determine position, orientation and velocity w.r.t. reference points in environment
2. Control (*low-level control*) — use actuators to go from current state to a desired state
3. Motion Planning (*high-level control*) — compute appropriate trajectories for moving through environment
   - Path Planning — computation of large-scale trajectories that satisfy constraints and are optimal in some sense, can be done offline
   - Trajectory Planning — computation of short-range trajectories that that deviate slightly from path but generally return to path in time; computing in real time for obstacle avoidance, etc.

Overview of Marine Vehicle Control

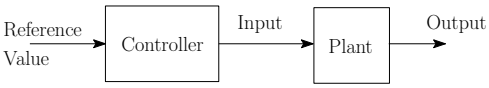

Open loop control system.

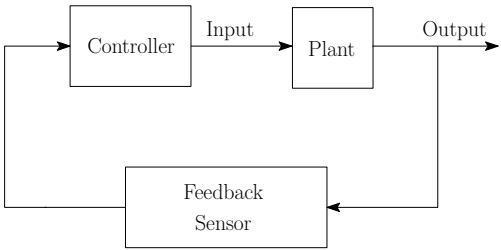

Closed Loop **Stabilization**, drive output to zero.

Overview of Marine Vehicle Control

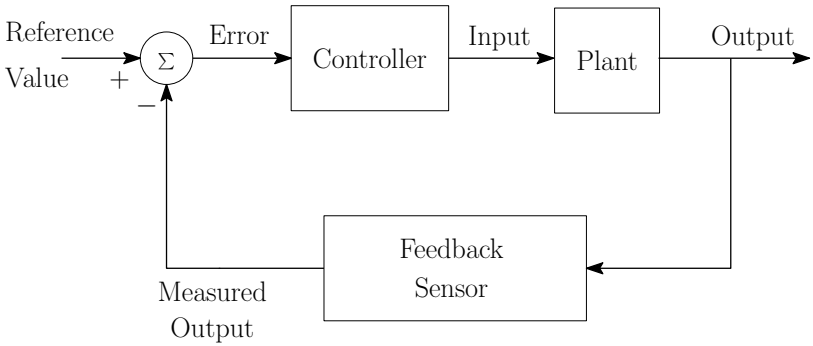

Closed Loop **Regulation** — constant reference signal & **Tracking** — time varying reference signal.

Overview of Marine Vehicle Control

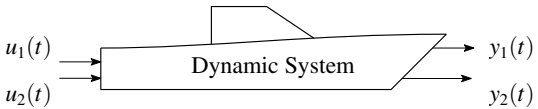

System plant.

Input–output system has form

$$\dot{\boldsymbol{x}} = \boldsymbol{f}(\boldsymbol{x}, \boldsymbol{u}), \quad \boldsymbol{y} = \boldsymbol{h}(\boldsymbol{x}, \boldsymbol{u}),$$

where $\boldsymbol{x} = \{x_1, \ldots, x_n\} \in \mathbb{R}^n$ is the state, $\boldsymbol{u} \in \mathbb{R}^p$ is the input and $\boldsymbol{y} \in \mathbb{R}^q$ is the output. The smooth maps $\boldsymbol{f} : \mathbb{R}^n \times \mathbb{R}^p \to \mathbb{R}^n$ and $\boldsymbol{h} : \mathbb{R}^n \times \mathbb{R}^p \to \mathbb{R}^q$ represent the dynamics and feedback measurements of the system.

Definition (State Variables)

A set of state variables $(x_1, x_2, \ldots, x_n)$ is a set of variables for which knowledge of the initial values of the state variables $[x_1(t_0), x_2(t_0), \ldots, x_n(t_0)]$ at the initial time t_0, and of the input signals $u_1(t)$ and $u_2(t)$ for $t \geq t_0$, **suffices** to determine the future values of the outputs and state variables.

Equations of Motion

Control design and stability analysis strongly depends on the dynamics of a system

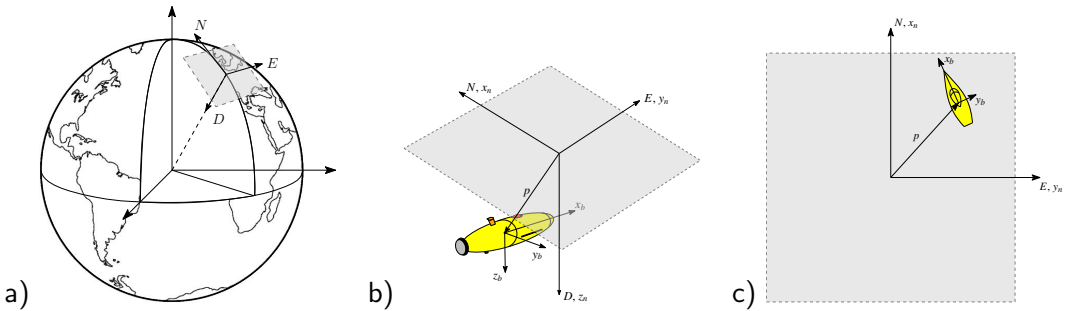

a) *NED* coordinate system referenced to an Earth–fixed, Earth–centered coordinate system.
b) Underwater vehicle referenced with respect to the NED coordinate system.
c) Surface vehicle referenced with respect to NED coordinate system.
Motion of surface vessels typically assumed to lie within plane of N–E axes.

Equations of Motion

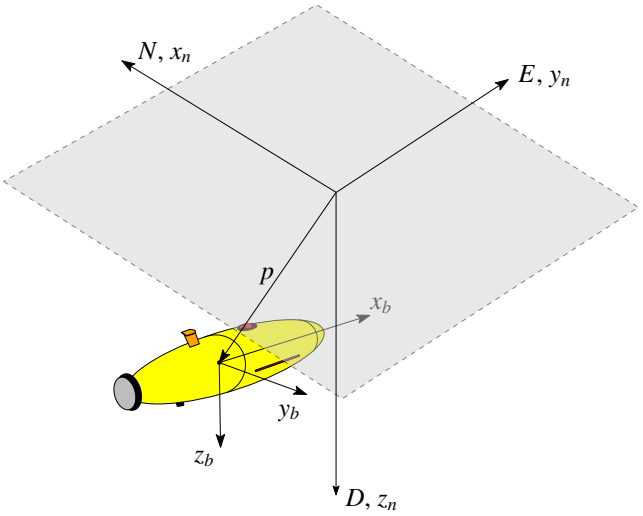

$$\boldsymbol{p} = \begin{bmatrix} x_n \\ y_n \\ z_n \end{bmatrix},$$

$$\Theta = \begin{bmatrix} \phi \\ \theta \\ \psi \end{bmatrix},$$

Euler angles measure of cumulative angular change over time between the *NED* and body-fixed coordinate systems.

Equations of Motion

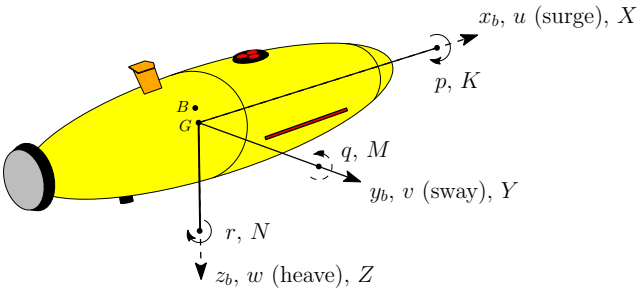

Body-fixed coordinate system with origin located at center of gravity G of an Autonomous Underwater Vehicle (AUV).

$$\boldsymbol{v} = \begin{bmatrix} u \\ v \\ w \end{bmatrix},$$

$$\boldsymbol{\omega} = \begin{bmatrix} p \\ q \\ r \end{bmatrix} = \begin{bmatrix} \dot{\phi} \\ \dot{\theta} \\ \dot{\psi} \end{bmatrix}.$$

$$\boldsymbol{f} = \begin{bmatrix} X \\ Y \\ Z \end{bmatrix}. \qquad \boldsymbol{m} = \begin{bmatrix} K \\ M \\ N \end{bmatrix}.$$

Equations of Motion

Fossen's *robot-like* model for equations of motion [Fossen, 2011]

$$\dot{\boldsymbol{\eta}} = \boldsymbol{J}(\boldsymbol{\eta})\boldsymbol{\nu}$$

$$\boldsymbol{M}\dot{\boldsymbol{\nu}} + \boldsymbol{C}(\boldsymbol{\nu})\boldsymbol{\nu} + \boldsymbol{D}(\boldsymbol{\nu})\boldsymbol{\nu} + \boldsymbol{g}(\boldsymbol{\eta}) = \boldsymbol{\tau} + \boldsymbol{w}_d,$$

where the first equation describes the kinematics of the vehicle (as above) and the second equation represents its kinetics.

Mathematical properties of $\boldsymbol{M}$, $\boldsymbol{C}(\boldsymbol{\nu})$ and $\boldsymbol{D}(\boldsymbol{\nu})$.

$$\boldsymbol{M} = \boldsymbol{M}^T > 0 \Rightarrow \boldsymbol{x}^T\boldsymbol{M}\boldsymbol{x} > 0, \forall \boldsymbol{x} \neq 0$$

$$\boldsymbol{C}(\boldsymbol{\nu}) = -\boldsymbol{C}^T(\boldsymbol{\nu}) \Rightarrow \boldsymbol{x}^T\boldsymbol{C}(\boldsymbol{\nu})\boldsymbol{x} = 0, \forall \boldsymbol{x}$$

$$\boldsymbol{D}(\boldsymbol{\nu}) > 0 \Rightarrow \tfrac{1}{2}\boldsymbol{x}^T[\boldsymbol{D}(\boldsymbol{\nu}) + \boldsymbol{D}^T(\boldsymbol{\nu})]\boldsymbol{x} > 0, \forall \boldsymbol{x} \neq 0$$

Equations of Motion

Define new state vector

$$\boldsymbol{x} := \begin{bmatrix} \boldsymbol{\eta} \\ \\ \boldsymbol{\nu} \end{bmatrix}, \qquad \dot{\boldsymbol{x}} = \begin{bmatrix} \boldsymbol{J}(\boldsymbol{\eta})\boldsymbol{\nu} \\ \\ -\boldsymbol{M}^{-1}\left[\boldsymbol{C}(\boldsymbol{\nu})\boldsymbol{\nu} + \boldsymbol{D}(\boldsymbol{\nu})\boldsymbol{\nu} + \boldsymbol{g}(\boldsymbol{\eta})\right] \end{bmatrix} + \begin{bmatrix} \boldsymbol{0}_{n\times n} \\ \\ \boldsymbol{M}^{-1} \end{bmatrix} \boldsymbol{B}\boldsymbol{u}.$$

Can be written variously as

$$\begin{aligned} \dot{\boldsymbol{x}} &= \boldsymbol{f}(\boldsymbol{x}) + \boldsymbol{G}\boldsymbol{B}\boldsymbol{u}, \\ &= \boldsymbol{f}(\boldsymbol{x}) + \boldsymbol{G}\boldsymbol{\tau}, \\ &= \boldsymbol{f}(\boldsymbol{x}) + \sum_{i=1}^{r} \boldsymbol{g}_i \tau_i, \end{aligned}$$

where

$$\boldsymbol{f}(\boldsymbol{x}) = \begin{bmatrix} \boldsymbol{J}(\boldsymbol{\eta})\boldsymbol{\nu} \\ \\ -\boldsymbol{M}^{-1}\left[\boldsymbol{C}(\boldsymbol{\nu})\boldsymbol{\nu} + \boldsymbol{D}(\boldsymbol{\nu})\boldsymbol{\nu} + \boldsymbol{g}(\boldsymbol{\eta})\right] \end{bmatrix},$$

$$\boldsymbol{G}(\boldsymbol{x}) = \begin{bmatrix} \boldsymbol{0} \\ \\ \boldsymbol{M}^{-1} \end{bmatrix},$$

Equations of Motion

Forms are interchangeable

$$\dot{\eta} = \boldsymbol{J}(\eta)\boldsymbol{v}$$

$$\boldsymbol{M}\dot{\boldsymbol{v}} + \boldsymbol{C}(\boldsymbol{v})\boldsymbol{v} + \boldsymbol{D}(\boldsymbol{v})\boldsymbol{v} + \boldsymbol{g}(\eta) = \boldsymbol{\tau} + \boldsymbol{w}_d, \quad \Leftrightarrow$$

$$\dot{\boldsymbol{x}} = \boldsymbol{f}(\boldsymbol{x}) + \boldsymbol{G}\boldsymbol{B}\boldsymbol{u},$$

$$= \boldsymbol{f}(\boldsymbol{x}, \boldsymbol{u})$$

Time Invariant and Time Varying Feedback Systems, Let $\boldsymbol{x} = \boldsymbol{x}(t)$.

State Feedback *Autonomous* System ($\boldsymbol{w}_d = 0$)	$\boldsymbol{u} = \boldsymbol{\alpha}(\boldsymbol{x})$	$\dot{\boldsymbol{x}} = \boldsymbol{f}(\boldsymbol{x})$
State Feedback, Time Varying System ($\boldsymbol{w}_d(t) \neq 0$)	$\boldsymbol{u} = \boldsymbol{\alpha}(\boldsymbol{x})$	$\dot{\boldsymbol{x}} = \boldsymbol{f}(\boldsymbol{x}, t)$
Time Varying Feedback (e.g. Adaptive Control)	$\boldsymbol{u} = \boldsymbol{\alpha}(\boldsymbol{x}, t)$	$\dot{\boldsymbol{x}} = \boldsymbol{f}(\boldsymbol{x}, t)$

Bibliography I

T. I. Fossen. *Handbook of marine craft hydrodynamics and motion control*. John Wiley & Sons, 2011.

W. B. Klinger, I. R. Bertaska, K. D. von Ellenrieder, and M. R. Dhanak. Control of an unmanned surface vehicle with uncertain displacement and drag. *IEEE Journal of Oceanic Engineering*, 42(2):458–476, 2017.

E. I. Sarda, H. Qu, I. R. Bertaska, and K. D. von Ellenrieder. Station-keeping control of an unmanned surface vehicle exposed to current and wind disturbances. *Ocean Engineering*, 127:305–324, 2016.

K. D. von Ellenrieder. *Control of marine vehicles*. Springer, 2021.

Fundamentals of Marine Vehicle Control: Sliding Mode Control

Karl D. von Ellenrieder

Field Robotics Lab South Tyrol
Facoltà di Scienze e Tecnologie, Libera Università di Bolzano
39100 Bolzano, Italia
Email: karl.vonellenrieder@unibz.it

MTS/IEEE Global OCEANS 2022: Chennai, India

21 February 2022

Introduction: Overview of Tutorial

Basic concepts of:

- Introduction
- Basic Stability
- Control of Underactuated Vehicles
- Feedback Linearization by Dynamic Inversion & Nonlinear Backstepping
- Adaptive Control
- Sliding Mode Control

Background

Marine vehicle dynamics:

$$\dot{\boldsymbol{\eta}} = \boldsymbol{R}(\psi)\boldsymbol{\nu},$$

$$\boldsymbol{M}\dot{\boldsymbol{\nu}} = -\boldsymbol{C}(\boldsymbol{\nu})\boldsymbol{\nu} - \boldsymbol{D}(\boldsymbol{\nu})\boldsymbol{\nu} + \boldsymbol{\tau} + \boldsymbol{d},$$

Control Challenges:

a) $\boldsymbol{M}$, $\boldsymbol{C}$, $\boldsymbol{D}$ and $\boldsymbol{\tau}$ uncertain.
b) $\boldsymbol{d}$ unknown/time-varying (but bounded).
c) Nonlinear $\rightarrow$ exacerbates points a & b

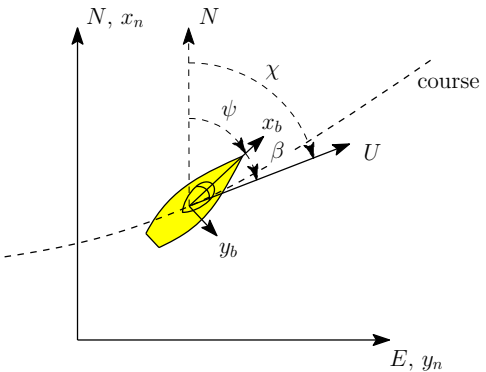

Maneuvering coordinates.

Background

Robust Control:

- Adaptive Control: control parameters adjust online to accommodate uncertainties.
- Disturbance Observer Based Control: include estimate $\hat{\boldsymbol{d}}$ in control signal to cancel real $\boldsymbol{d}$.
- Sliding mode control techniques.

Background

Robust Control:

- Adaptive Control: control parameters adjust online to accommodate uncertainties.
- Disturbance Observer Based Control: include estimate $\hat{\boldsymbol{d}}$ in control signal to cancel real $\boldsymbol{d}$.
- Sliding mode control techniques.

Advantages of sliding mode control include:

- robustness to uncertain plant model parameters, unmodeled dynamics and exogenous disturbances;
- finite-time convergence;
- reduced order dynamics (dynamical collapse).

Linear Control

Consider effects of uncertainty and external disturbance on linear control.

$$\begin{aligned} \dot{x}_1 &= x_2, \\ \dot{x}_2 &= u + d(x_1, x_2, t), \end{aligned} \tag{1}$$

where u is control input and d is bounded disturbance ($L \geq |d|$, $L > 0$).
Let $u = -k_1 x_1 - k_2 x_2$. When $d = 0$, closed loop system has state space form

$$\dot{\boldsymbol{x}} = \frac{\mathrm{d}}{\mathrm{d}t} \begin{bmatrix} x_1 \\ x_2 \end{bmatrix} = \begin{bmatrix} 0 & 1 \\ -k_1 & -k_2 \end{bmatrix} \begin{bmatrix} x_1 \\ x_2 \end{bmatrix} = \boldsymbol{A}\boldsymbol{x}.$$

CL system stable when $\boldsymbol{A}$ is Hurwitz (real part of all eigenvalues of $\boldsymbol{A} < 0$).

Linear Control

Eigenvalues of $\boldsymbol{A}$ are

$$\lambda_{1,2} = -\frac{k_2}{2} \pm \frac{1}{2}\sqrt{k_2^2 - 4k_1}.$$

For $\mathrm{Re}\{\boldsymbol{A}\} < 0$, we require $k_2 > 0$ and $k_1 > k_2^2/4$.

a)

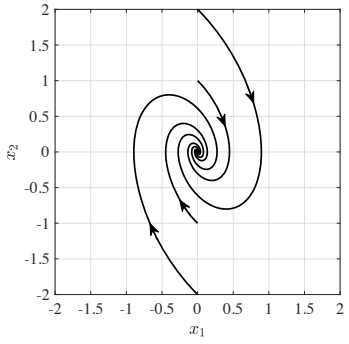

b)

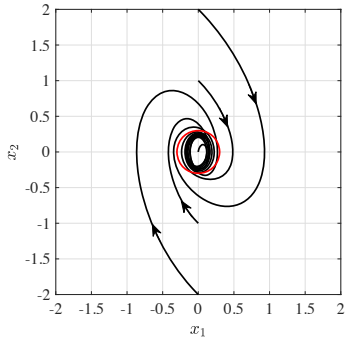

Phase portrait ($k_1 = 2$, $k_2 = 1$) for: a) $d = 0$ and b) $d = 0.25\sin(1.5t)$.

Lyapunov Functions

Lyapunov function V continuously differentiable, non-negative, energy-like function that always decreases along the solution trajectories. Minimum of V is an asymptotically stable equilibrium point.

a. V is a radially unbounded function of the state variables, i.e.

$$\lim_{|x_1|\to\infty, |x_2|\to\infty} V(x_1, x_2) \to \infty,$$

and

b. the time derivative of V is negative definite,

$$\dot{V} < 0, \quad \forall x_1, x_2 \neq 0.$$

Lyapunov Functions

Examine CL stability of (1) with linear control $u = -k_1 x_1 - k_2 x_2$ using

$$V = \frac{1}{2}x_1^2 + \frac{1}{2}x_2^2.$$

Select control gains so $\dot{V} < 0, \forall x_1, x_2 \neq 0$. It can be shown that

$$\begin{aligned} \dot{V} &\leq -\frac{(k_1 - 1)}{2}x_1^2 - \left[\frac{(k_1 - 1) + 2k_2 - 1}{2}\right] x_2^2 + \frac{1}{2}d^2, \\ &\leq -\mu_1 x_1^2 - \mu_2 x_2^2 + C_d, \end{aligned}$$

where

$$C_d := \sup_{\{x_1, x_2, t\}} \left|\frac{1}{2}d^2\right|.$$

Lyapunov Functions

Let

$$\mu := \min\{\mu_1, \mu_2\}.$$

Then

$$\dot{V} \leq -2\mu V + C_d.$$

which can be solved to show

$$V \leq \left(V_0 - \frac{C_d}{2\mu}\right) \mathrm{e}^{-2\mu t} + \frac{C_d}{2\mu},$$

where V_0 is the value of V at time $t = 0$.

As in phase portrait above, when $d \neq 0$, $V = \frac{1}{2}x_1^2 + \frac{1}{2}x_2^2 \to \frac{C_d}{2\mu} \neq 0$.

Sliding Mode Control

When $d = 0$, a stable linear controller would have the form

$$\dot{x}_1 = -cx_1, \quad c > 0.$$

Since, $x_2 := \dot{x}_1$, then the general solution is

$$\begin{aligned} x_1(t) &= x_1(0)\mathrm{e}^{-ct}, \\ x_2(t) &= \dot{x}_1(t) = -cx_1(0)\mathrm{e}^{-ct}. \end{aligned}$$

Note:

- Both $x_1(t)$ and $x_2(t)$ exponentially converge to zero.
- Ideally, $d(x_1, x_2, t) \neq 0$ will not affect our desired solution.

Sliding Mode Control

Can we "reverse engineer" closed loop dynamics to drive system to desired equilibrium?

Introduce a new variable

$$s = x_2 + cx_1, \quad c > 0.$$

We seek a control input u that drives $s \to 0$ in finite time.

Time derivative of s brings control input into desired dynamics of CL system

$$\dot{s} = \dot{x}_2 + c\dot{x}_1 = u + d(x_1, x_2, t) + cx_2.$$

Now take

$$V = \frac{1}{2}s^2.$$

To ensure CL system converges to equilibrium in finite time, we require V to satisfy

$$\dot{V} \leq -\alpha V^{1/2}, \quad \alpha > 0.$$

Sliding Mode Control

Integrating this inequality using separation of variables gives

$$V^{1/2} \leq -\frac{\alpha t}{2} + V_0^{1/2}.$$

Thus V becomes zero in the finite time t_r, which is bounded by

$$t_r \leq \frac{2V_0^{1/2}}{\alpha}.$$

Differentiating V allows us to find a control input u so that $\dot{V} \leq 0$,

$$\dot{V} = s\dot{s} = s\left(cx_2 + d(x_1, x_2, t) + u\right)$$

Take $u = -cx_2 + \nu$ to get

$$\dot{V} = s\left[d(x_1, x_2, t) + \nu\right] = sd(x_1, x_2, t) + s\nu \leq |s|L + s\nu.$$

Sliding Mode Control

If we take $\nu = -\rho \text{sgn}(s), \rho > 0$, where

$$\text{sgn}(s) := \begin{cases} +1, & s > 0, \\ -1, & s < 0 \end{cases} \quad \text{and} \quad \text{sgn}(0) \in [-1, 1].$$

Noting that $\text{sgn}(s)s = |s|$, then

$$\dot{V} \leq L|s| - \rho \text{sgn}(s)s = (L - \rho)|s|.$$

$\dot{V}$ can also be written as

$$\dot{V} \leq -\frac{\alpha}{\sqrt{2}}|s|.$$

Equating these inequalities, gives

$$(L - \rho) = -\frac{\alpha}{\sqrt{2}} \quad \Rightarrow \quad \rho = L + \frac{\alpha}{\sqrt{2}}.$$

Then, the sliding mode control law is

$$\boxed{u = -cx_2 - \rho \text{sgn}(s)}$$

Sliding Mode Control

Definition

The surface $s = 0$ (the straight line $x_2 + cx_1 = 0$ in 2 dimensions) is a **sliding surface**.

Definition

The equation

$$\dot{V} = s\dot{s} \leq -\frac{\alpha}{\sqrt{2}}|s|,$$

is a **reachability condition**. When met, trajectory of CL system is driven towards sliding surface and remains on it after reached.

Definition

A control law that drives the state variables to the sliding surface in finite time t_r and keeps them on the surface thereafter in the presence of a bounded disturbance is called a sliding mode controller. An ideal sliding mode is taking place when $t > t_r$.

Sliding Mode Control: Example

Consider response of system (1) when control input is $u = -cx_2 - \rho \mathrm{sgn}(s)$

Let $c = 1.5$, $\rho = 2$ and $d(x_1, x_2, t) = 0.25 \sin(1.5t)$ and initial conditions be $x_1(0) = 0$, $x_2(0) = 2$.

Then

$$V_0 = \frac{1}{2}(x_2(0) + cx_1(0))^2 = 2.$$

If we take $L = 0.25$,

$$\alpha = \sqrt{2}(\rho - L) = 2.475$$

and the estimated reaching time is

$$t_r \leq \frac{2V_0^{1/2}}{\alpha} = \frac{2\sqrt{2}}{2.475} = 1.143 \text{ secs.}$$

Sliding Mode Control: Example

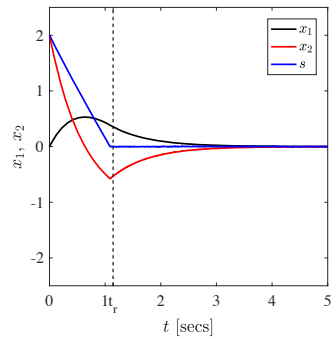

a)

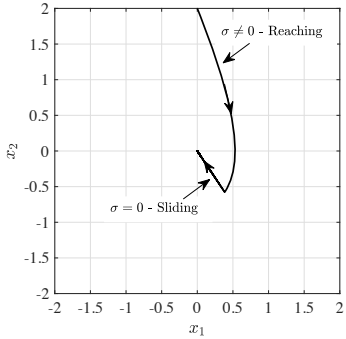

b)

a) Time response and b) phase portrait of the system in (1) when the control input is taken to be $u = -cx_2 - \rho \mathrm{sgn}(s)$ with $c = 1.5$, $\rho = 2$ and $d(x_1, x_2, t) = 0.25 \sin(1.5t)$ and initial conditions $x_1(0) = 0$, $x_2(0) = 2$.

Sliding Mode Control: Example

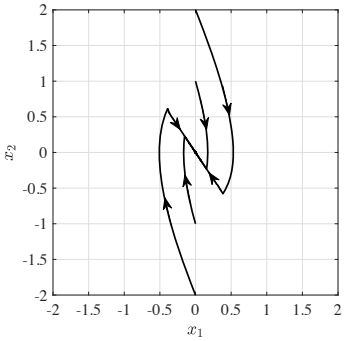

Phase portrait of the sliding mode controller with $c = 1.5$ and $\rho = 2$ and disturbance $d = 0.25 \sin(1.5t)$.

Sliding Mode Control: Example

But there's a catch...

Sliding Mode Control: Example

But there's a catch...chattering

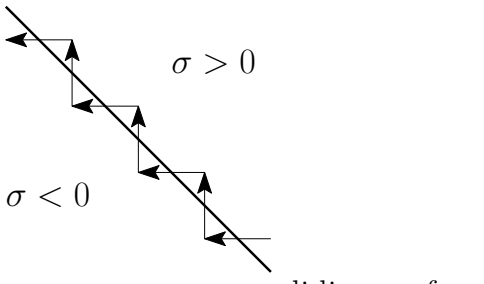

a)

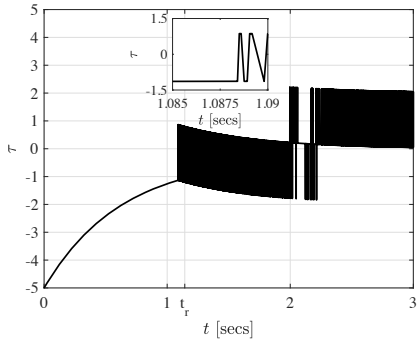

b)

a) Zig-zag motion of solution trajectory across sliding surface $s = 0$ during chattering.
b) Chattering of control input when using the sliding mode controller. Inset shows control signal rapidly switching.

Equivalent Control

When $t \geq t_r$ trajectory of CL system on sliding surface $s = x_2 + cx_1 = 0$.

Once on sliding surface, trajectory remains there $\Rightarrow s = \dot{s} = 0$.

Examine condition $\dot{s} = 0$ more closely

$$\dot{s} = cx_2 + d(x_1, x_2, t) + u = 0, \quad s(t \geq t_r) = 0.$$

Condition would be satisfied by an "equivalent control" input of form

$$u_{\text{eq}} = -cx_2 - d(x_1, x_2, t)$$

Not possible to implement u_{eq} in practice — $d(x_1, x_2, t)$ represents exogenous disturbances and model uncertainty, which we do not know.

Equivalent Control

However, our sliding mode control law $u = -cx_2 - \rho \mathrm{sgn}(s)$ works!

Comparing u and u_{eq} suggests average effect of high frequency switching in sliding mode control law produces a control like u_{eq}.

Approximate u_{eq} using low pass filtered version of sliding mode control law:

$$\hat{u}_{\mathrm{eq}} = -cx_2 - \rho \mathrm{LPF}\left[\mathrm{sgn}(s)\right], \quad t \geq t_r.$$

Implement low pass filter as 1^{st} order differential equation

$$\begin{aligned} \hat{u}_{\mathrm{eq}} &= -cx_2 - \rho z, \\ \tau \dot{z} &= -z + \mathrm{sgn}(s), \end{aligned}$$

$\tau \in [0, 1)$ is filter time constant (small as possible, but larger than sampling time).

$\mathrm{LPF}\left[\mathrm{sgn}(s)\right]$ disturbance observer for combined disturbance & model uncertainty

Summary: Standard Sliding Mode Control

1) Two main tasks in conventional sliding mode control design:
   a) Design 1^{st} order sliding surface $s = 0$.
   b) Design control u to drive sliding variable $s \to 0$ using sliding variable dynamics.
2) Application of sliding mode control law gives CL dynamics

$$\begin{aligned} \dot{x}_1 &= x_2, \\ \dot{x}_2 &= -cx_2 - \rho \operatorname{sgn}(s) + d(x_1, x_2, t). \end{aligned}$$

   In sliding mode ($t \geq t_r$), CL system driven by equivalent dynamics, s.t.

$$\begin{aligned} \dot{x}_1 &= x_2, \\ \dot{x}_2 &= \underbrace{-cx_2 - d(x_1, x_2, t)}_{u_{\text{eq}}} + d(x_1, x_2, t) = -cx_2 = -c\dot{x}_1 \end{aligned} \quad \Rightarrow \quad \begin{cases} \dot{x}_1 = x_2, \\ \dot{x}_2 = -cx_1. \end{cases}$$

   In sliding mode, dynamics of system 1^{st} order, but original system 2^{nd} order $\Rightarrow$ *partial dynamical collapse*
3) In sliding mode CL dynamics do not depend on $d(x_1, x_2, t)$. But, upper limit of d accounted for when selecting controller gain.
4) Discontinuous $\operatorname{sgn}(s)$ term in u causes undesireable chattering.

Stabilization vs. Tracking

So far, we examined control input designed to drive the system to a fixed equilibrium point $\Rightarrow$ **stabilization problem**.

Many important marine applications require a control law to track desired "moving equilibrium point", i.e. a desired trajectory $y_d \Rightarrow$ **tracking problem**.

Relative Degree of System — number of times r output must be differentiated before the control input u explicitly appears

- When order of system n is same, i.e. when $n = r$, no internal dynamics (e.g. dynamics which cannot be directly controlled using the control input u).
- When $r < n$, additional analysis necessary to ensure internal dynamics are stable.

For example, let $y = x_1$ in

$$\begin{aligned} \dot{x}_1 &= x_2, \\ \dot{x}_2 &= u + d(x_1, x_2, t). \end{aligned}$$

Since $\ddot{y} = \ddot{x}_1 = \dot{x}_2 = u + d(x_1, x_2, t)$ relative degree of system is $r = n = 2$ (no internal dynamics).

Super-Twisting Sliding Mode Control

Sliding mode control very nice features, but chattering a show stopper in real systems.

Can we modify the basic sliding mode control to produce a continuous control signal?

Modify definition of sliding variable to solve an output tracking problem $\Rightarrow$
$e := (y - y_d)$, then

$$s = \dot{e} + ce, \quad c > 0.$$

We seek a control input that drives $s \to 0$ in finite time and keeps it there, s.t.

$$\begin{aligned} \dot{s} &= \ddot{e} + c\dot{e}, \\ &= \ddot{y}_d - \ddot{y} + c\dot{y}_d - c\dot{y}, \\ &= \underbrace{\ddot{y}_d + c\dot{y}_d - c\dot{y} - d(x_1, x_2, t)}_{\phi(y,\dot{y},t)} - u = 0, \end{aligned}$$

where $\phi(y, \dot{y}, t)$ is a *cumulative* disturbance term, upperbounded by a positive constant M, e.g. $|\phi(y, \dot{y}, t)| \leq M$.

Super-Twisting Sliding Mode Control

When $\phi(y, \dot{y}, t) = 0$ the control input

$$u = c|s|^{1/2}\mathrm{sgn}(s), \quad c > 0$$

makes compensated dynamics in the sliding mode become

$$\dot{s} = -c|s|^{1/2}\mathrm{sgn}(s), \quad s(0) = s_0.$$

This can be integrated to get

$$|s|^{1/2} - |s_0|^{1/2} = -\frac{c}{2}t.$$

Taking $s = 0$, we find that the corresponding reaching time would be given by

$$t_r \geq \frac{2}{c}|s_0|^{1/2}.$$

Unfortunately, when $\phi(y, \dot{y}, t) \neq 0$, these relations no longer hold $\Rightarrow$ can add another term to the controller to cancel the effects of cumulative disturbance?

Super-Twisting Sliding Mode Control

Here, we can apply our experience with equivalent control.

Assuming time derivative of cumulative error upper bounded, i.e. $\dot{\phi}(y, \dot{y}, t) \leq C$, can modify controller above to get,

$$\boxed{\begin{aligned} u &= c|s|^{1/2}\mathrm{sgn}(s) + w, \quad c = 1.5\sqrt{C} \\ \dot{w} &= b\mathrm{sgn}(s), \quad b = 1.1C \end{aligned}}$$

This makes compensated s-dynamics become

$$\begin{aligned} \dot{s} &= \phi(y, \dot{y}, t) - c|s|^{1/2}\mathrm{sgn}(s) - w, \\ \dot{w} &= b\mathrm{sgn}(s). \end{aligned}$$

w acts like an equivalent control term — produces a low pass filtered estimate of $\phi(y, \dot{y}, t)$.

When w converges to $\phi(y, \dot{y}, t)$, remaining $c|s|^{1/2}\mathrm{sgn}(s)$ term in u can drive $s \to 0$ in finite time.

Summary: Super-Twisting Sliding Mode Control

1. Super-twisting control u continuous: $c|s|^{1/2}\mathrm{sgn}(s)$ and $w = \int b\mathrm{sgn}(s)\mathrm{d}t$ are continous — high frequency switching in $\mathrm{sgn}(s)$ term smoothed by integral.
2. w and augmented system $\dot{w} = b\mathrm{sgn}(s)$ mandatory for canceling $\phi(y, \dot{y}, t)$.
3. Once $\phi(y, \dot{y}, t)$ cancelled, super-twisting controller uses nonlinear sliding manifold $\dot{s} = -c|s|^{1/2}\mathrm{sgn}(s)$ to drive $\dot{s} \to 0$ and $s \to 0$ in finite time — conventional sliding mode control uses linear sliding surface to drive only $s \to 0$ in finite time.

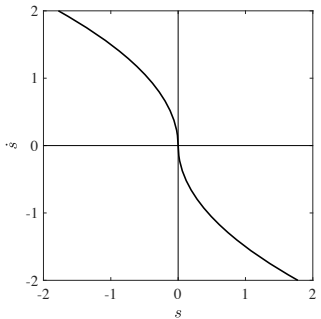

The super-twisting sliding surface given by $\dot{s} = -1.5|s|^{1/2}\mathrm{sgn}(s)$.

Summary: Super-Twisting Sliding Mode Control

4. Let $\tilde{x}_1 := e$ and $\tilde{x}_2 := \dot{e}$, then $s = \tilde{x}_2 + c\tilde{x}_1$.

   $\dot{s} \to 0$ in finite time implies $s \to 0$ in finite time, so compensated dynamics in sliding mode are

$$\begin{aligned} \tilde{x}_2 &= -c\tilde{x}_1 \\ \dot{s} &= 0. \end{aligned}$$

   Complete dynamical collapse achieved in sliding mode — 2^{nd} order uncompensated dynamics of original system reduced to the algebraic equations $\tilde{x}_2 = \tilde{x}_1 = 0$ in finite time.

   Guarantees control input eliminates any inner loop dynamics or parasitic dynamics.

Super-Twisting Sliding Mode Control: Example

Consider the vertical tracking control of an unmanned aerial vehicle (UAV) lifting a small 5 N payload

$$m\ddot{x} = -mg - C_d\dot{x}|\dot{x}| + u + d,$$

$x_1 = x$ is UAV position, $x_2 = \dot{x}$ is speed, $g = 9.81$ m/s^2 is gravitational acceleration, u is thrust and $d = -5$ N is a disturbance (payload weight).

Let $\dot{y}_d = U = 1$ m/s, so that $y_d = Ut$ m for $C_d = 0.5$ kg/m and $m = 2$ kg.

Estimate cumulative error bounds as $C = 20$, s.t. $b = 1.1C$ and $c = 5\sqrt{(C)}$.

Super-Twisting Sliding Mode Control: Example

a)

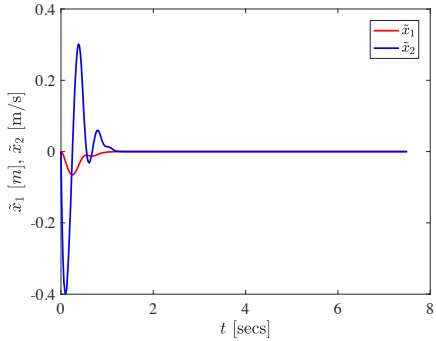

b)

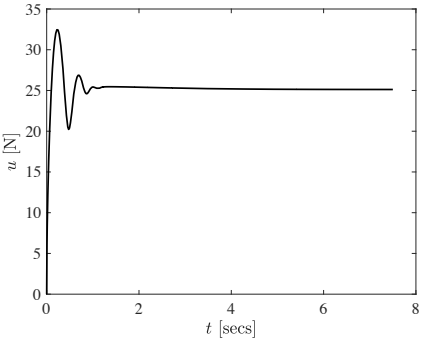

Super-twisting controller: a) Tracking errors, b) control input.

Super-Twisting Sliding Mode Control: Example

a)

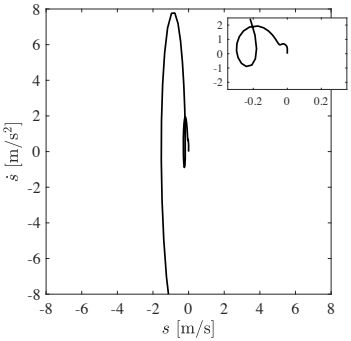

b)

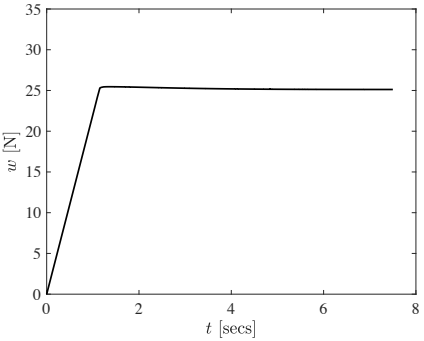

Super-twisting controller: a) s, $\dot{s}$ vs. time, b) Disturbance error estimate.

Summary

So we have covered the fundamentals principles of

- Marine Control Systems & Stability Analysis
- Feedback Linearization by Dynamic Inversion & Nonlinear Backstepping
- Control of Underactuated Vehicles
- Adaptive Control
- Sliding Mode Control

in a **very short** period of time.

Thank You!!

We hope that you enjoyed the tutorial and have found it informative and useful!

Fundamentals of Marine Vehicle Control: Basic Stability

Karl D. von Ellenrieder

Field Robotics Lab South Tyrol
Facoltà di Scienze e Tecnologie, Libera Università di Bolzano
39100 Bolzano, Italia
Email: karl.vonellenrieder@unibz.it

MTS/IEEE Global OCEANS 2022: Chennai, India

21 February 2022

Introduction: Overview of Tutorial

Basic concepts of:

- Introduction
- Basic Stability
- Control of Underactuated Vehicles
- Feedback Linearization by Dynamic Inversion & Nonlinear Backstepping
- Adaptive Control
- Sliding Mode Control

Basic Stability: Introduction

- Before a control system for a marine vehicle is widely implemented in practice, must characterize its stability over a range of conditions
- Dynamics of marine vehicles generally very nonlinear
  - Familiar linear analysis tools can't be easily applied
  - Nonlinear Lyapunov stability methods often used — can show stability of a closed loop system, even when no equilibrium point exists (disturbances)
  - Often one doesn't need an exact solution to the equations of motion, only an understanding of its properties, e.g. boundedness, asymptotic behavior

Basic Stability: 1D Flow along a line

Consider the one dimensional autonomous system $\dot{x} = f(x)$, where $x = x(t)$.

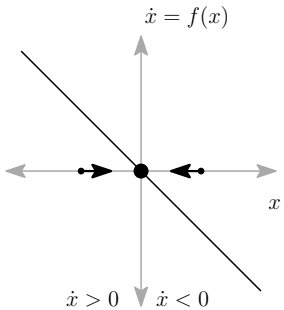

$f(0) = 0$

Stable

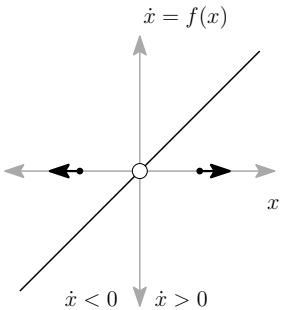

$f(0) = 0$

Unstable

x position of particle
$\dot{x}$ speed of particle
$\dot{x} = 0$ equilibrium point
$\dot{x} < 0$ particle moves left
$\dot{x} > 0$ particle moves right

Stable: particles move towards equilibrium point from both sides

Basic Stability: 1D Flow along a line

Example: speed control of a surface vessel

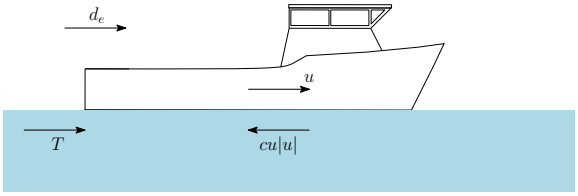

Equation of motion
$m\dot{u} = -cu|u| + T + d_e$

Equilibrium $\dot{u} = 0$

Open Loop Control:
Let $d_e = 0$ and $T = cu_0|u_0|$
Then, $\dot{u} = 0$ when $u = u_0$

What if $d_e \neq 0$ and drag coefficient is *uncertain*, i.e. our estimate is off, e.g. $c + \delta c$?
Then, with $d := \delta c u_0|u_0| + d_e$

$$\begin{aligned} m\dot{u} &= -cu|u| + (c + \delta c)u_0|u_0| + d_e, \\ &= -cu|u| + cu_0|u_0| + d. \end{aligned}$$

Basic Stability: 1D Flow along a line

Example: speed control of a surface vessel

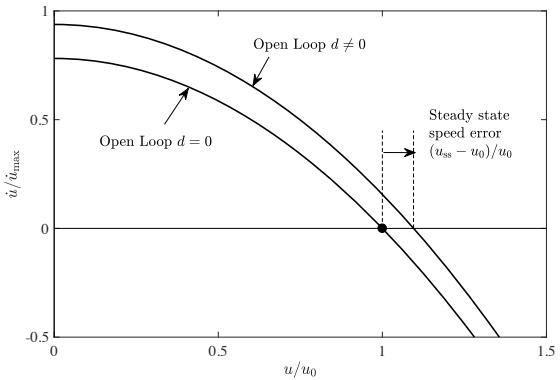

Now, the new equilibrium speed is

$$\lim_{t\to\infty} u = u_{ss} = \sqrt{u_0^2 + d/c}.$$

Open loop: No way to mitigate speed error with disturbance and model uncertainty!

Basic Stability: 1D Flow along a line

Example: speed control of a surface vessel

Now, use feedback. Let

$$
\begin{aligned}
T &= (c+\delta c)u_0|u_0| - k_p(u-u_0), \\
m\dot{u} &= -cu|u| + (c+\delta c)u_0|u_0| - k_p(u-u_0) + d_e,
\end{aligned}
$$

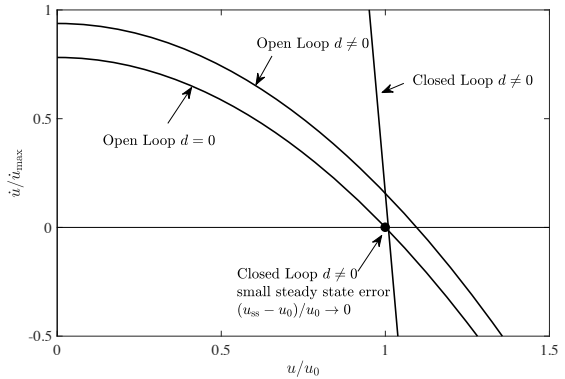

Then, after linearizing about $u = u_0$

$$m\dot{u} \approx -(k_p + 2cu_0)(u-u_0) + d.$$

Now, new equilibrium speed is

$$
\begin{aligned}
\lim_{t\to\infty} u &= u_{ss} \\
&= u_0 + \frac{d}{k_p + 2cu_0}
\end{aligned}
$$

Closed loop: can mitigate speed error with disturbance and model uncertainty using $k_p \gg 1$.

Basic Stability: 2D Phase Portrait

Example: pitch control of an AUV

$$(I_y - M_{\dot{q}})\ddot{\theta} = (I_y - M_{\dot{q}})\dot{q} = -U^2 \sin\theta\cos\theta(Z_{\dot{w}} - X_{\dot{u}}) - k_p\theta - k_d\dot{\theta}.$$

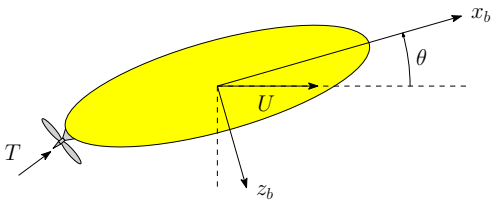

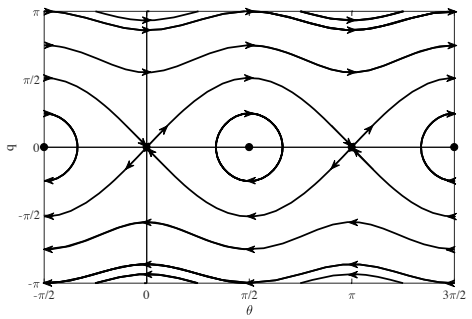

Uncontrolled, $k_p = 0, k_d = 0$.

Basic Stability: 2D Phase Portrait

Example: pitch control of an AUV

$$(I_y - M_{\dot{q}})\ddot{\theta} = (I_y - M_{\dot{q}})\dot{q} = -U^2 \sin\theta\cos\theta(Z_{\dot{w}} - X_{\dot{u}}) - k_p\theta - k_d\dot{\theta}.$$

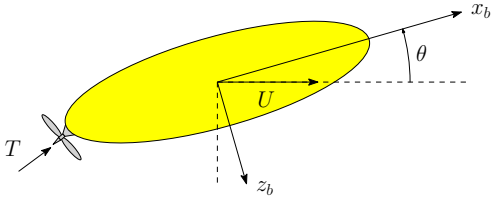

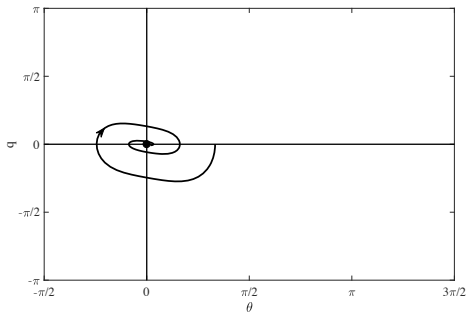

Controlled, $k_p > 0, k_d > 0$.

Basic Stability: Stability Analysis

- Controlled marine systems generally represented with ordinary differential equations
- Not interested in solving the equations, only in understanding behavior of the solutions, e.g. boundedness, . . .

Generally, nonlinear stability theory consists of three main components:

1. *definitions* of the different kinds of stability, which provide insight into the behavior of a closed loop system;
2. the different *conditions* that a closed loop system must satisfy in order to possess a certain type of stability; and
3. *criteria* that enable one to check whether or not the required conditions hold, **without having to explicitly compute the solution of the differential equations describing the time evolution of the closed loop system**.

The *conditions* and *criteria* required to establish the various types of stability are often presented in the form of mathematical theorems.

Basic Stability: Stability Analysis

Consider a system of the form

$$\begin{aligned} \dot{\boldsymbol{x}} &= \boldsymbol{f}(\boldsymbol{x}, \boldsymbol{u}), \quad \boldsymbol{x} \in \mathbb{R}^n, \boldsymbol{u} \in \mathbb{R}^p \\ \boldsymbol{y} &= \boldsymbol{h}(\boldsymbol{x}), \quad \boldsymbol{y} \in \mathbb{R}^q, \end{aligned}$$

where $\boldsymbol{f}$ is a locally Lipschitz continuous function.

Definition (Lipschitz Continuous)

A function $\boldsymbol{f}(\boldsymbol{x})$ is defined to be *Lipschitz continuous* if for some constant $c > 0$,

$$\|\boldsymbol{f}(\boldsymbol{x}_2) - \boldsymbol{f}(\boldsymbol{x}_1)\| < c\|\boldsymbol{x}_2 - \boldsymbol{x}_1\|, \quad \forall\ \boldsymbol{x}_1, \boldsymbol{x}_2,$$

where $\| \bullet \|$ denotes the 2-norm (Euclidean norm) of a vector. A sufficient condition for a function to be Lipshitz continuous is that its Jacobian

$$\boldsymbol{A} = \frac{\partial \boldsymbol{f}}{\partial \boldsymbol{x}}$$

is uniformly bounded for all $\boldsymbol{x}$.

Basic Stability: Stability Analysis

Consider the system $\dot{\boldsymbol{x}} = \boldsymbol{f}(\boldsymbol{x}, \boldsymbol{u})$

Definition (Stable)

Let $\epsilon > \delta > 0$, $\boldsymbol{x}_e$ is a *stable equilibrium point*, if for a given initial condition $\boldsymbol{x}_0 = \boldsymbol{x}(t_0)$, where $\|\boldsymbol{x}_0 - \boldsymbol{x}_e\| < \delta$, the solution trajectories $\boldsymbol{x}(t)$ of the system remain in the region ϵ for all $t > t_0$, i.e. such that $\|\boldsymbol{x}(t) - \boldsymbol{x}_e\| < \epsilon,\ \forall t > t_0$. We also say the system is stable *in the sense of Lyapunov*.

Definition (Unstable)

The equilibrium point $\boldsymbol{x}_e$ is *unstable*, if it is not stable.

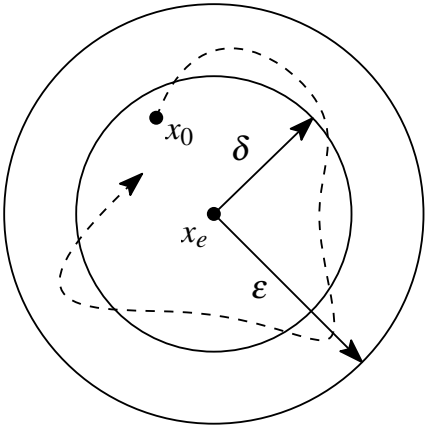

Basic Stability: Stability Analysis

In practice, simple stability is not enough, we want to know

- more about the nature of the stability
- and under what initial conditions a system is stable.

Definition (Asymptotically Stable)

A system is *asymptotically stable* if, 1) it is stable and 2) the solution trajectories of the state $\boldsymbol{x}$ converge to $\boldsymbol{x}_e$ for initial conditions sufficiently close to $\boldsymbol{x}_e$, i.e. a δ can be chosen so that

$$\|\boldsymbol{x}_0 - \boldsymbol{x}_e\| < \delta \Rightarrow \lim_{t\to\infty} \|\boldsymbol{x}(t) - \boldsymbol{x}_e\| = 0.$$

Basic Stability: Stability Analysis

Definition (Exponentially Stable)

An equilibrium point $\boldsymbol{x}_e$ is *exponentially stable* if there exist positive constants δ, k and λ such that all solutions with $\|\boldsymbol{x}_0 - \boldsymbol{x}_e\| \leq \delta$ satisfy the inequality

$$\|\boldsymbol{x}(t) - \boldsymbol{x}_e\| \leq k\|\boldsymbol{x}_0 - \boldsymbol{x}_e\|e^{-\lambda t}, \quad \forall t \geq t_0.$$

The constant λ is often referred to as the *convergence rate*.

Asymptotic and exponential stability are local concepts. Convergence guaranteed if x_0 is within a radius δ (basin of attraction) of x_e. If not, $x(t)$ may not converge, it could even diverge!

Basic Stability: Stability Analysis

Definition (Globally Attractive)

Generally, the asymptotic stability and exponential stability of an equilibrium point are local properties of a system. However, when the region of attraction of an equilibrium point includes the entire space of $\mathbb{R}^n$, i.e. $\delta \to \infty$, the equilibrium point is *globally attractive*.

Definition (Globally Asymptotically Stable)

An equilibrium point x_e is *globally asymptotically stable* (GAS), if it is stable and the state converges to x_e for any initial state x_0.

Definition (Globally Exponentially Stable)

An equilibrium point x_e is *globally exponentially stable* (GES), if it is stable and the state converges exponentially fast to x_e for any initial state x_0.

Basic Stability: Stability Analysis

So how do we use these definitions?

The most common approach is to find a controller that will make the closed loop system Lyapunov stable and to use the definitions to characterize the resulting stability.

How do we do that?

Basic idea:

- Lyapunov noticed that if the total energy of a system is continuously dissipated, the system tends towards an equilibrium.
- If we can identify an energy-like scalar function $V(\boldsymbol{x})$ for our system and show that a controller makes it decreases in time, we have shown that the closed loop controlled system is stable.

Basic Stability: Stability Analysis

Lyapunov's Second (Direct) Method

Let $(\boldsymbol{x} - \boldsymbol{x}_e) := \tilde{\boldsymbol{x}} \in \mathbb{R}^n$ and consider the nonlinear time-invariant system

$$\dot{\tilde{\boldsymbol{x}}} = \boldsymbol{f}(\tilde{\boldsymbol{x}}),$$

with a local equilibrium point $\boldsymbol{x}_e$, such that $\boldsymbol{f}(\tilde{\boldsymbol{x}} = 0) = 0$.

For time-invariant systems $V(\tilde{\boldsymbol{x}})$ is an implicit function of time t, such that

$$\frac{\mathrm{d}V}{\mathrm{d}t} = \dot{V}(\tilde{\boldsymbol{x}}) = \frac{\partial V}{\partial \tilde{\boldsymbol{x}}} \boldsymbol{f}(\tilde{\boldsymbol{x}}).$$

Theorem (Lyapunov Stability)

Suppose there exists a continuous function $V : \mathbb{R}^n \to \mathbb{R}$ where $V(\tilde{\boldsymbol{x}}) > 0$ for all $\boldsymbol{x} \neq \boldsymbol{x}_e$ and $\dot{V}$ is negative semidefinite for all $\boldsymbol{x}$, i.e. $\dot{V}(\tilde{\boldsymbol{x}}) \leq 0$, then the system is stable. If $\dot{V}$ is negative definite, i.e. $\dot{V}(\tilde{\boldsymbol{x}}) < 0$ for all $\boldsymbol{x} \neq \boldsymbol{x}_e$, then the system is asymptotically stable. If, in the latter case, $V(\tilde{\boldsymbol{x}}) \to \infty$ for $\tilde{\boldsymbol{x}} \to \infty$, then it is GAS.

Basic Stability: Stability Analysis

Example: speed control of a surface vessel

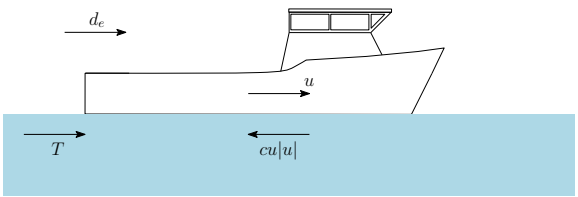

Take $d_e = 0$. Equation of motion is $m\dot{u} = -cu|u| + T$

Say we want to track speed $u_d(t)$.

Let $\tilde{u} := u - u_d$, then
$m\dot{\tilde{u}} = -cu|u| + T - m\dot{u}_d$

Consider the Lyapunov function

$$V = \frac{1}{2}\tilde{u}^2$$

Then

$$\dot{V} = \tilde{u}\dot{\tilde{u}} = \tilde{u}\left(-\frac{c}{m}u|u| + \frac{T}{m} - \dot{u}_d\right)$$

What if we pick control input $T = cu|u| + m\dot{u}_d - k_u m\tilde{u}$?

Basic Stability: Stability Analysis

Example: speed control of a surface vessel

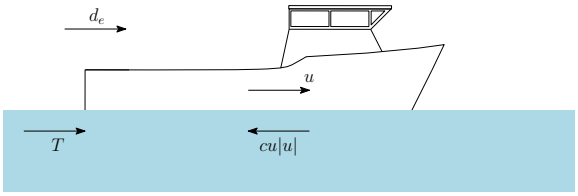

Then we have

$$\dot{V} = -k_u \tilde{u}^2.$$

So, overall we have

$$V > 0, \dot{V} < 0, \forall \tilde{u} \neq 0,$$

and

$$\lim_{\tilde{u} \to \infty} V \to \infty,$$

so system is GAS.

However, we can also see that we have a stronger type of stability because

$$\dot{V} = -k_u \tilde{u}^2 = -2k_u V$$

so that $V = V_0 \mathrm{e}^{-2k_u t}$, where V_0 is V at time $t = t_0$.

Then, $\|\tilde{u}\| = \sqrt{2V_0}\mathrm{e}^{-k_u t}$, so that system is GES to $\tilde{u} = 0$.

Basic Stability: Stability Analysis

Other important Lyapunov-based stability analysis methods for nonlinear systems (see lecture notes):

- **Invariant Set Theorem:** when you can only find a CLF with $\dot{V} \leq 0$, but still need to characterize stability of a closed loop system.
- **Use of Comparison Functions:** to analyze time-varying nonlinear systems.
- **Input to state stability:** when you need to show that system is stable to bounded disturbances.
- **Ultimate Boundedness:** an equilibrium point does not exist and you need to show that solution trajectories remain within a bounded region of state space.
- **Practical Stability:** When a system has actuator constraints and operates in the presence of disturbances, it does not approach an equilibrium point. Practical stability permits one to characterize the size of the region of the state space the solutions trajectories converge to, based on the magnitudes of the control gains.
- **Barbalat's Lemma:** Often used to analyze stability of adaptive systems, which generally have $\dot{V} \leq 0$.

Fundamentals of Marine Vehicle Control: Control of Underactuated Vehicles

Karl D. von Ellenrieder

Field Robotics Lab South Tyrol
Facoltà di Scienze e Tecnologie, Libera Università di Bolzano
39100 Bolzano, Italia
Email: karl.vonellenrieder@unibz.it

MTS/IEEE Global OCEANS 2022: Chennai, India

21 February 2022

Introduction: Overview of Tutorial

Basic concepts of:

- Introduction
- Basic Stability
- Control of Underactuated Vehicles
- Feedback Linearization by Dynamic Inversion & Nonlinear Backstepping
- Adaptive Control
- Sliding Mode Control

Control of Underactuated Vehicles

Basic Ideas:

- Important to distinguish between underactuated vehicles and fully-actuated vehicles.
- Underactuated systems cannot be arbitrarily moved from some initial pose to some final pose because
  - they cannot generate control forces/moments along every degree of freedom (missing actuators), or
  - because actuator magnitude constraints, or rate limits, restrict their ability to accelerate in a certain direction.
- Generally easier to control a fully-actuated vehicle, because underactuation limits the control objectives that can be satisfied.
- Most marine vehicles are underactuated, as full-actuation is often impractical, because of cost, weight or energy consumption.

Control of Underactuated Vehicles

Basic Ideas:

- In *trajectory tracking control* a marine vehicle must track a desired, time varying pose $\boldsymbol{\eta}_d(t)$.
- A fully-actuated vehicle without actuator constraints can track any arbitrary time-dependent trajectory.
- Even if a vehicle possesses actuators that can produce forces in any desired direction, if the forces required to maintain speed or acceleration required to catch up to and track a rapidly varying pose exceed the capabilities of the actuators, the vehicle is underactuated.

Here, we explore use of vehicle kinematics and dynamics to generate a dynamically feasible trajectory, which can then be tracked using a standard control approach.

Strategy: when possible, better to incorporate natural open loop dynamics of an underactuated system into control design, rather than trying to overcome them, because doing so requires fewer actuators and lower control effort.

Basic Concepts in Control of Underactuated Vehicles

Definition (Configuration Space)

The *n*-dimensional *configuration space* is the set of all configurations, i.e all possible positions and orientations, a vehicle can have, possibly subject to external constraints.

Definition (Degrees of Freedom – DOF)

A marine vehicle is said to have *n degrees of freedom* if its configuration can be minimally specified by *n* parameters. A marine vehicle that freely moves in three dimensions has six DOF: three translational DOF (linear displacements) and three rotational DOF (angular displacements).

Definition (Number of Independent Control Inputs)

The *number of independent control inputs r* is the number of *independently controlled directions* in which a vehicle's actuators can generate forces/moments.

Basic Concepts in Control of Underactuated Vehicles

Definition (Underactuated Marine Vehicles)

A marine vehicle is *underactuated* if it has fewer control inputs than generalized coordinates ($r < n$).

Definition (Fully Actuated Marine Vehicles)

A marine vehicle is *fully actuated* if the number of control inputs is equal to, or greater than, the number of generalized coordinates ($r \geq n$).

Definition (Workspace)

An underactuated vehicle can only produce independent control forces in $r < n$ directions. When designing a controller, it makes sense to explore whether or not a space of fewer dimensions $m < n$ might exist in which the vehicle can be suitably controlled. The workspace is a reduced space of dimension $m < n$ in which the control objective is defined Fossen [2011].

Basic Concepts in Control of Underactuated Vehicles

Basic Ideas:

- Underactuated vehicles have more states in their configuration space n than independent control inputs r.
- Some vehicle states are uncontrollable (unreachable).
- While it is possible to design a controller for an underactuated marine vehicle when its workspace is fully-actuated $m = r$, one must ensure zero dynamics of closed loop system are stable when dimension of configuration space is reduced to that of workspace.
- Uncontrolled equations of motion appear as k constraints that must have bounded solutions to prevent system from becoming unstable.

Motion Constraints

Basic Ideas:

- Constraints can arise from both input and state limitations.
- Examples of dynamic constraints include missing actuators, but could also be caused by magnitude or rate limitations of the actuators present.
- Constraints can also arise because of a physical barrier in the environment, e.g. a ship is generally constrained to move along the free surface of the water.

Constraints that depend on both vehicle state and inputs can be expressed as

$$h(\boldsymbol{\eta}, \boldsymbol{u}, t) \geq 0.$$

Often constraints are separated into those that depend only on input (e.g. actuator constraints, also called *input constraints*) $h(\boldsymbol{u}) \geq 0$ and those that depend on vehicle pose $h(\boldsymbol{\eta}) \geq 0$, which are known as *state constraints*.

Motion Constraints

Since $\boldsymbol{\eta}$ is an n-dimensional vector, if k geometric constraints exist,

$$h_i(\boldsymbol{\eta}) \geq 0, \quad i = 1, \ldots, k$$

the possible motions of vehicle are restricted to an $(n-k)$-dimensional submanifold (space) $\Rightarrow$ state constraints reduce dimensionality of system's available state space.

When constraints have the form

$$h_i(\boldsymbol{\eta}) = 0, \quad i = 1, \ldots, k < n,$$

they are known as *holonomic constraints*.

Motion Constraints

System constraints that depend on both pose and its first time derivative are *first order constraints*

$$h_i(\boldsymbol{\eta}, \dot{\boldsymbol{\eta}}) = 0, \quad i = 1, \ldots, k < n,$$

and are also called *kinematic constraints*, or *velocity constraints*.
First order kinematic constraints limit possible motions of a vehicle by restricting the set of velocities $\dot{\boldsymbol{\eta}}$ that can be obtained in a given configuration. These constraints are usually encountered in the form

$$\boldsymbol{A}^T(\boldsymbol{\eta})\dot{\boldsymbol{\eta}} = 0.$$

Holonomic constraints of this form imply kinematic constraints of the form

$$\nabla h \cdot \dot{\boldsymbol{\eta}} = 0.$$

But, the converse is not true. Kinematic constraints cannot always be integrated.
When this is true, the constraints (and system) are *nonholonomic*.

Motion Constraints

In many underactuated systems, including (especially) marine vehicles, nonholonomic constraints usually of *second order* and involve the *acceleration* of system. They can be represented in the form

$$h_i(\boldsymbol{\eta}, \dot{\boldsymbol{\eta}}, \ddot{\boldsymbol{\eta}}) = 0, \quad i = 1, \ldots, k < n.$$

Nonholonomic constraints limit mobility of systems differently than holonomic constraints:

- Nonholonomic constraints do not reduce the number of possible configurations of the system, only how each configuration can be reached.
- Nonholonomic constraints confine velocity or acceleration to an $m = (n - k)$ dimensional subspace (the workspace), but the entire n dimensional configuration space of the system can still be reached.
- Holonomic constraints reduce the number of degrees of freedom of a system by one $\Rightarrow$ motion of a holonomic system with k constraints is constrained to an $(n - k)$ dimensional subset of full n dimensional configuration space De Luca and Oriolo [1995].

Dynamics of underactuated surface vessels

In three DOF, the kinematic equations reduce to

$$\dot{\boldsymbol{\eta}} = \boldsymbol{R}(\psi)\boldsymbol{v},$$

where ψ is the heading angle of the vehicle, $\boldsymbol{R}(\psi)$ is the transformation matrix from the body-fixed system to the a North-East-Down (NED) inertial coordinate system, which is given by

$$\boldsymbol{R}(\psi) := \begin{bmatrix} \cos\psi & -\sin\psi & 0 \\ \sin\psi & \cos\psi & 0 \\ 0 & 0 & 1 \end{bmatrix} \in SO(3),$$

and

$$\boldsymbol{\eta} := \begin{bmatrix} x_n \\ y_n \\ \psi \end{bmatrix} \in \mathbb{R}^2 \times \mathcal{S}, \quad \text{and} \quad \boldsymbol{v} := \begin{bmatrix} u \\ v \\ r \end{bmatrix} \in \mathbb{R}^3$$

are the position and orientation (pose) vector and velocity vector (in body-fixed coordinates), respectively.

Dynamics of underactuated surface vessels

Consider the kinetic equation of motion

$$\boldsymbol{M}\dot{\boldsymbol{\nu}} + \boldsymbol{C}(\boldsymbol{\nu})\boldsymbol{\nu} + \boldsymbol{D}(\boldsymbol{\nu})\boldsymbol{\nu} = \boldsymbol{\tau},$$

where

$$\boldsymbol{M} := \begin{bmatrix} m - X_{\dot{u}} & 0 & 0 \\ 0 & m - Y_{\dot{v}} & -Y_{\dot{r}} \\ 0 & -N_{\dot{v}} & I_z - N_{\dot{r}} \end{bmatrix}$$

$$= \begin{bmatrix} m_{11} & 0 & 0 \\ 0 & m_{22} & m_{23} \\ 0 & m_{32} & m_{33} \end{bmatrix}.$$

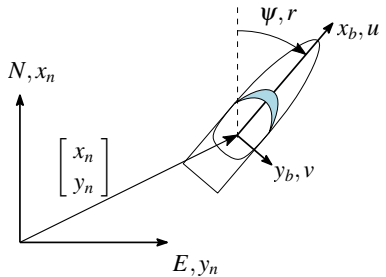

3 DOF maneuvering coordinate system definitions.

Dynamics of underactuated surface vessels

$$\boldsymbol{C}(\boldsymbol{v}) := \begin{bmatrix} 0 & 0 & -m_{22}v - \dfrac{(m_{23}+m_{32})}{2}r \\ 0 & 0 & m_{11}u \\ m_{22}v + \dfrac{(m_{23}+m_{32})}{2}r & -m_{11}u & 0 \end{bmatrix},$$

$$\boldsymbol{D}_{nl}(\boldsymbol{v}) := -\begin{bmatrix} X_{u|u|}|u| & 0 & 0 \\ 0 & Y_{v|v|}|v| + Y_{v|r|}|r| & Y_{r|v|}|v| + Y_{r|r|}|r| \\ 0 & N_{v|v|}|v| + N_{v|r|}|r| & N_{r|v|}|v| + N_{r|r|}|r| \end{bmatrix},$$

$$\text{and} \quad \boldsymbol{D}_{l} := -\begin{bmatrix} X_u & 0 & 0 \\ 0 & Y_v & Y_r \\ 0 & N_v & N_r \end{bmatrix}.$$

Dynamics of underactuated surface vessels

Let the total drag $\boldsymbol{D}(\boldsymbol{v})\boldsymbol{v}$, which the sum of the nonlinear drag $\boldsymbol{D}_{nl}(\boldsymbol{v})\boldsymbol{v}$ and the linear drag $\boldsymbol{D}_{l}\boldsymbol{v}$, be represented as

$$\boldsymbol{D}(\boldsymbol{v})\boldsymbol{v} = \left[\boldsymbol{D}_{nl}(\boldsymbol{v}) + \boldsymbol{D}_{l}\right]\boldsymbol{v} = \begin{bmatrix} d_x \\ d_y \\ d_\psi \end{bmatrix}.$$

Then, expanding terms, the equations of motion can be rewritten component-wise as

$$\begin{aligned}
&m_{11}\dot{u} - m_{22}vr - \left(\frac{m_{23} + m_{32}}{2}\right) r^2 + d_x = \tau_x, \\
&m_{22}\dot{v} + m_{23}\dot{r} + m_{11}ur + d_y = 0, \\
&m_{32}\dot{v} + m_{33}\dot{r} + (m_{22} - m_{11})uv + \left(\frac{m_{23} + m_{32}}{2}\right) ur + d_\psi = \tau_\psi.
\end{aligned}$$

Dynamics of underactuated surface vessels

These equations can be rearranged to write separate expressions for the accelerations $\dot{u}$, $\dot{v}$ and $\dot{r}$, to get

$$\begin{aligned} \dot{u} &= f_x + \frac{\tau_x}{m_{11}}, \\ \dot{v} &= f_y + a_y \frac{\tau_\psi}{m_{33}}, \\ \dot{r} &= f_\psi + a_\psi \frac{\tau_\psi}{m_{33}}, \end{aligned}$$

where f_x, f_y and f_ψ are functions of the velocities (u, v and r), and

$$a_\psi = \frac{m_{22} m_{33}}{m_{22} m_{33} - m_{23} m_{32}} \quad \text{and} \quad a_y = -\frac{m_{23}}{m_{22}} a_\psi.$$

The sway and yaw acceleration terms are coupled through the added mass term m_{23}.

Dynamics of underactuated surface vessels

Let $\boldsymbol{x} := [x_n \;\; y_n \;\; \psi \;\; u \;\; v \;\; r]^T$. The combined kinematic and dynamic equations can be written as

$$\dot{\boldsymbol{x}} = \begin{bmatrix} u\cos\psi - v\sin\psi \\ u\sin\psi + v\cos\psi \\ r \\ f_x \\ f_y \\ f_\psi \end{bmatrix} + \begin{bmatrix} 0 \\ 0 \\ 0 \\ \dfrac{1}{m_{11}} \\ 0 \\ 0 \end{bmatrix} \tau_x + \begin{bmatrix} 0 \\ 0 \\ 0 \\ 0 \\ \dfrac{a_y}{m_{33}} \\ \dfrac{a_\psi}{m_{33}} \end{bmatrix} \tau_\psi,$$

which has the control affine form

$$\dot{\boldsymbol{x}} \;\; = \;\; \boldsymbol{f}(\boldsymbol{x}) + \boldsymbol{G}\boldsymbol{u}.$$

Computing dynamically feasible trjactories

Given a set of $x_d(t), y_d(t)$ positions that we would like to follow, we can determine the corresponding values of $\psi(t)$ that are dynamically feasible (i.e. that satisfy the acceleration constraints) [Ashrafiuon et al., 2017].

The approach has the following main steps:

1. Use the kinematic equations of motion to determine the corresponding sway acceleration $\dot{v}_d(t)$.
2. The kinetic equations of motion for sway and yaw are coupled by the m_{23} added mass term. We use this coupling to find a virtual control input relating $\dot{r}$ to $\dot{v}_d$.

Computing dynamically feasible trjactories

The velocity of the vessel in the body-fixed frame can be related to its velocity in the inertial (NED) frame, as

$$\boldsymbol{v} = \boldsymbol{R}^{-1}(\psi)\dot{\boldsymbol{\eta}} = \boldsymbol{R}^{T}(\psi)\dot{\boldsymbol{\eta}}.$$

Then, the sway speed v is related to the velocities in the NED frame as

$$v = -\dot{x}_n \sin\psi + \dot{y}_n \cos\psi.$$

Let $(x_d(t), y_d(t))$ be a sufficiently smooth trajectory in the NED reference frame. Then, $v_d(t)$ is

$$v_d(t) = -\dot{x}_d \sin\psi + \dot{y}_d \cos\psi.$$

Taking the time derivative of this gives the desired sway acceleration

$$\dot{v}_d(t) = -\ddot{x}_d \sin\psi - \dot{x}_d r \cos\psi + \ddot{y}_d \cos\psi - \dot{y}_d r \sin\psi.$$

Computing dynamically feasible trjactories

Next we find the relationship between $\dot{r}$ and $\dot{v}_d$. By solving for τ_ψ in our expression for $\dot{r}$ we rewrite the equation for $\dot{v}$ as

$$\dot{v} = f_y + \frac{a_y}{a_\psi}\left[\dot{r} - f_\psi\right].$$

To find the virtual control input $\dot{r}_d$ that gives the heading angle required for a dynamically feasible trajectory, define the sway acceleration error as $\dot{\tilde{v}} := \dot{v} - \dot{v}_d$. Then, we have

$$\dot{\tilde{v}} = f_y + \frac{a_y}{a_\psi}\left[\dot{r} - f_\psi\right] - \dot{v}_d,$$

so that the virtual control input $\dot{r}_d$ that makes $\dot{\tilde{v}} = 0$ is given by

$$\dot{r}_d = \frac{a_\psi}{a_y}\left[\dot{v}_d - f_y\right] + f_\psi.$$

Computing dynamically feasible trjactories

Thus, given $(x_d(t), y_d(t))$ one can specify the dynamically feasible time-dependent pose $\boldsymbol{\eta}_d(t) = [x_d \;\; y_d \;\; \psi_d]^T$ using the associated sway acceleration $\dot{v}_d(t)$ and integrating twice to obtain the desired heading angle $\psi_d(t)$, subject to initial conditions $\psi_d(t = t_0)$ and $\dot{\psi}_d(t = t_0)$.

Given a dynamically feasible trajectory, we can also determine a set of feedforward control inputs τ_x and τ_ψ that generate the desired motion, using the equations we developed for $\dot{u}$ and $\dot{r}$.

We start by computing u_d in the NED frame, as

$$u_d = \dot{x}_d \cos\psi + \dot{y}_d \sin\psi.$$

The desired surge acceleration is then

$$\dot{u}_d = \ddot{x}_d \cos\psi - \dot{x}_d r \sin\psi + \ddot{y}_d \sin\psi + \dot{y}_d r \cos\psi.$$

Computing dynamically feasible trjactories

Replacing $\dot{u}$ with $\dot{u}_d$ in our equation for surge acceleration and solving for τ_x gives

$$\tau_x = m_{11} \left(\dot{u}_d - f_x \right).$$

Similarly, replacing $\dot{r}$ with $\dot{r}_d$ in equation for yaw acceleration and solving for τ_ψ gives

$$\tau_\psi = \frac{m_{33}}{a_\psi} \left(\dot{r}_d - f_\psi \right).$$

These control inputs produce desired dynamically feasible trajectory in absence of disturbances.

A separate feedback controller can be used to ensure system is robust to disturbances and modeling uncertainties.

Computing dynamically feasible trjactories: Example

Construct dynamically feasible trajectories for a USV with

$$M = \begin{bmatrix} 189.0 & 0.0 & 0.0 \\ 0.0 & 1036.4 & -543.5 \\ 0.0 & -543.5 & 2411.1 \end{bmatrix}.$$

Then, a_y and a_ψ are

$$a_y = 0.595 \quad \text{and} \quad a_\psi = 1.134.$$

Assume linear drag with coefficients

$$D = \begin{bmatrix} 50.0 & 0.0 & 0.0 \\ 0.0 & 948.2 & 385.4 \\ 0.0 & 385.4 & 1926.9 \end{bmatrix}.$$

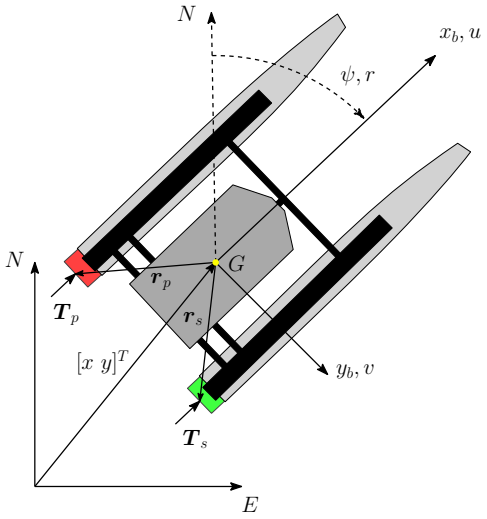

Computing dynamically feasible trjactories: Example

Vehicle follows circular trajectory radius $R = 10$ m in clockwise direction, starting from $(x_0, y_0) = (0, 0)$ at $t_0 = 0$ and finishing at same point $(x_f, y_f) = (0, 0)$ at $t_f = 50$ secs, where (x, y) coordinates specified in meters.
Center of circle located at point $(x_c, y_c) = (0, 10)$.
The trajectory is given by

$$\begin{aligned} x_d(t) &= R\sin(\omega_d t), \\ y_d(t) &= R[1 - \cos(\omega_d t)], \end{aligned}$$

where $\omega_d = 2\pi/t_f$.

Computing dynamically feasible trjactories: Example

a)

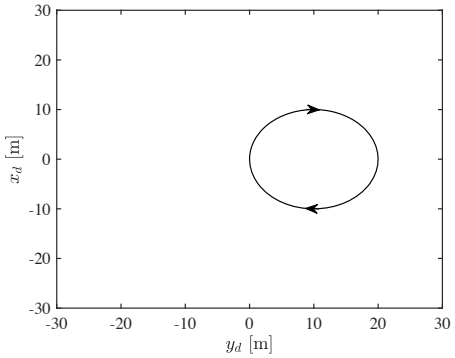

b)

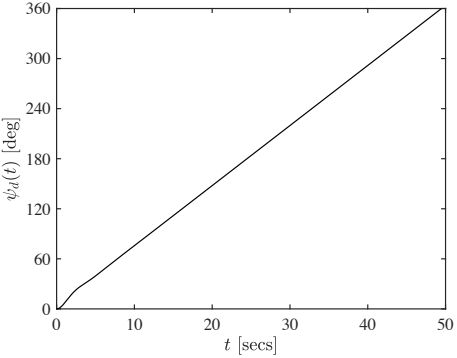

a) trajectory and b) desired heading angle.

Computing dynamically feasible trjactories: Example

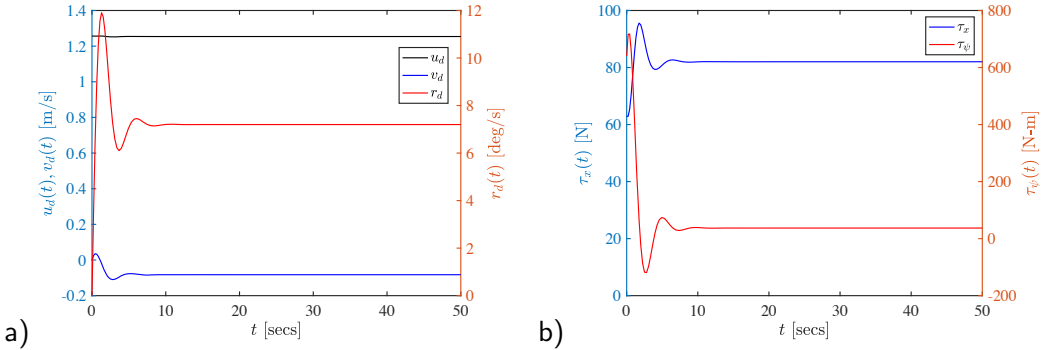

Case c: a) desired body-fixed velocities and b) control inputs.

After small initial transient, desired yaw rate is constant $r_d = \omega_d$.

To maintain turn, vehicle has small v_d and τ_ψ throughout the trajectory.

Bibliography I

H. Ashrafiuon, S. Nersesov, and G. Clayton. Trajectory tracking control of planar underactuated vehicles. *IEEE Trans Autom Control*, 62(4):1959–1965, 2017.

A. De Luca and G. Oriolo. Modelling and control of nonholonomic mechanical systems. In *Kinematics and dynamics of multi-body systems*, pages 277–342. Springer, 1995.

T. I. Fossen. *Handbook of marine craft hydrodynamics and motion control*. John Wiley & Sons, 2011.